N°d'ordre NNT : 2016LYSE1045

THESE de DOCTORAT DE L'UNIVERSITE DE LYON
opérée au sein de
l'Université Claude Bernard Lyon 1

Ecole Doctorale N° 206
(Chimie de Lyon)

Spécialité de doctorat : Chimie

Soutenue publiquement le 29/03/2016, par :
Thaíssa de Camargo Chaparro

Synthèse de nanocomposites avec des propriétés anisotropes par polymérisation radicalaire contrôlée en émulsion

---

Devant le jury composé de :

CASSAGNAU, Philippe	Professeur, Université Claude Bernard Lyon 1	Président
HEUTS, Johan P.A.	Professeur, Université Technique d'Eindhoven	Rapporteur
PREVOT, Vanessa	Chargée de Recherche HDR CNRS, Institut de Chimie de Clermont-Ferrand	Rapporteur
GIUDICI, Reinaldo	Professeur, Université de São Paulo	Examinateur
BOURGEAT-LAMI, Elodie	Directrice de Recherche CNRS C2P2	Directrice de thèse
DOS SANTOS Amilton M.	Professeur, Université de São Paulo	Co-Directeur de thèse

THAÍSSA DE CAMARGO CHAPARRO

Synthesis of nanocomposites with anisotropic properties by controlled radical emulsion polymerization

Lorena
2016

THAÍSSA DE CAMARGO CHAPARRO

Synthesis of nanocomposites with anisotropic properties by controlled radical emulsion polymerization

A thesis submitted in partial fulfillment of the requirements for the degree of Doctor of Philosophy in Sciences in the area of Conventional and Advanced Materials at the Engineering School of Lorena of the University of São Paulo, and in Chemistry at the University Claude Bernard Lyon 1.

Supervisors:

Dr. Amilton Martins dos Santos
Dr. Elodie Bourgeat-Lami

Reprinted and corrected edition
The original edition is available at the Engineering School of Lorena

Lorena
May, 2016

THAÍSSA DE CAMARGO CHAPARRO

Synthesis of nanocomposites with anisotropic properties by controlled radical emulsion polymerization

Tese apresentada à Escola de Engenharia de Lorena da Universidade de São Paulo para a obtenção do título de Doutora em Ciências na área de Materiais Convencionais e Avançados e à Universidade Claude Bernard Lyon 1 para a obtenção do título de Doutora em Química.

Orientadores:

Dr. Amilton Martins dos Santos
Dr. Elodie Bourgeat-Lami

Edição reimpressa e corrigida
A versão original encontra-se disponível na Escola de Engenharia de Lorena

Lorena
Maio, 2016

AUTORIZO A REPRODUÇÃO E DIVULGAÇÃO TOTAL OU PARCIAL DESTE TRABALHO, POR QUALQUER MEIO CONVENCIONAL OU ELETRÔNICO, PARA FINS DE ESTUDO E PESQUISA, DESDE QUE CITADA A FONTE

Ficha catalográfica elaborada pelo Sistema Automatizado
da Escola de Engenharia de Lorena,
com os dados fornecidos pelo(a) autor(a)

Chaparro, Thaíssa de Camargo
Synthesis of nanocomposites with anisotropic properties by controlled radical emulsion polymerization / Thaíssa de Camargo Chaparro; orientador Amilton Martins dos Santos; co orientadora Elodie Bourgeat-Lami - ed. reimp., corr. - Lorena, 2016.
240 p.

Tese (Doutorado em Ciências - Programa de Pós Graduação em Engenharia de Materiais na Área de Materiais Convencionais e Avançados) - Escola de Engenharia de Lorena da Universidade de São Paulo. 2016
Orientador: Amilton Martins dos Santos

1. Laponita. 2. Polimerização em emulsão sem surfatante. 3. Raft. 4. Látex. 5. Encapsulação. I. Título. II. dos Santos, Amilton Martins, orient. III. Bourgeat-Lami, Elodie, co-orient.

Acknowledgments

I would like to dedicate my sincere recognition to everyone who helped me accomplish this work. I thank Fundação de Amparo à Pesquisa do Estado de São Paulo, FAPESP, for the financial support that allowed the development of my Ph.D. research studies, as well as the development of part of the studies abroad. I thank, additionally, the International Union of Pure and Applied Chemistry (IUPAC) and the Centre national de la recherche scientifique (CNRS) for supporting researches related to this Ph.D study.

I would like to thank my supervisors Professor Dr. Amilton Martins dos Santos and Dr. Elodie Bourgeat-Lami and express my true appreciation for their support, patience and encouragement, and for competently executing this joint supervision. By sharing their knowledge with experienced and honest advices, they have enriched me as a professional and, for this reason, I admire and profoundly acknowledge them.

I would also like to thank Dr. Johan P. A. Heuts, Dr. Vanessa Prévot, Dr. Philippe Cassagnau and Dr. Reinaldo Giudici for serving as my committee members, and for their feedback, assistance and the valuable contribution to my work.

I would like to extend my gratitude to the all of the faculty and staff from the Lorena Engineering School of the University of São Paulo (EEL-USP) and from Université Claude Bernard Lyon I (UCBL), in special from the Programa de Pós-Graduação em Engenharia de Materiais (PPGEM), Comissão de Pós-Graduação (CPG), and the libraries of EEL-USP (in particular to Tavânia Cavasso, Regina Horta, Ludmila Osuna and Bruno Marton for their solicitude and enthusiasm) and from the Direction de la Recherche et des Etudes Doctorales (DRED) at UCBL.

I especially appreciate the contribution of everyone involved in the ENCIRCLE project and would like to thank Ana Maria Cenacchi Pereira, Rodrigo Duarte Silva, Gizelda Maria Alves, Dr. Muriel Lansalot, Dr. Frank D'Agosto, Dr. Ana M. Barros Timmons, Liliana Melro, Paula Lacerda and, of course, my supervisors. The knowledge and time shared by these individuals with discussions have been important to enlighten me towards the best direction and, therefore, to enrich my research.

My gratitude is extended to Pierre-Yves Dugas from LCPP for Cryo-TEM analysis; to Dr. Florent Dalmas, Dr. Laurent Chazeau and Baptiste Gary from MATEIS Laboratory (INSA of Lyon) for DMA and FIB-SEM analyses and for the valuable discussion and advices that added so much to my work; to Manel Taam and Olivier Boyron for SEC support and to Nathalie Jouglard for all the support in LCPP.

I thank Professor Jayne Carlos de Souza Barboza, Barbara Pereira and Professor Francisco Carlos Biaggio, from EEL-USP, for, respectively, NMR analysis, FTIR analysis and general support, and Juliana Livi Antoniassi from LCT (Poli-USP) for XRD analysis.

I would especially like to thank all members of LabPol, in Lorena. More than just coworkers, this group can been considered members of a second family that share knowledge with solidarity and an incredible good humor. I thank Marli for everything that she taught me, and all the friends Vanessa, Ana, Mari, Lella, Fábio, Isa, Lucas, Thiago, Simone, Rafael, Bárbara, Paulo, Brunão, Taline, João, Thales, Júlia, Victor, Raíssa, Igor, Arthur, Felipe, Gabi, Bruno, Rodolpho, Anthony, Grazi, Rodolfo, Isa, Jessica, Clarice, Cleise, Paulo and all the others for the sincere friendship and for making the past few years an enjoyable part of my life. I thank especially Rodrigo, for sharing his knowledge with such a good heart, and Giza for her joy, good will and, especially, for creating the LabPol spirit.

Thanks are also extended to everyone from the LCPP group. All of you have made my time in France an unforgettable experience. Special thanks to Keran, Sam, Bastian, Julien, Isabelle and Emilie, who have been great friends, as well as Anthony, Anderson and Gigi for all the adventures and fun times shared during my stay in Lyon. Appreciation is also expressed to Juliën, Ana, Emilie and Elizabeth for letting conferences in Thailand and China be an enjoyable and fun moment. Very special thanks go to Thiago and Barbara. For the honest, creative, genuine and eternal friendship.

Finally, special recognition goes to my family. To my sisters Emi and Laila, as well as my brothers-in-law David and Rodrigo and my nieces and nephews, for the support and patience and for understanding (or accepting) my lack of visit during these past few years. To my cousin and godmother Bete, and my entire family, whose encouragement and prayers sustained me during the most challenging moments. To my parents, who have been my inspiration in life, I cannot thank you enough for the motivation you have provided during my career, for your positive influence and for the sacrifices that you have made on my behalf. I dedicate this work to you.

And last but not least, I thank God for letting me come this far.

Abstract

CHAPARRO, T. C. **Synthesis of nanocomposites with anisotropic properties by controlled radical emulsion polymerization**. 2016. 240 p. Thesis (Doctoral in science) – Escola de Engenharia de Lorena, Universidade de São Paulo, Lorena, 2016.

The aim of this work is to prepare Laponite RD-based nanocomposite latexes by aqueous emulsion polymerization, using the reversible addition-fragmentation chain transfer (RAFT) polymerization. Laponite platelets were selected as the inorganic filler due, especially, to their anisotropic shape, which allows the production of nanostructured films, but also for their thermal and mechanical properties, their high chemical purity and the uniform dispersity of the platelets. Hydrophilic polymers (macroRAFT) composed of poly(ethylene glycol) (PEG), acrylic acid (AA) or N,N-dimethylaminoethyl methacrylate (DMAEMA) and comprising hydrophobic n-butyl acrylate (BA) units (in some cases) and trithiocarbonate terminal group were initially synthesized. Then, the interaction between the macroRAFTs and the clay was studied through the plot of adsorption isotherms. By acting as coupling agents and stabilizers, the macroRAFT agents were used in the emulsion copolymerization of methyl (meth)acrylate and BA by semi-continuous process in the presence of the clay. Hybrid latex particles with different morphologies were obtained and the results were associated to the nature and concentration of the RAFT (co)polymers, to the pH of the macroRAFT/Laponite dispersion, the glass transition temperature of the final copolymer (function of the composition of the hydrophobic monomers mixture) and to the polymerization conditions. The cryo-TEM images indicate the formation of polymer-decorated Laponite platelets (several latex particles located at the surface of the platelets), dumbbell-like, janus, Laponite-decorated (armored) latex particles, and multiple encapsulated particles (several platelets inside each latex particle). The mechanical properties of polymer/Laponite films were studied by dynamic mechanical analysis and correlated with the particles morphology and the films microstructure.

Keywords: Laponite, layered silicate, surfactant-free emulsion polymerization, RAFT, morphology, encapsulation, latex, nanocomposites, films.

Resumo

CHAPARRO, T. C. **Síntese de nanocompósitos com propriedades anisotrópicas via polimerização radicalar controlada em emulsão**. 2016. 240 p. Tese (Doutorado em ciências) – Escola de Engenharia de Lorena, Universidade de São Paulo, Lorena, 2016.

Este trabalho de tese tem como objetivo a preparação de látices nanocompósitos à base da argila Laponita RD em emulsão aquosa, via polimerização radicalar controlada por transferência de cadeia via adição-fragmentação reversível (RAFT). A Laponita foi escolhida como carga inorgânica devido principalmente à forma anisotrópica de suas lamelas, o que permite a elaboração de filmes nanoestruturados, mas também por suas propriedades térmicas e mecânicas, por sua alta pureza química e pela distribuição uniforme, em termos de tamanho, de suas partículas. Inicialmente, polímeros hidrofílicos (macroRAFT) à base de poli(etileno glicol) (PEG), de ácido acrílico (AA) ou de metacrilato de N,N-dimetilaminoetila (DMAEMA) que contêm unidades hidrofóbicas de acrilato de *n*-butila (ABu) (em alguns casos) e um grupo tritiocarbonílico terminal foram sintetizados. Em seguida, a interação entre os macroagentes de controle (macroRAFTs) e a argila foi estudada através de isotermas de adsorção. Atuando como agentes de acoplamento e estabilizantes, esses macroRAFTs foram então utilizados na copolimerização em emulsão do (met)acrilato de metila e do ABu em processo semicontínuo na presença da argila Laponita. Partículas de látex híbrido de diferentes morfologias foram obtidas e os resultados foram correlacionados à natureza e à concentração dos macroRAFTs, ao pH da dispersão macroRAFT/Laponita, à temperatura de transição vítrea do copolímero final (função da composição da mistura de monômeros hidrofóbicos) e às condições de polimerização. As análises de cryo-TEM indicam a formação de lamelas de Laponita decoradas com partículas de polímero (várias partículas de látex localizadas na superfície das lamelas), de partículas do tipo *dumbbell*, *janus*, blindadas (partículas de látex decoradas com lamelas de argila em sua superfície) ou ainda de partículas multiencapsuladas (diversas lamelas encapsuladas dentro de uma única partícula de látex). As propriedades mecânicas dos filmes de polímero/Laponita foram estudadas por análise dinâmico-mecânica e correlacionadas à morfologia das partículas e à microestrutura dos filmes.

Palavras-chave : Laponita, silicato lamelar, polimerização em emulsão sem surfatante, RAFT, morfologia, encapsulação, látex, nanocompósitos, filmes.

Résumé

CHAPARRO, T. C. **Synthèse de nanocomposites avec des propriétés anisotropes par polymérisation radicalaire contrôlée en émulsion**. 2016. 240 p. Thèse (Doctorale en sciences) – Escola de Engenharia de Lorena, Universidade de São Paulo, Lorena, 2016.

L'objectif de ce travail de thèse est de préparer des latex nanocomposites à base d'argile, la Laponite RD, en émulsion aqueuse, à l'aide de la polymérisation radicalaire contrôlée par transfert de chaîne réversible par addition-fragmentation (RAFT). Les plaquettes de Laponite ont été choisies comme charge inorganique surtout pour leur anisotropie de forme, ce qui pourrait permettre l'elaboration de films nanostructurés, mais aussi pour leurs propriétés thermiques et mécaniques, leur pureté chimique élevée et la distribution uniforme en taille des plaquettes. Des polymères hydrophiles (macroRAFT) à base de polyéthylène glycol (PEG), d'acide acrylique (AA) ou de méthacrylate de N,N- diméthylaminoéthyle (DMAEMA) et comportant des unités hydrophobes d'acrylate de n-butyle (ABu) (dans certains cas) et un groupe trithiocarbonate terminal, ont été tout d'abord synthétisés. Ensuite, l'interaction entre les macroRAFTs et l'argile a été étudiée à travers le tracé des isothermes d'adsorption. En agissant comme des agents de couplage et des stabilisants, ces macroRAFTs ont eté utilisés dans la copolymérisation en émulsion du (méth)acrylate de méthyle et de l'ABu en mode semi-continu en presence d'argile. Des particules de latex hybrides de différentes morphologies ont été obtenues et les morphologies ont été reliées à la nature et à la concentration de l'agent macroRAFT, au pH de la dispersion macroRAFT/Laponite, à la température de transition vitreuse du copolymère final (fonction de la composition du mélange de monomères hydrophobes) et aux conditions de polymérisation. Les analyses par cryo-MET indiquent des plaquettes de Laponite décorées par des particules de polymère (plusieurs particules de latex en surface des plaquettes d'argile), des particules 'haltère', janus, 'carapace' (particules de latex décorées en surface par les plaquettes de Laponite) ou encore des particules multi-encapsulées (plusieurs plaquettes encapsulées dans chaque particule de latex). Les propriétés mécaniques des films de polymère/Laponite ont été etudiées par spectrométrie mécanique dynamique et corrélées à la morphologie des particules et à la microstructure des films.

Mots clés : Laponite, silicate lamellaire, polymérisation en émulsion sans tensioactif, RAFT, morphologie, encapsulation, latex, nanocomposites, films.

Abbreviations

2D	Two-dimensional
3D	Three-dimensional
α_L	Langmuir isotherm constant
AA	Acrylic acid
ACPA	4,4′-azobis(cyanovaleric acid)
ADIBA	2,2'-azobis(*N,N′* -dimethyleneisobutyramidine) dihydrochloride
AEC	Anionic exchange capacity
AGET	Activator generated by electron transfer
AIBA	2,2'-Azobisisobutyramidinedihydrochloride
AIBN	2,2'-azobisisobutyronitrile
ATRP	Atom-transfer radical polymerization
BA	*n*-Butyl acrylate
C_0	Initial concentration
CC	Clay content
C_e	Equilibrium concentration in the supernatant
CEC	Cation exchange capacity
CMC	Critical micelle concentration
CNT	Carbon nanotubes
CRP	Controlled radical polymerization
CTμ	Centre technologique des microstructures
CTA	Chain transfer agent
CTPPA	4-cyano-4-thiothiopropylsulfanyl pentanoic acid
Đ	Dispersity
DCC	N,N'-dicyclohexyl carbodiimide
DLS	Dynamic light scattering
DMA	Dynamic mechanical analysis
DMAEMA	2-(dimethylamino)ethyl methacrylate
DMAP	4-dimethylaminopyridine
DMF	Dimethylformamide
DMSO	Dimethyl sufoxide-d_6
DSC	Differential scanning calorimetry
FIB	Focused Ion Beam
GO	Graphene oxide
HA	Humic acid
HPLC	High performance liquid chromatography
IEP	Isoelectric point
INSA	Institut national des sciences appliquées
IR	Infrared spectroscopy
k_{-add}	Fragmentation rate constant
k_a	Activation rate constant
k_{add}	Addition rate constant
k_c	Recombination rate constant
k_d	Decomposition rate constant

K_F	Freundlich isotherm constant
k_p	Propagation rate constant
K_L	Binding energy constant
KPS	Potassium persulfate
LbL	Layer-by-layer
LDH	Layered double hydroxide
LSPN	Layered silicate polymer nanocomposites
MA	Methyl acrylate
MacroRAFT	Macromolecular RAFT agent
MADIX	Macromolecular Design via the Interchange of Xanthates
MMA	Methyl methacrylate
Mt	Montmorillonite
$M_{n,exp}$	Experimental number-average molar mass (g mol^{-1})
$M_{n,theo}$	Theoretical number-average molar mass (g mol^{-1})
M_n:	Number-average molar mass (g mol^{-1})
mPEG	Poly(ethylene glycol) methyl ether
MR	MacroRAFT
MWCNT	Multi-walled carbon nanotubes
NMP	Nitroxide-mediated polymerization
NMR	Nuclear magnetic resonance
PAA	Poly(acrylic acid)
PAH	Poly(allylamine hydrochloride)
PDMAEMA	Poly(2-(dimethylamino)ethyl methacrylate)
PEG	Poly(ethylene glycol)
PEGA	Poly(ethylene glycol) methyl ether acrylate
PEO	Poly(ethylene oxide)
PISA	Polymerization-induced self-assembly
PMMA	Poly(methyl methacrylate)
QD	Quantum dots
Q_e	Adsorbed amount of macroRAFT agent
Q_{max}	Adsorbed amount at saturation
RAFT	Reversible addition-fragmentation chain transfer
RDRP	Reversible deactivation radical polymerization
REEP	MacroRAFT-assisted encapsulating emulsion polymerization
SANS	Small-angle neutron scattering
SE	Secondary electron
SEM	Scanning Electron Microscopy
SEC	Size Exclusion Chromatography
SI	Surface-initiated
Sty	Styrene
TEM	Transmission electron microscopy
Tg	Glass transition temperature
THF	Tetrahydrofuran
XRD	X-Ray diffraction
$Z_{av.}$	Hydrodynamic average particle diameter

Table of contents

1 Introduction 15
1.1 General introduction 15
1.2 Aim and outline of the thesis 17
References 23
2 Bibliographic review on reversible deactivation radical polymerization (RDRP) and macroRAFT-assisted encapsulating emulsion polymerization (REEP) 29
2.1 Introduction 29
2.2 Free radical polymerization 30
2.3 Reversible deactivation radical polymerization (RDRP) 31
2.3.1 Nitroxide-mediated polymerization (NMP) 31
2.3.2 Atom transfer radical polymerization (ATRP) 33
2.3.3 Reversible addition-fragmentation chain transfer (RAFT) 34
2.3.3.1 RAFT in dispersed media 36
***2.3.3.1.1 Emulsion polymerization* 37**
***2.3.3.1.2 Conventional RAFT emulsion polymerization* 39**
***2.3.3.1.3 Polymerization-induced self-assembly RAFT emulsion polymerization* 40**
***2.3.3.1.4 RAFT-encapsulating emulsion polymerization of inorganic particles* 42**
2.4 Conclusions 49
References 50
3 MacroRAFT/Laponite interactions 59
3.1 Introduction 59
3.2 Bibliographic review 60
3.2.1 Clays or layered silicates 60
3.2.2 Laponite clay 61
3.2.2.1 Laponite crystal structure 61
3.2.3 Laponite surface modification 64
3.2.3.1 Interaction of Laponite with polymers 65
3.2.3.1.1. Anionic polyelectrolytes 67
3.2.3.1.2. Cationic polyelectrolytes 69
3.2.3.1.3. Nonionic polymers 70
3.3 Synthesis of macroRAFT agents 73
3.3.1 Experimental section 73
3.3.1.1 Materials 73
3.3.1.2 Methods 73
3.3.1.3 Characterizations 76
3.3.2 Results and Discussion 77
3.3.2.1 Synthesis of PAA-based macroRAFT agents 78
3.3.2.1.1. PAA_{42}-CTPPA (MR1) 78
3.3.2.1.2. P(AA_{16}-co-BA_{16})-CTPPA (MR2) 78
3.3.2.2 Synthesis of PEG-based macroRAFT agents 79

3.3.2.2.1. PEG$_{45}$-CTPPA (MR3) 79
3.3.2.2.2. PEG$_{45}$-b-PAA$_{49}$-CTPPA (MR4) 80
3.3.2.2.3. P(AA$_{40}$-b-PEGA$_5$)-CTPPA (MR5) 81
3.3.2.2.4. PAA$_{40}$-b-P(PEGA$_7$-co-BA$_4$)-CTPPA (MR6) 82
3.3.2.2.5. P(AA$_{16}$-co-BA$_{16}$)-b-P(PEGA$_7$-co-BA$_4$)-CTPPA (MR7) 83
3.3.2.2.6. P(PEGA$_7$-co-BA$_4$)-CTPPA (MR8) 84
3.3.2.2.7. P(AA$_5$-co-PEGA$_5$-co-BA$_5$)-CTPPA (MR 9) 85
3.3.2.2.8. P(AA$_{10}$-co-PEGA$_{10}$-co-BA$_{10}$)-CTPPA (MR10) 86
3.3.2.3 Synthesis of DMAEMA-based macroRAFT agents 87
3.3.2.3.1. P(DMAEMA$_{10}$-co-BA$_5$)-CTPPA (MR 11) 87
3.3.2.3.2. P(DMAEMA$_{20}$-co-BA$_{20}$)-CTPPA (MR 12) 89
3.3.2.4 Verification of the living character of the copolymers 90
3.4 Adsorption isotherms of macroRAFT agents onto Laponite 93
3.4.1 Experimental section 93
3.4.1.1 Materials 93
3.4.1.2 Methods 94
3.4.1.3 Characterizations 96
3.4.2 Results and Discussion 96
3.4.2.1 Adsorption isotherm of PAA-based macroRAFT agents 97
3.4.2.2 Adsorption isotherms of PEG-based macroRAFT agents 99
3.4.2.3 Adsorption isotherms of DMAEMA-based macroRAFT agents 103
3.5 Conclusions 107
References 109
4 Synthesis of hybrid latexes 119
4.1 Introduction 119
4.2 Bibliographic Review 121
4.2.1 Nanocomposites 121
4.2.1.1 Layered silicate polymer nanocomposites (LSPN) 123
4.2.2 Colloidal nanocomposites 126
4.2.2.1 Synthesis of colloidal nanocomposites 128
4.2.2.2 MacroRAFT-assisted encapsulating emulsion polymerization of layered particles 131
4.3 Experimental Section 138
4.3.1 Materials 138
4.3.2 Methods 138
4.3.3 Characterizations 139
4.4 Results and discussion 141
4.4.1 Synthesis of hybrid latexes in the presence of PEG$_{45}$-CTPPA 141
4.4.2 Synthesis of hybrid latexes in the presence of PAA$_{40}$-CTPPA 144
4.4.3 Synthesis of hybrid latexes in the presence of PEG$_{45}$-$_b$-PAA$_{42}$-CTPPA 146
4.4.4 Synthesis of hybrid latexes in the presence of P(AA$_{40}$-*b*-PEGA$_4$)-CTPPA 148

4.4.5 Synthesis of hybrid latexes in the presence of PAA_{40}-*b*-($PEGA_6$-*co*-BA_4)-CTPPA 151
4.4.6 Synthesis of hybrid latexes in the presence of P(AA_{16}-*co*-BA_{16})-*b*-($PEGA_6$-*co*-BA_4)-CTPPA 156
4.4.7 Synthesis of hybrid latexes in the presence of P($PEGA_5$-*co*-BA_3)-CTPPA 158
4.4.8 Synthesis of hybrid latexes in the presence of P(AA_{16}-*co*-BA_{16})-CTPPA 160
4.4.9 Synthesis of hybrid latexes in the presence of P(AA-*co*-PEGA-*co*-BA)-CTPPA 162
4.4.10 Synthesis of hybrid latexes in the presence of P($DMAEMA_{10}$-*co*-BA_4)-CTPPA 166
4.4.11 Synthesis of hybrid latexes in the presence of P($qDMAEMA_{19}$-*co*-BA_{14})-CTPPA 169
4.4.11.1 Effect of macroRAFT concentration 170
4.4.11.2 Effect of monomer composition 173
4.4.11.3 Effect of the nature of the initiator 177
4.4.11.4 Effect of clay content 178
4.4.12 Layer-by-layer technique 182
4.4.13 Mechanical behavior and microstructural characterization of Laponite polymer nanocomposite films 186
4.5 Conclusions 192
References 196
5 Conclusions and perspectives 207
References 214
Annexes 215
Annex 1 Extended abstracts 221
Annex 2 Calibration curves for the adsorption isotherms 233
Annex 3 X-ray diffraction analysis 239

1 Introduction

1.1 General introduction

Nanocomposites are an interesting type of material that has been gaining growing importance in recent years due to the many benefits offered over traditional composites. Among them, layered silicate polymer nanocomposites (LSPN) are of particular interest, since they combine the best attributes of layered silicates with the excellent processing and handling aspects of organic polymers.[1-6] Since the reinforcement efficiency of inorganic fillers is strongly related to their aspect ratio, anisotropic particles, such as clay platelets, are considered exceptional fillers. Besides bringing several gains to the mechanical properties of these materials, including enhancements in hardness, mechanical strength and scratch resistance, clay platelets can also contribute to various other improvements, such as better optical, thermal and gas barrier properties, as well as significant weight and cost reductions.

However, preserving and controlling the unique physical properties of anisotropic nano-objects in order to maintain their nanoscale integrity and achieve uniform dispersions is particularly challenging. The control over nanoparticle arrangement and distribution within the polymer matrix has been the focus of a great number of researches, as the alignment of anisotropic particles into polymeric hosts affects positively the mechanical, electrical or optical properties, as well as the macroscopic performance of composite materials. One of the most attractive ways to achieve an exceptional dispersion and a controlled distribution of nanoparticles within the polymer matrix is by encapsulating them with a polymer layer. A variety of methods has been reported in the recent literature to synthesize these materials, including heterocoagulation, layer-by-layer assembly techniques, and *in situ* polymerization.[7] Among the most suitable synthetic methods adopted, living/reversible deactivation radical polymerization (RDRP) techniques allow a precise control of the composition, thickness and functionality of the polymer layer.

Even though there are plenty of solvent-borne synthetic strategies involving RDRP techniques available to coat the surface of inorganic particles with polymers, waterborne methods involving emulsion, suspension, dispersion or miniemulsion polymerization are still underexplored. The current available strategies to produce polymer-encapsulated inorganic particles through emulsion polymerization still have limitations that impede them from being universal techniques.

The field of composite latex particles (hereafter referred to as colloidal nanocomposites) is growing and becoming the focus of numerous academic and industrial researches.[8, 9] Emulsion polymerization, a free radical polymerization process widely used in industries to manufacture paints, adhesives, impact modifiers and a variety of other products is particularly interesting. The use of conventional (i.e. non-controlled) emulsion polymerization to encapsulate individual inorganic particles by this technique, however, can be complicated and, in many cases, the targeted core-shell morphology is replaced by complex morphologies such as currant-bun, snowman-like, strawberry-like, daisy-shaped, janus and armored particles. Although successful encapsulation has been reported for spherical particles,[9] it seems that the particle shape and the high aspect ratio associated with the high surface energy of anisotropic particles prevent them from being efficiently encapsulated.[10, 11]

Recently, a new method for the synthesis of organic/inorganic nanocomposites by RDRP in emulsion has been reported by Hawkett and coworkers to encapsulate hydrophobic organic (phthalocyanine blue pigment) and hydrophilic inorganic pigment particles (alumina and zirconia-coated titanium dioxide),[12] and subsequently applied by Daigle and Claverie for different metal, metal oxide and metal nitride spherical particles.[13] Although, in theory, the same method can be applied to Nitroxide-Mediated Polymerization (NMP)[14] and Atom Transfer Radical Polymerization (ATRP)[15], this field is still insufficiently explored and the attention has been dedicated, almost exclusively, to the use of Reversible Addition-Fragmentation chain Transfer **(**RAFT**)** process, one of the most robust and versatile controlled radical polymerization techniques.[16] The strategy, recently called RAFT-encapsulating emulsion polymerization (REEP),[17, 18] relies on the use of hydrophilic macromolecular RAFT agents (also referred to as macroRAFTs) as coupling agents and precursors of stabilizers. The thiocarbonylthio compounds have conveniently chosen R and Z groups and, through successive active/dormant cycles, which minimizes radical-radical termination processes, mediate the simultaneous growth of polymer chains from the inorganic substrate.[19, 20]

The macroRAFT agents used by Hawkett et al.[12] to stabilize the dispersions of inorganic pigments were hydrosoluble amphipathic copolymers of randomly distributed acrylic acid (AA) and *n*-butyl acrylate (BA) units. For the formation of an encapsulating hydrophobic shell around the pigment particles, the RAFT functionality of the copolymers was further reactivated for the polymerization of a hydrophobic monomer under starve-feed

emulsion polymerization. The presence of the macroRAFT agents is fundamental for the process not only to control polymerization, but mostly to define the inorganic surface as the polymerization locus and potentially stabilize the hybrid latex particles. Diverse other particles have been successfully encapsulated by the RAFT-mediated emulsion polymerization, including cadmium sulfide[21] and lead sulfide[22] quantum dots, cerium oxide,[23-26] carbon nanotubes,[27, 28] Gibbsite,[29] Montmorillonite clay[30] and even graphene oxide.[31] The encapsulation of anisotropic nano-objects, such as clays, however, is not so trivial. The disk shape morphology, large aspect ratio and high surface energy of layered minerals difficult the encapsulation process and most attempts to encapsulate unmodified[32] and, in some cases, surface-modified[7, 10, 33] clay platelets by emulsion polymerization result in the formation of the so-called armored structures, in which the clay is located at the particle surface. Several parameters, related especially to kinetic and/or thermodynamic control mechanisms, must be optimized for successful encapsulation. In addition to encapsulating clay, there is specific interest in forming a thin polymer layer at the particle surface so that the anisotropy of the particle shape is preserved. The production of such anisotropic "core-shell" composite latex particles is attracting increasing interest since these particles are more likely to induce anisotropy into the final film, which is highly desirable as it generates materials with potentially improved properties that can find applications in the fields of coatings or adhesives,[34] for instance. For this reason, having control over the orientation of clay platelets in the final polymeric film, which is fundamental for the final coating properties of the material, is currently a very inviting challenge.

1.2 Aim and outline of the thesis

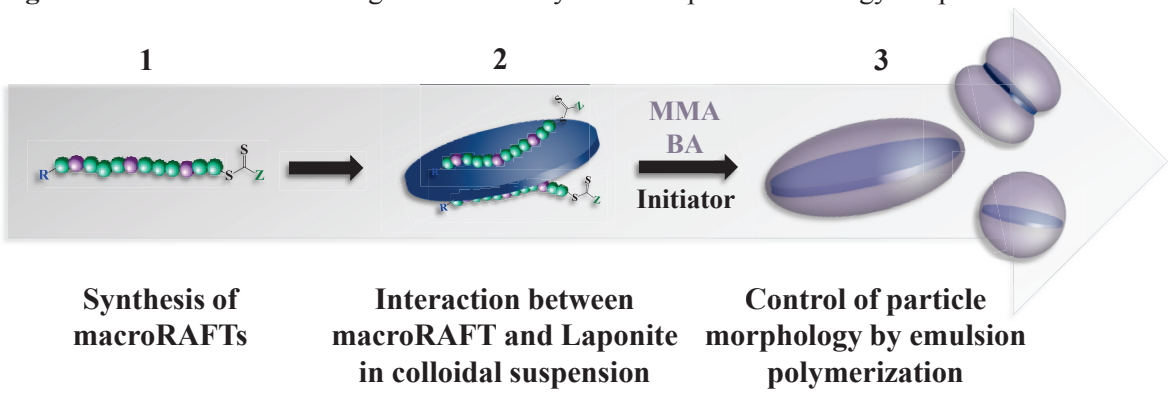
This thesis was part of an international multidisciplinary project entitled "polymer **enc**apsulation of anisotropic **i**no**r**ganic nanoparti**cle**s by RAFT-mediated emulsion polymerization (ENCIRCLE), enabled by the International Union of Pure and Applied Chemistry (IUPAC). The aim of the project was to develop a knowledge-based method involving RAFT-mediated emulsion polymerization for the encapsulation of anisotropic inorganic nano-objects, in order to form nanostructured latex films. Different types of inorganic materials were investigated by three different partners: layered double hydroxides particles and Imogolite nanotubes were studied in Lyon, France, silica-coated luminescent $Gd_2O_3:Eu^{3+}$ nanotubes in Aveiro, Portugal, and natural (Montmorillonite) and synthetic (Laponite) smectite-type layered silicates in Lorena, Brazil.

In fact, Montmorillonite and hectorite (and notably Laponite) are among the most frequently used smectite clays for the preparation of nanocomposites.[2, 5] This type of clays presents unique properties, including a large chemically active surface area, a high exchange capacity and special hydration characteristics. Laponite, specifically, was chosen for this work since it has some other additional advantages that make it an ideal model substrate, such as a high chemical purity, a uniform dispersity of the elementary platelets and the ability to produce clear dispersions.

A part of this present work was developed in the Laboratory of Polymers, in the Engineering School of Lorena (EEL-USP), in Lorena-SP, Brazil and another part in the Laboratory of Chemistry, Catalysis, Polymers and Processes (C2P2) in Lyon, France.

The synthetic strategy of RAFT-based emulsion polymerization proposed in this work to encapsulate Laponite particles represents an important tool for preparing a wide variety of particle morphologies that result in latex films with different controlled nanostructures. It is composed of three main steps, as schematically represented in Figure 1.1.

Figure 1.1 – Scheme illustrating the different synthetic steps of the strategy adopted.



Source: elaborated by the author.

1) **Synthesis of designed RAFT and macroRAFT agents:** The initial part of the strategy had as main objective designing and synthesizing appropriate amphipathic macroRAFT agents that were capable of interacting with the inorganic particles, by carrying suitable anchor groups, for the further preparation of stable macroRAFT-inorganic colloidal suspensions. The RAFT copolymers synthesized carry a thiocarbonylthio functionality that allow them to control the radical polymerization of methyl methacrylate (MMA) or methyl acrylate (MA) and *n*-butyl acrylate (BA) monomers. A trithiocarbonate compound was chosen due to its higher efficiency as control agent when used in

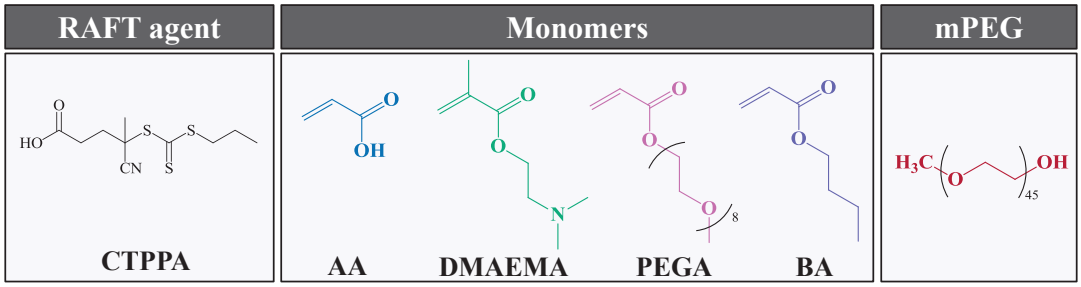
dispersed media.[35-40] The Z and R groups of the RAFT agent were carefully selected, and the 4-cyano-4-thiothiopropylsulfanyl pentanoic acid (CTPPA), a (thiocarbonyl)sulfanyil chain transfer agent that carries a short hydrophobic alkyl chain end (thiopropyl) as Z group, was chosen as RAFT agent.

To allow strong interaction of these macroRAFT agents with the inorganic particles, twelve different macroRAFTs with the R group bearing either a quaternary ammonium group (from N,N-dimethylaminoethyl methacrylate, DMAEMA) or neutral polyethylene glycol (PEG) side chains were carefully designed and synthesized by solution polymerization.

Each monomer was chosen for specific purposes. The presence of charged or ionizable monomers of DMAEMA, with opposite charge to that of the inorganic particle surface, is strategic to promote strong electrostatic interaction of the macroRAFT copolymers with the negatively charged clay particles. As an alternative to cationic macroRAFT agents, PEG-based homo and copolymers were also selected considering their potential to adsorb on clay particles. In addition, (co)polymers containing BA, AA and poly(ethylene glycol) acrylate (PEGA) units were also designed to tune the interaction of the macroRAFT agents with the inorganic surface, since AA can potentially have some affinity with the positively charged rims of the clay. In addition, the RAFT (co)polymers should ensure sufficient colloidal stability of the inorganic particles before polymerization and allow subsequent growth of a polymer shell without secondary nucleation. In this aspect, random macroRAFT copolymers were preferred over block copolymers to avoid the self-assembly of these copolymers in the aqueous phase and prevent the formation of new pure polymer particles. Both polyelectrolytes of AA and DMAEMA, as well as the pending or linear polar blocks of ethylene glycol, are also expected to provide stability to the hybrid particles. The addition of some BA units, on the other hand, aimed to increase the hydrophobicity of the clay environment, which is generally highly hydrophilic, in order to attract the growing hydrophobic polymeric block close to the Laponite/macroRAFT domain.

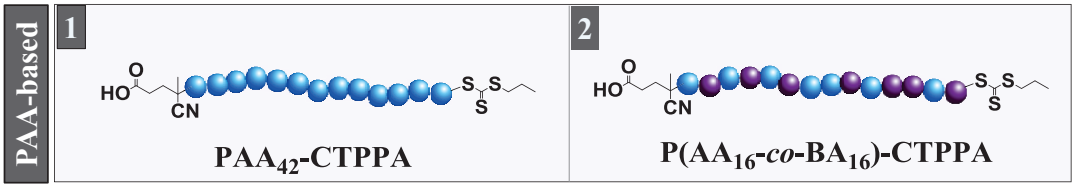
The RAFT agent, monomers used and poly(ethylene glycol) methyl ether (mPEG) are represented in Figure 1.2, while AA-based, PEGA-based and DMAEMA-based designed structures are schematically represented in Figure 1.3, Figure 1.4 and Figure 1.5, respectively.

Figure 1.2 – RAFT agent, monomers and mPEG used for the synthesis of macroRAFT agents.



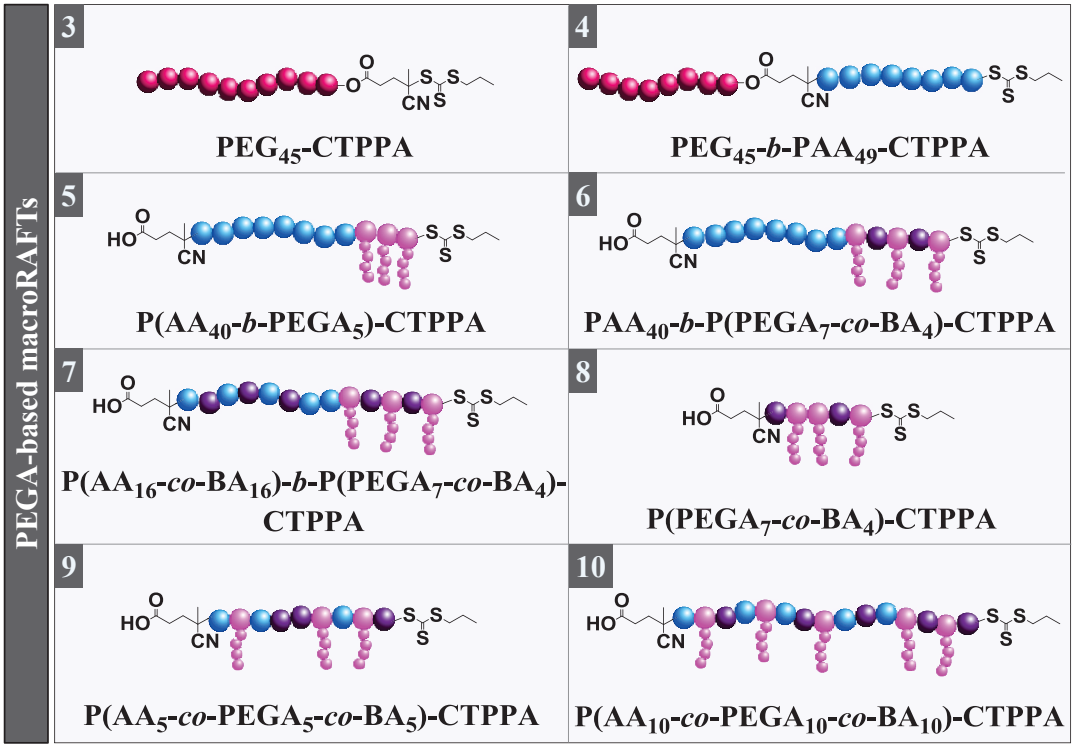
Source: elaborated by the author.

Figure 1.3 – Schematic representation of AA-based macroRAFT agents synthesized in this work: PAA_{42}-CTPPA (MR1) and P(AA_{16}-*co*-BA_{16})-CTPPA (MR2).



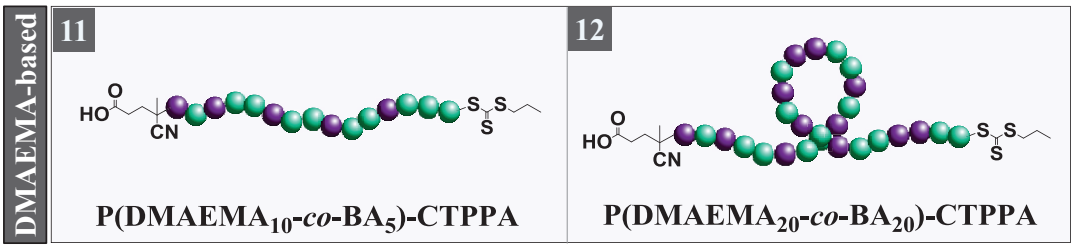
Source: elaborated by the author.

Figure 1.4 – Schematic representation of PEGA-based macroRAFT agents synthesized in this work: PEG_{45}-CTPPA (MR3); PEG_{45}-*b*-PAA_{49}-CTPPA (MR4); P(AA_{40}-*b*-$PEGA_5$)-CTPPA (MR5); PAA_{40}-*b*-P($PEGA_7$-*co*-BA_4)-CTPPA (MR6); P(AA_{16}-*co*-BA_{16})-*b*-P($PEGA_7$-*co*-BA_4)-CTPPA (MR7); P($PEGA_7$-*co*-BA_4)-CTPPA (MR8); P(AA_5-*co*-$PEGA_5$-*co*-BA_5)-CTPPA (MR9) and P(AA_{10}-*co*-$PEGA_{10}$-*co*-BA_{10})-CTPPA (MR10).



Source: elaborated by the author.

Figure 1.5 – Schematic representation of DMAEMA-based macroRAFT agents synthesized in this work: P(DMAEMA$_{10}$-*co*-BA$_5$)-CTPPA (MR11) and P(DMAEMA$_{20}$-*co*-BA$_{20}$)-CTPPA (MR12).



Source: elaborated by the author.

2) **Colloidal suspensions of macroRAFT-inorganic particles:** The second step of the strategy aimed the preparation of aqueous colloidal suspensions of the clay particles with the different macroRAFT agents synthesized in the previous step. For this purpose, the colloidal dispersions of the inorganic particles were introduced into the preformed water-soluble RAFT copolymers, for the adsorption of macroRAFT agents onto the negatively charged Laponite layers. Special attention was paid to the stability of the colloidal dispersions and, in this aspect, the entire exfoliation of the platelets is highly desirable. Particular attention was additionally paid to the suspension pH, which was carefully adjusted. The interactions between the macroRAFT agents and the inorganic particles were evaluated by measurement of adsorption isotherms and fitted to the Langmuir and Freundlich models, giving important insights into the adsorption capacity and the affinity of the different structures for Laponite surface.
3) **Polymer-encapsulation of Laponite particles by RAFT-mediated emulsion polymerization:** In this task, the macroRAFT-modified Laponite platelets prepared previously were used as seeds in waterborne emulsion polymerization. For this purpose, a careful selection of the experimental conditions was required. The formation of secondary nucleated particles is highly undesirable, since the presence of pure polymer latex particles may affect the successful ordering and organization of the anisotropic particles inside the film. No additional free surfactant was used due to the ability of the AA and DMAEMA units (combined or not with PEG segments) to efficiently stabilize the core-shell particles. Indeed, the presence of free macroRAFT agents in the aqueous phase is also required to maintain colloidal stability, since they are suspected to adsorb from the water phase on the growing particles and confer them extra stability. To ensure an efficient control of chain extension while maintaining a good colloidal stability of the polymer-coated inorganic particles, the monomer mixtures were fed into the reactor at a sufficiently low monomer addition rate, to ensure rapid monomer consumption and avoid

the formation of monomer droplets. Indeed, the presence of monomer droplets might disturb the system. Inorganic particles can potentially adsorb on them and, in addition, monomer droplets can cause macroRAFT partitioning by competing with the inorganic particle for the amphipathic copolymer adsorption, thus affecting the colloidal stability of the macroRAFT-Laponite suspension. So, to ensure immediate consumption of the monomers, the RAFT-mediated polymerizations were conducted preferentially under starve-feed conditions. The morphology of the final latex particles was accessed by transmission electronic microscopy at cryogenic temperature (cryo-TEM). The most promising composite latexes were adapted to film-forming formulations, to afford copolymers with low glass transition temperature (T_g) that can film-form at room temperature. Films were prepared by casting and characterized in order to understand the relationship between synthetic parameters and the 3D microstructure of the films obtained. The mechanical properties of the composite films were, then, studied by dynamic mechanical analysis (DMA) and the results obtained were compared with blanks (latex films without fillers).

This manuscript is divided into four more chapters.

In **Chapter 2**, a quick overview of some topics that are directly connected to the synthesis of nanocomposites by macroRAFT-assisted encapsulating emulsion polymerization (REEP) of inorganic particles is presented. The basis and the main aspects of the techniques that led to the development of the REEP (such as the free radical polymerization and the reversible deactivation radical polymerization techniques, the emulsion polymerization process and the polymerization-induced self-assembly approach) are presented in order to give a better understanding of the strategy used in this work.

Chapter 3 is dedicated to the functionalization of Laponite platelets with all RAFT (co)polymers synthesized. Prior to the results section, a bibliographic review on the subject is given. This review section concerns a detailed description of Laponite crystal structure and surface chemistry, as well as some topics related to the surface modification of Laponite with polyelectrolytes and PEG. In the following section, preceding the adsorption study part, the results obtained in the synthesis of the macroRAFT agents is briefly described. Finally,

the results obtained in the adsorption study (adsorption isotherms and the fitting of these isotherms to Langmuir and Freundlich models) are shown and discussed.

Chapter 4 focuses on the synthesis of polymer/Laponite hybrids by the REEP strategy, using different RAFT copolymers. First, a bibliographic review on clay/polymer nanocomposites and REEP strategy to encapsulate platelet-like materials is given. Then, the results obtained in the emulsion polymerization of MMA (or MA) and BA, carried out in the presence of the Laponite platelets modified with the chain transfer agents (CTA) to generate nanocomposite latex particles, are described. Various parameters were explored in the RAFT-mediated emulsion polymerization in the presence of Laponite particles. The main parameter studied was the nature of the macroRAFT agent, and molecules with different compositions, hydrophilic-lipophilic balance and the chain length were evaluated in the synthesis of the hybrid latexes. Some other important parameters that were studied in this work include the RAFT copolymer concentration, pH, type and concentration of initiator and temperature. Finally, the film-forming experiments are described, as well as the mechanical characterization of the nanocomposite films.

In **Chapter 5**, some conclusions and perspectives for future works are drawn.

References

1 ALEXANDRE, M.; DUBOIS, P. Polymer-layered silicate nanocomposites: Preparation, properties and uses of a new class of materials. **Materials Science & Engineering R-Reports,** v. 28, n. 1-2, p. 1-63, jun. 2000.

2 RAY, S. S.; OKAMOTO, M. Polymer/layered silicate nanocomposites: A review from preparation to processing. **Progress in Polymer Science,** v. 28, n. 11, p. 1539-1641, nov. 2003.

3 OKAMOTO, M. Recent advances in polymer/layered silicate nanocomposites: An overview from science to technology. **Materials Science and Technology,** v. 22, n. 7, p. 756-779, july 2006.

4 PAVLIDOU, S.; PAPASPYRIDES, C. D. A review on polymer-layered silicate nanocomposites. **Progress in Polymer Science,** v. 33, n. 12, p. 1119-1198, dec. 2008.

[5] RAY, S. S. Recent trends and future outlooks in the field of clay-containing polymer nanocomposites. **Macromolecular Chemistry and Physics,** v. 215, n. 12, p. 1162-1179, june 2014.

[6] MITTAL, V. Polymer layered silicate nanocomposites: A review. **Materials,** v. 2, n. 3, p. 992-1057, sept. 2009.

[7] BOURGEAT-LAMI, E. Organic-inorganic nanostructured colloids. **Journal of Nanoscience and Nanotechnology,** v. 2, n. 1, p. 1-24, feb. 2002.

[8] BALMER, J. A.; SCHMID, A.; ARMES, S. P. Colloidal nanocomposite particles: Quo vadis? **Journal of Materials Chemistry,** v. 18, n. 47, p. 5722-5730, dec. 2008.

[9] BOURGEAT-LAMI, E.; LANSALOT, M. Organic/inorganic composite latexes: The marriage of emulsion polymerization and inorganic chemistry. **Advances in Polymer Science,** v. 233, p. 53-123, may 2010.

[10] NEGRETE-HERRERA, N.; PUTAUX, J.-L.; DAVID, L.; DE HAAS, F.; BOURGEAT-LAMI, E. Polymer/Laponite composite latexes: Particle morphology, film microstructure, and properties. **Macromolecular Rapid Communications,** v. 28, n. 15, p. 1567-1573, aug. 2007.

[11] ESTEVES, A. C.; NEVES, M. C.; BARROS-TIMMONS, A.; BOURGEAT-LAMI, E.; LIZ-MARZAN, L.; TRINDADE, T. Synthesis of SiO_2-coated Bi_2S_3/poly(styrene) nanocomposites by in-situ polymerization. **Journal of Nanoscience and Nanotechnology,** v. 6, n. 2, p. 414-420, feb. 2006.

[12] NGUYEN, D.; ZONDANOS, H. S.; FARRUGIA, J. M.; SERELIS, A. K.; SUCH, C. H.; HAWKETT, B. S. Pigment encapsulation by emulsion polymerization using macro-RAFT copolymers. **Langmuir,** v. 24, n. 5, p. 2140-2150, 2008.

[13] DAIGLE, J.-C.; CLAVERIE, J. P. A simple method for forming hybrid core-shell nanoparticles suspended in water. **Journal of Nanomaterials,** v. 2008, p. 1-8, 2008.

[14] QIAO, X. G.; DUGAS, P. Y.; CHARLEUX, B.; LANSALOT, M.; BOURGEAT-LAMI, E. Synthesis of multipod-like silica/polymer latex particles via nitroxide-mediated polymerization-induced self-assembly of amphiphilic block copolymers. **Macromolecules,** v. 48, n. 3, p. 545-556, 2015.

[15] LOIKO, O. P.; SPOELSTRA, A. B.; VAN HERK, A. M.; MEULDIJK, J.; HEUTS, J. P. A. An ATRP-based approach towards water-borne anisotropic polymer-gibbsite nanocomposites. **Polymer Chemistry**, 2016.

[16] BARNER-KOWOLLIK, C. Introduction. In: _____ (Ed.). **Handbook of RAFT polymerization**: Wiley-VCH Verlag GmbH & Co. KGaA, 2008. p.1-4.

[17] CENACCHI-PEREIRA, A. M. **Synthesis of anisotropic polymer/inorganic composite particles via RAFT-mediated emulsion polymerization**. 2014. 286 (Ph.D.). École doctorale de chimie, University of Lyon, Lyon.

[18] PAVLOVIC, M.; ADOK-SIPICZKI, M.; NARDIN, C.; PEARSON, S.; BOURGEAT-LAMI, E.; PREVOT, V.; SZILAGYI, I. Effect of macroRAFT copolymer adsorption on the colloidal stability of layered double hydroxide nanoparticles. **Langmuir,** v. 31, n. 46, p. 12609-12617, nov. 2015.

[19] ZETTERLUND, P. B.; THICKETT, S. C.; PERRIER, S.; BOURGEAT-LAMI, E.; LANSALOT, M. Controlled/living radical polymerization in dispersed systems: An update. **Chemical Reviews,** v. 115, p. 9745−9800, 2015.

[20] BOURGEAT-LAMI, E.; D'AGOSTO, F.; LANSALOT, M. Synthesis of nanocapsules and polymer/inorganic nanoparticles through controlled radical polymerization at and near interfaces in heterogeneous media. In: VANA, P. (Ed.). **Controlled radical polymerization at and from solid surfaces**. Heidelberg: Springer International Publishing, 2016.v.270, p.123-161. (Advances in polymer science).

[21] DAS, P.; ZHONG, W.; CLAVERIE, J. P. Copolymer nanosphere encapsulated CdS quantum dots prepared by RAFT copolymerization: Synthesis, characterization and mechanism of formation. **Colloid and Polymer Science,** v. 289, n. 14, p. 1519-1533, sept. 2011.

[22] DAS, P.; CLAVERIE, J. P. Synthesis of single-core and multiple-core core-shell nanoparticles by RAFT emulsion polymerization: Lead sulfide-copolymer nanocomposites. **Journal of Polymer Science Part A: Polymer Chemistry,** v. 50, n. 14, p. 2802-2808, jul. 2012.

[23] ZGHEIB, N.; PUTAUX, J.-L.; THILL, A.; BOURGEAT-LAMI, E.; D'AGOSTO, F.; LANSALOT, M. Cerium oxide encapsulation by emulsion polymerization using hydrophilic macroRAFT agents. **Polymer Chemistry,** v. 4, n. 3, p. 607-614, 2013.

[24] GARNIER, J.; WARNANT, J.; LACROIX-DESMAZES, P.; DUFILS, P. E.; VINAS, J.; VANDERVEKEN, Y.; VAN HERK, A. M. An emulsifier-free RAFT-mediated process for the efficient synthesis of cerium oxide/polymer hybrid latexes. **Macromolecular Rapid Communications,** v. 33, n. 16, p. 1388-1392, aug. 2012.

[25] GARNIER, J.; WARNANT, J.; LACROIX-DESMAZES, P.; DUFILS, P.-E.; VINAS, J.; VAN HERK, A. Sulfonated macro-RAFT agents for the surfactant-free synthesis of cerium oxide-based hybrid latexes. **Journal of Colloid and Interface Science,** v. 407, p. 273-281, oct. 2013.

[26] WARNANT, J.; GARNIER, J.; VAN HERK, A.; DUFILS, P.-E.; VINAS, J.; LACROIX-DESMAZES, P. A CeO_2/pvdc hybrid latex mediated by a phosphonated macro-RAFT agent. **Polymer Chemistry,** v. 4, n. 23, p. 5656-5663, dec. 2013.

[27] NGUYEN, D.; SUCH, C. H.; HAWKETT, B. S. Polymer coating of carboxylic acid functionalized multiwalled carbon nanotubes via reversible addition-fragmentation chain transfer mediated emulsion polymerization. **Journal of Polymer Science Part A: Polymer Chemistry,** v. 51, n. 2, p. 250-257, jan. 2013.

[28] ZHONG, W.; ZEUNA, J. N.; CLAVERIE, J. P. A versatile encapsulation method of noncovalently modified carbon nanotubes by RAFT polymerization. **Journal of Polymer Science Part A: Polymer Chemistry,** v. 50, n. 21, p. 4403-4407, 2012.

[29] ALI, S. I.; HEUTS, J. P. A.; HAWKETT, B. S.; VAN HERK, A. M. Polymer encapsulated gibbsite nanoparticles: Efficient preparation of anisotropic composite latex particles by RAFT-based starved feed emulsion polymerization. **Langmuir,** v. 25, n. 18, p. 10523-10533, sept. 2009.

[30] MBALLA MBALLA, M. A.; ALI, S. I.; HEUTS, J. P. A.; VAN HERK, A. M. Control of the anisotropic morphology of latex nanocomposites containing single montmorillonite clay particles prepared by conventional and reversible addition-fragmentation chain transfer based emulsion polymerization. **Polymer International,** v. 61, n. 6, p. 861-865, 2012.

[31] HUYNH, V. T.; NGUYEN, D.; SUCH, C. H.; HAWKETT, B. S. Polymer coating of graphene oxide via reversible addition-fragmentation chain transfer mediated emulsion polymerization. **Journal of Polymer Science Part A: Polymer Chemistry,** v. 53, n. 12, p. 1413-1421, june 2015.

[32] CAUVIN, S.; COLVER, P. J.; BON, S. A. F. Pickering stabilized miniemulsion polymerization: Preparation of clay armored latexes. **Macromolecules,** v. 38, n. 19, p. 7887-7889, sept. 2005.

[33] PUTLITZ, B. Z.; LANDFESTER, K.; FISCHER, H.; ANTONIETTI, M. The generation of "armored latexes" and hollow inorganic shells made of clay sheets by templating cationic miniemulsions and latexes. **Advanced Materials,** v. 13, n. 7, p. 500-503, apr. 2001.

[34] WANG, T.; COLVER, P. J.; BON, S. A. F.; KEDDIE, J. L. Soft polymer and nano-clay supracolloidal particles in adhesives: Synergistic effects on mechanical properties. **Soft Matter,** v. 5, n. 20, p. 3842-3849, 2009.

[35] FERGUSON, C. J.; HUGHES, R. J.; PHAM, B. T. T.; HAWKETT, B. S.; GILBERT, R. G.; SERELIS, A. K.; SUCH, C. H. Effective ab initio emulsion polymerization under RAFT control. **Macromolecules,** v. 35, n. 25, p. 9243-9245, dec. 2002.

[36] FERGUSON, C. J.; HUGHES, R. J.; NGUYEN, D.; PHAM, B. T. T.; GILBERT, R. G.; SERELIS, A. K.; SUCH, C. H.; HAWKETT, B. S. Ab initio emulsion polymerization by RAFT-controlled self-assembly. **Macromolecules,** v. 38, n. 6, p. 2191-2204, mar. 2005.

[37] GANEVA, D. E.; SPRONG, E.; DE BRUYN, H.; WARR, G. G.; SUCH, C. H.; HAWKETT, B. S. Particle formation in ab initio RAFT mediated emulsion polymerization systems. **Macromolecules,** v. 40, n. 17, p. 6181-6189, aug. 2007.

[38] RIEGER, J.; STOFFELBACH, F.; BUI, C.; ALAIMO, D.; JEROME, C.; CHARLEUX, B. Amphiphilic poly(ethylene oxide) macromolecular RAFT agent as

a stabilizer and control agent in ab initio batch emulsion polymerization. **Macromolecules,** v. 41, n. 12, p. 4065-406, may 2008.

39 RIEGER, J.; OSTERWINTER, G.; BUI, C.; STOFFELBACH, F.; CHARLEUX, B. Surfactant-free controlled/living radical emulsion (co)polymerization of n-butyl acrylate and methyl methacrylate via RAFT using amphiphilic poly(ethylene oxide)-based trithiocarbonate chain transfer agents. **Macromolecules,** v. 42, n. 15, p. 5518-5525, 2009.

40 MOAD, G.; RIZZARDO, E.; THANG, S. H. Radical addition-fragmentation chemistry in polymer synthesis. **Polymer,** v. 49, n. 5, p. 1079-1131, mar. 2008.

2 Bibliographic review on reversible deactivation radical polymerization (RDRP) and macroRAFT-assisted encapsulating emulsion polymerization (REEP)

2.1 Introduction

Organic/inorganic nanocomposites[1-3] are an important type of material that find diverse applications, including in the coating and pharmaceutical fields, for instance. The incorporation of inorganic nanoparticles into polymeric matrixes brings significant improvements to the final properties of nanocomposite materials, as compared to the corresponding pure polymers. When the polymeric matrix and the inorganic part interact with good affinity, the fillers are homogeneously distributed in the matrix, and the mechanical properties of the final material are enhanced. However, these components do not, typically, present good affinity with each other, so special attention must be paid to this matter. One of the most currently used strategies to improve the affinity between the organic and inorganic parts is the modification of the inorganic particle with organic molecules, such as polymers. For this purpose, the use of reversible deactivation radical polymerization has been extremely attractive, allowing the synthesis of hybrid particles with controlled morphologies. Many publications have been dedicated to the synthesis of these materials through the grafting-from[4-6] and the grafting-to[7, 8] techniques (further discussed in Chapter 4) in solution. However, the adaptation of these methods to miniemulsion [9-14] and, more specifically, to emulsion systems, allowed by the development of the polymerization-induced self-assembly (PISA) technique, has opened new horizons for the synthesis of nanocomposites.[15]

The synthesis of organic/inorganic nanocomposites by RDRP in emulsion relies on the use of hydrophilic living copolymers that work as coupling agents and stabilizers. Although it can be applied to nitroxide-mediated polymerization (NMP), leading to a surface-initiated polymerization, little work has been done in this field[16] and the attention has been dedicated, almost exclusively, to the use of reversible addition-fragmentation chain transfer (RAFT) polymerization. In this strategy, recently called macroRAFT-assisted encapsulating emulsion polymerization (REEP),[17] amphiphilic macroRAFT agents are used to promote the interaction between the inorganic surface and the growing hydrophobic polymeric block, which will later form the encapsulating shell around the inorganic particle.

For this reason, hydrosoluble control agents are initially adsorbed onto the inorganic particles, and then submitted to a chain extension with hydrophobic monomers, in aqueous media, generating amphipathic block copolymers either directly on the surface of the particle or in the aqueous phase, where they suffer a self-assembly process.

In this chapter, a quick overview of some topics that are directly connected to the synthesis of nanocomposites by macroRAFT-assisted encapsulating emulsion polymerization of inorganic particles is presented. The basis and the main aspects of the techniques that led to the development of the RAFT-encapsulating emulsion polymerization (such as the free radical polymerization and the reversible deactivation radical polymerization techniques, the emulsion polymerization process and the polymerization-induced self-assembly approach) are presented in order to give a better understanding of the strategy used in this work.

2.2 Free radical polymerization

Free radical polymerization has been raised as an alternative to ionic polymerization in large-scale processes, due to its ability to overcome some of the limitations of the ionic process, such as the restriction to water-borne systems (limited choice of solvents) and the intolerance to functionality and impurities. It is now one of the most versatile polymerization techniques available, and is widely applied industrially. The industrial success of free radical polymerization can be attributed, among other factors, to the compatibility of this method with a variety of functional monomers and water. Free-radical polymerization consists in a chain-growth mechanism, and proceeds basically through four types of reactions involving free radicals:

1) Initiation: radicals are generated from nonradical species;
2) Propagation: radicals are added to a substituted alkene to increase the chain length of the growing polymer;
3) Chain transfer and termination by disproportionation: polymer chains are terminated by atom transfer and atom abstraction reactions;
4) Termination by combination/coupling: besides disproportionation, polymer chains can be terminated by radical-radical recombination.

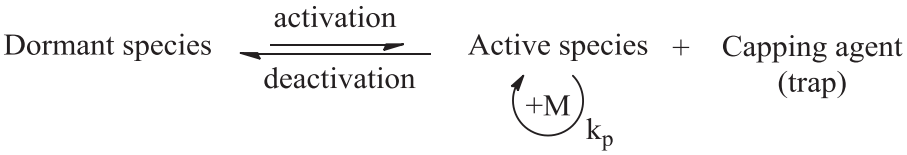
In the pursuit of improved materials with innovative architectures and interesting commercial applications, new mechanisms have been developed from the free radical

polymerization. The use of control agents to control molar mass and end-group functionality of polymers was first reported in the 1980s. However, it was only in the 1990s that these techniques, called reversible deactivation radical polymerization (RDRP), suffered a major growth. NMP, atom transfer radical polymerization (ATRP) and RAFT approaches have emerged as successful routes to produce polymer chains with controlled molar mass, narrow dispersity and specific architectures, from complex stars, combs, brushes, and dendritic structures, to block and gradient copolymers.[18]

2.3 Reversible deactivation radical polymerization (RDRP)

The principle of reversible deactivation radical polymerization methods is to establish a dynamic equilibrium between the growing free radicals and dormant species.[19] The mechanisms involved in the propagation and termination of free radicals are similar to the conventional radical polymerization, however, only a small fraction of radicals and a major amount of dormant species are present in RDRP. For this reason, propagating species in RDRP are forced to stay inert to premature termination and transfer reactions, in order to ensure a good control over polymer composition, architecture and functionality and to guarantee that polymer chains with homogeneous molar mass are obtained (**Scheme 2.1**).

Scheme 2.1 – Dynamic equilibrium involved in the reversible activation/deactivation process in RDRP mechanisms.



Source: elaborated by the author.

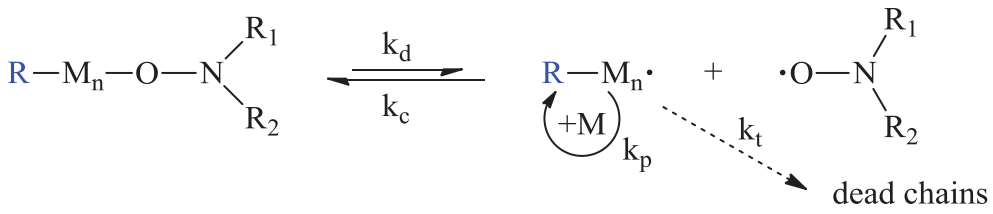
The three most well-established RDRP techniques are NMP,[20] ATRP[21] and RAFT,[22] which have been extensively explored and investigated in the literature.

2.3.1 Nitroxide-mediated polymerization (NMP)

The nitroxide-mediated polymerization (NMP) was the first RDRP technique to be described in 1993, by Georges et al.[23] In this technique, a (macro)alkoxyamine, which is considered the dormant species, is thermally or photochemically dissociated into an

active/propagating and a stable (persistent) radical, as shown in Scheme 2.2. A reversible termination reaction between the stable free radical nitroxide and the growing active (macro)radical forms, again, the (macro)alkoxyamine. This dormant molecule is also the predominant species, so the propagating radical concentration is limited to levels that guarantee a controlled character to the polymerization. There are two possible pathways for NMP. In the first one, the alkoxyamine is formed *in situ* by the addition of two components that will generate both radicals (for this reason it is referred to as bicomponent): a conventional radical initiator and a free nitroxide. In opposition, the second pathway relies on the initial use of a preformed alkoxyamine (which gave it the title of monocomponent initiating system). The bicomponent pathway was the original mechanism of the first NMP works, however it has some disadvantages related to kinetics and control that led to the development of the monocomponent systems.

Scheme 2.2 – NMP activation/deactivation equilibrium.



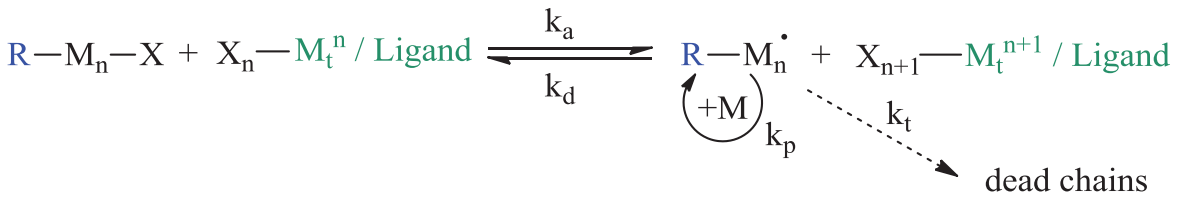
with k_d = dissociation rate constant and k_c = recombination rate constant.
Source: elaborated by the author.

The use of NMP, as well as most of RDRP techniques, in aqueous polymerization is challenging.[24, 25] To avoid the loss of the "living" character and to guarantee the colloidal stability of the resulting latexes, special attention must be paid to the solubility of radical mediators in the water phase, and their partitioning in organic and aqueous phases. The employment of NMP in emulsion polymerization has been successful through the use of some techniques that prevent monomer droplet nucleation and ensure a sufficiently high nitroxide concentration in the particles, such as the self-assembly or the seeded emulsion polymerization techniques. Since 2008, however, less works have been dedicated to emulsion NMP, in comparison to other RDRP techniques.[26]

2.3.2 Atom transfer radical polymerization (ATRP)

ATRP was developed in 1994 simultaneously by the groups of Sawamoto[27] and Matyjaszweski[28] and, similarly to NMP, it is based on a reversible termination reaction. In this technique, an alkyl halide is activated by a transition metal complex catalyst to form a radical that can initiate polymerization. The addition of monomers to this radical generates a growing polymeric radical, which is also called the active species ($R–M_n^{\bullet}$). This active propagating radical, when reacted with the transition metal halide formed in the previous step ($X_{n+1}–M_t^{n+1}$/Ligand), is deactivated and generates the dormant species ($R–M_n–X$). The C–X bond of this dormant species (where X is a halogen atom of Cl or Br) is, again, homolitically cleaved by a reversible redox reaction catalyzed by the transition metal complex, and the catalyst oxidizes again by the transfer of the halogen atom from the dormant species. Through these activation/deactivation cycles, an equilibrium is established between dormant and active species and the growth of polymer chains happen at a similar rate, so termination is almost null in the process. Similar to NMP, the equilibrium between dormant and active species heavily favors the dormant state. ATRP mechanism is schematically represented in Scheme 2.3.

Scheme 2.3 – ATRP activation/deactivation equilibrium.



k_a = activation rate constant and k_d = deactivation rate constant.
Source: elaborated by the author.

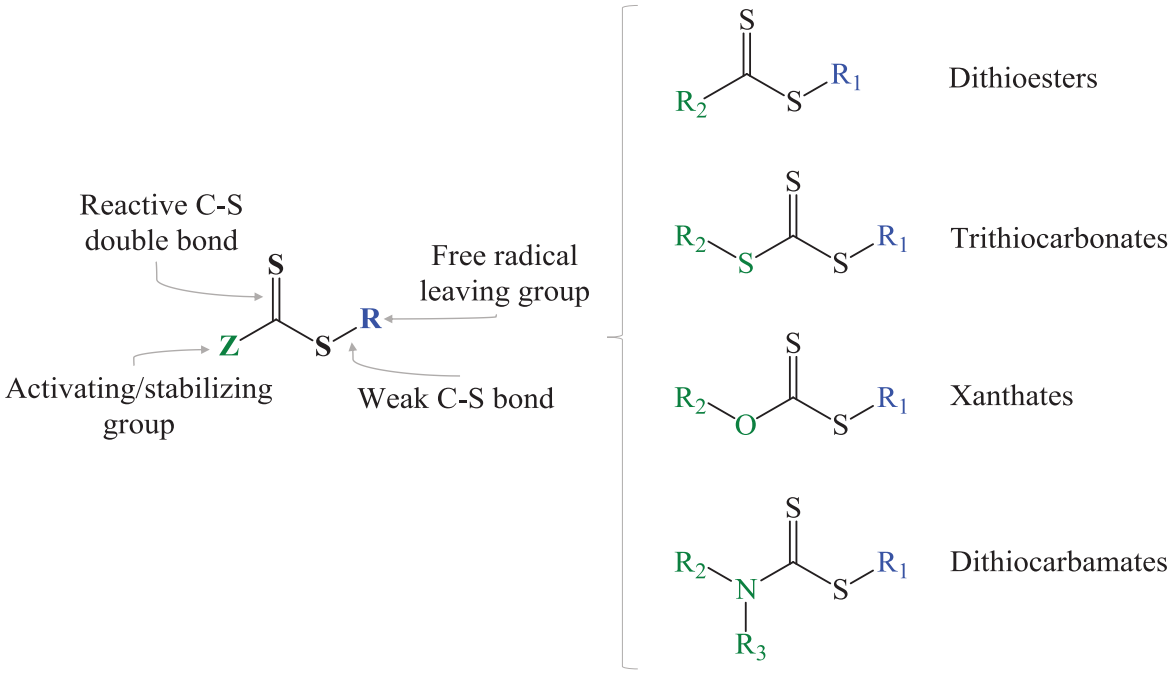
A variety of polymers can be prepared by ATRP technique, however, the extension of this process to water-borne systems, such as emulsion polymerization, is not so trivial.[29] A careful selection of components (monomer, catalyst, growing and dormant species) must be done in order to obtain a successful polymerization[30] In the last decade, some works have described the use of direct and reverse ATRP in *ab initio* emulsion polymerization, using either conventional or activator generated by electron transfer (AGET) ATRP.[26] AGET ATRP combines all the benefits of conventional ATRP process with the additional benefit of requiring significantly smaller amounts of the high-oxidation-state catalyst. By the addition of a reducing agent that is capable of reacting with the oxidatively stable Cu^{II}

complex, it is possible to generate the transition metal complex when it is in its lower oxidation state. In fact, AGET ATRP has many other advantages that circumvent some of the limitations of the conventional ATRP process, including reduced sensitivity to oxygen and humidity.[31]

2.3.3 Reversible addition-fragmentation chain transfer (RAFT)

RAFT is a relatively new RDRP technique. It was only in the 1990s that addition-fragmentation chain transfer agents were used to provide a living character to radical polymerization. It was first described by two groups, that used different chain transfer agents (CTA): the group of Rizzardo[32] and the French group of Bouhadir,[33] that named it MADIX, for Macromolecular Design via the Interchange of Xanthates. In the RAFT mechanism, the conventional free radical polymerization of a substituted monomer takes place in the presence of a suitable CTA. The CTA, also referred to as RAFT agent, is typically composed of thiocarbonylthio species that possess a thiocarbonylthio group (S=C-S) with substituents R and Z, as shown in Figure 2.1. Depending on the Z group, a wide range of CTAs can be employed including, among others, dithioesters, trithiocarbonates, xanthates and dithiocarbamates.[32; 34, 35]

Figure 2.1 – Different types of RAFT agents: dithioesters, trithiocarbonates, xanthates and dithiocarbamates.



Source: elaborated by the author.

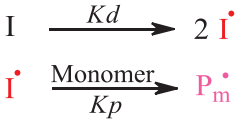
Unlike the other controlled radical polymerization techniques such as ATRP and NMP, RAFT is based on the principle of reversible chain transfer. In RAFT, primary radicals are formed by the decomposition of a free radical initiator, as shown in Scheme 2.4. In the second step (reversible chain transfer, also referred to as pre-equilibrium), an intermediate radical is formed by the addition of the primary radical to the thiocarbonylthio group of the chain transfer agent, due to its weak covalent bond. This intermediate radical can fragment on the opposite side, generating a polymeric RAFT agent, which is temporary deactivated, and a new active radical. This radical is able to reinitiate the polymerization and form new radicals that propagate by adding monomer units until they enter the dormant state again by encountering a CTA molecule. In this addition-fragmentation equilibrium between the propagating radicals and the main intermediate radical, the RAFT main equilibrium occurs and continuously generates the active and dormant species. Irreversible termination can happen at any point, by combination or disproportionation. However, to minimize the amount of active radicals and decrease termination, RAFT polymerizations are usually performed using high [RAFT]/[initiator] ratios.

Some disadvantages of the RAFT technique can be cited, such as the need of a multiple-step procedure for the synthesis of the RAFT agent, as well as the purification of the final product. Besides, RAFT agents can become unstable after a long period of time, may have strong colors and odor, due to the presence of sulfur, which may be undesirable for some applications, and may have some toxicity associated with the trithiocarbonate-termination, which is undesirable for biomedical applications.[36] With some extra chemical and physical purification steps, though, these drawbacks can be overcome.

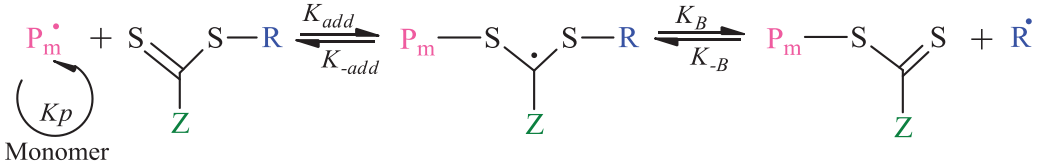
In spite of these minor drawbacks, RAFT has become one of the most important RDRP methods due to its numerous advantages. It is a highly versatile technique for the controlled synthesis of various polymer architectures, it can operate under moderate conditions, such as mild temperatures, and is less sensible to the presence of oxygen and other impurities, in comparison to conventional radical polymerization. RAFT is suitable for a broad variety of monomers and can be performed in a wide range of solvents, including water.[37] The direct employment of RAFT polymerization in aqueous dispersed media, however, cause some inconveniences, but they can be easily overcome if some specific measures are taken.[26, 38-41]

Scheme 2.4 – Mechanism of RAFT polymerization mediated by a thiocarbonylthio RAFT agent.

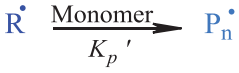
Initiation:



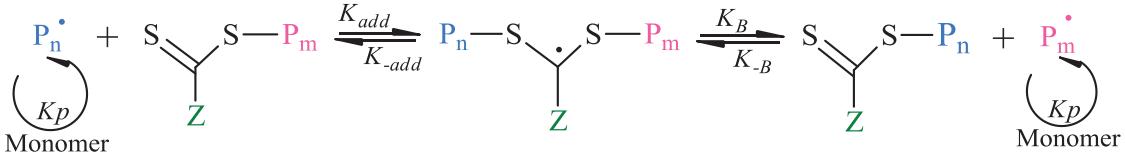
Reversible chain transfer/pre-equilibrium:



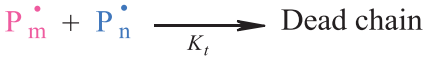
Re-initiation and propagation:



RAFT main equilibrium:



Termination:



K_{add} = addition rate constant
K_{-add} = fragmentation rate constant
Source: Adapted from ref. [22, 42].

2.3.3.1 RAFT in dispersed media

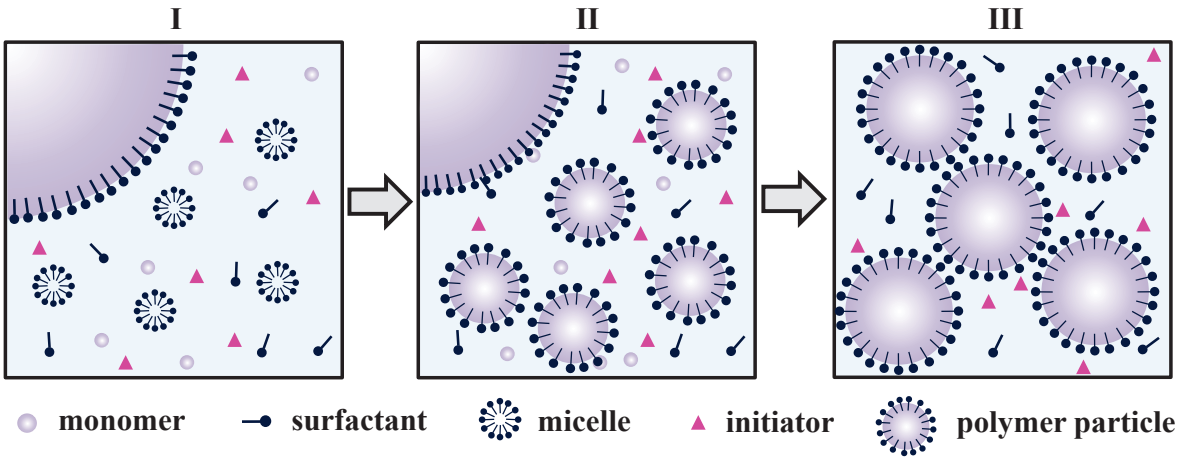
The main difficulty of using RAFT agents in aqueous dispersed media can be attributed to an inefficient diffusion of this molecule, which is usually hydrophobic, from the water phase to inside the micelles. This diffusion issue can cause control and stability problems and, to be avoided, miniemulsion or seeded polymerization[39] can be used, for instance. However, the many advantages of emulsion polymerization led to the development of new techniques that allow the association of both methods. To better explain these techniques, a quick overview of the emulsion process is given in the following section.

2.3.3.1.1 Emulsion polymerization

Emulsion polymerization is a free radical polymerization technique performed in heterogeneous media that has, as main components, monomer(s), water-soluble initiator and surfactant. It has many advantages over other free radical polymerization processes such as bulk, solution or suspension, that include the production of polymer chains with high molar mass at relatively high reaction rates, the obtainment of high solids contents with moderate viscosity increase, good heat transfer control, tolerance to a wide range of monomers and the environmental advantage of avoiding volatile organic solvents by having water as the most common continuous phase. Emulsion polymerization has been widely employed industrially to manufacture different products, such as coatings, paints and adhesives.[43]

Three regimes, or intervals, can be identified in emulsion polymerization, as illustrated in Figure 2.2.

Figure 2.2 – Schematic representation of the emulsion polymerization intervals.



Source: elaborated by the author.

The first interval (Interval I) corresponds to the beginning of polymerization, in which particle nucleation takes place. In this interval, the system initially consists of an oil-in-water dispersion of monomer droplets in an aqueous solution containing the surfactant. Surfactants are composed of a non-polar tail that contains in one of its extremities a polar head. Above a certain concentration (known as Critical Micelle Concentration, CMC), these molecules assemble to minimize their surface energy, by forming micelles with the hydrophilic heads outside protecting the hydrophobic core. Monomers are either reserved inside big monomer droplets, confined in the interior of the micelles or soluble in the water phase, in small amounts. Initiation starts in the aqueous phase by the decomposition of the

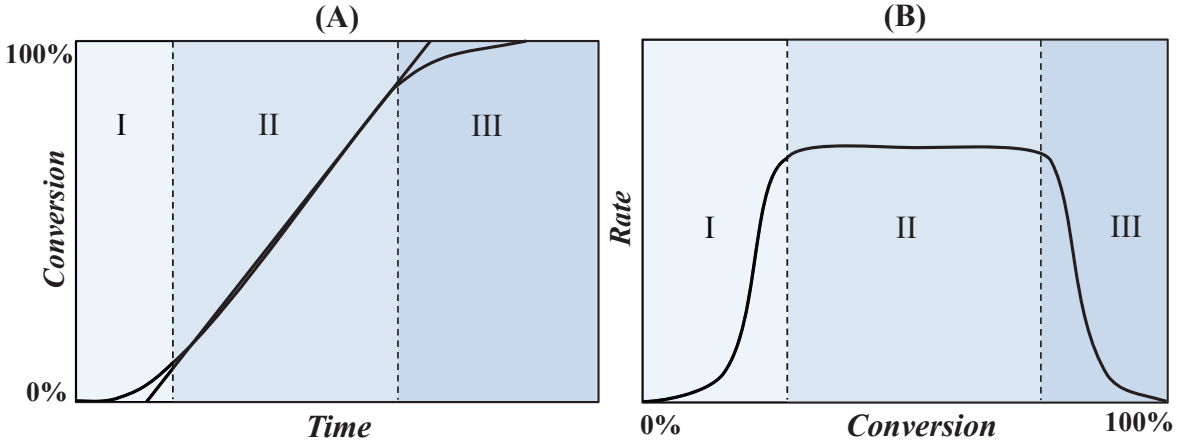
water-soluble free radical initiator to form radicals. The reaction of these radicals with the monomer that is soluble in the aqueous phase generates oligoradicals. These propagating radicals grow in the water phase by the addition of a few monomer units until their length compromises their solubility in water. At this point, they become sufficiently hydrophobic to either migrate to inside the micelles (in a micellar nucleation process), or precipitate (homogeneous or coagulative nucleation). The micelles become, then, the main polymerization loci, allowing polymerization to proceed inside these new small particles.

In the second interval (Interval II), the particles that were nucleated in the previous step grow by the consumption of the monomer present in the swollen particles. These particles are constantly fed with the monomer present in the monomer droplets that diffuses through the water phase. During this interval, the number of particles and the polymerization rate stay constant. Particles grow in size, while the monomer droplets decrease until their total disappearance. At this point, after the total consumption of monomer droplets, the last interval starts.

The last interval (Interval III) is known as the end of polymerization, and only the monomer that remains in the particles is polymerized. The final product of emulsion, the latex, is an aqueous dispersion of submicron solid polymer particles (with diameters of around 50 to 500 nm) that are stabilized by the surfactant molecules.

This division of the emulsion process in three different phases was proposed by Smith and Ewart.[44] The kinetic representation of the emulsion process and the different levels of conversion and polymerization rate for each interval are shown in Figure 2.3. It can be seen that the Phase I is a transitory and quick phase, in which conversion generally goes from 0 to 15%. In this phase, polymerization rate increases until the number of particles is defined. Then starts Phase II, in which the polymerization rate is constant, as well as the number of particles. The transition between phases II and III occurs at conversions of 80 to 90%, depending on the solubility of the monomer in the aqueous phase. Polymerization rate decreases progressively, since only the monomer from the particles is present in the system, and it is gradually disappearing.

Figure 2.3 – Typical kinetic profile of emulsion polymerization, showing the different levels of (A) conversion and (B) polymerization rate for each interval.



Source: adapted from ref. [43]

It is important to mention that the different mechanisms of nucleation can take place concomitantly during phase I of emulsion polymerization. The micellar nucleation is the predominant phenomenon, and is characterized by the migration of the radicals or oligoradicals to inside the micelles.[43, 45] For this reason, the emulsifier concentration must be above the CMC, in order to exist micelles in the medium. However, depending on the surfactant concentration, as well as the temperature and the nature of the monomer, other mechanisms of nucleation can occur. In the absence of micelles, or when the concentration of monomer in the aqueous phase is considerably high, the homogeneous nucleation may take place.[46] In this process of nucleation, oligoradicals precipitate when they reach the critical length (j_{crit}). The coagulative nucleation is considered an extension of the homogeneous process. It considers that two or more primary particles, formed by the coagulation of unstable oligoradicals, aggregate to form new and larger particles.[47]

The application of RAFT technique to emulsion polymerization can be successfully employed through two approaches. One of these approaches is similar to a conventional emulsion polymerization (with radical initiator and surfactant), but it has the presence of the RAFT agent as the main difference. The second strategy involves a self-assembly process, in which RAFT agents act simultaneously as control agents and surfactants.

2.3.3.1.2 Conventional RAFT emulsion polymerization

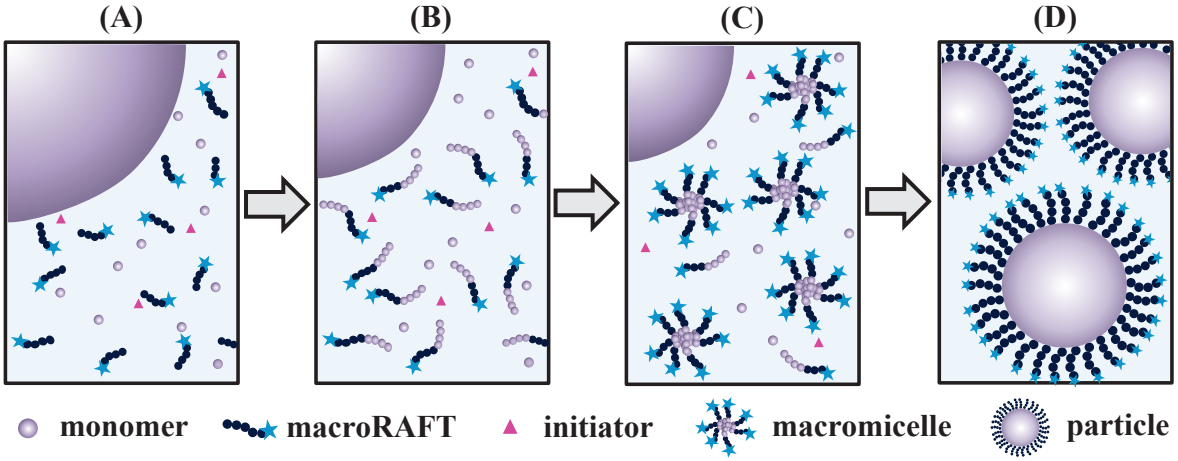
The first works describing *ab initio* emulsion polymerization under RAFT control[25, 26, 39, 41] were not successful and indicated the high complexity of this system. The association of the RAFT technique with the emulsion process was frequently described as uncontrolled

polymerizations that led to the formation of latexes with unsatisfactory colloidal stability. Indeed, the presence of RAFT agent in the medium can cause some issues, such as the phase separation and formation of a colored oil layer, loss of stability with the formation of aggregates and low molar mass control. These issues were later attributed to the partitioning of the RAFT agent, that cannot be properly transported between aqueous phase, monomer droplets and the polymerizing particles and to the superswelling effect of the polymer particles.[48-54] In 2002,[55] a new method has been described for the effective *ab initio* RAFT emulsion polymerization. In this novel strategy, hydrophilic RAFT agents that contain short stabilizing segments of hydrophilic monomers were used in the emulsion polymerization of hydrophobic monomers to form amphipathic species that self-assemble to form micelles. Since then, various works have described the use of polymerization-induced self-assembly (PISA) of amphipathic macroRAFT in emulsion polymerizations, and this technique is now the most used method for this purpose.[55-57]

2.3.3.1.3 Polymerization-induced self-assembly RAFT emulsion polymerization

The application of the RAFT technique to emulsion polymerization is an excellent strategy for the controlled production of polymers with well-defined structures, as well as latexes with special morphologies. Since the pioneer works of Ferguson et al.[55, 56] using the PISA concepts, which allowed the successful combination of all of the advantages of the RAFT process with the benefits of emulsion polymerization, many researches have been focused on this approach. The general mechanism of PISA RAFT emulsion polymerization is shown in Figure 2.4. Amphipathic RAFT agents are synthesized *in situ* by RAFT-mediated *ab initio* emulsion polymerization. The RAFT copolymers, or oligomers, act as steric or electrosteric surfactants, functionalizing the surface of the particles and controlling the particle growth. As a result, latex particles are stabilized by the hydrophilic segment of the macroRAFT agents, so there is no need for any additional conventional surfactant. This is an interesting advantage of this method, considering that low molar mass surfactants can suffer diffusion during film formation and deteriorate some film properties, such as permeability, whitening, or adhesion.[58-60]

Figure 2.4 – Schematic overview of the polymerization-induced self-assembly RAFT emulsion polymerization process (PISA). (A) Initial state; (B) chain extension; (C) self-assembly of block copolymers in macromicelles and (D) final state.



Source: elaborated by the author.

In Ferguson's work, the RAFT aqueous solution polymerization of a water-soluble monomer (AA), followed by the addition of a hydrophobic monomer (BA), to form AA-*b*-BA-RAFT oligomers was reported. In water, these oligomers were able to form micelles that, swollen by hydrophobic monomer (BA or styrene), yielded core-shell particles composed of block copolymers, with the hydrophobic block forming the core and the hydrophilic segment composing the shell of PAA. The hydrophobic monomer was continuously fed into the reactor, avoiding the formation of monomer droplets. However, some modifications of this PISA process have been proved to be successful as well.[61-70]

Manguian et al. performed the PISA process in batch.[61] The hydrophilic block synthesized by the authors was a polycation, the poly 2-(diethylamino)ethyl methacrylate chain transfer agent, synthesized by a dithiobenzoate-mediated solution polymerization. The chain extension with styrene was performed in emulsion polymerization, after purification of the precursor polymer. Stable latexes were obtained and the authors suggested that the nano-objects were formed by the self-assembly of macroRAFT block copolymers originated from the oligoradicals. The group also concluded that the pH of the medium had influence on the colloidal stability of the particles, since the stabilization role is attributed to the copolymer's hydrophilic block. In other pioneer works, Santos et al.[62] and Charleux, et al.[63] showed that poly(ethylene oxide)-based macroRAFT agents (PEO-RAFT) have a crucial role in the steric stabilization of particles formed by the PISA mechanism, as well as in the particle nucleation and, under some conditions, in controlling the molar mass of the chains. The PISA mechanism has also been explored as an efficient method for the morphological

control of latex particles, allowing the production of nonspherical objects. Depending on the hydrophilic/hydrophobic character of the block copolymer, different morphologies can be obtained, such as rods or fibers and vesicles.[26, 64, 65, 71]

Even though some works report the PISA method as a multiple-step process,[65] in which the initial hydrophilic block is usually synthesized by solution polymerization and needs to be purified before the chain extension step by emulsion polymerization to form the hydrophobic core of the latex particles, a growing number of works [66-68, 71] has described the one-pot synthesis of self-stabilized particles. In this strategy, the whole process is carried out in water, excluding the purification step. The hydrophilic block is synthesized by aqueous solution polymerization and, after complete monomer consumption, a new charge of monomer (a hydrophobic one, this time) and initiator is added to the reactor. This second synthesis proceeds according to the PISA RAFT emulsion mechanism. The one-pot synthesis has been proved to be an interesting strategy with many advantages over the conventional PISA process. It is a simple and efficient tool that avoids the employment of organic solvents.

The PISA process has been applied to other RDRP techniques.[69, 70] However, RAFT remains as the most studied method due to its versatility to a wide range of monomers and the lower (compared to NMP and ATRP) temperatures required for efficient polymerization.

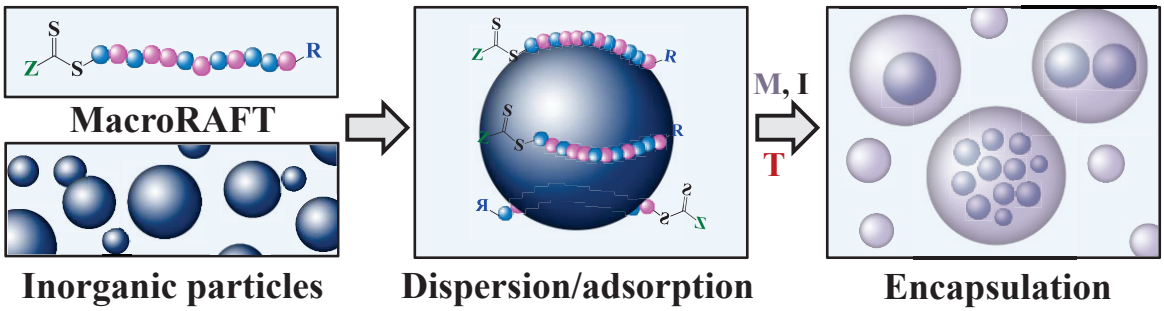
2.3.3.1.4 RAFT-encapsulating emulsion polymerization of inorganic particles

The many advances made in the field of RDRP-mediated emulsion polymerization have opened new directions for the synthesis of nanocomposites.[14, 15, 26] Different inorganic particles have been encapsulated using the combination of RDRP and miniemulsion polymerization.[9-13] In fact, encapsulation can be easily achieved by RDRP in miniemulsion if a preview step of organic modification of the inorganic surface is added to the process in order to improve the compatibility between inorganic particles and organic liquids (hydrophobic monomers, for instance), increasing the dispersability of the inorganics inside the monomer droplets.[26] However, the many advantages of the emulsion process make it more attractive for this purpose, since it is a less energy-consuming (it does not require a high shear device for emulsification) and can be considered a more versatile technique than miniemulsion, being widely employed in many industrial sectors. The development of the PISA approach has been an important step forward into the direction of RAFT-encapsulating emulsion polymerization of inorganic particles.

The methodology to encapsulate inorganic particles by RAFT-mediated emulsion polymerization was first described in 2008[72, 73] and relies on the use of amphipathic RAFT agents that adsorb onto the inorganic particles and induce the growth of the hydrophobic polymer layer from the inorganic surface, according to the PISA process, promoting encapsulation. In most works reported, authors generally use RAFT agents based on AA, monomer that interacts with the inorganic particles by electrostatic interaction and promotes the adsorption of the molecule containing the RAFT functionality onto the inorganic surface. The AA units (or other hydrophilic monomer) are also responsible for the formation of the hydrophilic segment that, later (after the chain extension process), stabilizes the hybrid particles. In addition, some works report that the macroRAFT structure also requires the presence of some BA units to increase the hydrophobicity of the macroRAFT/inorganic environment, improving the affinity between the particles and the growing hydrophobic shell. Besides, hydrophobic BA units may also be associated with increasing the driving force for adsorption since, in order to minimize their interaction with the aqueous medium, BA units tend to adsorb at the surface of the inorganic particles, in a process driven by hydrophobic interactions.[74, 75]

An overview of the REEP strategy is shown in Figure 2.5. After the synthesis of the macroRAFT agent by solution polymerization, the product is purified and dissolved in water under a convenient pH for the appropriate ionization of its ionizable groups (if necessary). Then, the inorganic particles are added into the macroRAFT agent solution. In this step, the interaction between the macroRAFT and the inorganic particles is promoted and it is crucial for the REEP strategy. A good adsorption of the macromolecule onto the surface of the particle, with a good coverage of the inorganic surface and minimum amount of free molecules in the aqueous phase, is essential for the success of the encapsulation process. It is fundamental, as well, that the macroRAFT works as an efficient stabilizer and, in order to guarantee the obtainment of a stable dispersion, some works describe the use of sonication to increase the dispersability of the macroRAFT/inorganic particles. In a second step, the emulsion polymerization of hydrophobic monomers is carried out in the presence of the inorganic particles containing the adsorbed macroRAFT. This complex works as a seed in the emulsion polymerization and the chain extension of the macroRAFT agent, which is adsorbed at the surface of the particles, guarantees that the hydrophobic polymer layer is formed from the inorganic surface, encapsulating the particles.

Figure 2.5 – Schematic representation showing the dispersion and encapsulation steps of the macroRAFT-assisted encapsulating emulsion polymerization of inorganic particles. M = monomers; I = water-soluble initiator and T = temperature.



M = monomers; I = water-soluble initiator and T = temperature.
Source: elaborated by the author.

In 2008, Nguyen et al.[72] reported the encapsulation of hydrophobic organic particulate materials (phthalocyanine blue pigment) and inorganic hydrophilic particles (alumina and zirconia-coated titanium dioxide), by RAFT-mediated emulsion polymerization. The authors synthesized amphipathic random copolymers composed of AA and BA by RAFT polymerization in solution of 1,4-dioxane and used these molecules as RAFT control agents to encapsulate the particulate materials. In the strategy proposed by the authors, the random copolymers have a crucial role in the encapsulation mechanism. The amphipathic molecules are not only capable of interacting with the organic and inorganic particles, but they can also successfully stabilize these particles and behave as a precursor for the chain extension reaction with hydrophobic monomers, to form the uniform polymer shell around the surface of the pigments, generating core-shell particles according to the PISA process. The use of water-soluble random copolymers can be cited as one of the key points of the work, since they avoided the formation of micelles in the water phase and they did not suffer chain extension in the aqueous phase, which avoided the nucleation of pure polymer particles and increased the encapsulation efficiency. In addition, the use of macroRAFT agents with low molar mass was described as another important factor because it maximized the number of molecules on the inorganic surface (facilitating the rapid transfer of polymer growth between polymer chains) and it guaranteed that final particles were composed of a short hydrophilic block (minimizing the water sensitivity of the polymer shell). Nonetheless, a part of the macroRAFT agents should remain free in the aqueous phase before polymerization in order to adsorb on the growing hybrid particles during the encapsulation process and stabilize the new objects that are being formed.

In the same year, Daigle and Claverie[73] reported the encapsulation of various spherical inorganic particles via RAFT mechanism in emulsion. The authors used ten different inorganic nanoparticles with different characteristics, such as metals, metal oxides and metal nitrides. For this purpose, trithiobenzyl carbonate was used as RAFT agent to produce AA-based macroRAFT agents composed of one PAA block in each extremity. Using a small amount of surfactant (below CMC) to enhance the stability of the particles, the group successfully encapsulated the inorganic particles by batch emulsion polymerization of styrene or copolymerization of styrene with BA. Despite the very diverse adsorption behavior presented by each macroRAFT/inorganic system, all cases resulted in successful encapsulation, indicating the high versatility of this method to form core-shell particles. Besides, as reminded by the authors, the method eliminates the need for any chemical surface treatment of the commercial inorganic nanoparticles.

In 2011, cadmium sulfide (CdS) quantum dots (QDs) were encapsulated using the REEP strategy by Claverie's group.[76] Random RAFT copolymers composed of AA and BA, or homopolymers of AA, were used to disperse the nanoparticles and guarantee their encapsulation in nanospheres of polystyrene. The strategy used by the authors was similar to the strategy reported in 2008 by the group,[73] however, the most interesting aspect of this work was the size of the encapsulated particles (around 5 nm). There was no control over the number of QD units per polymer particle, and particles with multiple QD were obtained. The reasons why core-shell nanoparticles composed of single-CdS QD core were not obtained were not completely elucidated by the authors. They attribute it, however, as one of the possibilities, to the loss of stability of the single-core particles during the formation of the polymer shell. In this process, as size of the particles increased, the amount of macroRAFT and surfactant became no longer enough to stabilize the objects and particles aggregated, forming the multiple-core morphology.

Das and Claverie[77] reported in 2012 the incorporation of lead sulfide QDs into polystyrene nanospheres and obtained core-shell particles with individual cores. The authors used a trithiocarbonate macroRAFT agent composed of random units of AA and BA, similarly to the previous work with CdS/QDs. Nevertheless, monoencapsulation was additionally achieved in this work, depending on the amounts of PbS, surfactant and monomer used.

In 2012, Nguyen, Such and Hawkett[78] described, again, the encapsulation of titanium dioxide nanoparticles by RAFT-mediated emulsion polymerization. The novelty, in this case, was the formation of air voids that surrounded the pigment particles to form polymer

nanorattles. In the method used by the authors, the pigment was encapsulated by two polymer layers, first a hydrophilic internal layer, composed of an ionizable monomer (methacrylic acid), followed by an external, hard and hydrophobic shell. The strategy proposed by the group was based on the neutralization of the inner layer with ammonium hydroxide at high temperature, which led to the expansion of this layer and, after drying, resulted in the nanorattle particles. The use of macroRAFT agents based on AA and BA, as in the first approach, was not interesting in this case since the carboxylic groups of AA would be protonated during the addition of the ionizable monomer for the formation of the inner layer. For this reason, in this work, authors have used a macroRAFT agent based on 4-styrenesulfonic acid that, copolymerized with AA and BA, guaranteed the stability of the particles even at low pH.

In the work of Garnier et al.,[79, 80] the encapsulation of negatively charged cerium oxide nanoparticles (containing residual amount of dispersant citrate) was attempted using various poly(AA-*co*-BA) macroRAFT agents. The presence of the citrate layer bonded to the inorganic particles, however, seems to have limited the adsorption of the copolymer onto the nanoceria, causing electrostatic repulsion between the negatively charged particles and the anionic macroRAFT agent. For this reason, CeO_2 particles were located at the surface of the final hybrid particles, instead of being effectively encapsulated. The authors have also tried to use macroRAFT agents containing sulfonic[80] or phosphonic[81] acid groups, in replacement of carboxylic acid groups from AA. However, this attempt did not increase the macroRAFT agent adsorption and still resulted in non-encapsulated particles, with CeO_2 located at the polymer/water interface. These results indicate that there is a strong relationship between the adsorption mechanism (and consequently the nature of the inorganic surface) and the encapsulation process. Indeed, successful multi-encapsulation of bare, and therefore positively charged, cerium oxide particles using a similar amphipathic macroRAFT agent composed of AA and BA was later achieved by Zgheib and coworkers.[82]

The encapsulation of very small spherical nanoparticles, such as CeO_2 and QDs seems to be quite challenging due to large surface area of these particles and, in most cases, particles seem to form aggregates that result in the formation of core-shell particles with multiple cores. Some particles with high aspect ratio, such as nanotubes and platelet-like particles, however, have been successfully encapsulated through the REEP technique.

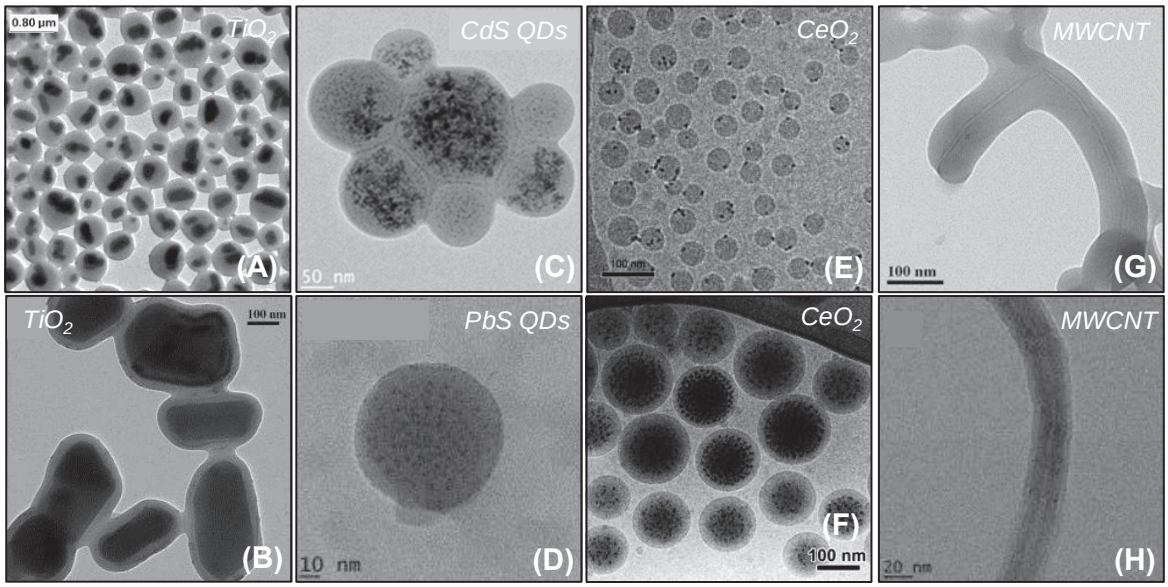
In 2012, Nguyen et al.[83] developed a strategy to encapsulate carbon nanotubes using a layer-by-layer (LbL) approach. The authors used multi-walled carbon nanotubes

(MWCNT) functionalized with carboxylic groups and their intention was to promote, initially, a charge inversion of the surface of carbon nanotubes by the use of a cationic polymer, so that poly(AA-*co*-BA) macroRAFT agents could be effectively adsorbed onto the surface of the nanotubes. This approach led to the encapsulation of the particles with a uniform polymer layer that followed the tubular shape of the particles, via the REEP process.

A more direct method was proposed by Zhong, Zeuna and Claverie[84] to encapsulate unmodified carbon nanotubes. The authors proposed only two steps for this purpose. Initially, the nanotubes were dispersed in water with low molar mass macroRAFT agents based on AA and BA or styrene, without any covalent bonding with the surface of the nanotubes. The affinity between the macroRAFT agents and the unmodified nanotubes was poor, though, as reported by the authors, but the interaction was enough to promote the efficient dispersion of the nanotubes. In a second step, the macroRAFT/nanotubes dispersed particles worked as a polymerization locus for the growth of a polystyrene layer from the nanotubes surface, by emulsion polymerization, promoting encapsulation. A uniform covering of the nanotubes with polymer was achieved, however, only when specific polymerization conditions were applied.

Figure 2.6 summarizes some of the particles that have been encapsulated until now. The REEP strategy has been well explored to a variety of particles with different characteristics. Sheets or platelet-like particles, that have higher aspect ratio than nanotubes, such as Gibbsite,[85] Montmorillonite clay,[86] and even graphene oxide,[87] have been encapsulated through RAFT-mediated emulsion polymerization, but this topic will be further discussed in Chapter 4.

Figure 2.6 – TEM and Cryo-TEM images of encapsulated inorganic nanoparticles by RAFT-encapsulating emulsion polymerization. (A) TiO_2; (B) TiO_2; (C) CdS QDs; (D) PbS QDs; (E) CeO_2; (F) CeO_2; (G) MWCNT and (H) MWCNT.



Source: reprinted with permission from ref [72, 76-79, 82-84].

Until now, RAFT has been the preferred RDRP method for the encapsulation of inorganic nano-objects by emulsion polymerization. Nonetheless, any other RDRP technique could be potentially used. NMP, for instance, was the choice of Qiao et al.[16] to synthesize polymer/silica latex particles by emulsion polymerization. For this purpose, a water-soluble polymer based on poly(ethylene oxide) methacrylate was synthesized to be used as NMP macroinitiator, as well as a coupling agent between the silica nanoparticles and the growing hydrophobic polymer shell. Even though the strategy used by the authors was very similar to the REEP method commonly used, some minor differences, such as the nature of the coupling agent, might have led to the obtainment of multipod-like particles, instead of the core-shell morphology. In the case of this present work, however, the RAFT technique was the method of choice since it requires milder conditions, in terms of temperature, over NMP, and it is more tolerant to functional monomers, when compared to ATRP. Moreover, acrylic (and methacrylic) acid cannot be directly polymerized by ATRP due to interactions of the ATRP catalyst with the monomer carboxyl group, and most macroRAFT agents proposed in this work are based on AA.

2.4 Conclusions

The REEP technique is an extremely interesting method for the direct preparation of colloidal nanocomposites in water and it has been proved to be versatile and efficient for the encapsulation of a large variety of inorganic (or even organic, in some cases) particles. It associates all the advantages of emulsion polymerization and RDRP techniques to produce unique nanocomposite materials. Among the key features of this method, the use of amphipathic RAFT agents that work both as coupling agents and stabilizers of the hybrid particles leads to the two main advantages of the techniques: no sophisticated chemical treatment of the inorganic surface is required, so nanocomposite latex particles can be synthesized by one simple step of emulsion polymerization through the PISA mechanism, and it eliminates the need for conventional surfactant to stabilize the final latex particles, which is desirable not only for environmental but also for quality-related reasons, since the presence of free surfactant in the latex has a negative effect on the properties of the film.[15, 26, 88]

Some prerequisites must be fulfilled for the successful encapsulation of inorganic particles by RAFT-mediated emulsion polymerization. The first and main prerequisite is the use of amphipathic macroRAFT agents, as mentioned above. These molecules must be composed of some hydrophobic monomer units, in order to increase the affinity of macroRAFT/inorganic particles with the hydrophobic monomer and decrease the macroRAFT hydrophilicity, which would force molecules to stay, mainly, in the water phase, leading to secondary nucleation of particles. Nonetheless, some molecules must be free in the aqueous phase to adsorb on the growing hybrid particles and stabilize the new objects that are being formed. In addition, the hydrophilic and hydrophobic units must be, preferably, randomly distributed in the copolymers to avoid their self-assembly into micelles and, consequently, the formation of new particles by micellar nucleation. Some works also indicate that the system should be under monomer starve-feed conditions to avoid the presence of monomer droplets in the water phase, which could lead to the partitioning of macroRAFT (or even the inorganic particles) between the macroRAFT/inorganic particle complexes, the water phase and the monomer droplets.

So, a careful selection of the macroRAFT agent must be performed, to guarantee that macroRAFT has an adequate hydrophilic/hydrophobic balance. Besides, the molecule must be planned based on the chemical nature of the inorganic particle to guarantee an adequate adsorption of the macroRAFT agent onto the inorganic surface. In fact, the adsorption is

another crucial factor for the successful REEP, and for this reason it will be the central topic in Chapter 3.

To summarize, despite requiring a careful planning of best conditions and selection of components, the REEP of inorganic particles is a versatile process that can be easily implemented. Final materials obtained by this method could find applications in diverse fields, such as paints, coatings, adhesives or in the biomedical field.

References

1 SANCHEZ, C.; JULIAN, B.; BELLEVILLE, P.; POPALL, M. Applications of hybrid organic-inorganic nanocomposites. **Journal of Materials Chemistry,** v. 15, n. 35-36, p. 3559-3592, 2005.

2 BOURGEAT-LAMI, E.; LANSALOT, M. Organic/inorganic composite latexes: The marriage of emulsion polymerization and inorganic chemistry. **Advances in Polymer Science,** v. 233, p. 53-123, may 2010.

3 GOMEZ-ROMERO, P. Hybrid organic-inorganic materials - in search of synergic activity. **Advanced Materials,** v. 13, n. 3, p. 163-174, feb. 2001.

4 BARBEY, R.; LAVANANT, L.; PARIPOVIC, D.; SCHUEWER, N.; SUGNAUX, C.; TUGULU, S.; KLOK, H.-A. Polymer brushes via surface-initiated controlled radical polymerization: Synthesis, characterization, properties, and applications. **Chemical Reviews,** v. 109, n. 11, p. 5437-5527, nov. 2009.

5 BRINKS, M. K.; STUDER, A. Polymer brushes by nitroxide-mediated polymerization. **Macromolecular Rapid Communications,** v. 30, n. 13, p. 1043-1057, jul 2009.

6 EDMONDSON, S.; OSBORNE, V. L.; HUCK, W. T. S. Polymer brushes via surface-initiated polymerizations. **Chemical Society Reviews,** v. 33, n. 1, p. 14-22, jan. 2004.

7 HOMENICK, C. M.; LAWSON, G.; ADRONOV, A. Polymer grafting of carbon nanotubes using living free-radical polymerization. **Polymer Reviews,** v. 47, n. 2, p. 265-290, 2007.

8 BADRI, A.; WHITTAKER, M. R.; ZETTERLUND, P. B. Modification of graphene/graphene oxide with polymer brushes using controlled/living radical polymerization. **Journal of Polymer Science Part A: Polymer Chemistry,** v. 50, n. 15, p. 2981-2992, aug. 2012.

9 MICUSIK, M.; BONNEFOND, A.; PAULIS, M.; LEIZA, J. R. Synthesis of waterborne acrylic/clay nanocomposites by controlled surface initiation from macroinitiator modified montmorillonite. **European Polymer Journal,** v. 48, n. 5, p. 896–905, may 2012.

[10] SAMAKANDE, A.; SANDERSON, R. D.; HARTMANN, P. C. Encapsulated clay particles in polystyrene by RAFT mediated miniemulsion polymerization. **Journal of Polymer Science Part a-Polymer Chemistry,** v. 46, n. 21, p. 7114-7126, nov. 2008.

[11] _____. Rheological properties of RAFT-mediated poly(styrene-co-butyl acrylate)-clay nanocomposites p(S-co-BA)-PCNS : Emphasis on the effect of structural parameters on thermo-mechanical and melt flow behaviors. **Polymer,** v. 50, n. 1, p. 42-49, jan. 2009.

[12] ESTEVES, A. C. C.; HODGE, P.; TRINDADE, T.; BARROS-TIMMONS, A. M. M. V. Preparation of nanocomposites by reversible addition-fragmentation chain transfer polymerization from the surface of quantum dots in miniemulsion. **Journal of Polymer Science Part a-Polymer Chemistry,** v. 47, n. 20, p. 5367-5377, oct. 2009.

[13] MA, J.; LU, M.; CAO, C.; ZHANG, H. Synthesis and characterization of PMMA/SiO_2 organic-inorganic hybrid materials via RAFT-mediated miniemulsion polymerization. **Polymer Composites,** v. 34, n. 5, p. 626-633, may 2013.

[14] CHARLEUX, B.; D'AGOSTO, F.; DELAITTRE, G. Preparation of hybrid latex particles and core-shell particles through the use of controlled radical polymerization techniques in aqueous media. In: VAN HERK, A. M.;LANDFESTER, K. (Ed.). **Hybrid latex particles: Preparation with (mini) emulsion polymerization**. Berlin Heidelberg: Springer, 2010. p.125-183. (Advances in polymer science).

[15] BOURGEAT-LAMI, E.; D'AGOSTO, F.; LANSALOT, M. Synthesis of nanocapsules and polymer/inorganic nanoparticles through controlled radical polymerization at and near interfaces in heterogeneous media. In: VANA, P. (Ed.). **Controlled radical polymerization at and from solid surfaces**. Heidelberg: Springer International Publishing, 2016.v.270, p.123-161. (Advances in polymer science).

[16] QIAO, X. G.; DUGAS, P. Y.; CHARLEUX, B.; LANSALOT, M.; BOURGEAT-LAMI, E. Synthesis of multipod-like silica/polymer latex particles via nitroxide-mediated polymerization-induced self-assembly of amphiphilic block copolymers. **Macromolecules,** v. 48, n. 3, p. 545-556, 2015.

[17] CENACCHI-PEREIRA, A. M. **Synthesis of anisotropic polymer/inorganic composite particles via RAFT-mediated emulsion polymerization**. 2014. 286 (Ph.D.). École doctorale de chimie, University of Lyon, Lyon.

[18] MATYJASZEWSKI, K. General concepts and history of living radical polymerization. In: (Ed.). **Handbook of radical polymerization**. New York: John Wiley & Sons, Inc., 2003. p.361-406.

[19] BRAUNECKER, W. A.; MATYJASZEWSKI, K. Controlled/living radical polymerization: Features, developments, and perspectives. **Progress in Polymer Science,** v. 32, n. 1, p. 93-146, jan. 2007.

[20] NICOLAS, J.; GUILLANEUF, Y.; LEFAY, C.; BERTIN, D.; GIGMES, D.; CHARLEUX, B. Nitroxide-mediated polymerization. **Progress in Polymer Science,** v. 38, n. 1, p. 63-235, 2013.

[21] MATYJASZEWSKI, K. Atom transfer radical polymerization (ATRP): Current status and future perspectives. **Macromolecules,** v. 45, n. 10, p. 4015-4039, 2012.

[22] KEDDIE, D. J.; MOAD, G.; RIZZARDO, E.; THANG, S. H. RAFT agent design and synthesis. **Macromolecules,** v. 45, n. 13, p. 5321-5342, 2012.

[23] GEORGES, M. K.; VEREGIN, R. P. N.; KAZMAIER, P. M.; HAMER, G. K. Narrow molecular weight resins by a free-radical polymerization process. **Macromolecules,** v. 26, p. 2987-2988, may. 1993.

[24] CHARLEUX, B.; NICOLAS, J. Water-soluble SGL-based alkoxyamines: A breakthrough in controlled/living free-radical polymerization in aqueous dispersed media. **Polymer,** v. 48, n. 20, p. 5813-5833, sept. 2007.

[25] SAVE, M.; GUILLANEUF, Y.; GILBERT, R. G. Controlled radical polymerization in aqueous dispersed media. **Australian Journal of Chemistry,** v. 59, n. 10, p. 693-711, 2006.

[26] ZETTERLUND, P. B.; THICKETT, S. C.; PERRIER, S.; BOURGEAT-LAMI, E.; LANSALOT, M. Controlled/living radical polymerization in dispersed systems: An update. **Chemical Reviews,** v. 115, p. 9745−9800, 2015.

[27] KATO, M.; KAMIGAITO, M.; SAWAMOTO, M.; HIGASHIMURA, T. Polymerization of methyl methacrylate with the carbon tetrachloride/dichlorotris-(triphenylphosphine) ruthenium(ii) /methylaluminum bis(2,6-di-tert-butylphenoxide) initiating system: Possibility of living radical polymerization. **Macromolecules,** v. 28, p. 1721-1723, 1995.

[28] WANG, J.-S.; MATYJASZEWSKI, K. Controlled/"living" radical polymerization. Atom transfer radical polymerization in the presence of transition-metal complexes. **Journal of the American Chemical Society,** v. 117, n. 20, p. 5614-5615, 1995.

[29] MATYJASZEWSKI, K. State-of-the-art of controlled radical polymerization (reversible deactivation radical polymerization). **Abstracts of Papers of the American Chemical Society,** v. 248, aug. 2014.

[30] MATYJASZEWSKI, K.; QIU, J.; SHIPP, D. A.; GAYNOR, S. G. Controlled/“living” radical polymerization applied to water-borne systems. **Macromolecular Symposia,** v. 155, n. 1, p. 15-29, 2000.

[31] JAKUBOWSKI, W.; MATYJASZEWSKI, K. Activator generated by electron transfer for atom transfer radical polymerization. **Macromolecules,** v. 38, n. 10, p. 4139-4146, may 2005.

[32] CHIEFARI, J.; CHONG, Y. K.; ERCOLE, F.; KRSTINA, J.; JEFFERY, J.; LE, T. P. T.; MAYADUNNE, R. T. A.; MEIJS, G. F.; MOAD, C. L.; MOAD, G.; RIZZARDO, E.; THANG, S. H. Living free-radical polymerization by reversible addition-fragmentation chain transfer: The RAFT process. **Macromolecules,** v. 31, n. 16, p. 5559-5562, july 1998.

[33] CHARMOT, D.; CORPART, P.; ADAM, H.; ZARD, S. Z.; BIADATTI, T.; BOUHADIR, G. Controlled radical polymerization in dispersed media. **Macromolecular Symposia,** v. 150, n. 1, p. 23-32, feb. 2000.

[34] MAYADUNNE, R. T. A.; RIZZARDO, E.; CHIEFARI, J.; KRSTINA, J.; MOAD, G.; POSTMA, A.; THANG, S. H. Living polymers by the use of trithiocarbonates as reversible addition-fragmentation chain transfer (RAFT) agents: ABA triblock copolymers by radical polymerization in two steps. **Macromolecules,** v. 33, n. 2, p. 243-245, jan. 2000.

[35] MAYADUNNE, R. T. A.; RIZZARDO, E.; CHIEFARI, J.; CHONG, Y. K.; MOAD, G.; THANG, S. H. Living radical polymerization with reversible addition-fragmentation chain transfer (RAFT polymerization) using dithiocarbamates as chain transfer agents. **Macromolecules,** v. 32, n. 21, p. 6977-6980, oct. 1999.

[36] FAIRBANKS, B. D.; GUNATILLAKE, P. A.; MEAGHER, L. Biomedical applications of polymers derived by reversible addition - fragmentation chain-transfer (RAFT). **Advanced Drug Delivery Reviews,** v. 91, p. 141-152, aug. 2015.

[37] KEDDIE, D. J. A guide to the synthesis of block copolymers using reversible-addition fragmentation chain transfer (RAFT) polymerization. **Chemical Society Reviews,** v. 43, n. 2, p. 496-505, 2014.

[38] CHARLEUX, B.; DELAITTRE, G.; RIEGER, J.; D'AGOSTO, F. Polymerization-induced self-assembly: From soluble macromolecules to block copolymer nano-objects in one step. **Macromolecules,** v. 45, n. 17, p. 6753-6765, sept. 2012.

[39] CUNNINGHAM, M. F. Controlled/living radical polymerization in aqueous dispersed systems. **Progress in Polymer Science,** v. 33, n. 4, p. 365-398, apr. 2008.

[40] MONTEIRO, M. J.; CUNNINGHAM, M. F. Polymer nanoparticles via living radical polymerization in aqueous dispersions: Design and applications. **Macromolecules,** v. 45, n. 12, p. 4939-4957, june 2012.

[41] ZETTERLUND, P. B.; KAGAWA, Y.; OKUBO, M. Controlled/living radical polymerization in dispersed systems. **Chemical Reviews,** v. 108, n. 9, p. 3747-3794, sept. 2008.

[42] BARNER-KOWOLLIK, C.; BLINCO, J. P.; DESTARAC, M.; THURECHT, K. J.; PERRIER, S. Reversible addition fragmentation chain transfer (RAFT) polymerization: Mechanism, process and applications. In: STUDER, C. C.;ARMIDO (Ed.). **Encyclopedia of radicals in chemistry, biology and materials**: John Wiley & Sons, Ltd, 2012.

[43] ODIAN, G. Emulsion polymerization. In: _____ (Ed.). **Principles of polymerization**. 4th. Hoboken, New Jersey: John Wiley & Sons, Inc., 2004. p.350-371.

[44] SMITH, W. V.; EWART, R. H. Kinetics of emulsion polymerization. **Journal of Chemical Physics,** v. 16, p. 592-599, 1948.

[45] HARKINS, W. D. A general theory of the mechanism of emulsion polymerization. **Journal of the American Chemical Society,** v. 69, n. 6, p. 1428-1444, june 1947.

[46] PRIEST, W. J. Particle growth in the aqueous polymerization of vinyl acetate. **Journal of Physical Chemistry,** v. 56, p. 1077-1082, 1952.

[47] FEENEY, P. J.; NAPPER, D. H.; GILBERT, R. G. Surfactant-free emulsion polymerizations: Predictions of the coagulative nucleation theory. **Macromolecules,** v. 20, n. 11, p. 2922-2930, nov. 1987.

[48] NOZARI, S.; TAUER, K. Calorimetric study on the influence of the nature of the RAFT agent and the initiator in ab initio aqueous heterophase polymerization. **Polymer,** v. 46, n. 4, p. 1033-1043, 2005.

[49] TAUER, K.; NOZARI, S.; ALI, A. M. I. Experimental reconsideration of radical entry into latex particles. **Macromolecules,** v. 38, n. 21, p. 8611-8613, 2005.

[50] NOZARI, S.; TAUER, K.; ALI, A. M. I. RAFT agent concentration in polymer particles during emulsion polymerization. **Macromolecules,** v. 38, n. 25, p. 10449-10454, 2005.

[51] URBANI, C. N.; NGUYEN, H. N.; MONTEIRO, M. J. RAFT-mediated emulsion polymerization of styrene using a non-ionic surfactant. **Australian Journal of Chemistry,** v. 50, n. 10, p. 728-732, 2006.

[52] LUO, Y.; CUI, X. Reversible addition–fragmentation chain transfer polymerization of methyl methacrylate in emulsion. **Journal of Polymer Science Part A: Polymer Chemistry,** v. 44, n. 9, p. 2837-2847, 2006.

[53] LUO, Y.; WANG, X.; LI, B.-G.; ZHU, S. Toward well-controlled ab initio RAFT emulsion polymerization of styrene mediated by 2-(((dodecylsulfanyl)carbonothioyl)sulfanyl)propanoic acid. **Macromolecules,** v. 44, n. 2, p. 221-229, 2011.

[54] MCLEARY, J. B.; KLUMPERMAN, B. RAFT mediated polymerisation in heterogeneous media. **Soft Matter,** v. 2, n. 1, p. 45-53, dec. 2006.

[55] FERGUSON, C. J.; HUGHES, R. J.; PHAM, B. T. T.; HAWKETT, B. S.; GILBERT, R. G.; SERELIS, A. K.; SUCH, C. H. Effective ab initio emulsion polymerization under RAFT control. **Macromolecules,** v. 35, n. 25, p. 9243-9245, dec. 2002.

[56] FERGUSON, C. J.; HUGHES, R. J.; NGUYEN, D.; PHAM, B. T. T.; GILBERT, R. G.; SERELIS, A. K.; SUCH, C. H.; HAWKETT, B. S. Ab initio emulsion polymerization by RAFT-controlled self-assembly. **Macromolecules,** v. 38, n. 6, p. 2191-2204, mar. 2005.

[57] SPRONG, E.; LESWIN, J. S. K.; LAMB, D. J.; FERGUSON, C. J.; HAWKETT, B. S.; PHAM, B. T. T.; NGUYEN, D.; SUCH, C. H.; SERELIS, A. K.; GILBERT, R. G. Molecular watchmaking: Ab initio emulsion polymerization by RAFT-controlled self-assembly. **Macromolecular Symposia,** v. 231, n. 1, p. 84-93, 2006.

[58] BOURSIER, T.; CHADUC, I.; RIEGER, J.; D'AGOSTO, F.; LANSALOT, M.; CHARLEUX, B. Controlled radical polymerization of styrene in miniemulsion mediated by PEO-based trithiocarbonate macromolecular RAFT agents. **Polymer Chemistry,** v. 2, n. 2, p. 355-362, feb. 2011.

[59] ZHAO, C. L.; DOBLER, F.; PITH, T.; HOLL, Y.; LAMBLA, M. Surface-composition of coalesced acrylic latex films studied by XPS and SIMS. **Journal of Colloid and Interface Science,** v. 128, n. 2, p. 437-469, mar. 1989.

[60] MCKENNA, T. F. L.; CHARLEUX, B.; BOURGEAT-LAMI, E.; D'AGOSTO, F.; LANSALOT, M. Novel technologies and chemistries for waterborne coatings. **Journal of Coatings Technology and Research,** v. 11, n. 2, p. 131-141, mar. 2014.

[61] MANGUIAN, M.; SAVE, M.; CHARLEUX, B. Batch emulsion polymerization of styrene stabilized by a hydrophilic macro-RAFT agent. **Macromolecular Rapid Communications,** v. 27, n. 6, p. 399-404, 2006.

[62] MARTINS DOS SANTOS, A.; LE BRIS, T.; GRAILLAT, C.; D'AGOSTO, F.; LANSALOT, M. Use of a poly(ethylene oxide) macroRAFT agent as both a stabilizer and a control agent in styrene polymerization in aqueous dispersed system. **Macromolecules,** v. 42, n. 4, p. 946-956, jan. 2009.

[63] RIEGER, J.; STOFFELBACH, F.; BUI, C.; ALAIMO, D.; JEROME, C.; CHARLEUX, B. Amphiphilic poly(ethylene oxide) macromolecular RAFT agent as a stabilizer and control agent in ab initio batch emulsion polymerization. **Macromolecules,** v. 41, n. 12, p. 4065-406, may 2008.

[64] BOISSE, S.; RIEGER, J.; BELAL, K.; DI-CICCO, A.; BEAUNIER, P.; LI, M.-H.; CHARLEUX, B. Amphiphilic block copolymer nano-fibers via RAFT-mediated polymerization in aqueous dispersed system. **Chemical Communications,** v. 46, n. 11, p. 1950-1952, mar. 2010.

[65] ZHANG, X.; BOISSE, S.; ZHANG, W.; BEAUNIER, P.; D'AGOSTO, F.; RIEGER, J.; CHARLEUX, B. Well-defined amphiphilic block copolymers and nano-objects formed in situ via RAFT-mediated aqueous emulsion polymerization. **Macromolecules,** v. 44, n. 11, p. 4149-4158, may 2011.

[66] ZHANG, W.; D'AGOSTO, F.; DUGAS, P.-Y.; RIEGER, J.; CHARLEUX, B. RAFT-mediated one-pot aqueous emulsion polymerization of methyl methacrylate in presence of poly(methacrylic acid-co-poly(ethylene oxide) methacrylate)

trithiocarbonate macromolecular chain transfer agent. **Polymer,** v. 54, n. 8, p. 2011-2019, apr. 2013.

[67] CHADUC, I.; ZHANG, W.; LANSALOT, M.; D'AGOSTO, F.; CHARLEUX, B. Amphiphilic block copolymers from a direct and one-pot RAFT synthesis in water. **Macromolecular Rapid Communications,** v. 32, n. 16, p. 1270-1276, aug. 2011.

[68] CHADUC, I.; GIROD, M.; ANTOINE, R.; CHARLEUX, B.; D'AGOSTO, F.; LANSALOT, M. Batch emulsion polymerization mediated by poly(methacrylic acid) macroRAFT agents: One-pot synthesis of self-stabilized particles. **Macromolecules,** v. 45, n. 15, p. 5881-5893, july 2012.

[69] DELAITTRE, G.; DIRE, C.; RIEGER, J.; PUTAUX, J.-L.; CHARLEUX, B. Formation of polymer vesicles by simultaneous chain growth and self-assembly of amphiphilic block copolymers. **Chemical Communications**, n. 20, p. 2887-2889, may. 2009.

[70] GROISON, E.; BRUSSEAU, S.; D'AGOSTO, F.; MAGNET, S.; INOUBLI, R.; COUVREUR, L.; CHARLEUX, B. Well-defined amphiphilic block copolymer nanoobjects via nitroxide-mediated emulsion polymerization. **Acs Macro Letters,** v. 1, n. 1, p. 47-51, jan. 2012.

[71] ZHANG, W.; D'AGOSTO, F.; BOYRON, O.; RIEGER, J.; CHARLEUX, B. Toward a better understanding of the parameters that lead to the formation of nonspherical polystyrene particles via RAFT-mediated one-pot aqueous emulsion polymerization. **Macromolecules,** v. 45, n. 10, p. 4075-4084, may 2012.

[72] NGUYEN, D.; ZONDANOS, H. S.; FARRUGIA, J. M.; SERELIS, A. K.; SUCH, C. H.; HAWKETT, B. S. Pigment encapsulation by emulsion polymerization using macro-RAFT copolymers. **Langmuir,** v. 24, n. 5, p. 2140-2150, 2008.

[73] DAIGLE, J.-C.; CLAVERIE, J. P. A simple method for forming hybrid core-shell nanoparticles suspended in water. **Journal of Nanomaterials,** v. 2008, p. 1-8, 2008.

[74] MULLER, D.; MALMSTEN, M.; TANODEKAEW, S.; BOOTH, C. Adsorption of diblock copolymers of poly(ethylene oxide) and poly(lactide) at hydrophilic silica from aqueous solution. **Journal of Colloid and Interface Science,** v. 228, n. 2, p. 317-325, aug. 2000.

[75] VANGEYTE, P.; LEYH, B.; ROJAS, O. J.; CLAESSON, P. M.; HEINRICH, M.; AUVRAY, L.; WILLET, N.; JEROME, R. Adsorption of poly(ethylene oxide)-b-poly(e-caprolactone) copolymers at the silica-water interface. **Langmuir,** v. 21, n. 7, p. 2930-2940, mar. 2005.

[76] DAS, P.; ZHONG, W.; CLAVERIE, J. P. Copolymer nanosphere encapsulated CdS quantum dots prepared by RAFT copolymerization: Synthesis, characterization and mechanism of formation. **Colloid and Polymer Science,** v. 289, n. 14, p. 1519-1533, sept. 2011.

[77] DAS, P.; CLAVERIE, J. P. Synthesis of single-core and multiple-core core-shell nanoparticles by RAFT emulsion polymerization: Lead sulfide-copolymer nanocomposites. **Journal of Polymer Science Part A: Polymer Chemistry,** v. 50, n. 14, p. 2802-2808, jul. 2012.

[78] NGUYEN, D.; SUCH, C.; HAWKETT, B. Polymer-TiO_2 composite nanorattles via RAFT-mediated emulsion polymerization. **Journal of Polymer Science Part a-Polymer Chemistry,** v. 50, n. 2, p. 346-352, jan. 2012.

[79] GARNIER, J.; WARNANT, J.; LACROIX-DESMAZES, P.; DUFILS, P. E.; VINAS, J.; VANDERVEKEN, Y.; VAN HERK, A. M. An emulsifier-free RAFT-mediated process for the efficient synthesis of cerium oxide/polymer hybrid latexes. **Macromolecular Rapid Communications,** v. 33, n. 16, p. 1388-1392, aug. 2012.

[80] GARNIER, J.; WARNANT, J.; LACROIX-DESMAZES, P.; DUFILS, P.-E.; VINAS, J.; VAN HERK, A. Sulfonated macro-RAFT agents for the surfactant-free synthesis of cerium oxide-based hybrid latexes. **Journal of Colloid and Interface Science,** v. 407, p. 273-281, oct. 2013.

[81] WARNANT, J.; GARNIER, J.; VAN HERK, A.; DUFILS, P.-E.; VINAS, J.; LACROIX-DESMAZES, P. A CeO_2/PVDC hybrid latex mediated by a phosphonated macro-RAFT agent. **Polymer Chemistry,** v. 4, n. 23, p. 5656-5663, dec. 2013.

[82] ZGHEIB, N.; PUTAUX, J.-L.; THILL, A.; BOURGEAT-LAMI, E.; D'AGOSTO, F.; LANSALOT, M. Cerium oxide encapsulation by emulsion polymerization using hydrophilic macroRAFT agents. **Polymer Chemistry,** v. 4, n. 3, p. 607-614, 2013.

[83] NGUYEN, D.; SUCH, C. H.; HAWKETT, B. S. Polymer coating of carboxylic acid functionalized multiwalled carbon nanotubes via reversible addition-fragmentation chain transfer mediated emulsion polymerization. **Journal of Polymer Science Part A: Polymer Chemistry,** v. 51, n. 2, p. 250-257, jan. 2013.

[84] ZHONG, W.; ZEUNA, J. N.; CLAVERIE, J. P. A versatile encapsulation method of noncovalently modified carbon nanotubes by RAFT polymerization. **Journal of Polymer Science Part A: Polymer Chemistry,** v. 50, n. 21, p. 4403-4407, 2012.

[85] ALI, S. I.; HEUTS, J. P. A.; HAWKETT, B. S.; VAN HERK, A. M. Polymer encapsulated gibbsite nanoparticles: Efficient preparation of anisotropic composite latex particles by RAFT-based starved feed emulsion polymerization. **Langmuir,** v. 25, n. 18, p. 10523-10533, sept. 2009.

[86] MBALLA MBALLA, M. A.; ALI, S. I.; HEUTS, J. P. A.; VAN HERK, A. M. Control of the anisotropic morphology of latex nanocomposites containing single montmorillonite clay particles prepared by conventional and reversible addition-fragmentation chain transfer based emulsion polymerization. **Polymer International,** v. 61, n. 6, p. 861-865, 2012.

[87] HUYNH, V. T.; NGUYEN, D.; SUCH, C. H.; HAWKETT, B. S. Polymer coating of graphene oxide via reversible addition-fragmentation chain transfer mediated

emulsion polymerization. **Journal of Polymer Science Part A: Polymer Chemistry,** v. 53, n. 12, p. 1413-1421, june 2015.

88 CENACCHI-PEREIRA, A.; GRANT, E.; D'AGOSTO, F.; LANSALOT, M.; BOURGEAT-LAMI, E. Encapsulation with the use of controlled radical polymerization. In: KOBAYASHI, S.;MÜLLEN, K. (Ed.). **Encyclopedia of polymeric nanomaterials**. Berlin, Heidelberg: Springer Berlin Heidelberg, 2014. p.1-13.

3 MacroRAFT/Laponite interactions

3.1 Introduction

The interaction between the macroRAFT agent and the inorganic surface is a crucial parameter for the successful encapsulation of inorganic particles through the macroRAFT-assisted encapsulating emulsion polymerization (REEP) strategy. A good adsorption of the macromolecule onto the particle, with a good coverage of its surface and minimum amount of free molecules in the aqueous phase, guarantees that the macroRAFT agents are effective coupling agents and precursors of stabilizers for the synthesis of nanocomposites in aqueous dispersed media.

The strategy proposed in this work, which is based on the method first described by Nguyen et al.[1] and Claverie et al.[2] relies on the synthesis of macroRAFT agents that are capable of interacting with the inorganic particles and, for this reason, the leaving group (R) of the macroRAFT agent was carefully selected. Functional thiocarbonylthio compounds were synthesized, with the R group bearing either a quaternary ammonium group (from 2-(dimethylamino)ethyl methacrylate, DMAEMA), negatively charged polymers (based on acrylic acid, AA) or neutral polyethylene glycol (PEG) side chains. The presence of charged or ionizable monomers of DMAEMA, with opposite charge to that of the inorganic particle surface, is strategic to promote strong electrostatic interaction of the macroRAFT copolymers with the negatively charged clay particles.[3-6] As an alternative to cationic macroRAFT agents, PEG-based homo and copolymers were also selected considering their potential to adsorb on clay particles.[7-12] When compared to positively charged molecules, a weaker interaction is expected for neutral PEG polymers, so some of these molecules were also designed containing negatively charged carboxylic acid groups (AA) as an attempt to promote interaction with the positively charged rims of the platelets as well. It is also expected that the AA units help in the stabilization of the final hybrid particles.

This chapter is dedicated to the functionalization of Laponite platelets with all RAFT (co)polymers synthesized. Prior to the results section, a bibliographic review on the subject is given. This review section concerns a detailed description of Laponite crystal structure and surface chemistry, as well as some topics related to the surface modification of Laponite with polyelectrolytes and PEG. In the following section, preceding the adsorption study part, the results obtained in the synthesis of the macroRAFT agents are briefly described. Finally,

the results obtained in the adsorption study (adsorption isotherms and the fitting of these isotherms to Langmuir and Freundlich models) are shown and discussed.

3.2 Bibliographic review

3.2.1 Clays or layered silicates

Clay minerals are hydrous aluminum phyllosilicates that form an important group of the phyllosilicates. They have the interesting ability to disperse into individual layers (for this reason they are also known as layered silicates) and to exchange their interlayer ions with organic and inorganic cations, tuning their surface chemistry. These two characteristics make these materials excellent fillers for polymeric nanocomposites, generating the so-called layered silicate polymer nanocomposites (LSPN).

Among this family of minerals, smectite clays are considered one of the largest and most important classes. Their chemical composition, structure, exchangeable ions and small crystal size are responsible for several of the unique properties of smectite clays. These layered silicates have a large chemically active surface area, being characterized by a 2:1 layer structure composed by two outer tetrahedral silica sheets and a central octahedral magnesia or alumina layer.[13] Often referred to as "swelling clays", smectites can hydrate and expand their interlayer space. The separation between the individual sheets varies depending on the amount of water in the medium, until a complete dispersion into individual layers. With a high exchange capacity, smectites have their variable net negative charges balanced by the adsorption of Na, Ca or Mg ions externally on the interlamellar surfaces. Two of the most important smectite clays are Montmorillonite (Mt) and Hectorite (and notably Laponite), which are among the most commonly used smectite-type layered silicates for the preparation of nanocomposites.[14] Table 3.1 shows some of the 2:1 phyllosilicates most commonly used for the production of LSPN and their general formula.

Table 3.1 – Chemical structure of most commonly used 2:1 phyllosilicates in LSPN.

2:1 Phyllosilicate	General Formula
Montmorillonite	$M_x(Al_{4-x}Mg_x)Si_8O_{20}(OH)_4$
Hectorite	$M_x(Mg_{6-x}Li_x)Si_8O_{20}(OH)_4$
Saponite	$M_xMg_6(Si_{8-x}Al_x)O_{20}(OH)_4$

M = monovalent cation; x= degree of isomorphous substitution (between 0.5 and 1.3).
Source: adapted from ref.[15]

Hectorites offer many advantages that make them attractive for many industrial sectors and for academic studies. These advantages include their low iron content, light color and, specially, their great swelling capacity on contact with water.[16]

3.2.2 Laponite clay

Laponite is a synthetic crystalline hydrous sodium lithium magnesium layered silicate produced by BYK Additives Ltd (former Rockwood Additives Ltd) and supplied in the disc form of a white fine powder. In terms of crystal structure and composition, Laponite is very similar to hectorites but, comparatively to the natural clay, Laponite presents a higher chemical purity, produces exceptionally clear dispersions and have smaller and more uniform, in terms of dispersity, elementary platelets. For these reasons, Laponite is often used in studies as a model system. In addition, Laponite can find many industrial applications, including:

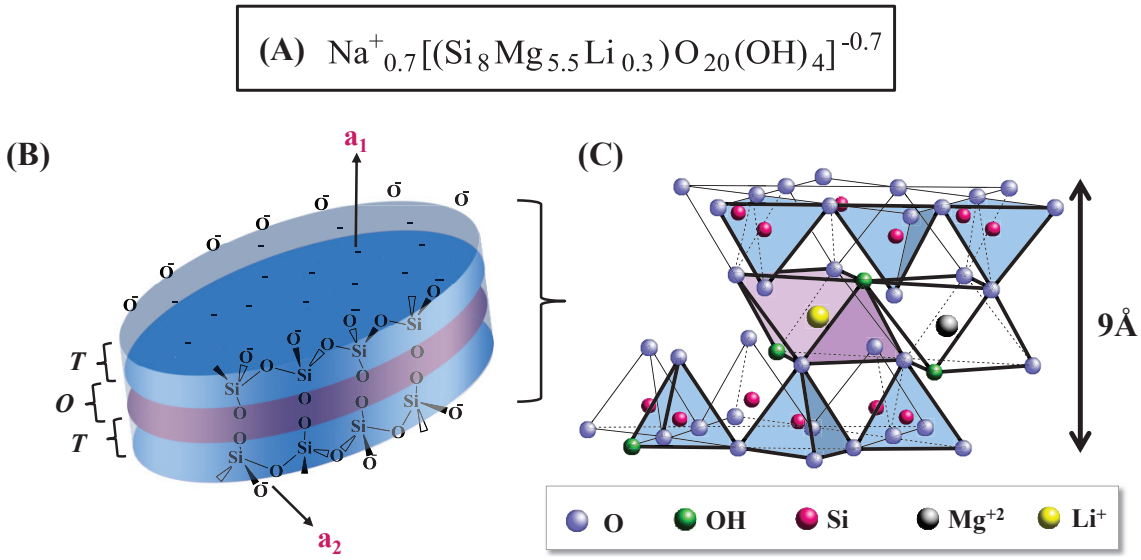
- As rheological additives: when added to the formulation of waterborne products such as surface coatings, household cleaners and personal care products (as a thickener, for instance);
- As film-forming agents: when coated onto a substrate, Laponite can produce coatings with electrical (conductive/antistatic), antiblocking and barrier properties;
- To build optimized nanocomposites.

3.2.2.1 Laponite crystal structure

Laponite has a layer structure comparable with those of natural hectorite and bentonite, being disposed in the form of disc-shaped crystals when dispersed in water. The unit cell of the crystal structure formed by the empirical formula of Laponite is shown in

Figure 3.1. The idealized structure of Laponite would be composed of a central octahedral sheet containing six divalent magnesium ions (giving a positive charge of twelve) sandwiched between two tetrahedral layers containing four silicon atoms. Twenty atoms of oxygen and four hydroxyl groups complete the balance of these layers, forming the magnesia octahedral and the silica tetrahedral sheets, which should have a neutral charge. However, in practice, Laponite has a surface negative charge that can be attributed to two factors: the isomorphic substitution and the broken edges, as shown in Figure 3.1A.[17] In the isomorphic substitution, some magnesium ions are substituted within the lattice structure by monovalent lithium ions (and some positions are empty) generating permanent negative charges.

Figure 3.1 – (A) Empirical formula of Laponite. (B) Schematic representation of the tetrahedral (T) and octahedral (O) sheets of Laponite, indicating the source of negative charges. (C) Perspective representation of Laponite idealized structural formula, showing the isomorphic substitution between magnesium and lithium ions.



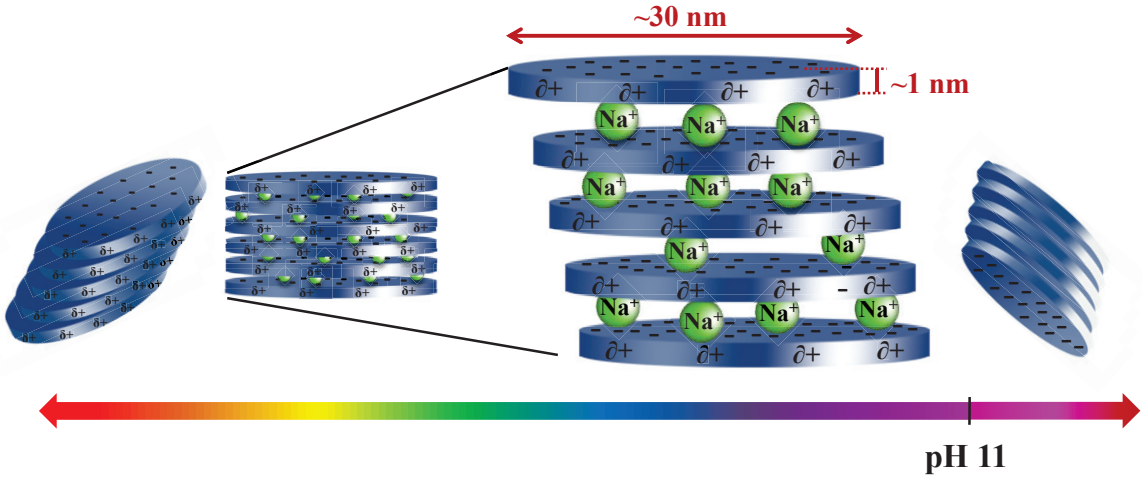
a_1 represents the negative charges by isomorphic substitution in octahedral sheets
a_2 represents the negative charges arising from the silanol groups located on the broken edges of the clay sheets
Source: (A) Adapted from ref.[16] ; (B) adapted from ref.[17] and (C) adapted from ref.[14]

The charges of the edges of the structure, which vary according to the pH, can be attributed to the presence of MgOH, LiOH and SiOH amphoteric groups where the crystal structure terminates. Depending on the pH of the medium, these groups can be protonated or deprotonated. Laponite dispersions are always found at pH around 10[18] and, below this pH, MgOH and LiOH are positively charged, while SiOH groups are negatively charged.[19] A number of works report that the rims of the mineral have small localized positive charges (typically 4-5 mmol/g, representing less than 10% of the total cation exchange capacity of

the mineral), that slightly decrease with increasing the pH.[20] Tawari and his group[21] suggested that the rim charge is neutralized above pH 11, and it is expected that at higher pH values, the deprotonation of the rims is favored and they may even become negative.

The negative charges of the crystal faces are counterbalanced by the adsorption of cations (predominantly Na^+) in the interlayer space of Laponite, as shown in Figure 3.2. The neutralization of the charges through cation exchange is a highly regular phenomenon that starts at the edges of the particles and proceeds towards the center.[22] The sharing of sodium ions between Laponite crystals holds these layers together electrostatically, with a regular van der Waals gap between the layers (the interlayer space or gallery), and guarantees that platelets are arranged together into stacks.[23] The repetition of Laponite unit cell in two directions results in a disc-shape crystal, shown in Figure 3.2, while its height (0.92 nm) is equivalent to the thickness of the Laponite crystal.

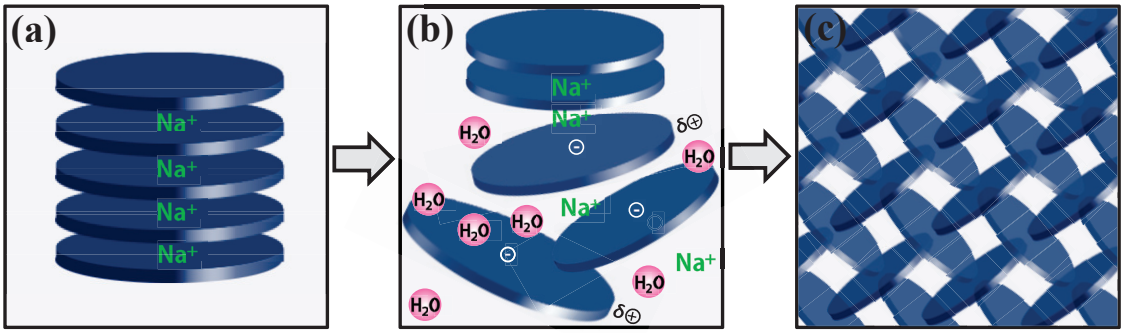
Figure 3.2 – Schematic representation of Laponite platelets and their arrangement into stacks, showing the sharing of Na^+ ions and the pH dependent charges of the edges.



Source: elaborated by the author.

During the dispersion of Laponite particles in water, the platelets hydrate and swell, and the interlayer Na^+ ions are released. The platelets are stabilized by electrostatic repulsion between the negative charges of the faces. In mediums with high ionic concentration and at pH below the rim isoelectric point, the positive edges are attracted to the negatively charged layers of the faces.[24, 25] When this is the dominating interaction phenomenon, electrostatic bonds are formed between the positively charged rims and the negatively charged faces and particles aggregate in a three-dimensional network, called “house of cards” structure. This structure, shown in Figure 3.3, is typical of the high-density gel state of Laponite.[26, 27]

Figure 3.3 – Schematic representation of the preparation of the clay aqueous suspension and the formation of the house-of cards structure: (a) Laponite clay; (b) dispersion (exfoliation) of the clay platelets in water, and (c) house of cards structure.



Clay (Hectorite) **"House of cards" structure**

Source: adapted from ref. [28]

To avoid the rim-to-face interactions, sodium pyrophosphate ($Na_4P_2O_7$) has been added to some of the commercially available grades of Laponite. The idea is that the tetravalent negatively charged ions of pyrophosphate adsorb onto the positively charged rims and work as an effective barrier to the electrostatic attraction.

Laponite is often used as a model substrate for adsorption studies, as it is composed of relatively monodisperse disc-shape platelets of around 1 nm thickness and ~30 nm diameter, with a large specific surface area available (370 m^2 g^{-1}) for the adsorption of various chemical compounds[29], and notably macroRAFT agents, and a cation exchange capacity (CEC) of 0.75 meq/g.[29, 30]

Among some of the aspects that differentiate Laponite of natural sodium Montmorillonite (e.g., Na Cloisite), another extensively studied smectite clay, the much larger aspect ratio of Montmorillonite can be cited as one of the most important differences, since platelets of more than 100 nm diameter, with a less uniform dispersity, are found in Mt. In addition, both clays have different structural organization of the octahedral layer[31] and, while Laponite solutions are stable predominantly at high pH, the dispersion of Montmorillonite platelets is possible down to pH 4, which allows the neutralization of edges charges (eliminating the oppositely charged surface/rims) under more acidic conditions.[32]

3.2.3 Laponite surface modification

The ability of layered silicates to fine-tune their surface chemistry with organic and inorganic cations through ion exchange reactions is one of the characteristics that make these materials extremely interesting for the synthesis of nanocomposites. To this regard, the

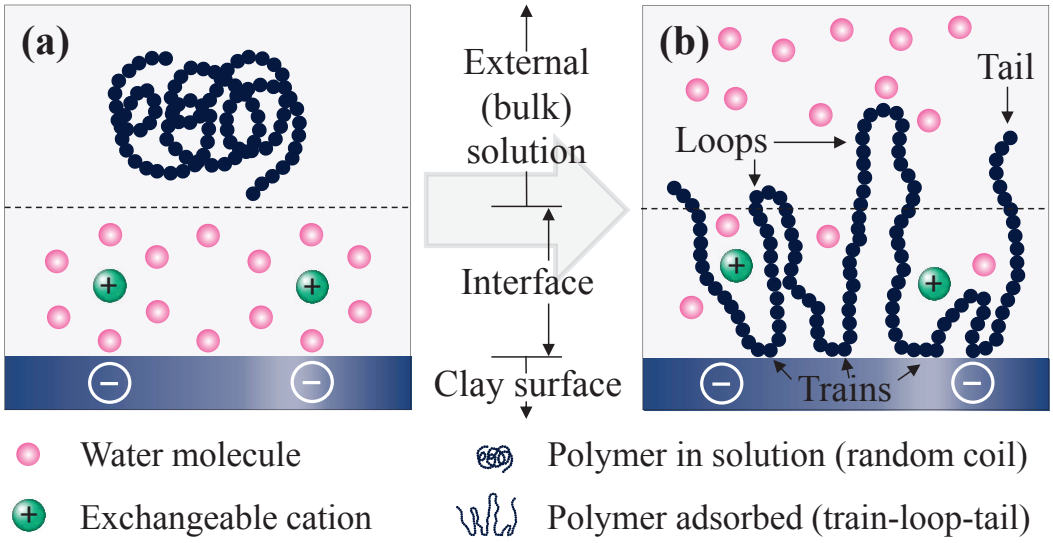
replacing of the alkali metal originally present on the clay surface with small molecules or large organic cations can be easily done, as the forces that hold the platelets together are relatively weak, rendering these hydrophilic phyllosilicates more organophilic. The hydrated interlayer cations of Laponite have been exchanged with various cationic molecules, including dyes,[33-35] surfactants such as alkylammonium[36-39] or alkylphosphonium salts,[40] free radical initiators,[17, 41, 42] monomers,[17] and so forth. While organic cations adsorb by cation exchange with the counterions, the adsorption of uncharged polar organic molecules is also possible and can be attributed to interaction between the functional groups of these molecules and the gallery cations of the clay. Another technique largely applied for the synthesis of clay/polymer nanocomposites is the exploitation of the reactivity of silanol groups present on the edges of the clay platelets by grafting alkoxysilanes onto the clay rims.[29]

The ion-exchanging process of replacing the inorganic counterions in the pristine mineral for organic cations results, in general, in a larger interlayer spacing. The modified clay, also referred to as organoclay, has its surface energy lowered and becomes more compatible for the intercalation of organic polymers or polymer precursors.[15] Even the direct intercalation of water soluble polymers into the galleries of inorganic layered materials has already been reported in the literature.

3.2.3.1 Interaction of Laponite with polymers

The interaction of organic polymers with clay surfaces is different in some aspects from that of non-polymeric species, especially because polymers are long, flexible and often polyfunctional molecules. The counterions present in the galleries of 2:1 phyllosilicates attract water molecules, attributing a significant enthalpy of hydration to these minerals. To receive a macromolecule, many of the water molecules must be desorbed. Thus, the system gains translational entropy, providing the driving force for the adsorption of the polymer molecule, as shown in Figure 3.4. Adsorption, which is normally an exothermic phenomenon, increases with the chain length of the polymer due to an increase in the contribution of van der Waals forces to the overall adsorption energy. In addition, considering that chains are flexible and, often, polyfunctional, the molecules can be attached to the mineral surface by several trains, which are segment-surface bonds, as shown in Figure 3.4b, leaving some unattached free segments (the loops or tails).[43]

Figure 3.4 – Uncharged and flexible polymer adsorption onto clay mineral surface from a dilute aqueous solution. (a) Polymer in solution adopting a random coil conformation and (b) on adsorption, the polymer chain uncoils and adopts a train-loop-tail conformation, displacing ordered water molecules from the interface into the external (bulk) solution.

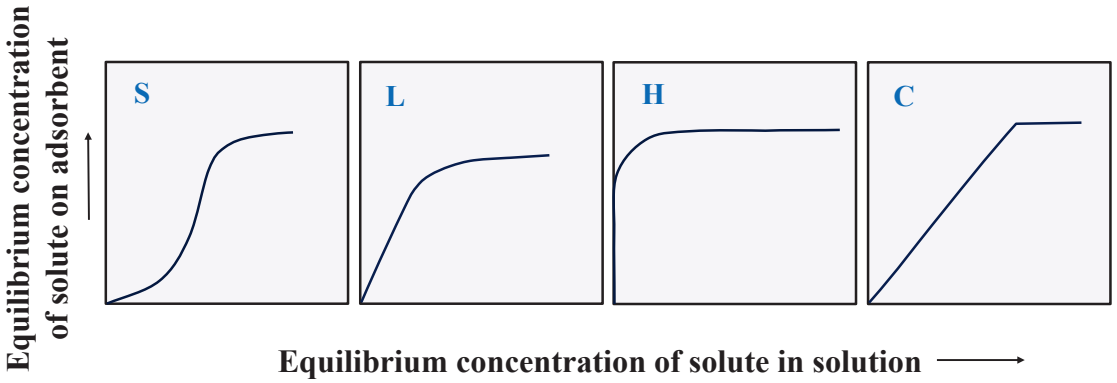


Source: adapted from ref. [43]

Clay-polymer interactions find various practical applications that are included, mainly, in agricultural and industrial segments.[44] In agriculture, polymers are used as "soil conditioners" to improve the quality of soils. In this regard, clays are linked to organic matter, such as humic substances,[45] polysaccharides[46] and synthetic anionic or nonionic polymers, to improve the stability of soil aggregates to water. Industrial examples of clay-polymer interactions include the production of composites (aiming the reinforcement of the polymeric material) or in papermaking (in which clays are used as fillers and coating materials of paper). In the last years, there have been several developments in the synthesis and characterization of clay/polymer nanocomposites. With the actual and potential applications of these new hybrid materials, increasing attention has been dedicated recently to better understand clay-polymer interactions.

A quantitative study that describes how polymers behave in the presence of a solid mineral interface, and that includes information about the conformational state of the adsorbed polymer chain, is not so trivial to be carried out. The determination of adsorption isotherms is probably the most used technique for this purpose. The shape of the isotherm give important information about the adsorption process and, based on the initial slope, four main types of solid-solution adsorption isotherms were listed by Giles et al. in 1960,[47] as shown in Figure 3.5.

Figure 3.5 – Different types of solid-solution adsorption isotherms.



Source: Adapted from ref. [47]

Among these four main shapes of isotherm most commonly observed, the C-curves (for constant partition) are found when there is a constant ratio between the concentration of solute remaining in the bulk solution and adsorbed on the solid surface is the same at any concentration. The S-type isotherm is characterized by a sigmoidal curve with a point of inflection. It is the result of a phenomenon called ‘‘cooperative adsorption’’, in which the adsorption of a first adsorbate helps making the adsorption of a second molecule easier. This type of curve is typically observed for non-polar organic compounds and surfactants, but rarely for polymers. Some works report cooperative adsorption of amphipathic block copolymers on hydrophilic substrates.[48, 49] The profile of the ‘‘L’’ (for Langmuir) isotherm is a concave curve, due to a progressive saturation of the solid, as the ratio between the concentration of the compound remaining in solution and adsorbed on the solid decreases with increasing solute concentration. The curve usually reaches a plateau when the solute concentration is above the solid’s adsorption capacity. In the ‘‘H’’ isotherm (for high-affinity), the initial region (the slope) of the curve is very steep because the affinity between solute and the solid substrate is very high even at minimal concentrations of solute. It is considered a particular case of the ‘‘L’’ isotherm, and solid-solution adsorption isotherms of most polymers are of the H-type. However, when measured at low concentration of solute, isotherms of polymers are frequently of the L-type.[43]

3.2.3.1.1. Anionic polyelectrolytes

It was in the nineteen-fifties that the interactions of negatively charged polymers and clays started to be studied with the purpose of using synthetic polyanions to stabilize natural soil aggregates since they can simulate the action of negatively charged soil polymers (humic substances and polyuronides, for instance).

When present in aqueous clay dispersions, polyanion molecules are capable of attaching themselves to more than one clay platelet at once, causing inter-particle bridging and, consequently, the flocculation of the particles. In fact, a considerable part of the literature on the interaction between clays and polyanions is related to the ability that the adsorbate has to affect the stability of clay dispersions. However, adsorption of polyanions does not result, necessarily, in flocculation. A group of conditions, related mainly to the polymer chain length or its molar mass, must be satisfied for effective flocculation. Otherwise, polyanions can have the opposite effect and, by increasing the stability of the clay dispersion, prevent flocculation. Indeed, the control of some factors, such as the ionic strength and the pH of the solution, may favor adsorption, contrary to the expectation that the negatively charged polymers are repelled by the negative charges of the clay surface.[50] The variations in the pH are responsible for changing the ionization and chain conformation of the polyanions, as well as the edge charges of the clay platelets and, in general, adsorption of polyanions increases with decreasing the pH.[51]

Some works based on X-ray diffractions indicate that, contrary to cationic and nonionic polymers, polyanions in general do not penetrate the galleries of 2:1 phyllosilicates. The mechanism by which the negatively charged polymers are attached to the platelets of these materials is still not fully understood, and different propositions have been elaborated, including electrostatic attraction or "anion exchange", hydrogen bonding between the surface hydroxyls and the C=O groups of the polymer, physical (van der Waals) interactions, hydrophobic bonding between the carbon chain of the polyanion and the uncharged basal surfaces of the clay and ligand exchange between the hydroxyl groups of the clay surface and the carboxylic groups of the polymer.[50]

Fulvic, humic and acrylic acids, however, seem to have been successfully intercalated into Montmorillonite at low pH (lower than 4). Ramos-Tejeda and coworkers[52] studied the effect of humic acid (HA) in flow properties of Mt dispersions, finding a significantly high adsorption of HA onto the platelets, as previously verified by Tombácz et al.[53]. The authors concluded that adsorption is not only explained by electrostatic attraction on the edges (which is the main phenomenon), but also by repulsive interactions between faces and HA molecules. In addition, the authors also consider coordinative and hydrophobic interactions.

While more in-depth studies have been carried out with Montmorillonite, a few works associate anionic polymers with Laponite (although, the edge surface area in

Laponite, compared to the total surface area of the platelets, is more representative than in Mt). The presence of negatively charged molecules in Laponite dispersions reduces the electrostatic attraction among surfaces and edges of different clay discs, avoiding the formation of 'House of Cards' structures.[54] A significant amount of the works that describe the addition of anionic polyelectrolytes to Laponite aim to increase the clay content in nanocomposite hydrogels, in order to enhance the gel strength. However, the success in preparing ionic nanocomposite hydrogels has been limited, since the addition of ionic monomers to clay dispersion causes aggregation and gelation, due to an increase in the ionic strength, which causes a decrease in the electrostatic repulsion among the platelets.[55, 56] Some successful examples include the use of sodium polyacrylate as anionic polyelectrolyte,[57] or the direct addition of acrylic acid (AA) into a $Na_4P_2O_7$-modified Laponite dispersion followed by *in situ* polymerization, to produce ionic PAA/Laponite hydrogels with improved mechanical properties.[56]

3.2.3.1.2. Cationic polyelectrolytes

Since Laponite is a cationic exchanger, polycations, such as the protonated form of poly(2-(dimethylamino)ethyl methacrylate) (PDMAEMA), can adsorb on its surface by electrostatic interaction between the opposite charges of the electrolytes and the platelet surface. Nonetheless, the use of positively charged polymers for the formation of clay/polymer complexes has received less attention than uncharged and negatively charged polymers in the last years. Most of the recent work in this area report the use of these polycations/clay complexes for the controlled release of herbicide, as sorbents for organic pollutants or as catalysts for organic reactions.[43]

Even at low concentrations, and in the absence of neutral molecules, positively charged polymers are effective in causing aggregation, since these molecules function as both coagulants and flocculants. While coagulation is caused by the charge neutralization and compression of the double layer around the platelets, flocculation is attributed to the interparticle bridging. Charge neutralization is usually the predominant phenomenon, however, the flocculation effect (bridging) can be more recurrent for polycations of high molar mass. In comparison to uncharged and anionic polymers, polycations are more effective, in general, in destabilizing clay dispersions.

Some works reported the capacity of different polycations to intercalate into Na^+ Mt, replacing the interlayer Na^+ cations.[58-60] The measurement of the basal spacing for the interlayer complex of Mt with polycations indicated that the intercalation of these molecules

happens in a flat (extended) conformation[6, 61] or, as obtained by Churchman et al.,[4] by multilayer intercalation. By measuring the anionic exchange capacity (AEC) of the complexes, and comparing it with the evolution of the cationic exchange capacity, Ueda et al. attested that loops and tails can be formed along polycations chains.[62] As the amount of adsorbed polycations increases, the polymer/Mt complex acquires an AEC different from the original CEC of the unmodified clay. The neutralization of the surface charges of Mt is caused by the train segments of the polycations, however, the appearance of an AEC can be attributed to the fact that part of the segments are presented as positively charged loops and tails. Some other factors that have a considerable effect on the conformation of the adsorbed polycation chains affect also their adsorption behavior, including molar mass and cationicity of the polycation and ionic strength of the suspension medium.[3, 5]

3.2.3.1.3. Nonionic polymers

There is a variety of uncharged, linear water soluble polymers that, possessing polar functional groups along their chain, can form complexes with clays.[10-12, 51, 63-70] These molecules are solvated by water and, by displacing the water molecules from the mineral surface, they can associate with the exchangeable cations through ion-dipole interactions. Various hydrophilic polymers interact with clay minerals in aqueous medium, among which are poly(vinyl alcohol),[63-65] poly(vinyl pyrrolidone)[66, 67] and nonionic polyacrylamide,[51, 68, 69] however, the attention in this section will be dedicated exclusively to poly(ethylene glycol) (PEG)/poly(ethylene oxide) (PEO).[10-12, 70]

In fact, as a general rule, the terms PEG and PEO have been considered synonyms for polymeric structures containing two hydroxyl groups bound to different carbon atoms (glycol groups). As a tendency, the term PEG has been used in the literature when referring to polymers with low molar mass (usually below 20000 g mol^{-1}), while PEO has been applied for larger polymer chains (in some cases above 2000 g mol^{-1}). In addition, the end-group contribution can be considered an important factor in the nomenclature of these structures, as end groups play an increasing role in the solubility of the polymer or oligomer in water as the molar mass of the compound decreases. However, no official definition of a transition molar mass region has been defined yet. Therefore, the compounds used in this work will be referred to as PEG, since they present low molar mass, however, as some authors use these terms interchangeably or according to their application, the term PEO will be maintained when referring to other works, respecting the choice of the authors.

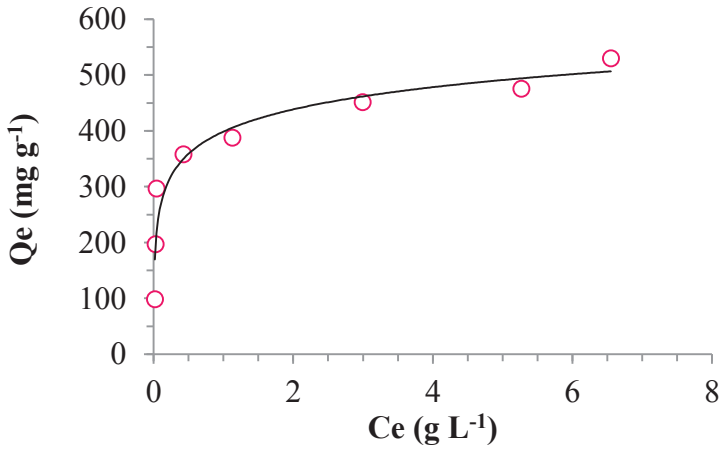
The interaction of Laponite with PEG, and other nonionic polymers, is more controversial than most polyelectrolytes. Most believe that PEG chains adsorb onto clay disks by hydrogen bond between the hydrogen from the silanol groups (SiOH), available at the clay surface, and the oxygen present in the PEG chains, but others claim that it is not the hydrophilic but the hydrophobic ethylene groups of PEG structure that interact with the siloxane groups of Laponite by hydrophobic interaction. Adsorption can also be attributed to other phenomena, such as ion−dipole interactions between the exchangeable cation present in the interlayer region of the platelets (Na^+) and the polar nonionic polymer chains (capable of donating electrons), as mentioned above, or van der Waals forces, for instance.[9] Nevertheless, even though the mechanism of adsorption is not completely elucidated yet, being still under debate, it is known that PEO has a good interaction with Laponite, and has considerable effects on the stability of the clay suspension.

Mongondry et al.[10] studied the effect of PEO of different molar masses on the aggregation and gelation of Laponite dispersions. The authors used PEO of 2000 g mol^{-1}, 10000 g mol^{-1} and 20000 g mol^{-1} and, by analysis of the adsorption isotherms of these molecules and the fitting of the data to the Langmuir model, obtained adsorbed amounts at saturation (Q_{max}) between 590 and 870 mg g^{-1} for the polymers of 2000 and 20000 g mol^{-1}, respectively. The authors concluded that PEO chains, by adsorbing onto the Laponite particles, inhibit aggregation of the platelets by increasing the activation energy for face-to-rim association due to steric hindrance. Even though it may be expected that aggregation decreases with increasing molar mass, this was not observed. Longer PEO chains can be associated to the bridging between different particles, which leads to less effective protection against aggregation. The reduction of aggregation rate depends, in fact, on the molar mass, however, authors concluded that it is maximal at about 1000 g mol^{-1}.

Andrew Nelson and Terence Cosgrove[11] investigated the adsorption of PEO on Laponite as a function of the molar mass using small-angle neutron scattering (SANS) combined with contrast variation. Results indicated that adsorption of PEO follows a core-shell model in which polymer is present not only on the face of the clay particles but also extends over the edges, “wrapping” the rims of the platelets (not meaning, however, that the molecules adsorb on the edges). The polymer layers were found to be unusually thin, with little influence of molar mass. The edge layer thickness, on the other hand, grew with a power law dependence on the molar mass. These results were explained by a possible accumulation of the additional polymer segments around the edge of the particles rather than on the face.

In 2010, Bourgeat-Lami et al. reported the use of a methyl ether acrylate-terminated poly(ethylene glycol) macromonomer to promote the association of Laponite platelets with hydrophobic polymer by soap-free emulsion copolymerization of styrene and *n*-butyl acrylate (BA). The strategy led to armored film-forming latex particles with high solids content.[71] Some years later, the same group[12] extended the technique and used a trithiocarbonate poly(ethylene glycol)-based macromolecular RAFT agent, with a molar mass of 2000 g mol^{-1}, as coupling agent between Laponite platelets and the hydrophobic polymer, which was synthesized *in situ* by emulsion polymerization. An adsorption study carried out by the group revealed a high affinity of the PEG-based macroRAFT for Laponite and the isotherm data fitted well to the Langmuir adsorption model, as shown in Figure 3.6. With the linearized form of the Langmuir equation, the Langmuir parameters were determined. An adsorbed amount at saturation of 515 mg g^{-1} and a binding energy constant, K_L, of 5.8 L mg^{-1} were obtained. The authors also concluded that the thiocarbonylthio end group of the macroRAFT agent had no considerable effect on the adsorption.

Figure 3.6 – Adsorption Isotherm of PEO-CTPPA onto Laponite (10 g L^{-1}). The solid line is the fitting to the Langmuir equation. The experimental data fitted well to the Langmuir adsorption model with a high correlation coefficient.



Source: Adapted from ref. [12]

3.3 Synthesis of macroRAFT agents

3.3.1 Experimental section

3.3.1.1 Materials

Sodium 1-propanethiolate (Aldrich, 99%), carbon disulfide (Aldrich, >99%), potassium hexacyanoferrate (III) ($K_3Fe(CN)_6$, Aldrich, ≥99,99%), N,N'-dicyclohexyl carbodiimide (DCC, Fluka, 99%), 4-dimethylaminopyridine (DMAP, Aldrich, 99%), 4,4′-azobis(cyanovaleric acid) (ACPA, ≥98%, Sigma-Aldrich), (trimethylsilyl)diazomethane (Aldrich, solution 2.0 M in diethyl ether), silica gel (Gerduran® Si 60, 40-63 μm pore size, Merck) and 1,3,5-trioxane (>99%, Sigma-Aldrich) were all used as received. Anhydrous dichloromethane (CH_2Cl_2, 99%), 1,4-dioxane (> 99.5%), diethyl ether (> 99.5%) petroleum ether (p.a.) and ethyl acetate were purchased from Sigma-Aldrich and used with no further purification. Tetrahydrofuran (THF) (VWR Recaptur, stabilized) was used as solvent in the methylation of AA-containing macroRAFT agents and iodomethane (ICH_3, Vetec, 99%) was used for the quaternization of DMAEMA-based macroRAFTs.

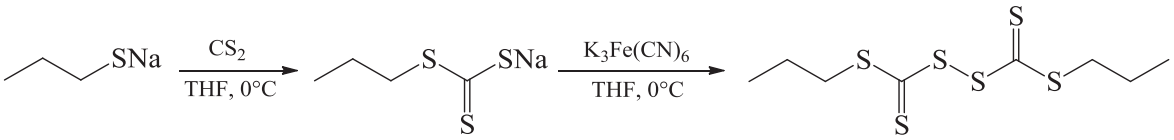
Poly(ethylene glycol) methyl ether (mPEG) 2000 g mol^{-1} (Fluka, 99.5%) was distilled twice with toluene before use and the monomers: acrylic acid (AA, anhydrous, 99% Sigma-Aldrich), poly(ethylene glycol) methyl ether acrylate (PEGA, 480 g mol^{-1}, 99%, Sigma-Aldrich), 2-(dimethylamino)ethyl methacrylate (DMAEMA, 99% stabilized, Acros Organics) and *n*-butyl acrylate (BA, 99%, Sigma-Aldrich) were all used as received. Deuterated chloroform ($CDCl_3$), deuterium oxide (D_2O), dimethyl sufoxide-d_6 (DMSO-d_6, 99%, Sigma-Aldrich) were used for ^1H NMR analysis and THF (HPLC, stabilized/BHT, Sigma-Aldrich), N,N-dimethylformamide (DMF for HPLC, ≥99.5%, Sigma-Aldrich) and lithium bromide were used for SEC analysis.

3.3.1.2 Methods

The RAFT agent: 4-cyano-4(propylsulfanylthiocarbonyl) sulfanylpentanoic acid (CTPPA) was synthesized according to a methodology described elsewhere.[72, 73] The synthesis of this trithiocarbonate ester is composed of two main steps: first, the synthesis of the intermediate bis(propyl-sulfanylthiocarbonyl) disulfide, and the further reaction of this

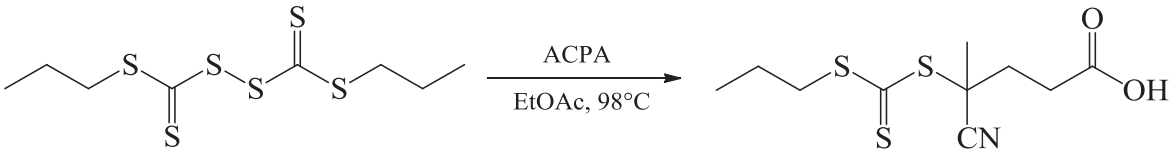
molecule with 4,4-azobis cyanovaleric acid (ACPA). Scheme 3.1 and Scheme 3.2 show both steps of the synthetic route towards the CTPPA RAFT agent.

Scheme 3.1 – Synthetic route towards bis(propyl-sulfanylthiocarbonyl) disulfide from sodium propanethiolate and carbon disulfide.



Source: elaborated by the author.

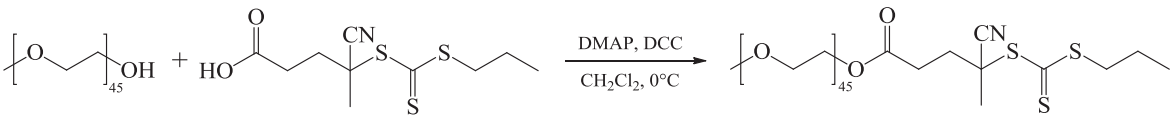
Scheme 3.2 – Synthetic route towards the CTPPA RAFT agent from bis(propyl-sulfanylthiocarbonyl) disulfide.



Source: elaborated by the author.

The product was purified using a silica gel column and stored after synthesis at 4 ºC under argon atmosphere. A trithiocarbonate macroRAFT agent composed of a linear block of poly(ethylene glycol), PEG-CTPPA, was synthesized via an esterification reaction between a 2000 g mol^{-1} mPEG and CTPPA, according to the procedure described in the literature[73] and shown in Scheme 3.3. This macroRAFT agent was synthesized to be applied as a precursor in the further chain extension with acrylic acid, in order to obtain the block copolymer, PEG-*b*-PAA-CTPPA, but also to be used directly as the mediator in the synthesis of P(MMA-*co*-BA)/Laponite hybrid latexes.

Scheme 3.3 – Synthetic route towards PEG$_{45}$-CTPPA macroRAFT.



Source: elaborated by the author.

For the synthesis of the macroRAFT agents MR2 to MR12, shown in Table 3.2, by solution polymerization, initially, the chain transfer agent (CTA) was added to a round-bottom glass flask, where the initiator, ACPA (10% of the molar concentration of RAFT agent) and the monomers were added. 1,3,5-Trioxane was used as an internal reference for determination of monomer conversion by ^{1}H NMR, in a molar ration of $^{1}/_{12}$ related to

monomer(s). The mixture was dissolved in 1,4-dioxane, in order to obtain a final monomer concentration of ~25% w/v and the reaction medium was purged for 30 min with nitrogen and then heated to 80 °C to start polymerization. Samples were taken periodically and, after ~7-8 hours, polymerization was quenched by immersing the flask into an ice bath. The final products were submitted to 3 precipitation cycles using a large volume of petroleum ether and dried overnight under vacuum at room temperature. The amounts of CTA and monomers used in the synthesis are shown in Table 3.2.

Some of the homo and copolymers synthesized were used, after purification, as a precursor in chain extension reactions, in order to obtain block copolymers. The synthesis of these macroRAFT agents was carried out using a similar procedure to the one described above, but the chain transfer agent CTPPA was replaced, in these cases, by the macroRAFT agents: PEG-CTPPA, PAA-CTPPA or P(AA-*co*-BA)-CTPPA.

Table 3.2 – MacroRAFT agents synthesized and recipes used in the synthesis.

Entry	MacroRAFT agent	[CTA] (mM)	[Monomer]$_0$ (M)			
			AA	PEGA	BA	DMAEMA
MR1	PAA_{42}-CTPPA	60.0	2.50	-	-	-
MR2	P(AA_{16}-*co*-BA_{16})-CTPPA	114.8	1.84	-	1.84	-
MR3	PEG_{45}-CTPPA	-	-	-	-	-
MR4	PEG_{45}-*b*-PAA_{49}-CTPPA	62.2	3.05	-	-	-
MR5	P(AA_{40}-*b*-$PEGA_5$)-CTPPA	74.6	-	0.36	-	-
MR6	PAA_{40}-*b*-($PEGA_7$-*co*-BA_4)-CTPPA	54.8	-	0.41	0.23	-
MR7	P(AA_{16}-*co*-BA_{16})-*b*-($PEGA_7$-*co*- BA_4)-CTPPA	50.9	-	0.35	0.20	-
MR8	P($PEGA_7$-*co*-BA_4)-CTPPA	54.5	-	0.36	0.22	-
MR9	P(AA_5-*co*-$PEGA_5$-*co*- BA_5)-CTPPA	60.9	0.31	0.30	0.30	-
MR10	P(AA_{10}-*co*-$PEGA_{10}$-*co*- BA_{10})-CTPPA	29.3	0.31	0.29	0.29	-
MR11	P($DMAEMA_{10}$-*co*-BA_5)-CTPPA	91.4	-	-	0.46	0.90
MR12	P($DMAEMA_{20}$-*co*-BA_{20})-CTPPA	34.9	-		0.68	0.68

Source: elaborated by the author.

MacroRAFT P($DMAEMA_{10}$-*co*-BA_5)-CTPPA (MR11) was submitted to a quaternization reaction with CH_3I.[74, 75] Initially, 34.30 g of the unpurified reaction product was dissolved in 100 mL of THF in a 250 mL glass reactor. This amount of unpurified product contains 6.78 g of the copolymer P($DMAEMA_{10}$-*co*-BA_5)-CTPPA, which represents 0.029 mol of DMAEMA repeating units. With a glass syringe, CH_3I (5.00 g or 0.035 mol) was added dropwise into the reactor under N_2 atmosphere at room temperature.

The quaternization of the copolymer could be visually monitored by the precipitation of quaternized chains and the reaction was maintained for 18 h. The quaternized product was a yellowish powder that was submitted to filtration with THF. It was, then, dried under vacuum to eliminate the solvent and residual CH_3I. A similar procedure was used for the quaternization of P(DMAEMA$_{20}$-*co*-BA$_{20}$)-CTPPA (MR12).

3.3.1.3 Characterizations

For the synthesis of macroRAFT agents, the final monomer conversions were monitored by proton nuclear magnetic resonance analysis (^{1}H NMR) at room temperature (Bruker DRX 300), by diluting the crude reaction medium in DMSO-d_6. By relying on the use of 1,3,5-trioxane an internal standard, the relative integration the vinylic protons of the monomers led to the determination of monomer conversion. Final products obtained after the synthesis of RAFT agent CTPPA and macroRAFT agents were dried under vacuum overnight at room temperature and characterized by ^{1}H NMR spectroscopy, using deuterated chloroform ($CDCl_3$) or deuterium oxide (D_2O) as solvents.

The average molar masses (number-average molar mass, M_n, and weight-average molar mass, M_w) and the molar mass dispersity ($Đ = M_w/M_n$) of macroRAFT agents were determined by Size Exclusion Chromatography (SEC). Measurements were performed using a Viscotek TDA305 system from Malvern Instruments equipped with a differential refractive index detector (RI) (λ=670 nm). The separation was carried out on three columns [T6000 M General Mixed Org (300 x 8 mm)]. AA-based molecules had their carboxylic groups methylated with tri(methylsilyl)diazomethane methylation agent, in a THF/H_2O mixture[76] before injection. All samples were filtrated through a 0.45 µm pore-size membrane and analyzed at the concentration of 5 mg mL^{-1}. For PEGA- and AA-based molecules, analyses were performed at 40 °C with THF as eluent at a flow rate of 1 mL min^{-1}, using toluene as a flow rate marker. For the analysis of DMAEMA-based macroRAFT agent, the eluent was DMF (with LiBr, 0.01 mol L^{-1}), with toluene as a flow rate marker. The analyses were performed at 50 °C, using an EcoSEC semi-micro SEC system from Tosoh, equipped with a dual flow refractive index detector and a UV detector. Separation was performed with a guard column and three PSS GRAM columns (7 µm, 300 × 7.5 mm). M_n, M_w and $Đ$ were obtained by deriving the RI signal and using a calibration curve based on polystyrene (PS) or PMMA standards (from Polymer Laboratories).

3.3.2 Results and Discussion

Three different types of macroRAFT agents, presenting anionic, cationic or nonionic (linear or pending) blocks, were synthesized. These (co)polymers have either acrylic acid, DMAEMA or PEG-based structures, and the addition of each of these components aims different types of interactions with Laponite. The results obtained in the synthesis are listed in Table 3.3. A brief description of each result is given individually in the following subsections.

Table 3.3 – Overall monomer conversion, theoretical and experimental molar mass and dispersity for the macroRAFT agents: PAA_{42}-CTPPA (MR1); P(AA_{16}-*co*-BA_{16})-CTPPA (MR2); PEG_{45}-CTPPA (MR3); PEG_{45}-*b*-PAA_{49}-CTPPA (MR4); P(AA_{40}-*b*-$PEGA_5$)-CTPPA (MR5); PAA_{40}-*b*-P($PEGA_7$-*co*-BA_4)-CTPPA (MR6); P(AA_{16}-*co*-BA_{16})-*b*-P($PEGA_7$-*co*-BA_4)-CTPPA (MR7); P($PEGA_7$-*co*-BA_4)-CTPPA (MR8); P(AA_5-*co*-$PEGA_5$-*co*-BA_5)-CTPPA (MR9); P(AA_{10}-*co*-$PEGA_{10}$-*co*-BA_{10})-CTPPA (MR10); P($DMAEMA_{10}$-*co*-BA_5)-CTPPA (MR11) and P($DMAEMA_{20}$-*co*-BA_{20})-CTPPA (MR12).

Entry	X [a] (%)	*nAA*[b]	*nPEGA*[b]	*nBA*[b]	*nDMAEMA*[b]	$M_{n,\,theo}$ (g mol^{-1})	$M_{n,\,exp}$ (g mol^{-1})	$Đ$
MR1	94.6	39.5	-	-	-	3120	3630	1.19
MR2	98.2	15.8	-	15.8	-	3440	3420	1.26
MR3[c]	-	-	-	-	-	2270	-	-
MR4[d]	85.9	42.1	-	-	-	5310	6710	1.18
MR5[e]	84.3		4.0	-	-	5460	4640	1.31
MR6[e]	87.4	-	6.4	3.7	-	7320	6130	1.21
MR7[f]	96.1	-	6.5	3.9	-	6820	4810	1.35
MR8	79.1	-	5.3	3.1	-	3070	2900	1.12
MR9	86.5	4.2	4.1	4.2	-	3100	3120	1.19
MR10	82.9	8.8	8.8	8.6	-	6230	5730	1.20
MR11	86.6	-	-	3.9	9.7	2310	950	1.24
MR12	81.1	-	-	14.2	18.5	4400	4560	1.40

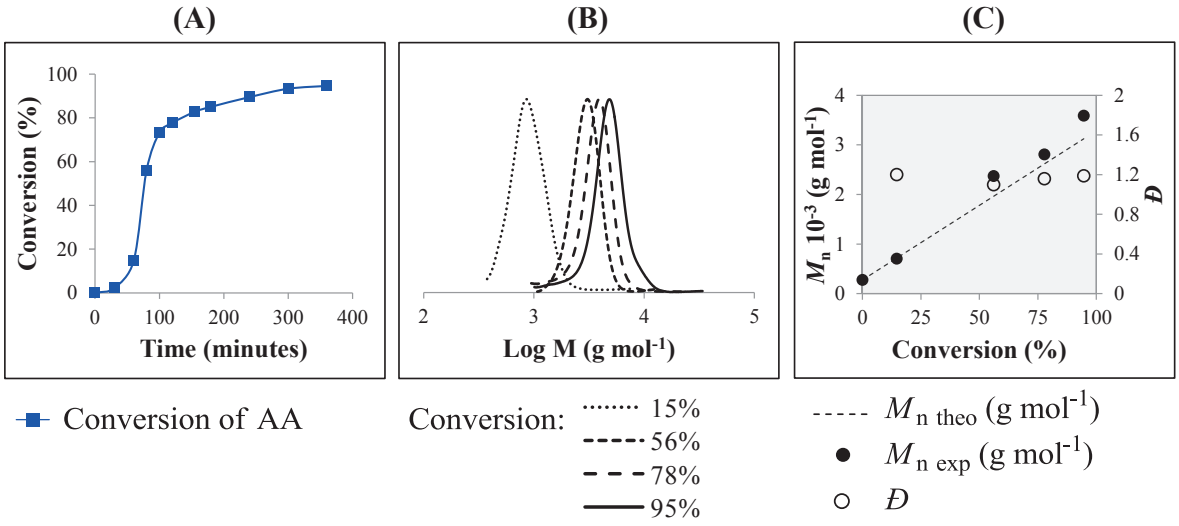
[a] X = overall monomer conversion;
[b] n = actual number of repeat units in the polymer chain based on the individual conversion of each comonomer.
[c] Synthesized via esterification reaction between mPEG and CTPPA.
[d] Synthesized using MR3, PEG-CTPPA, as precursor.
[e] Synthesized using MR1, PAA-CTPPA, as precursor.
[f] Synthesized using MR2, P(AA-*co*-BA)-CTPPA, as precursor.
Source: elaborated by the author.

3.3.2.1 Synthesis of PAA-based macroRAFT agents

3.3.2.1.1. PAA_{42}-CTPPA (MR1)

To synthesize the AA-based macroRAFT agent, PAA_{42}-CTPPA, the chain transfer agent CTPPA was used in the polymerization of AA. A theoretical molar mass of 3120 g mol^{-1} was aimed, which represents targeting the addition of 42 units of acrylic acid to the CTA. A final conversion of 94.6% was achieved after 6 hours of polymerization, as shown in Figure 3.7A, indicating that, if all RAFT agent was activated, 39.5 units were added. For the determination of the number average molar mass (M_n) and the dispersity ($Đ$) by SEC in THF, the product was purified and submitted to the methylation process. The final number average molar mass obtained ($M_{n\ exp}$ = 3630 g mol^{-1}) was slightly superior to the theoretical value. However, a good control over the homopolymerization of AA was achieved, as shown in the complete shift of the SEC chromatograms (Figure 3.7B), the linear increase of M_n with conversion (Figure 3.7C) and the narrow distribution of molar masses ($Đ$=1.19).

Figure 3.7 – RAFT polymerization of AA in solution of 1,4-dioxane at 80°C. (A) Evolution of AA conversion versus time, determined by ^{1}H NMR; (B) THF-SEC chromatogram peaks and (C) number-average molar masses (M_n; full symbols) and dispersities ($Đ$; open symbols) with overall monomer conversion at 0%, 56%, 78% and 95% conversions for the synthesis of PAA_{42}-CTPPA (MR1).



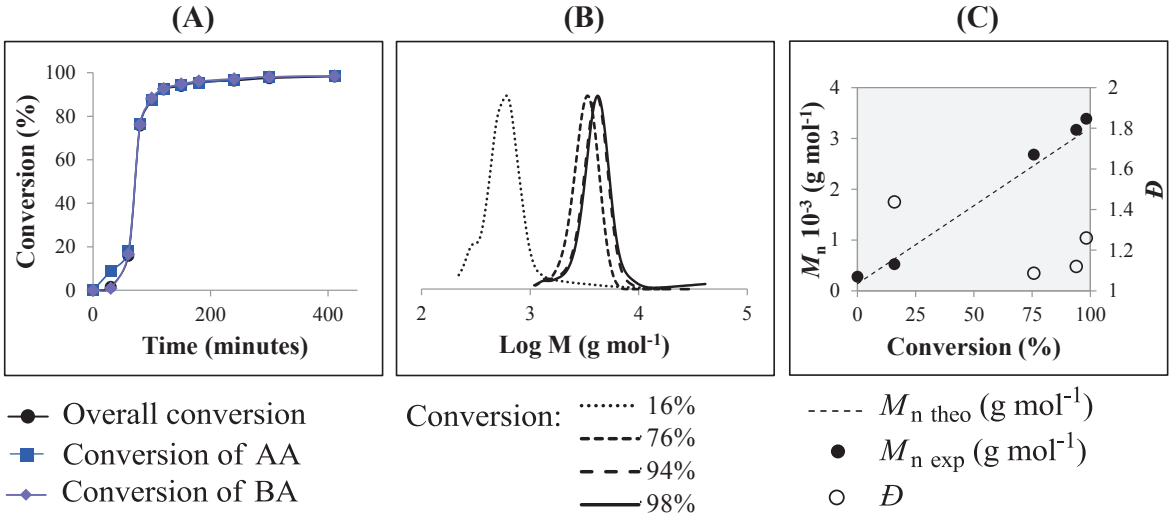
Source: elaborated by the author.

3.3.2.1.2. $P(AA_{16}$-co-$BA_{16})$-CTPPA (MR2)

MacroRAFT agent $P(AA_{16}$-*co*-$BA_{16})$-CTPPA was synthesized using the chain transfer agent CTPPA. The evolution of overall and individual acrylic acid and butyl acrylate conversions was determined by ^{1}H NMR spectroscopy, and it is shown in Figure 3.8A. The

molar mass of the macroRAFT agent was determined by SEC in THF and the chromatogram is shown in Figure 3.8B, as well as the evolution of molar mass and dispersity with conversion, in Figure 3.8C. It can be seen that M_n values increase linearly with conversion and they are close to the theoretical values, which is consistent with RAFT-mediated polymerizations. However, dispersity reached the value of 1.44 during the first 60 minutes of polymerization. Considering that the polymer samples were not purified after the methylation process, it can be speculated that the high dispersity obtained in the beginning of polymerization was due to the superposition of the peak from the sample with the signal from the methylation agent, since a low molar mass (560 g mol^{-1}) had been reached until this point. For the rest of polymerization, $Đ$ ranged from 1.09 to 1.26.

Figure 3.8 – RAFT copolymerization of AA with BA in solution of 1,4-dioxane at 80°C. (A) Evolution of monomer conversion with time; (B) size exclusion chromatogram peaks and (C) evolution of the number-average molar masses (M_n; full symbols) and dispersities ($Đ$; open symbols) with monomer conversion at 16%, 76%, 94% and 98% monomer conversions, for the synthesis of P(AA$_{16}$-*co*-BA$_{16}$)-CTPPA (MR2).



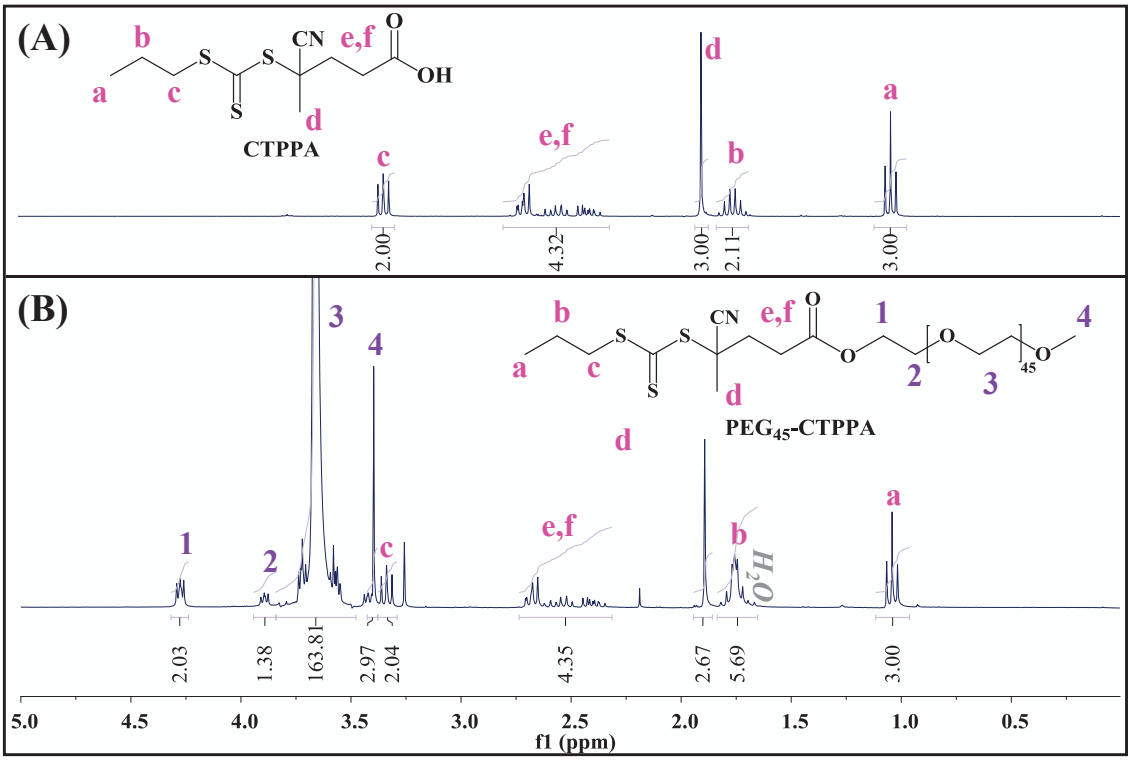
Source: elaborated by the author.

3.3.2.2 Synthesis of PEG-based macroRAFT agents

3.3.2.2.1. PEG$_{45}$-CTPPA (MR3)

PEG$_{45}$-CTPPA macroRAFT agent has been synthesized by an esterification reaction between mPEG (2000 g mol^{-1}) and CTPPA, as reported in the experimental section. The comparison between the ^{1}H NMR spectra of the RAFT agent CTPPA, shown in Figure 3.9A, and of the macroRAFT agent PEG$_{45}$-CTPPA, shown in Figure 3.9B, indicates that PEG$_{45}$-CTPPA with a high degree of purity was successfully obtained.

Figure 3.9 – ^{1}H NMR spectra of (A) CTPPA and (B) PEG_{45}-CTPPA macroRAFT agent (MR3).



Source: elaborated by the author.

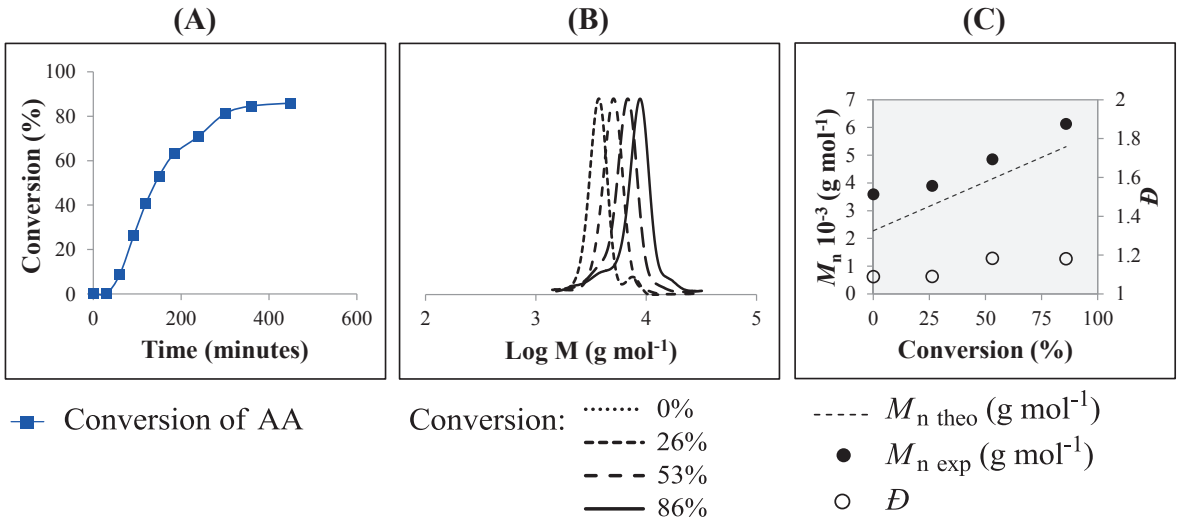
3.3.2.2.2. PEG_{45}-b-PAA_{49}-CTPPA (MR4)

For the synthesis of the PEG_{45}-*b*-PAA_{49}-CTPPA block copolymer, macroRAFT agent PEG_{45}-CTPPA was used as the precursor in the chain extension with AA. The effect of time of reaction on the conversion of acrylic acid when PEG_{45}-CTPPA was used as chain transfer agent is shown in Figure 3.10A. A final conversion of 86% was obtained after 450 minutes, at the end of polymerization, which indicates that 42 units of AA were added to PEG_{45}-CTPPA. The comparison between Figure 3.7A and Figure 3.10A indicates that both presented a short induction period, however, when PEG_{45}-CTPPA was used as the RAFT agent, the increase in conversion was slightly slower than with CTPPA. This could be attributed to the increase in viscosity caused by the PEG CTA.

Figure 3.10B shows the SEC chromatograms and a peak of low intensity that can be attributed to remaining PEG_{45}-CTPPA chains in the reaction medium that were not activated, appears as the molar mass increases. These molecules could also be residual mPEG from the synthesis of PEG_{45}-CTPPA. In addition, the first curve, corresponding to PEG_{45}-CTPPA, presents another peak of lower intensity that could be attributed to the existence of chains with higher molar mass in commercial mPEG or to coupling reactions between some PEG_{45}-CTPPA molecules. However, the living character of AA polymerization in the presence of

PEG_{45}-CTPPA was confirmed in Figure 3.10C by the linear increase of molar mass with conversion and by the low dispersities (1.09-1.18). Even though data showed a linear behavior, they did not follow the theoretical curve, from which they are deviating of approximately 1300 g mol^{-1}. A theoretical molar mass of 5310 g mol^{-1} was predicted and an experimental value of 6130 g mol^{-1} was obtained by SEC in THF. This difference could be explained by the use of PMMA standards, which are not the most indicated for PEG chains, due to the different characteristics of both molecules.

Figure 3.10 – RAFT polymerization of AA in solution of 1,4-dioxane at 80°C. (A) Evolution of AA, determined by ^{1}H NMR, versus time; (B) THF-SEC chromatogram peaks and (C) number-average molar masses (M_n; full symbols) and dispersities ($Đ$; open symbols) with overall monomer conversion at 0%, 26%, 53% and 86% conversions for the synthesis of PEG_{45}-*b*-PAA_{49}-CTPPA (MR4).

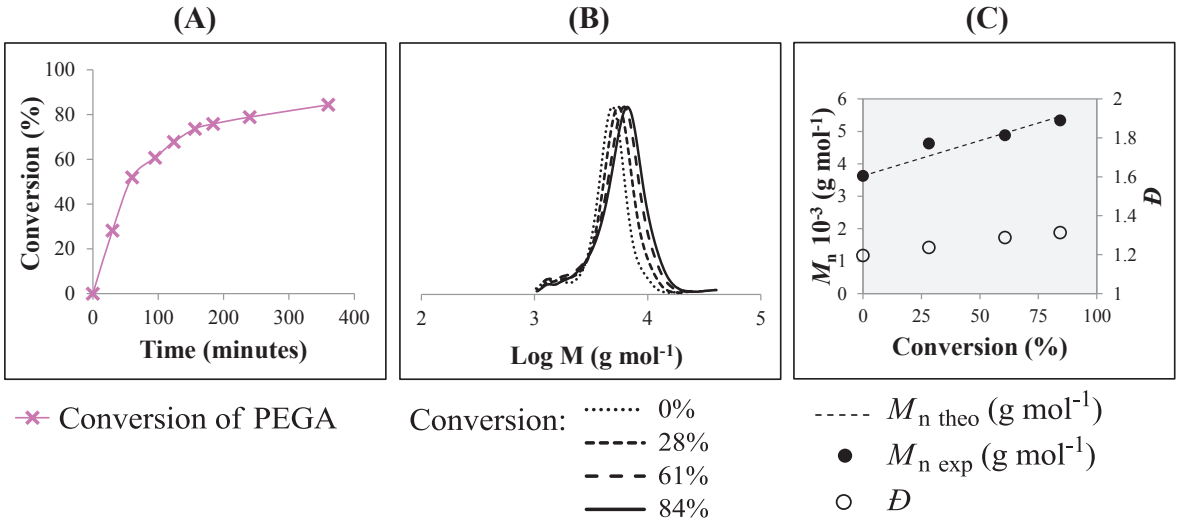


Source: elaborated by the author.

3.3.2.2.3. P(AA_{40}-b-$PEGA_5$)-CTPPA (MR5)

For the synthesis of block copolymer P(AA_{40}-*b*-$PEGA_5$), macroRAFT agent PAA_{40}-CTPPA (MR1) was used as precursor in the chain extension reaction with PEGA. After 6 hours of reaction, nearly 85% of conversion was obtained, and the curve is shown in Figure 3.11A. The chromatograms shown in Figure 3.11B indicate a modest shift of the SEC curves towards high molar masses, and the evolution of molar mass with conversion from Figure 3.11C indicates that the results fit well with the expected theoretical values. While a final M_n of 5460 g mol^{-1} was expected, the final sample had a molar mass of 4640 g mol^{-1} and a $Đ$ of 1.31.

Figure 3.11 – RAFT polymerization of PEGA in solution of 1,4-dioxane at 80°C. (A) Evolution of PEGA conversion, determined by ^{1}H NMR, versus time; (B) THF-SEC chromatogram peaks and (C) number-average molar masses (M_n; full symbols) and dispersities ($Đ$; open symbols) with overall monomer conversion at 0%, 28%, 61% and 84% conversions for the synthesis of P(AA_{40}-*b*-$PEGA_5$)-CTPPA (MR5).

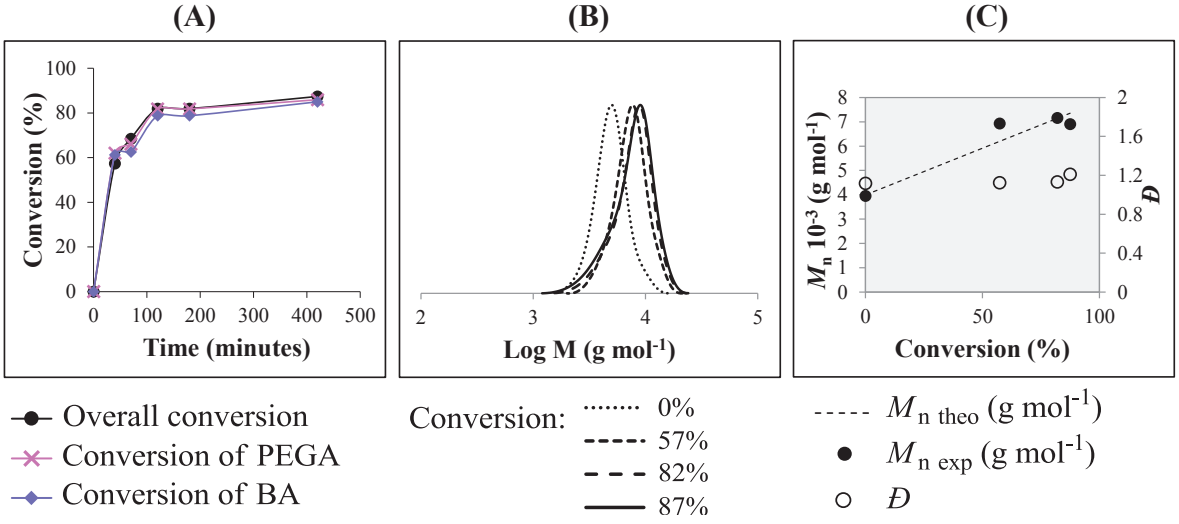


Source: elaborated by the author.

3.3.2.2.4. PAA_{40}-b-P($PEGA_7$-co-BA_4)-CTPPA (MR6)

MacroRAFT agent PAA_{40}-*b*-P($PEGA_7$-*co*-BA_4)-CTPPA was synthesized using PAA_{40}-CTPPA (MR1) as chain transfer agent and precursor for the chain extension with PEGA and BA. Figure 3.12A shows the conversion profiles for each monomer, as well as the overall conversion, versus time. Individual conversions were similar for both monomers, which indicates the absence of composition drift. A final overall conversion of 87% was achieved after 7 hours of polymerization. The SEC curves, shown in Figure 3.12B, indicate a clear shift from the PAA_{42}-CTPPA curve, however, it is possible to see a remaining shoulder, which indicates that some of the chains from the precursor were not activated and did not suffer chain extension with PEGA and BA. A dispersity of 1.21 was obtained and M_n, 6130 g mol^{-1}, was below the theoretical value of 7320 g mol^{-1}.

Figure 3.12 – RAFT polymerization of PEGA in solution of 1,4-dioxane at 80°C (A) Evolution of PEGA conversion, determined by ^{1}H NMR, versus time; (B) THF-SEC chromatogram peaks and (C) number-average molar masses (M_n; full symbols) and dispersities ($Đ$; open symbols) with overall monomer conversion at 0%, 57%, 82% and 87% conversions for the synthesis of PAA_{40}-*b*-$P(PEGA_7$-*co*-$BA_4)$-CTPPA (MR6).



Source: elaborated by the author.

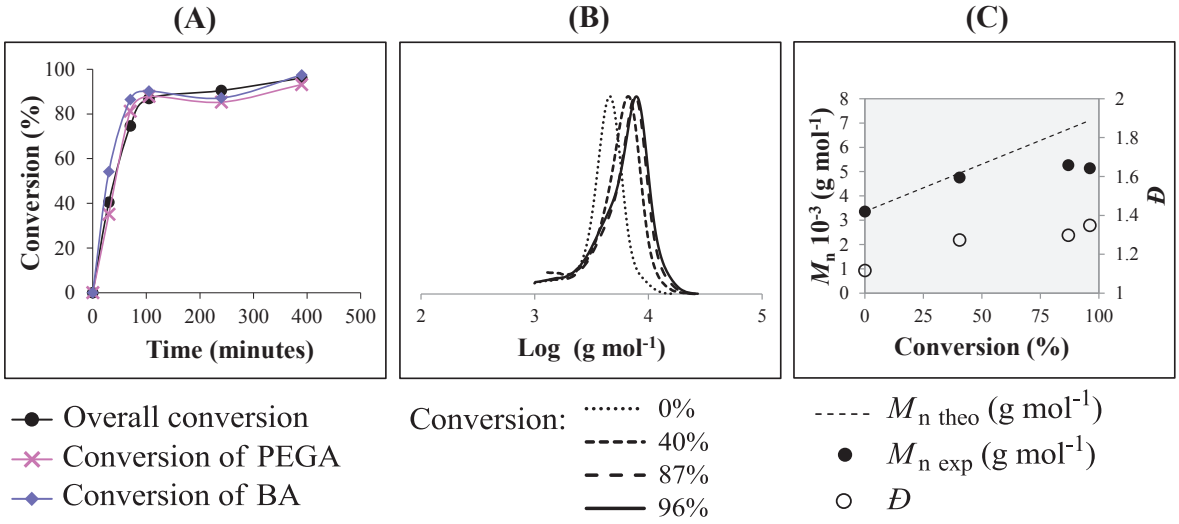
3.3.2.2.5. P(AA$_{16}$-co-BA$_{16}$)-b-P(PEGA$_7$-co-BA$_4$)-CTPPA (MR7)

MacroRAFT agent P(AA$_{16}$-*co*-BA$_{16}$)-*b*-P(PEGA$_7$-*co*-BA$_4$)-CTPPA was synthesized in two-steps. The first step consisted in the synthesis of the P(AA$_{16}$-co-BA$_{16}$) block (MR2). In the second step, this macroRAFT agent was used as the precursor on the block extension with PEGA and BA for the synthesis of P(AA$_{16}$-*co*-BA$_{16}$)-*b*-P(PEGA$_7$-*co*-BA$_4$)-CTPPA. A final global conversion of 96% was achieved after 390 minutes, as shown in Figure 3.13A. It can also be seen that high PEGA and BA individual conversions were achieved and a final copolymer containing 6.5 units of PEGA and 3.9 units of BA was obtained.

Figure 3.13C shows the evolution of number-average molar masses and dispersities with monomer conversion. Number-average molar mass of the final product, obtained by SEC analysis in THF, was 4810 g mol^{-1}, which is lower than the expected theoretical value (6820 g mol^{-1}). This could be attributed, again, to the different characteristics between PMMA standards and PEG chains, which, additionally, have the ethylene oxide segments disposed in a pending configuration. However, a comparison between the kinetic profile of MR6 and MR7 (both having the same pending configuration of PEG chains, with the same number of units), reveals that the events determining the molar mass of these copolymers go beyond the pending configuration of the PEG chains. It is possible to note that the experimental molar masses increase quite linearly with conversion for the synthesis of MR6, and a slight decrease in M_n is observed for the final values of conversion, which confirms

that this is a trend when using PEGA (although this was not observed for MR5, for which the molar masses are in agreement with the theoretical values). The most important effect could be, therefore, the different microstructures of both macroRAFT agents. In other words, the different conformation and distribution profile of AA units in the backbone of these copolymers results in different intramolecular interactions, with different intensities, between the blocks of AA and PEGA segments. It is possible that, in the case of MR7, the AA units are submitted to more interactions with the PEGA segments, resulting in a lower hydrodynamic volume (and, consequently, in lower molar masses). This experiment was not repeated, however, to confirm if this is a trend for this comonomer. A final dispersity of 1.35 was obtained and it can be seen by the size exclusion chromatogram peaks, shown in Figure 3.14B, that a small shoulder, relative to remaining P(AA_{16}-*co*-BA_{16})-CTPPA chains, is present in all samples.

Figure 3.13 – RAFT copolymerization of PEGA with BA in solution of 1,4-dioxane at 80°C. (A) Evolution of PEGA and BA conversions, determined by ^{1}H NMR, versus time; (B) THF-SEC chromatogram peaks and (C) number-average molar masses (M_n; full symbols) and dispersities ($Đ$; open symbols) with overall monomer conversion at 0%, 40%, 87% and 96% conversions for the synthesis of P(AA_{16}-*co*-BA_{16})-*b*-P($PEGA_7$-*co*-BA_4)-CTPPA (MR7).



Source: elaborated by the author.

3.3.2.2.6. P(PEGA$_7$-co-BA$_4$)-CTPPA (MR8)

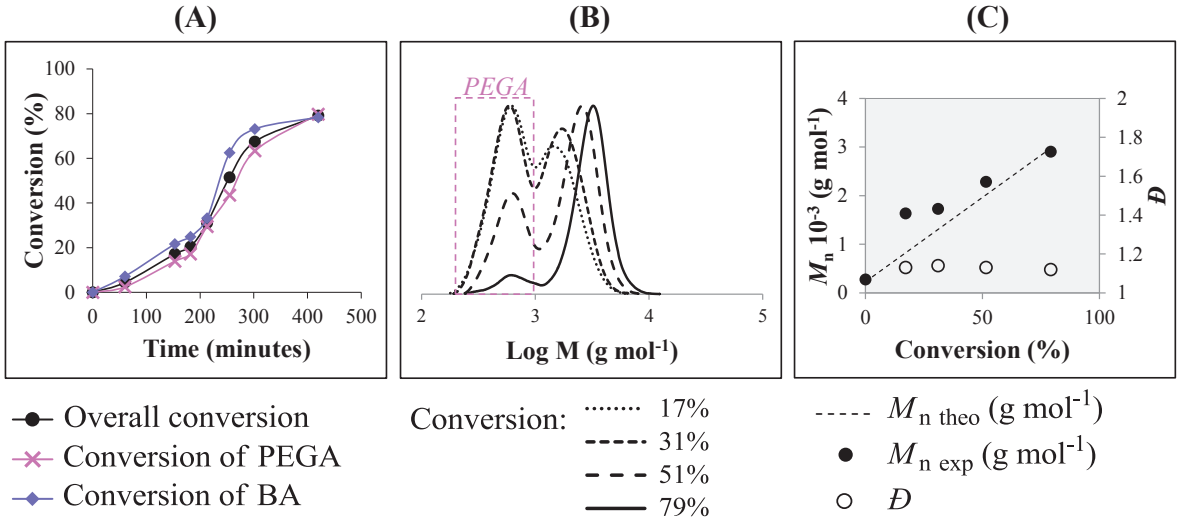
The synthesis of the PEGA- and BA-based copolymer presented a final global conversion of 79%. Evolution of monomer conversion with time can be seen in Figure 3.14A and it can be observed that, during most of the polymerization, BA had a slightly higher conversion than PEGA. However, PEGA and BA final individual conversions were 80 and

78%, respectively, which resulted in a macroRAFT agent composed of 5 units of PEGA and 3 units of BA.

The SEC results indicated a M_n of 2900 g mol^{-1} and a dispersity of 1.12. Molar mass results are in agreement with the theoretical expected values, as it can be seen in Figure 3.14C, showing the evolution of the number-average molar masses and dispersity with conversion.

The product was purified by three cycles of precipitation in petroleum ether, but SEC peaks, obtained in THF, show that the purification of the product was not complete, as traces of PEGA, present in all samples, indicate that the residual macromonomer was not totally removed from the copolymer. As this phenomenon was not observed for the previous samples (with the other PEGA-based macroRAFT agents), it is possible that this difficulty in removing the residual PEGA is due to the molar mass of this copolymer which is considerably low.

Figure 3.14 – RAFT copolymerization of PEGA with BA in solution of 1,4-dioxane at 80°C. (A) Evolution of monomer conversion with time; (B) size exclusion chromatogram peaks and (C) evolution of the number-average molar masses (M_n; full symbols) and dispersities ($Đ$; open symbols) with monomer conversion at 17%, 31%, 51% and 79% monomer conversions, for the synthesis of P(PEGA$_7$-*co*-BA$_4$)-CTPPA (MR8).



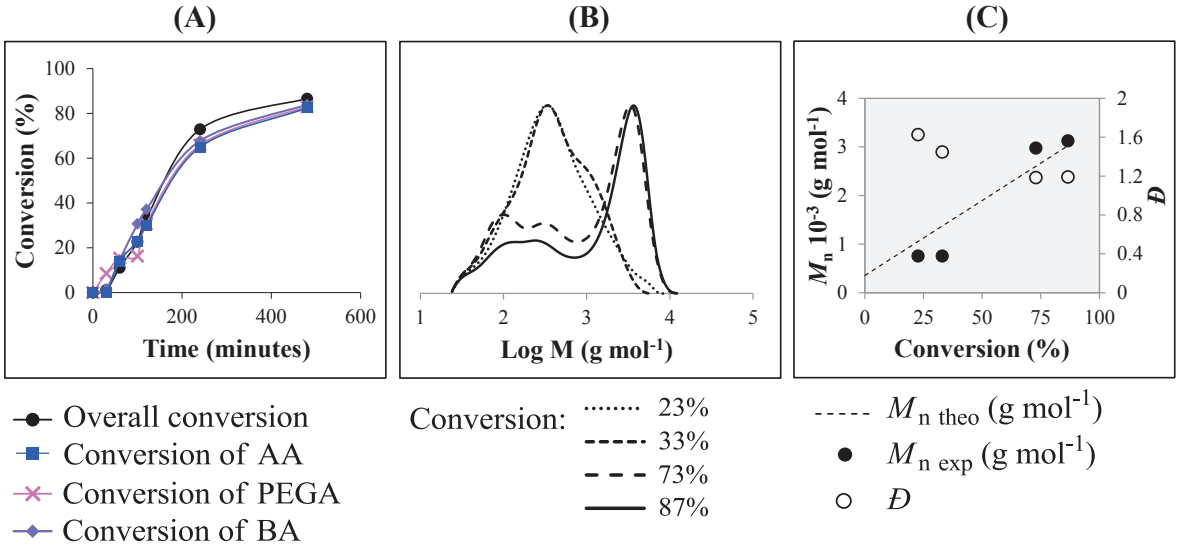
Source: elaborated by the author.

3.3.2.2.7. P(AA$_5$-co-PEGA$_5$-co-BA$_5$)-CTPPA (MR 9)

A random copolymer containing 5 units of AA, PEGA and BA was synthesized and the evolution of individual and overall conversions is shown in Figure 3.15A. A short induction period was observed for AA and BA during the first 30 minutes of polymerization and, during this initial period, PEGA had higher individual conversion, which may have

resulted in a composition drift. However, the final individual conversions were similar for all monomers and a final overall conversion of 87% was achieved after 8 hours of polymerization. SEC curves, shown in Figure 3.15B, cannot be considered as a representative result. Especially the first two curves, corresponding to samples withdrawn at 23% and 33% conversion, suffered a superposition with the methylation agent peak or even, as in the case of MR8, with residual macromonomer. After 73% conversion, the curves suffered a shift towards higher molar masses and a final molar mass of 3120 g mol^{-1} (with a dispersity of 1.19) was obtained, which is very close to the theoretical value of 3100 g mol^{-1}.

Figure 3.15 – RAFT copolymerization of AA, PEGA and BA in solution of 1,4-dioxane at 80°C. (A) Evolution of monomer conversion with time; (B) size exclusion chromatogram peaks and (C) evolution of the number-average molar masses (M_n; full symbols) and dispersities ($Đ$; open symbols) with monomer conversion at 23%, 33%, 73% and 87% monomer conversions, for the synthesis of P(AA_5-*co*-$PEGA_5$-*co*-BA_5)-CTPPA (MR9).



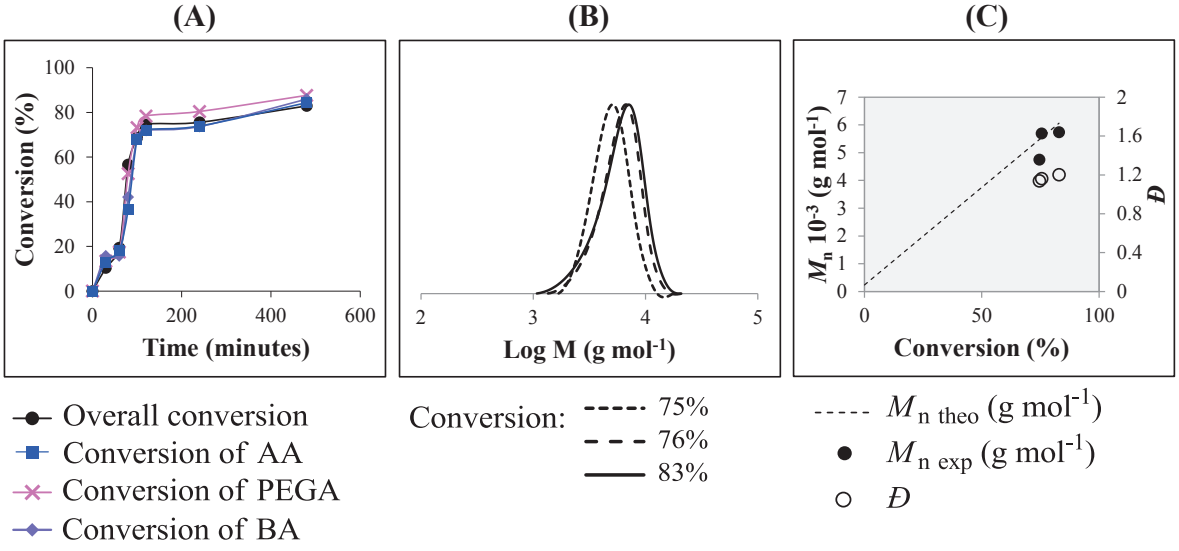
Source: elaborated by the author.

3.3.2.2.8. P(AA_{10}-co-$PEGA_{10}$-co-BA_{10})-CTPPA (MR10)

Another random copolymer containing, this time, 10 units of AA, PEGA and BA was synthesized and the profile of individual and overall conversions, shown in Figure 3.16A, was similar to that obtained for MR9. However, the short induction period observed for AA and BA during the first 30 minutes of polymerization for the shorter copolymer (MR9) was not observed for the longer molecule (MR10). A final individual conversion of 83% was obtained after 8 hours of polymerization. The SEC curves obtained for MR10, shown in Figure 3.16B, did not suffer a superposition with the methylation agent peak, since higher molar masses were obtained for this copolymer, in comparison to MR9. After 83%

conversion, a final molar mass of 5730 g mol^{-1}, with a dispersity of 1.20, was obtained, while the theoretical value was 6230 g mol^{-1}.

Figure 3.16 – RAFT copolymerization of AA, PEGA and BA in solution of 1,4-dioxane at 80°C. (A) Evolution of monomer conversion with time; (B) size exclusion chromatogram peaks and (C) evolution of the number-average molar masses (M_n; full symbols) and dispersities ($Đ$; open symbols) with monomer conversion at 75%, 76% and 83% monomer conversions, for the synthesis of P(AA$_{10}$-*co*-PEGA$_{10}$-*co*-BA$_{10}$)-CTPPA (MR10).



Source: elaborated by the author.

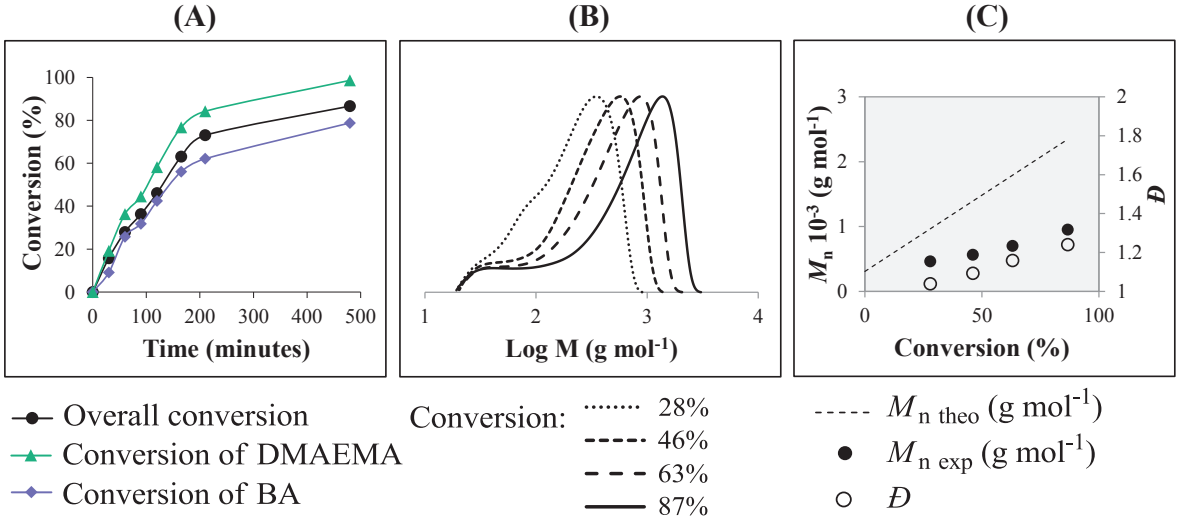
3.3.2.3 Synthesis of DMAEMA-based macroRAFT agents

3.3.2.3.1. P(DMAEMA$_{10}$-co-BA$_5$)-CTPPA (MR 11)

The synthesis of macroRAFT agent based on DMAEMA, the P(DMAEMA$_{10}$-*co*-BA$_5$)-CTPPA, resulted in a final overall conversion of 86.6%, as shown in Figure 3.17A. The analysis of the individual monomer consumption, however, reveals that the conversion of DMAEMA (98.6%) was higher than the conversion of BA (78.8%) since the beginning of polymerization, which resulted in a final copolymer containing 4 units of BA and 10 units of DMAEMA. The samples were characterized in terms of molar mass and dispersity by SEC using PMMA standards and THF as eluent. The chromatogram, shown in Figure 3.17B, indicates a clear shift of the curves, and the evolution of experimental M_n with conversion, shown in Figure 3.17C, reveals a considerable deviation from the theoretical values and a tail at low molar masses can be observed, resulting in high dispersities. These observations could be attributed to the characterization of this copolymer and the solvent (THF) used for the analysis, which may not be the most suitable choice in this case, rather than to the

copolymer itself. For final sample, a molar mass of 2313 g mol^{-1} was expected, but a value of 952 g mol^{-1} was obtained. This discrepancy has already been reported in the literature[77] and may be attributed to the use of PMMA standards, which are not the most suitable for DMAEMA based copolymers. A final *Đ* of 1.24 was obtained.

Figure 3.17 – RAFT copolymerization of DMAEMA and BA in solution of 1,4-dioxane at 80°C. (A) Evolution of monomer conversion with time; (B) size exclusion chromatogram peaks and (C) evolution of the number-average molar masses (M_n; full symbols) and dispersities (*Đ*; open symbols) with monomer conversion at 28%, 46%, 63% and 87% monomer conversions, for the synthesis of P(DMAEMA$_{10}$-*co*-BA$_5$)-CTPPA (MR11).



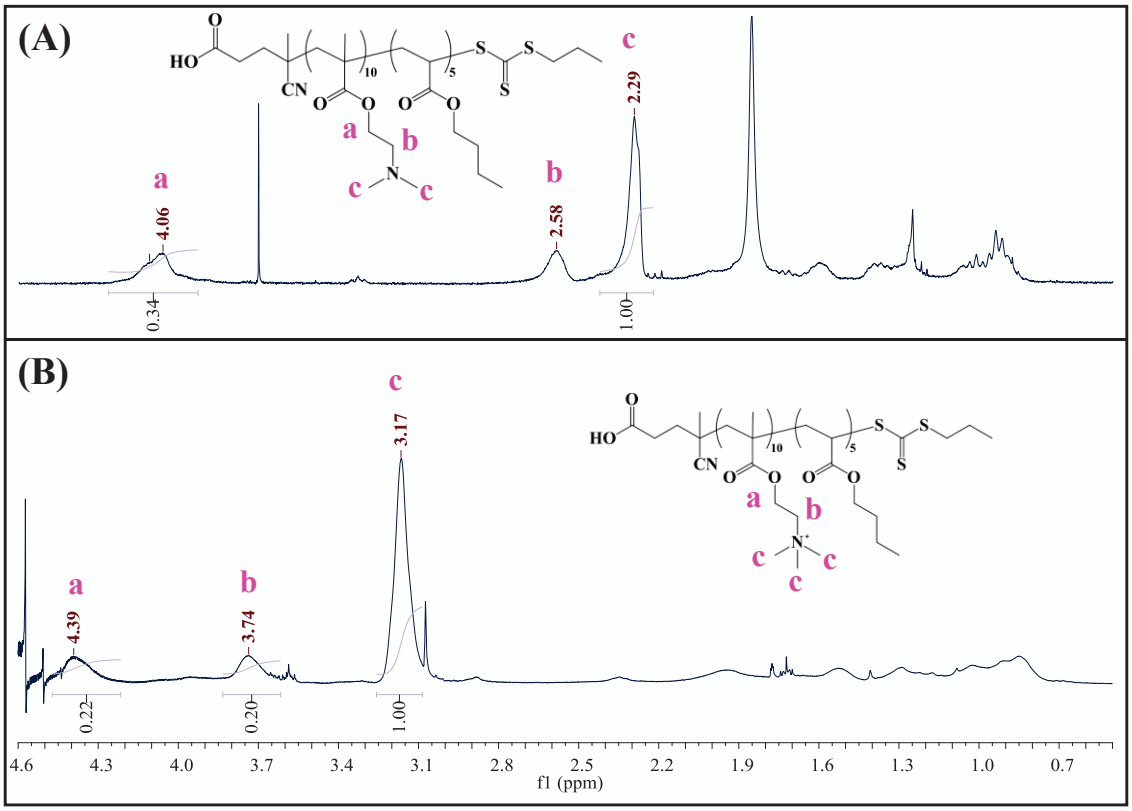
Source: elaborated by the author.

The final product of the synthesis was precipitated three times in cold n-hexane and dried under high vacuum. The ^{1}H NMR spectrum of the purified product is displayed in Figure 3.18A. At δ = 4.06 ppm, a characteristic chemical shift can be observed (signal **a**) and it is attributable to the methylene protons adjacent to the oxygen moieties of the ester linkages in the DMAEMA units. The other chemical shifts that are observed at δ = 2.58 (signal **b**) and 2.29 ppm (signal **c**) are related to the methylene and methyl protons, respectively, of the DMAEMA moieties in the copolymer.[78] At δ = 1.95 ppm, there is a chemical shift that could not be attributed to any proton. This peak was not observed in any spectrum of PDMAEMA-based polymers.[74, 79, 80] However, when the sample was analyzed in D_2O, this chemical shift at δ = 1.95 ppm was not observed.

Part of the unpurified macroRAFT agent was submitted to quaternization reaction with CH_3I and the ^{1}H NMR spectrum of the quaternized macroRAFT agent [P(qDMAEMA$_{10}$-*co*-BA$_5$)-CPP] is displayed in Figure 3.18B. Nine quaternary ammonium protons appear at δ = 3.17 ppm and the comparison of the integral of this peak with the signal

from the methylene proton at δ = 4.39 indicates 100% of quaternization.[74] Even though a small peak could be observed at δ = 2.3-2.4 ppm, its integral was neglected. It was considered that it suffered a total shift to the δ = 3.17 region.

Figure 3.18 – ^{1}H NMR spectrum of P(DMAEMA$_{10}$-*co*-BA$_5$)-CTPPA (A) before (300 MHz, $CDCl_3$) and (B) after quaternization (300 MHz, D_2O).



Source: elaborated by the author.

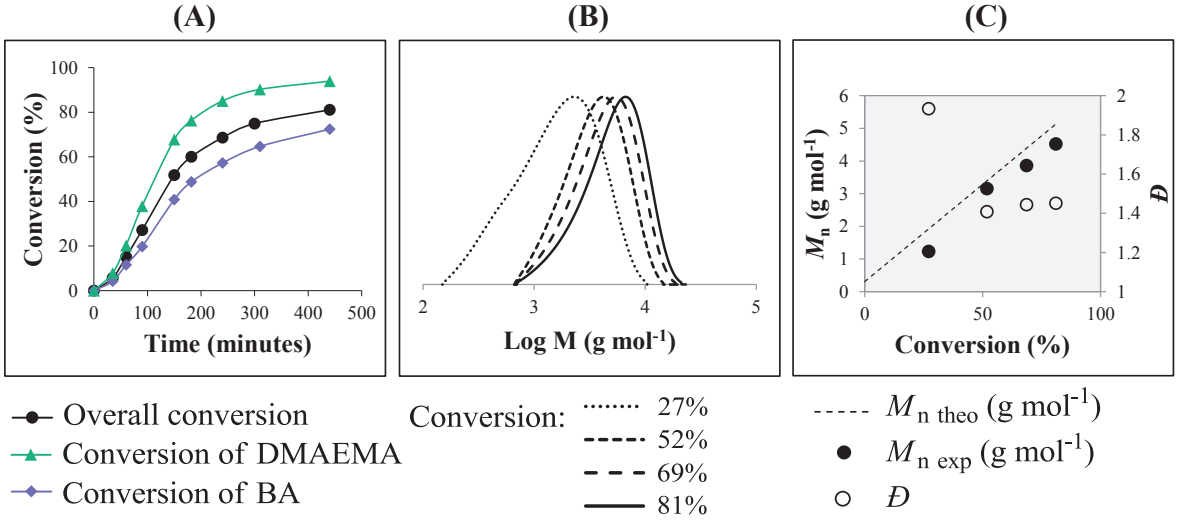
3.3.2.3.2. P(DMAEMA$_{20}$-co-BA$_{20}$)-CTPPA (MR 12)

A longer and more hydrophobic DMAEMA-based copolymer was synthesized, the P(DMAEMA$_{20}$-*co*-BA$_{20}$)-CTPPA, and its synthesis presented a final global conversion of 81%. The evolution of monomer overall and individual conversions with time is shown in Figure 3.19A. It can be observed that DMAEMA conversion was higher than BA conversion during all polymerization, and DMAEMA and BA final individual conversions were 94 and 72%, respectively, which resulted in a macroRAFT agent composed of 19 units of DMAEMA and 14 units of BA.

The product was characterized in terms of molar mass and dispersity by SEC using PMMA standards and THF with, exceptionally in the case of this macroRAFT, lithium bromide as eluent. A clear shift of SEC traces can be seen in Figure 3.19B, as the molar mass of the copolymer increased. SEC results indicated a M_n of 4560 g mol^{-1} and a dispersity of

1.40. Molar masses were in agreement with the theoretical expected values as it can be seen in Figure 3.19C, which shows the evolution of the number-average molar masses and dispersity with conversion. Even though the dispersities were quite high, it seems that a better agreement between the experimental and theoretical molar masses was obtained in this case, as compared to the SEC results obtained for MR11. In fact, the addition of LiBr to the mobile phase is a common procedure in SEC analysis to reduce possible interactions between polar samples and the negatively charged column packing.

Figure 3.19 – RAFT copolymerization of DMAEMA and BA in solution of 1,4-dioxane at 80°C. (A) Evolution of monomer conversion with time; (B) size exclusion chromatogram peaks and (C) evolution of the number-average molar masses (M_n; full symbols) and dispersities ($Đ$; open symbols) with monomer conversion at 27%, 52%, 69% and 81% monomer conversions, for the synthesis of P(DMAEMA$_{20}$-*co*-BA$_{20}$)-CTPPA (MR12).



Source: elaborated by the author.

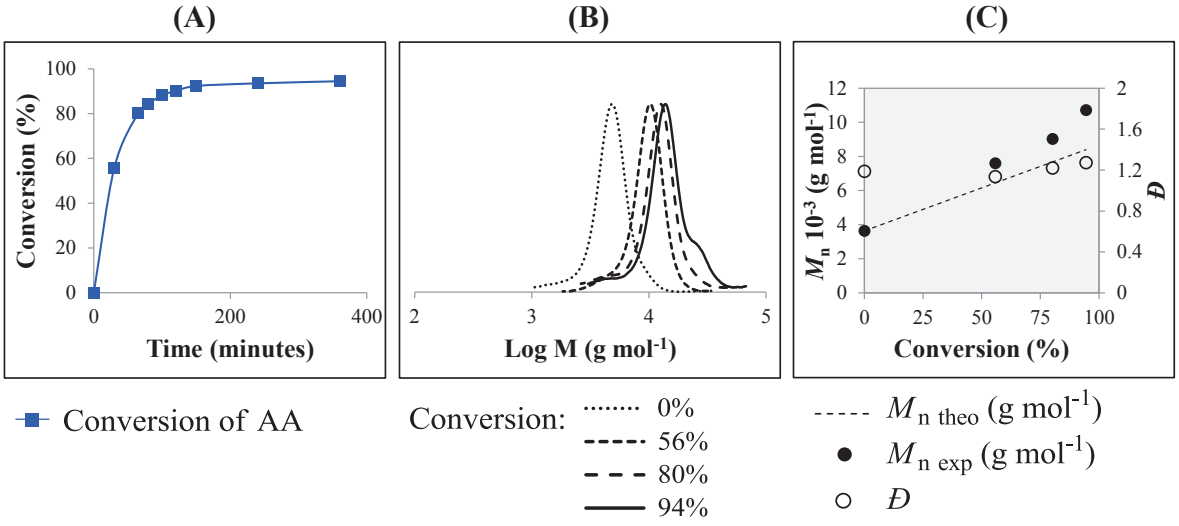
3.3.2.4 Verification of the living character of the copolymers

Two macroRAFT agents, PAA-CTPPA (MR1) and PAA-*b*-P(PEGA-*co*-BA)-CTPPA (MR6), were randomly chosen to be submitted to a chain extension with, respectively, AA and BA, in order to verify the living character of these molecules and guarantee their capacity to mediate the emulsion polymerizations via RAFT mechanism. Polymerizations were carried out using the same procedure as described above for the synthesis of macroRAFT agents.

The profile of monomer conversion versus time for the chain extension carried out with PAA-CTPPA is shown in Figure 3.20A, while SEC chromatograms are shown in Figure 3.20B. Narrow curves were obtained until the first 60 minutes of polymerization and, during

this first hour of reaction, a conversion of over 80% was achieved. However, last sample presented a shoulder that can be attributed to the formation of chains with higher values of molar mass, due to coupling reactions. The evolution of molar mass and dispersity with conversion is shown in Figure 3.20C. Molar mass increased linearly with conversion and $Đ$ values reached 1.27 at the end of the chain extension reaction.

Figure 3.20 – RAFT polymerization of AA in solution of 1,4-dioxane at 80°C. (A) Evolution of monomer conversion with time; (B) size exclusion chromatogram peaks and (C) evolution of the number-average molar masses (M_n; full symbols) and dispersities ($Đ$; open symbols) with monomer conversion at 0%, 56%, 80% and 94% monomer conversions, for the chain extension of PAA_{42}-CTPPA.

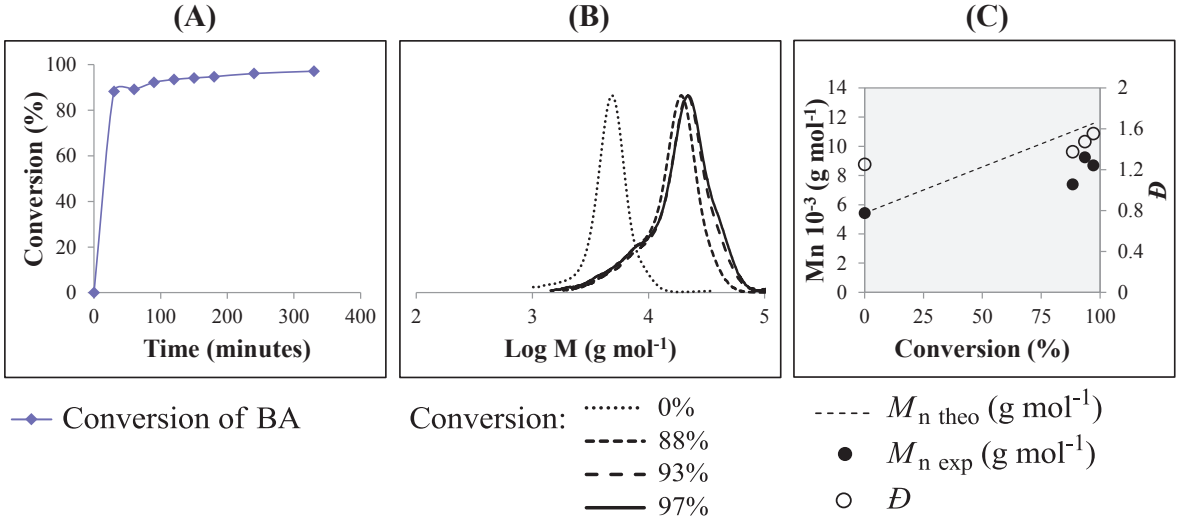


Source: elaborated by the author.

For the chain extension of the PAA-*b*-P(PEGA-*co*-BA)-CTPPA macroRAFT agent with AA, polymerization was faster and a conversion of nearly 90% was achieved within the first 30 minutes of reaction (Figure 3.21A). This can be considered an unexpected result for a controlled radical polymerization, and particularly for this experiment, since the nature of the propagating radical has not changed from the previous chain extension experiment. This kinetic behavior could be explained by factors related to the experimental conditions, however, as this experiment has not been repeated, this cannot be firmly affirmed. The control over the polymerization is not the main goal of this work and, instead, it is more desirable to guarantee the living character of the polymerization, since it allows the shift of the molar masses, as shown in the SEC curves of Figure 3.21B. This chain extension reaction resulted in broad SEC curves and SEC traces indicate that part of macroRAFT chains were not activated, since all curves presented a tail that corresponds to low molar masses. After 93 minutes of reaction, another shoulder appears at the region of high molar masses and can

be explained by coupling reactions, which are common for high conversions in RAFT polymerizations. For this reason, dispersity values ranged from 1.25 to 1.55 (Figure 3.21), and the presence of some dead macroRAFT chains resulted in M_n values above the expected ones.

Figure 3.21 – RAFT polymerization of BA in solution of 1,4-dioxane at 80°C. (A) Evolution of monomer conversion with time; (B) size exclusion chromatogram peaks and (C) evolution of the number-average molar masses (M_n; full symbols) and dispersities ($Đ$; open symbols) with monomer conversion at 0%, 88%, 93% and 97% monomer conversions, for the chain extension of PAA-*b*-P(PEGA-*co*-BA)-CTPPA.



Source: elaborated by the author.

In regard to the synthesis of the macroRAFT agents, it should be considered that the individual monomer conversions were not 100% and, for this reason, in most cases, the theoretical structures were not obtained according to the predicted number of repeat units. Therefore, in the following sections, the nomenclature used for the macroRAFT agents will consider the experimentally obtained structures and the abbreviations used to represent the macroRAFT agents will consider the actual number of repeat units in the polymer chain (based on the individual conversion of each comonomer), and not the theoretical values, as listed in Table 3.4.

Table 3.4 – Comparison between the theoretical predicted structures for the macroRAFT agents synthesized and the experimentally obtained structures considering the actual number of repeat units in the polymer chain, based on the individual conversion of each comonomer.

Entry	Theoretical structures	Experimentally obtained structures
MR1	PAA_{42}-CTPPA	PAA_{40}-CTPPA
MR2	P(AA_{16}-*co*-BA_{16})-CTPPA	P(AA_{16}-*co*-BA_{16})-CTPPA
MR3	PEG_{45}-CTPPA	PEG_{45}-CTPPA
MR4	PEG_{45}-*b*-PAA_{49}-CTPPA	PEG_{45}-*b*-PAA_{42}-CTPPA
MR5	P(AA_{40}-*b*-$PEGA_5$)-CTPPA	P(AA_{40}-*b*-$PEGA_4$)-CTPPA
MR6	PAA_{40}-*b*-($PEGA_7$-*co*-BA_4)-CTPPA	PAA_{40}-*b*-($PEGA_6$-*co*-BA_4)-CTPPA
MR7	P(AA_{16}-*co*-BA_{16})-*b*-($PEGA_7$-*co*- BA_4)-CTPPA	P(AA_{16}-*co*-BA_{16})-*b*-($PEGA_6$-*co*- BA_4)-CTPPA
MR8	P($PEGA_7$-*co*-BA_4)-CTPPA	P($PEGA_5$-*co*-BA_3)-CTPPA
MR9	P(AA_5-*co*-$PEGA_5$-*co*- BA_5)-CTPPA	P(AA_4-*co*-$PEGA_4$-*co*- BA_4)-CTPPA
MR10	P(AA_{10}-*co*-$PEGA_{10}$-*co*- BA_{10})-CTPPA	P(AA_9-*co*-$PEGA_9$-*co*- BA_9)-CTPPA
MR11	P($DMAEMA_{10}$-*co*-BA_5)-CTPPA	P($DMAEMA_{10}$-*co*-BA_4)-CTPPA
MR12	P($DMAEMA_{20}$-*co*-BA_{20})-CTPPA	P($DMAEMA_{19}$-*co*-BA_{14})-CTPPA

Source: elaborated by the author.

3.4 Adsorption isotherms of macroRAFT agents onto Laponite

3.4.1 Experimental section

3.4.1.1 Materials

The clay mineral chosen for this work was Laponite RD, a synthetic hectorite produced by BYK Additives Ltd (former Rockwood Additives Ltd, UK). There are different grades of Laponite available, and the RD grade is the most frequently studied grade. It is a fast-dispersing gel-forming grade that does not contain any added peptizer. Deionized water (Purelab Classic UV, Elga LabWater) was used and the macroRAFT agents used were synthesized as described in the previous sections. The peptizer (tetrasodium pyrophosphate, $Na_4P_2O_7$, 95%, Aldrich) was added to Laponite powder for adsorption studies carried out with nonionic macroRAFT agents PEG-CTPPA (MR3) and P(PEGA-*co*-BA)-CTPPA (MR8). The main purpose of adding a peptizing agent was to hinder gel formation, as this tetravalent negatively charged ion adsorbs on the rims of the platelets and protects them from

rim-to-face interactions. Since the AA units of AA-based macroRAFTs can potentially adsorb on the positively charged rims, performing the same function, and DMAEMA-based molecules can adsorb on the negative surface of the platelets, rendering the entire particle positively charged, the addition of peptizer was considered unnecessary for the rest of the macroRAFT agents.

3.4.1.2 Methods

In this work, the interaction of AA-based, PEG-based and DMAEMA-based macroRAFT agents with Laponite was investigated and equilibrium adsorption isotherms were determined for each macroRAFT agent synthesized. For this purpose, a stock dispersion of Laponite was initially prepared by adding 0.4 g of Laponite into 20 mL of water and left for 30 minutes under magnetic stirring. Exclusively for the PEG_{45}-CTPPA and P($PEGA_5$-*co*-BA_3)-CTPPA adsorption isotherm, peptizer pyrophosphate was added to Laponite powder in controlled amounts (10 wt% based on clay). Aliquots of 1 mL of the 20 g L^{-1} clay suspension were added to small flasks, where different volumes of a previously prepared macroRAFT agent solution were added. All flasks were completed with water until a final volume of 4 mL, obtaining macroRAFT/Laponite dispersions with a fixed final clay concentration of 5 g L^{-1} and different macroRAFT agent concentrations. The pH of each dispersion was carefully adjusted at this point, by adding droplets of NaOH or HCl. The dispersion was stirred for approximately 15 hours and further ultracentrifuged at 60 000 rpm for one hour (using a Sorvall™ MTX 150 Micro-Ultracentrifuge, from Thermo Scientific). The supernatant was recovered for determination of the amount of free macroRAFT agent by UV-visible analysis.

The results were fitted to Langmuir and Freundlich isotherm models. These isotherms apply over a wide concentration range, which explains why these are the most commonly used models to fit adsorption isotherm data. Even though these isotherms models are excessively simple to explain highly complex phenomena, such as the adsorption of macroRAFT agents onto Laponite, they can be satisfactorily employed as a comparative method to verify the adsorption behavior of the different molecules proposed. Langmuir[81] isotherm is a two-parameter model, characterized graphically by a plateau that corresponds to saturation equilibrium. In the Langmuir expression (Eq. (1)), K_L and a_L are Langmuir

constants, C_e is the adsorbate concentration in the liquid phase and Q_e is its concentration in the solid phase at equilibrium.

$$Q_e = \frac{K_L C_e}{1 + a_L C_e} \quad (1)$$

The Langmuir constants, K_L and a_L can be obtained by the linearization of Eq. (1), according to Eq. (2):

$$\frac{C_e}{Q_e} = \frac{1}{K_L} + \frac{a_L}{K_L} C_e \quad (2)$$

Langmuir assumes monolayer adsorption, so, after the saturation plateau is achieved, no more adsorption takes place and the solid has reached its adsorption capacity, Q_{max}., which is equal to K_L/a_L:

$$Q_{max} = \frac{K_L}{a_L} \quad (3)$$

By combining Eq. (2) and (3), Q_{max} can be obtained from the slope of Eq (4), according to:

$$\frac{C_e}{Q_e} = \frac{1}{Q_{max} a_L} + \frac{1}{Q_{max}} C_e \quad (4)$$

Freundlich [82] isotherm is an exponential equation so, contrary to Langmuir, a plateau is not reached and, theoretically, the concentration of adsorbate on the solid surface can increase until infinite adsorption. It can be applied to multilayer, non-ideal and reversible adsorption over heterogeneous surfaces. The empirical model (Eq (5)) is characterized by Freundlich constants K_F, related to the adsorption capacity, and *n*, the heterogeneity factor, related to the surface heterogeneity or the adsorption intensity.

$$Q_e = K_F C_e^n \quad (5)$$

The linear form of this equation, given by Eq. (6), is used to determine the constants K_F and *n*, from the intercept and the slope, respectively. The slope values range between 0 and 1 and slopes closer to zero are an indicative of more heterogeneous systems, while values below 1 indicate a chemisorption process and above one may indicate cooperative adsorption.

$$\ln Q_e = \ln K_F + n \ln C_e \quad (6)$$

3.4.1.3 Characterizations

The equilibrium concentration of macroRAFT agent in the supernatant, C_e (g L^{-1}), was determined by UV-visible spectroscopy at 310 nm using a pre-determined calibration curve. With the difference between the initial concentration of macroRAFT agent, C_0 (g L^{-1}) and the equilibrium concentration, it was possible to calculate the adsorbed amount of macroRAFT agent, Q_e (mg g^{-1}), according to Eq. (7):

$$Q_e = \frac{(C_0 - C_e)}{C_{clay}} \times 1000 \quad (7)$$

where C_{clay} is the concentration of Laponite in the sample (g L^{-1}).

The macroRAFT agents, which derive from CTPPA, contain a trithiocarbonate chain end that guarantees the absorbance of these compounds in the ultraviolet-visible spectral region, presenting an intense absorption at 310 nm. This wavelength was selected to carry out the measurements because the interference of the residual Laponite obtained after centrifugation is minimal in this spectral region.[12]

The hydrodynamic average particle diameter ($Z_{av.}$) and the dispersity of the samples (indicated by the Poly value) were determined by Dynamic Light Scattering (DLS) in a NanoZetasizer instrument from Malvern. Typically, one drop of the sample was diluted in pure deionized water before analysis and the reported particle size represents an average of 3 measurements. Samples were also characterized in terms of Zeta potential (ζ potential), with the same instrument.

3.4.2 Results and Discussion

In order to understand the mechanisms of nanocomposite particles formation through the RAFT encapsulating emulsion polymerization strategy in the presence of Laponite platelets, the adsorption of the macroRAFT agents on Laponite was studied. To quantify the amount of free macroRAFT agent in the supernatant by UV-visible spectroscopy, calibration curves were determined for each macroRAFT agent at 310 nm. A linear relationship between the macroRAFT concentration and the absorbance was obtained in all cases, according to the Beer-Lambert law (see Annex 1), indicating that the curves obtained were adequate for determining the equilibrium concentration of macroRAFT in the supernatant, C_e (g L^{-1}).

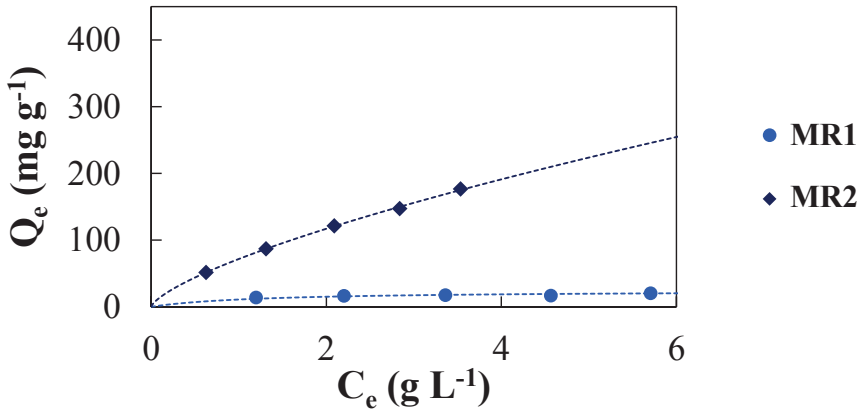
The adsorption of macroRAFT agents was expressed in terms of their mass concentration, alternatively to the molar concentration, because a considerable difference could be observed between the theoretical and the experimental molar masses obtained for some of these molecules. Considering that, in this work, the main intention was to analyze the adsorption of the different macroRAFT agents comparatively, this approach was considered to be the most loyal to reality and, therefore, the most adequate to express the equilibrium and adsorbed concentrations.

3.4.2.1 Adsorption isotherm of PAA-based macroRAFT agents

The adsorption behavior of macroRAFT agents PAA_{40}-CTPPA (MR1) and P(AA_{16}-*co*-BA_{16})-CTPPA (MR2) on Laponite was studied. The adsorption isotherms of these anionic macroRAFT agents, as well as all macroRAFT agents containing acrylic acid, were carried out at a fixed pH of 7.5. This pH was selected since it is high enough to guarantee the solubility of all macroRAFT agents in water, including the copolymers containing BA units, and low enough to guarantee the integrity of the RAFT functionality of the molecules.

The results are shown in Figure 3.22. A considerable higher adsorption was found for the macroRAFT agent P(AA_{16}-*co*-BA_{16})-CTPPA (MR2), compared to that of PAA_{40}-CTPPA (MR1), which indicates the importance of the hydrophobic domains for adsorption.

Figure 3.22 – Isotherm for macroRAFT adsorption onto the Laponite surface at pH = 7.5.



Laponite concentration = 5.0 g L^{-1}.
MR1 = PAA_{40}-CTPPA and
MR2 = P(AA_{16}-*co*-BA_{16})-CTPPA.
Dashed lines are fitting to the Langmuir (MR1) or Freundlich (MR2) equations.
Source: elaborated by the author.

However, the mechanism that drives the interaction between amphipathic copolymers with hydrophilic surface is not very obvious.[48, 49] The poor solubility of BA units in water can be considered as one of the explanations to the increase in adsorption caused by adsorbate's hydrophobicity. Hydrophobic units can adsorb on Laponite surface in order to minimize their interaction with the aqueous medium. Since the adsorption of pure PAA is almost absent at pH 7.5, this hydrophobicity-induced interaction might represent the main driving force for adsorption in the case of copolymer MR2.

The adsorption isotherms were fitted to the Langmuir and Freundlich models, and the Langmuir parameters (adsorbed amount at saturation, Q_{max}, binding energy constant, K_L, and Langmuir isotherm constant, α_L) and Freundlich parameters (Freundlich isotherm constant related to adsorption capacity, K_F, and slope, *n*) were determined with the linearized form of the equations, as listed in Table 3.5. The dashed lines from Figure 3.22 correspond to the best fitting to the models (the model that led to the highest value of correlation coefficient, R), according to the data shown in Table 3.5. So, for MR1, the dashed lines correspond to the Langmuir model, while for MR2, to the Freundlich model.

Table 3.5 – Langmuir and Freundlich constants and correlation coefficient for adsorption of macroRAFT agent PAA_{40}-CTPPA (MR1) at pH 7.5 and P(AA_{16}-*co*-BA_{16})-CTPPA (MR2) at pH 7.5 onto Laponite in water at 25 °C.

	Langmuir				**Freundlich**		
MacroRAFT	**Q_{max} (mg g^{-1})**	**α_L**	**K_L**	**R**	**Slope (*n*)**	**K_F (L mg^{-1})**	**R**
MR1	21.9	1.23	26.8	0.9807	0.21	13.4	0.9159
MR2	3.70×10^2	0.24	89.8	0.9828	0.71	71.6	0.9998

Source: elaborated by the author.

A comparison with some results obtained in the literature for the adsorption of PEG chains onto Laponite indicates that the adsorption of PAA-based macroRAFT agent is very low. Mongondry et al.[10] studied the adsorption of PEG chains of different molar masses onto Laponite and, by fitting the data to the Langmuir model, they obtained an adsorbed amount at saturation (Q_{max}) of 590 mg g^{-1} for the 2000 g mol^{-1} PEG, while and Bourgeat-Lami et al.[12] obtained, for the adsorption of a similar molecule (a trithiocarbonate PEG-based macroRAFT agent), an adsorbed amount at saturation of 515 mg g^{-1}. However, as the adsorption of MR1 was negligible at pH 7.5, the fitting to both models could be disregarded.

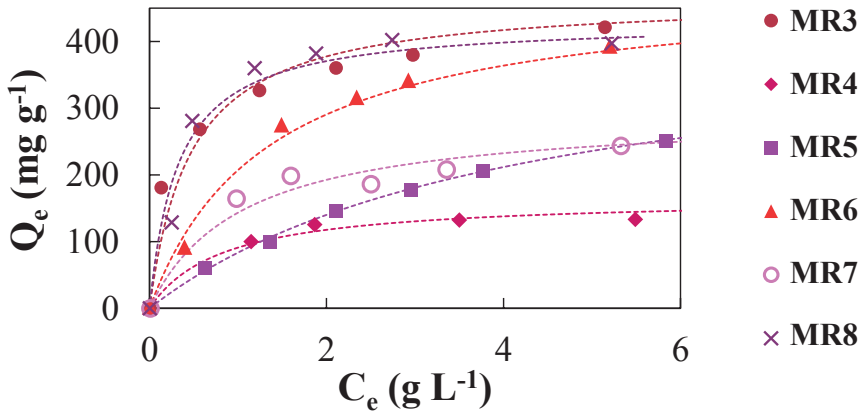
The adsorption behavior of MR2, on the other hand, fitted well to the Freundlich model. In this model, the slope of the curve, *n*, also known as the heterogeneity factor b_f, is a measure of adsorption intensity or surface heterogeneity. It ranges between 0 and 1 and values closer to one are an indicative of less heterogeneous systems.[83, 84] A Freundlich constant (K_F) of 71.62 L mg^{-1} was obtained and, as this constant is related to adsorption capacity, a relative low adsorption was obtained for this copolymer.

However, the concentration of MR2 on the surface of Laponite increases with the concentration of macroRAFT agent and, in theory, according to the Freundlich model, isotherm does not reach a plateau and infinite adsorption can occur.[85, 86]

3.4.2.2 Adsorption isotherms of PEG-based macroRAFT agents

The adsorption behavior of six different macroRAFT agents composed of linear or pending PEG blocks was investigated. In some cases, copolymers were also composed of hydrophilic AA units and/or hydrophobic BA units and, in these cases, the adsorption study was carried out at pH 7.5. Adsorption isotherms are shown in Figure 3.23.

Figure 3.23 – Isotherm for macroRAFT adsorption onto the Laponite surface.



Laponite concentration = 5.0 g L^{-1}.
MR3 = PEG_{45}-CTPPA at pH 10;
MR4 = PEG_{45}-*b*-PAA_{42}-CTPPA at pH 7.5;
MR5 = P(AA_{40}-*b*-$PEGA_4$)-CTPPA at pH 7.5;
MR7 = P(AA_{16}-*co*-BA_{16})-*b*-P($PEGA_6$-*co*-BA_4)-CTPPA at pH 7.5;
MR8 = P($PEGA_5$-*co*-BA_3)-CTPPA at pH 10.
Dashed lines are fits to the Langmuir equation.
Source: elaborated by the author.

The fitting of the isotherms to the Langmuir equation is represented by the dashed lines, and the data are shown in Table 3.6. The results were also fitted to the Freundlich

isotherm, and most isotherms fitted well to both models. In the Langmuir type of isotherm, the adsorbed amount of macroRAFT agent increases with the increase in the copolymer concentration until maximal adsorption capacity, represented by a plateau, is reached.[47] In this aspect, PAA_{40}-*b*-P($PEGA_6$-*co*-BA_4)-CTPPA (MR6) allowed a higher coverage of Laponite, as compared to the other macroRAFTs, since the amount of macroRAFT adsorbed at the plateau (Q_{max}) was 486.36 mg g^{-1}. It is possible to see that PEG_{45}-CTPPA (MR3) and P($PEGA_5$-*co*-BA_3)-CTPPA (MR8) displayed high adsorption capacities (465.78 mg g^{-1} and 430.46 mg g^{-1}, respectively) as well, with a stronger affinity for Laponite surface as the adsorption isotherms of both macroRAFT agents displayed a higher initial slope than the other curves.

Table 3.6 – Langmuir constants and correlation coefficients for adsorption of macroRAFT agents PEG_{45}-CTPPA (MR3); PEG_{45}-*b*-PAA_{42}-CTPPA (MR4) at pH 7.5; P(AA_{40}-*b*-$PEGA_4$)-CTPPA (MR5) at pH 7.5; PAA_{40}-*b*-P($PEGA_6$-*co*-BA_4)-CTPPA (MR6) at pH 7.5; P(AA_{16}-*co*-BA_{16})-*b*-P($PEGA_6$-*co*-BA_4)-CTPPA (MR7) at pH 7.5 and P($PEGA_5$-*co*-BA_3)-CTPPA (MR8) onto Laponite in water at 25 °C.

	Langmuir				Freundlich		
MacroRAFT	**Q_{max} (mg g^{-1})**	**α_L**	**K_L**	**R**	**Slope (*n*)**	**K_F (L mg^{-1})**	**R**
MR3	4.66×10^2	2.14	9.96×10^2	0.9979	0.23	2.99×10^2	0.9949
MR4	1.67×10^2	1.21	2.01×10^2	0.9986	0.32	86.5	0.9626
MR5	4.23×10^2	0.25	1.05×10^2	0.9943	0.66	84.2	0.9958
MR6	4.86×10^2	0.74	3.61×10^2	0.9966	0.51	1.80×10^2	0.9458
MR7	2.93×10^2	0.96	2.81×10^2	0.9916	0.22	1.65×10^2	0.9450
MR8	4.30×10^2	3.09	13.3×10^2	0.9966	0.34	2.82×10^2	0.8643

Source: elaborated by the author.

A comparison between PEG_{45}-CTPPA (MR3) and PEG_{45}-*b*-PAA_{42}-CTPPA (MR4), indicates a considerable lower affinity of the AA-containing molecule for Laponite surface. This lower affinity caused by the presence of the PAA block is expected, since a minor interaction is promoted between PAA and Laponite at pH 7.5, as discussed above (Figure 3.22). In addition, double-hydrophilic block copolymers composed of a proton-acceptor non-charged polymer, such as poly(ethylene oxide), with polycarboxylic acids are susceptible to the formation of intramolecular polycomplexes at low pH, via hydrogen bonding.[87-94] So, the association of a PEG block with PAA segment in the same structure may have led to

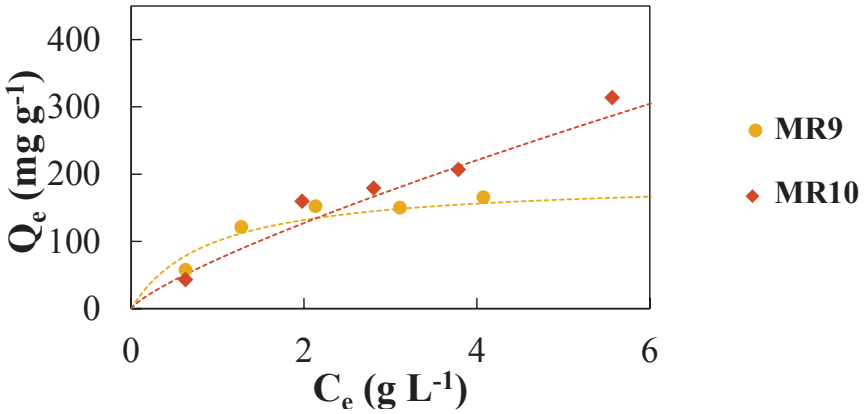
relatively strong interaction between both blocks, reducing therefore their interaction with the Laponite surface.

Nonetheless, when the PEG units are disposed in a pending conformation, as in the macroRAFT agent P(AA_{40}-*b*-$PEGA_4$)-CTPPA (MR5), a higher adsorption is observed, when compared to PEG_{45}-*b*-PAA_{42}-CTPPA (MR4). The pending disposition of the PEG segments might hinder their complexation with the poly(acrylic acid) block. Incrementing the non-charged segment with random units of BA in the macroRAFT PAA_{40}-*b*-P($PEGA_6$-*co*-BA_4)-CTPPA (MR6) seems to be favorable to adsorption, as already discussed for MR2, and the isotherm of this copolymer has a more defined equilibrium plateau, with a higher slope, in comparison to isotherm of MR5. However, if additional BA units are located in the PAA block as well, as in P(AA_{16}-*co*-BA_{16})-*b*-P($PEGA_6$-*co*-BA_4)-CTPPA (MR7), a reverse effect is observed and adsorption is reduced.

When comparing MR6 and MR8, a different behavior is observed at low concentrations, with a lower affinity of MR6 (which contains the AA block) for Laponite surface. This behavior is expected since the presence of AA units may increase the tendency of the copolymer to stay in the aqueous phase, rather than in the surface of Laponite, which, at pH 7.5, has an opposite charge to the charge of PAA. However, the adsorbed amount at the plateau is very similar for both copolymers, which indicates that, at higher concentrations, both copolymers are capable of providing similar coverage of Laponite surface. If we consider that MR8 has a lower molar mass (2900 g mol^{-1}) than MR6 (6130 g mol^{-1}), on the other hand, the surface coverage of Laponite provided by MR6 in terms of mol will be lower than the coverage provided by MR8, which is consistent with the assumption that the PAA block might hinder the adsorption of the PEG segment, instead of contributing to adsorption by adsorbing, for instance, on the positively charged edges of the clay.

The adsorption of two random copolymers composed of AA, PEGA and BA with different molar masses was also evaluated. The isotherms of P(AA_4-*co*-$PEGA_4$-*co*-BA_4)-CTPPA (MR9) and P(AA_9-*co*-$PEGA_9$-*co*-BA_9)-CTPPA (MR10) are shown in Figure 3.24.

Figure 3.24 – Isotherm for macroRAFT adsorption onto the Laponite surface at pH 7.5.



Laponite concentration = 5.0 g L^{-1}.
MR9 = P(AA$_4$-*co*-PEGA$_4$-*co*-BA$_4$)-CTPPA and
MR10 = P(AA$_9$-*co*-PEGA$_9$-*co*-BA$_9$)-CTPPA at pH 7.5.
Dashed lines are the fitting to the Langmuir (MR9) or Freundlich (MR10) equations.
Source: elaborated by the author.

In comparison to the other isotherms of PEG-based macroRAFT agents, the random copolymers of AA, BA and PEGA present considerably lower adsorption. With the linearized form of the Langmuir and the Freundlich equations, the adsorption parameters were determined and are listed in Table 3.7. While the copolymer with lower molar mass fitted well to the Langmuir model, the macroRAFT agent with longer chain fitted better to Freundlich equation. These fittings are represented by the dashed lines in Figure 3.24.

Table 3.7 – Langmuir constants and correlation coefficient for adsorption of macroRAFT agent P(AA$_4$-*co*-PEGA$_4$-*co*-BA$_4$)-CTPPA (MR9) at pH 7.5 and P(AA$_9$-*co*-PEGA$_9$-*co*-BA$_9$)-CTPPA (MR10) at pH 7.5 onto Laponite in water at 25 °C.

	Langmuir				Freundlich		
MacroRAFT	**Q_{max} (mg g^{-1})**	**α_L**	**K_L**	**R**	**Slope (*n*)**	**K_F (L mg^{-1})**	**R**
MR9	1.92×10^2	1.10	2.12×10^2	0.9860	0.42	90.0	0.8789
MR10	6.25×10^2	0.14	88.0	0.9014	0.79	73.5	0.9729

Source: elaborated by the author.

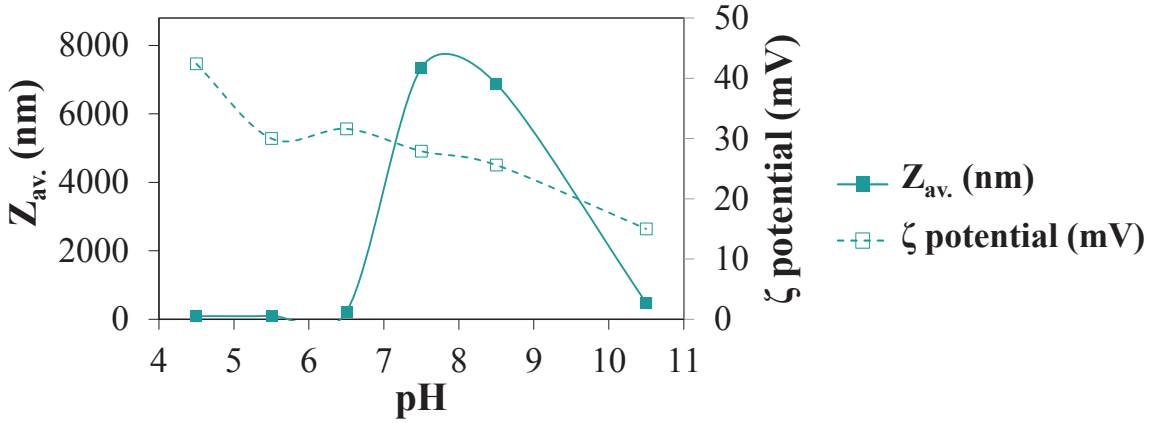
One might expect that chain length has a great effect on polymer adsorption, since high molar mass polymers are more prone to give rise to longer tails and loops than the smaller molecules, increasing the coverage of the particles and the affinity of the polymers for the clay surface (indicated by the initial slope).[95] In fact, in the case of MR9 and MR10,

adsorption of the longer chain was higher, however, the discrepancy between both curves can be considered minor.

3.4.2.3 Adsorption isotherms of DMAEMA-based macroRAFT agents

Two different cationic macroRAFT agents based on DMAEMA (MR11 and MR12) were synthesized and submited to a quaternization process, to guarantee the total ionization of the chains independently of the pH of the medium. These molecules were used in the adsorption study as well as the unquaternized MR12. The particle size and zeta potential of Laponite platelets functionalized with the untreated copolymer MR12 were measured at different pH values, as shown in Figure 3.25.

Figure 3.25 – Evolution of the average hydrodynamic diameters (full symbols and full line) and zeta potential (open symbols and dashed line) with pH for Laponite particles functionalized with P(DMAEMA$_{19}$-*co*-BA$_{14}$)-CTPPA (MR12).

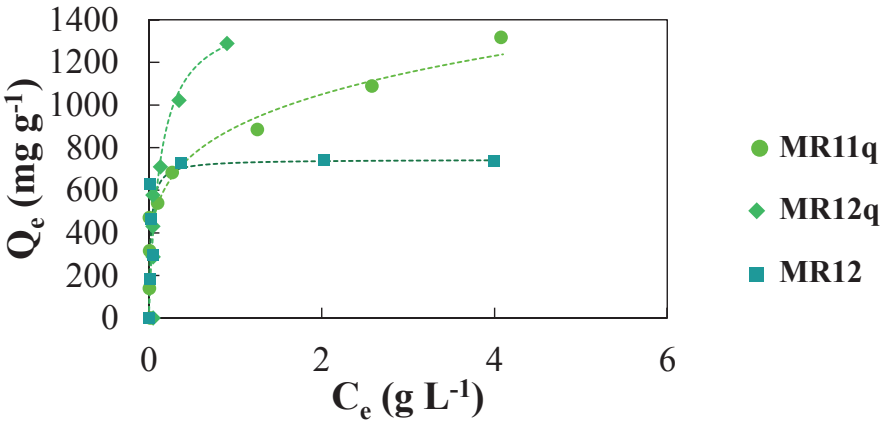


Laponite = 5.0 g L^{-1}. [MacroRAFT] = 10 g L^{-1}.
Source: elaborated by the author.

These results show that there is a wide aggregation zone between pH 6.5 and 10.5 and that the zeta potential of the macroRAFT/Laponite complex decreases with increasing the pH. For this reason, the selected pH to carry out the adsorption study with the untreated copolymer MR12 was 6, which preceds the aggregation zone.

The adsorption isotherm results for all macroRAFT agents are shown in Figure 3.26.

Figure 3.26 – Isotherms for macroRAFT adsorption onto the Laponite surface.



Laponite concentration = 5.0 g L^{-1}.
MR11 (q) = P(qDMAEMA$_{10}$-*co*-BA$_4$)-CTPPA at pH 10;
MR12 (q) = P(qDMAEMA$_{19}$-*co*-BA$_{14}$)-CTPPA at pH 10 and
MR12 = P(DMAEMA$_{19}$-*co*-BA$_{14}$)-CTPPA at pH 6.
Solid lines are fits to the Langmuir equation
Source: elaborated by the author.

As expected for the adsorption of positively charged polymers by clay minerals, high-affinity type isotherms were obtained for all DMAEMA-based macroRAFT agents. All data fitted better to the Langmuir adsorption model than to Freundlich, and a very good fit was obtained, in particular for the non quaternized copolymer MR12, as shown in Table 3.8.

Table 3.8 – Langmuir constants and correlation coefficient for adsorption of macroRAFT agents P(DMAEMA$_{10}$-*co*-BA$_4$)-CTPPA (MR11) quaternized at pH 10; P(DMAEMA$_{19}$-*co*-BA$_{14}$)-CTPPA (MR12) quaternized at pH 10 and P(DMAEMA$_{19}$-*co*-BA$_{14}$)-CTPPA (MR12) at pH 6 onto Laponite in water at 25 °C.

	Langmuir				Freundlich		
MacroRAFT	**Q_{max} (mg g^{-1})**	**α_L**	**K_L**	**R**	**Slope (*n*)**	**K_F (L mg^{-1})**	**R**
MR11 (q)	12.7×10^2	6.10	7.78×10^3	0.9886	0.23	8.95×10^2	0.8806
MR12 (q)	14.6×10^2	7.59	11.1×10^3	0.9923	0.50	15.7×10^2	0.8167
MR12	7.75×10^2	45.2	33.7×10^3	0.9999	0.16	6.76×10^2	0.7100

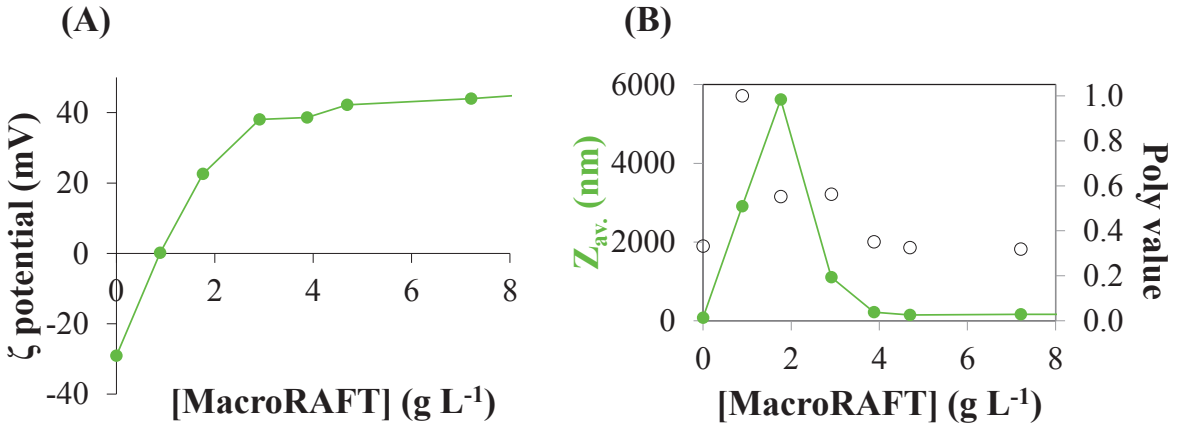
Source: elaborated by the author.

The high-affinity character of the isotherms indicates that the affinity of the macroRAFT agents for the surface of Laponite is high even at very low concentrations of copolymer, and saturation of adsorption is reached when molecules start to compete for space in the surface of the clay. However, the saturation point is above the point where there is a charge inversion of the particles. Adsorption beyond this point of zero charge (known as

isoelectric point, IEP) can be driven by hydrophobic interactions between the copolymer chains and by entropic effects (e. g. release of solvent and counterions from the charged copolymers). Additionally, it can be attributed to existence of some empty spaces on the surface of the platelets when the overall net charge of the platelets is zero, which can be occupied by additional macroRAFT chains.[96] The evolution of zeta potential, the average hydrodynamic diameters and poly value with the concentration of MR11q, shown in Figure 3.27, indicates that particles are totally neutralized (point of zero charge) at very low concentrations of copolymer (0.88 g L^{-1}), situation characterized by a severe coagulation. In fact, maximum aggregation commonly occurs for ζ potentials close to zero. For the successful synthesis of nanocomposite materials with controlled morphologies through the REEP technique, an efficient control over the initial dispersion of the macroRAFT/Laponite particles is a key factor, so it is crucial to guarantee that particles are well dispersed after the addition of macroRAFT agent. At elevated macroRAFT concentrations, the repulsive double-layer forces between the platelets (now positively charged, with platelets fully coated with macroRAFT chains) are reestablished, leading to highly stable dispersions.

At the point of zero charge, the macroRAFT agent presents a cationic charge of 0.73 meq per gram of Laponite, which can be compared to the cation exchange capacity of the clay (0.75 meq g^{-1}) (even though this value is an average value for the CEC of Laponite). The reversal of surface charges happens slightly below the CEC of Laponite, which can be explained by a discrete mismatch in charge separation between the cationic macroRAFT agent and the negative surface charges of Laponite (different average distances between negative charges in clay surface and between the quaternary nitrogen groups along the copolymer chain).[43, 97] In addition, this result represents a strong evidence that P(qDMAEMA$_{10}$-*co*-BA$_4$)-CTPPA (MR11q) is adsorbed preferentially in an extended configuration. Adsorption, however, can continue even after the neutralization of the negative surface charges of Laponite, and the adsorbed amount at saturation (Q_{max}), is considerably above the adsorbed amount found at point of charge inversion.

Figure 3.27 – Evolution of (A) Zeta (ζ) potential and (B) the average hydrodynamic diameters and poly value with macroRAFT agent concentration for MR11q.



Source: elaborated by the author.

A comparison between the adsorption isotherms of untreated and quaternized P(DMAEMA$_{19}$-*co*-BA$_{14}$)-CTPPA (MR12 and MR12q) indicates that a higher adsorption plateau was obtained for the quaternized macroRAFT agent. In fact, higher levels of quaternization lead to stronger interactions between the cationic copolymer and the inorganic surface. Therefore, it is expected that, in the case polymers with of lower cationicity, the adsorption of more molecules would be necessary to compensate the same amount of charges of the quaternized correspondent, leading to higher adsorbed amounts.[98, 99] In our case, some differences between both systems, concerning mainly the pH of the medium, should be considered though. The pH of the untreated macroRAFT complex was adjusted to 6 to guarantee the ionization of the amine groups of DMAEMA. This process resulted in an increase in the positive charge density of the edges of the platelets, which might have caused an electrostatic repulsion between the positively charged molecules and the positive edges, reducing adsorption. At a higher pH of ~10, which was the case for the quaternized copolymer, the edges of the platelets were almost neutral and, as a consequence, not opposing adsorption.

In addition, some other effects should be taken into account. The electrostatic interactions in this system involve not only the attraction between the negatively charged surfaces of Laponite and the positively charged segments, but also the mutual repulsive interaction between the charged units of the polymer. With high intramolecular repulsion interactions, the adsorbed polymer is found in a rather more extended (flat) chain conformation, with a great amount of "trains" (adsorbed segments), and the interaction between the segments and the surface is maximized. This phenomenon opposes adsorption

(leads to a lower adsorbed amount at saturation as the chains adopt a more extended conformation), and predominates for moderately to highly charged polyelectrolytes. As cationicity decreases, the development of long "loops" and "tails" is permitted. However, this is not what is observed for the untreated and the quaternized P(DMAEMA$_{19}$-*co*-BA$_{14}$)-CTPPA (MR12 and MR12q), and the adsorption of the quaternized copolymer is higher than the non quaternized one. It should also be considered, though, that as cationicity increases (either from higher degrees of ionization/quaternization or lower ionic strength), so increases the electrostatic repulsion and chains become more stretched and rigid until a point where they are adsorbed in a highly extended (flat) conformation, allowing the formation of bilayers of adsorbed polycations[5] (which could explain the higher adsorption of the quaternized molecule, in this case).

When both quaternized macroRAFT agents are compared in terms of adsorption, a lower adsorption plateau is achieved for the shorter and less hydrophobic copolymer P(qDMAEMA$_{10}$-*co*-BA$_4$)-CTPPA (MR11q). Two main factors determine that the chain conformation is flatter in this system than it is for the adsorption of P(qDMAEMA$_{19}$-*co*-BA$_{14}$)-CTPPA (MR12q). The first one is the lower molar mass of the chains. The fraction of polymer units effectively adsorbed onto the mineral surface decreases with the increase in molar mass so, with increasing chain length, the formation of loops and tails also increases. The second factor is that this copolymer has less hydrophobic units of BA, therefore, the rate of cationicity and, consequently, the electrostatic repulsion between identically charged groups along the same chain is higher for this molecule. In addition, as MR12q is richer in BA units (so it is a more flexible molecule) and only the cationic groups of the polymer can be adsorbed, this polyelectrolyte chain can adopt a more coiled and loopy conformation.[100]

3.5 Conclusions

The synthesis of 12 different macroRAFT agents by solution polymerization has been presented and it represents the initial step of this work towards the production of polymer/Laponite nanocomposite latexes by RAFT-mediated emulsion polymerization. Polymerizations were successfully carried out and the synthesis of most macroRAFT agents followed a controlled behavior, according to the RAFT mechanism. The low molar masses of the homo and copolymers, however, as well as the use of PEGA macromonomer and the methylation agent for SEC analysis, prejudiced the characterization of some of the products,

giving unrealistic values of M_n and $Đ$, as in the cases of P(PEGA$_5$-*co*-BA$_3$)-CTPPA (MR8) and P(AA$_4$-*co*-PEGA$_4$-*co*-BA$_4$)-CTPPA (MR9). The chain extensions of PAA-CTPPA and PAA-*b*-P(PEGA-*co*-BA)-CTPPA with AA and BA, were successfully carried out. Considering that obtaining controlled and uniform (in terms of dispersity) copolymers is not of fundamental importance for the synthesis of nanocomposite particles (and, therefore, it is not main objective of this work), the homo and copolymers obtained here are adequate for the intention proposed in this work,[101] since they can be chain-extended by a hydrophobic monomer to form block copolymers that adsorb onto the surface of Laponite and allow the formation of a polymeric layer from the clay surface.

With the growing potential applications of clay/polymer hybrid materials, increasing attention has been dedicated recently to better understand the typical interactions from these systems. So, the equilibrium adsorption of PAA, PEGA and DMAEMA-based macroRAFT agents has been studied by graphically plotting the solid phase concentration of these molecules against their liquid phase concentration, in adsorption isotherms. It represents the second step towards the production of polymer/Laponite nanocomposite latexes by RAFT-mediated emulsion polymerization, which is a key stage of this work.

The interpretation of these isotherms, however, can be complicated. The adsorption process suffers a strong influence of the polymeric chain conformation, and several factors interfere in this conformation, including the pH of the medium, the flexibility of the molecules, their cationicity, molar mass, concentration, and so forth. Many theories have been developed for the adsorption of ionic or nonionic polymers on charged interfaces from aqueous solution. The isotherms obtained in this work, measured for low concentrations of macroRAFT agents, were either of the L-type or the high-affinity type isotherms, and they were fitted to the Langmuir and Freundlich models.

The adsorption isotherms of anionic macroRAFT agents PAA$_{40}$-CTPPA (MR1) and P(AA$_{16}$-*co*-BA$_{16}$)-CTPPA (MR2) revealed that, at pH 7.5, the presence of hydrophobic domains is essential for the adsorption process. While the adsorption of PAA$_{40}$-CTPPA was almost nonexistent at neutral pH, the adsorption of the BA-containing copolymer, P(AA$_{16}$-*co*-BA$_{16}$)-CTPPA, fitted well to the Freundlich model, presenting a constant K_F of 71.62 L mg^{-1}, which indicates a high adsorption capacity

The favorable effect of BA units on adsorption was also revealed by the isotherms of PEGA-based macroRAFT agents. In addition, it was possible to conclude by these isotherms that, possibly, intermolecular complexes are formed between AA and linear PEG block,

interfering in adsorption of PEG-*b*-PAA-CTPPA (MR4). This effect, nonetheless, was reduced when ethylene glycol units were disposed as pending segments, as in P(AA-*b*-PEGA)-CTPPA (MR5), for which a higher adsorption plateau was obtained. The isotherms of random copolymers composed of AA, BA and PEGA indicated that the random distribution of these monomers in the structure of the macroRAFT agent is less favorable for adsorption than their segmental distribution in blocks, and a discrete effect of molar mass on adsorption was observed for these molecules. The only two totally uncharged macroRAFT agents, PEG-CTPPA (MR1) and P(PEGA-*co*-BA)-CTPPA (MR8), presented a high affinity for Laponite and, fitting well to the Langmuir model, as expected from the L-type shape of curves, they presented adsorbed amounts of macroRAFT agents at saturation (Q_{max}) of 463.78 and 430.46 mg g^{-1}, respectively. These values agree well with what has been reported in the literature for the adsorption of a similar molecule (PEG-CTPPA) onto Laponite.[12]

High-affinity-type curves were obtained for the adsorption of cationic macroRAFT agents onto Laponite, and all data fitted well to the Langmuir adsorption model. The adsorption seems to be dependent on the quaternization of the macroRAFT agents, since, when compared to the untreated copolymer, a different profile, with higher adsorption plateau, was obtained for the quaternized molecule. A general comparison between cationic, nonionic and anionic macroRAFT agents reveals a considerably higher affinity of the positively charged molecules for Laponite surface. Even though cationic systems can be more challenging in terms of colloidal stability, due to the greater ability of polycations to cause coagulation and bridging effects, the strong adsorption of these molecules onto clay minerals make them extremely attractive and promising for the synthesis of nanocomposites. However, uncharged macroRAFT agents PEG-CTPPA and P(PEGA-*co*-BA)-CTPPA are very interesting for this purpose as well, since a relatively strong adsorption was also obtained for these molecules. Furthermore, they have the advantage of not causing the charge inversion of the clay platelets and consequently are not associated to the stability issues caused by this phenomenon.

References

1 NGUYEN, D.; ZONDANOS, H. S.; FARRUGIA, J. M.; SERELIS, A. K.; SUCH, C. H.; HAWKETT, B. S. Pigment encapsulation by emulsion polymerization using macro-RAFT copolymers. **Langmuir,** v. 24, n. 5, p. 2140-2150, 2008.

[2] DAIGLE, J.-C.; CLAVERIE, J. P. A simple method for forming hybrid core-shell nanoparticles suspended in water. **Journal of Nanomaterials,** v. 2008, p. 1-8, 2008.

[3] DENOYEL, R.; DURAND, G.; LAFUMA, F.; AUDEBERT, R. Adsorption of cationic polyelectrolytes onto montmorillonite and silica - microcalorimetric study of their conformation. **Journal of Colloid and Interface Science,** v. 139, n. 1, p. 281-290, oct. 1990.

[4] CHURCHMAN, G. J. Formation of complexes between bentonite and different cationic polyelectrolytes and their use as sorbents for non-ionic and anionic pollutants. **Applied Clay Science,** v. 21, n. 3-4, p. 177-189, june 2002.

[5] DURANDPIANA, G.; LAFUMA, F.; AUDEBERT, R. Flocculation and adsorption properties of cationic polyelectrolytes toward Na-Montmorillonite dilute suspensions. **Journal of Colloid and Interface Science,** v. 119, n. 2, p. 474-480, oct. 1987.

[6] HUANG, X.; XU, S.; ZHONG, M.; WANG, J.; FENG, S.; SHI, R. Modification of Na-bentonite by polycations for fabrication of amphoteric semi-IPN nanocomposite hydrogels. **Applied Clay Science,** v. 42, n. 3-4, p. 455-459, jan. 2009.

[7] PARFITT, R. L.; GREENLAND, D. J. The adsorption of poly(ethylene glycols) on clay minerals. **Clay Minerals,** v. 8, p. 305-315, july 1970.

[8] ZHAO, X.; URANO, K.; OGASAWARA, S. Adsorption of polyethylene glycol from aqueous solution on montmorillonite clays. **Colloid and Polymer Science,** v. 267, n. 10, p. 899-906, oct. 1989.

[9] MORARIU, S.; BERCEA, M.; SACARESCU, L. Tailoring of clay/poly(ethylene oxide) hydrogel properties by chitosan incorporation. **Industrial & Engineering Chemistry Research,** v. 53, n. 35, p. 13690-13698, sept. 2014.

[10] MONGONDRY, P.; NICOLAI, T.; TASSIN, J. F. Influence of pyrophosphate or polyethylene oxide on the aggregation and gelation of aqueous Laponite dispersions. **Journal of Colloid and Interface Science,** v. 275, n. 1, p. 191-196, july 2004.

[11] NELSON, A.; COSGROVE, T. A small-angle neutron scattering study of adsorbed poly(ethylene oxide) on Laponite. **Langmuir,** v. 20, n. 6, p. 2298-2304, mar. 2004.

[12] GUIMARAES, T. R.; CHAPARRO, T. D. C.; D'AGOSTO, F.; LANSALOT, M.; DOS SANTOS, A. M.; BOURGEAT-LAMI, E. Synthesis of multi-hollow clay-armored latexes by surfactant-free emulsion polymerization of styrene mediated by poly(ethylene oxide)-based macroRAFT/Laponite complexes. **Polymer Chemistry,** v. 5, n. 22, p. 6611-6622, nov. 2014.

[13] KLOPROGGE, J. T.; KOMARNENI, S.; AMONETTE, J. E. Synthesis of smectite clay minerals: A critical review. **Clays and Clay Minerals,** v. 47, n. 5, p. 529-554, oct. 1999.

14 RAY, S. S.; OKAMOTO, M. Polymer/layered silicate nanocomposites: A review from preparation to processing. **Progress in Polymer Science,** v. 28, n. 11, p. 1539-1641, nov. 2003.

15 ALEXANDRE, M.; DUBOIS, P. Polymer-layered silicate nanocomposites: Preparation, properties and uses of a new class of materials. **Materials Science & Engineering R-Reports,** v. 28, n. 1-2, p. 1-63, jun. 2000.

16 RUZICKA, B.; ZACCARELLI, E. A fresh look at the Laponite phase diagram. **Soft Matter,** v. 7, n. 4, p. 1268-1286, 2011.

17 NEGRETE-HERRERA, N.; PUTAUX, J.-L.; BOURGEAT-LAMI, E. Synthesis of polymer/Laponite nanocomposite latex particles via emulsion polymerization using silylated and cation-exchanged Laponite clay platelets. **Progress in Solid State Chemistry,** v. 34, n. 2-4, p. 121-137, 2006.

18 CUMMINS, H. Z. Liquid, glass, gel: The phases of colloidal Laponite. **Journal of Non-Crystalline Solids,** v. 353, n. 41-43, p. 3891-3905, nov. 2007.

19 THOMPSON, D. W.; BUTTERWORTH, J. T. The nature of Laponite and its aqueous dispersions. **Journal of Colloid and Interface Science,** v. 151, n. 1, p. 236-243, june 1992.

20 MOURCHID, A.; LECOLIER, E.; VAN DAMME, H.; LEVITZ, P. On viscoelastic, birefringent, and swelling properties of Laponite clay suspensions: Revisited phase diagram. **Langmuir,** v. 14, n. 17, p. 4718-4723, aug. 1998.

21 TAWARI, S. L.; KOCH, D. L.; COHEN, C. Electrical double-layer effects on the brownian diffusivity and aggregation rate of Laponite clay particles. **Journal of Colloid and Interface Science,** v. 240, n. 1, p. 54-66, aug. 2001.

22 WALKER, G. F. Diffusion of exchangeable cations in vermiculite. **Nature,** v. 184, n. 4696, p. 1392-1393, 1959.

23 BRENNAN, L. J.; KOWALSKI, A. J.; RYAN, P. M.; SANDERSON, A. R.; WAGLE, A. S. **Externally structured aqueous isotropic liquid detergent compositions.** WO2013160022-A1, 2013.

24 NICOLAI, T.; COCARD, S. Structure of gels and aggregates of disk-like colloids. **European Physical Journal E,** v. 5, n. 2, p. 221-227, may 2001.

25 _____. Dynamic light-scattering study of aggregating and gelling colloidal disks. **Journal of Colloid and Interface Science,** v. 244, n. 1, p. 51-57, dec. 2001.

26 RAND, B.; PEKENC, E.; GOODWIN, J. W.; SMITH, R. W. Investigation into the existence of edge-face coagulated structures in Na-Montmorillonite suspensions. **Journal of the Chemical Society-Faraday Transactions I,** v. 76, p. 225-235, 1980.

27 DIJKSTRA, M.; HANSEN, J. P.; MADDEN, P. A. Gelation of a clay colloid suspension. **Physical Review Letters,** v. 75, n. 11, p. 2236-2239, sept. 1995.

[28] HARAGUCHI, K. Synthesis and properties of soft nanocomposite materials with novel organic/inorganic network structures. **Polymer Journal,** v. 43, n. 3, p. 223-241, mar. 2011.

[29] HERRERA, N. N.; LETOFFE, J. M.; REYMOND, J. P.; BOURGEAT-LAMI, E. Silylation of Laponite clay particles with monofunctional and trifunctional vinyl alkoxysilanes. **Journal of Materials Chemistry,** v. 15, n. 8, p. 863-871, 2005.

[30] LEVITZ, P.; LECOLIER, E.; MOURCHID, A.; DELVILLE, A.; LYONNARD, S. Liquid-solid transition of Laponite suspensions at very low ionic strength: Long-range electrostatic stabilisation of anisotropic colloids. **Europhysics Letters,** v. 49, n. 5, p. 672-677, mar. 2000.

[31] CADENE, A.; DURAND-VIDAL, S.; TURQ, P.; BRENDLE, J. Study of individual Na-Montmorillonite particles size, morphology, and apparent charge. **Journal of Colloid and Interface Science,** v. 285, n. 2, p. 719-730, may 2005.

[32] TOMBACZ, E.; SZEKERES, M. Colloidal behavior of aqueous montmorillonite suspensions: The specific role of pH in the presence of indifferent electrolytes. **Applied Clay Science,** v. 27, n. 1-2, p. 75-94, oct. 2004.

[33] YARIV, S. Combined DTA - mass-spectrometry of organo-clay complexes. **Journal of Thermal Analysis,** v. 36, n. 6, p. 1953-1961, sept.-oct. 1990.

[34] BORSACCHI, S.; GEPPI, M.; RICCI, L.; CARDELLI, A.; RUGGERI, G. Preparation, characterization and solid state NMR investigation of a dye-containing smectite clay. **Studia Universitatis Babes-Bolyai Chemia,** v. 56, n. 3, p. 15-26, 2011.

[35] SCHOONHEYDT, R. A.; HEUGHEBAERT, L. Clay adsorbed dyes - methylene-blue on Laponite. **Clay Minerals,** v. 27, n. 1, p. 91-100, mar. 1992.

[36] LAN, T.; KAVIRATNA, P. D.; PINNAVAIA, T. J. Mechanism of clay tactoid exfoliation in epoxy-clay nanocomposites. **Chemistry of Materials,** v. 7, n. 11, p. 2144-2150, nov. 1995.

[37] LIU, Q.; ZHANG, S.; SUN, D.; XU, J. Foams stabilized by Laponite nanoparticles and alkylammonium bromides with different alkyl chain lengths. **Colloids and Surfaces a-Physicochemical and Engineering Aspects,** v. 355, n. 1-3, p. 151-157, feb. 2010.

[38] BORSACCHI, S.; GEPPI, M.; RICCI, L.; RUGGERI, G.; VERACINI, C. A. Interactions at the surface of organophilic-modified Laponites: A multinuclear solid-state NMR study. **Langmuir,** v. 23, n. 7, p. 3953-3960, mar. 2007.

[39] KIM, Y. J.; LIU, Y. D.; CHOI, H. J.; PARK, S.-J. Facile fabrication of pickering emulsion polymerized polystyrene/Laponite composite nanoparticles and their electrorheology. **Journal of Colloid and Interface Science,** v. 394, p. 108-114, mar. 2013.

[40] MIRAU, P. A.; SERRES, J. L.; JACOBS, D.; GARRETT, P. H.; VAIA, R. A. Structure and dynamics of surfactant interfaces in organically modified clays. **Journal of Physical Chemistry B,** v. 112, n. 34, p. 10544-10551, aug. 2008.

[41] NEGRETE-HERRERA, N.; PUTAUX, J.-L.; DAVID, L.; BOURGEAT-LAMI, E. Polymer/Laponite composite colloids through emulsion polymerization: Influence of the clay modification level on particle morphology. **Macromolecules,** v. 39, n. 26, p. 9177-9184, dec. 2006.

[42] NEGRETE-HERRERA, N.; PUTAUX, J.-L.; DAVID, L.; DE HAAS, F.; BOURGEAT-LAMI, E. Polymer/Laponite composite latexes: Particle morphology, film microstructure, and properties. **Macromolecular Rapid Communications,** v. 28, n. 15, p. 1567-1573, aug. 2007.

[43] THENG, B. K. G. **Formation and properties of clay-polymer complexes**. Second. Elsevier Science, 2012. 511.

[44] HARVEY, C. C.; LAGALY, G. Chapter 10.1 conventional applications. In: FAÏZA BERGAYA, B. K. G. T.;GERHARD, L. (Ed.). **Developments in clay science**: Elsevier, 2006.v.1, p.501-540.

[45] PICCOLO, A.; PIETRAMELLARA, G.; MBAGWU, J. S. C. Use of humic substances as soil conditioners to increase aggregate stability. **Geoderma,** v. 75, n. 3-4, p. 267-277, feb. 1997.

[46] CHESHIRE, M. V.; DUMAT, C.; FRASER, A. R.; HILLIER, S.; STAUNTON, S. The interaction between soil organic matter and soil clay minerals by selective removal and controlled addition of organic matter. **European Journal of Soil Science,** v. 51, n. 3, p. 497-509, sept. 2000.

[47] GILES, C. H.; MACEWAN, T. H.; NAKHWA, S. N.; SMITH, D. Studies in adsorption .11. A system of classification of solution adsorption isotherms, and its use in diagnosis of adsorption mechanisms and in measurement of specific surface areas of solids. **Journal of the Chemical Society**, p. 3973-3993, oct. 1960.

[48] MULLER, D.; MALMSTEN, M.; TANODEKAEW, S.; BOOTH, C. Adsorption of diblock copolymers of poly(ethylene oxide) and poly(lactide) at hydrophilic silica from aqueous solution. **Journal of Colloid and Interface Science,** v. 228, n. 2, p. 317-325, aug. 2000.

[49] VANGEYTE, P.; LEYH, B.; ROJAS, O. J.; CLAESSON, P. M.; HEINRICH, M.; AUVRAY, L.; WILLET, N.; JEROME, R. Adsorption of poly(ethylene oxide)-b-poly(e-caprolactone) copolymers at the silica-water interface. **Langmuir,** v. 21, n. 7, p. 2930-2940, mar. 2005.

[50] HELLER, H.; KEREN, R. Anionic polyacrylamide polymer adsorption by pyrophyllite and montmorillonite. **Clays and Clay Minerals,** v. 51, n. 3, p. 334-339, june 2003.

[51] DENG, Y. J.; DIXON, J. B.; WHITE, G. N. Adsorption of polyacrylamide on smectite, illite, and kaolinite. **Soil Science Society of America Journal,** v. 70, n. 1, p. 297-304, jan.-feb. 2006.

[52] RAMOS-TEJADA, M. M.; DE VICENTE, J.; ONTIVEROS, A.; DURAN, J. D. G. Effect of humic acid adsorption on the rheological properties of sodium montmorillonite suspensions. **Journal of Rheology,** v. 45, n. 5, p. 1159-1172, sept.-oct. 2001.

[53] TOMBACZ, E.; FILIPCSEI, G.; SZEKERES, M.; GINGL, Z. Particle aggregation in complex aquatic systems. **Colloids and Surfaces a-Physicochemical and Engineering Aspects,** v. 151, n. 1-2, p. 233-244, june 1999.

[54] LIU, Y.; ZHU, M. F.; LIU, X. L.; ZHANG, W.; SUN, B.; CHEN, Y. M.; ADLER, H. J. P. High clay content nanocomposite hydrogels with surprising mechanical strength and interesting deswelling kinetics. **Polymer,** v. 47, n. 1, p. 1-5, jan. 2006.

[55] LUO, Y.; WANG, X.; LI, B.-G.; ZHU, S. Toward well-controlled ab initio RAFT emulsion polymerization of styrene mediated by 2-(((dodecylsulfanyl)carbonothioyl)sulfanyl)propanoic acid. **Macromolecules,** v. 44, n. 2, p. 221-229, 2011.

[56] DU, J.; ZHU, J.; WU, R.; XU, S.; TAN, Y.; WANG, J. A facile approach to prepare strong poly(acrylic acid)/Laponite ® ionic nanocomposite hydrogels at high clay concentrations. **Rsc Advances,** v. 5, n. 74, p. 60152-60160, 2015.

[57] LABANDA, J.; LLORENS, J. Rheology of Laponite colloidal dispersions modified by sodium polyacrylates. **Colloids and Surfaces a-Physicochemical and Engineering Aspects,** v. 249, n. 1-3, p. 127-129, nov. 2004.

[58] LAGALY, G.; ZIESMER, S. Sol-gel transitions of sodium montmorillonite dispersions by cationic end-capped poly (ethylene oxides) (surface modification of bentonites, iv). **Colloid and Polymer Science,** v. 284, n. 9, p. 947-956, june 2006.

[59] LOCHHEAD, R. Y.; HAYNES, C. T.; JONES, S. R.; SMITH, V. The high throughput investigation of polyphenolic couplers in biodegradable packaging materials. **Applied Surface Science,** v. 252, n. 7, p. 2535-2548, jan. 2006.

[60] HUSKIC, M.; ZAGAR, E.; ZIGON, M.; BRNARDIC, I.; MACAN, J.; IVANKOVIC, M. Modification of montmorillonite by cationic polyesters. **Applied Clay Science,** v. 43, n. 3-4, p. 420-424, mar. 2009.

[61] INYANG, H. I.; BAE, S. Polyacrylamide sorption opportunity on interlayer and external pore surfaces of contaminant barrier clays. **Chemosphere,** v. 58, n. 1, p. 19-31, jan. 2005.

[62] UEDA, T.; HARADA, S. Adsorption of cationic polysulfone on bentonite. **Journal of Applied Polymer Science,** v. 12, n. 11, p. 2395–2401, 1968.

63 STRAWHECKER, K. E.; MANIAS, E. Structure and properties of poly(vinyl alcohol)/Na^+ montmorillonite nanocomposites. **Chemistry of Materials,** v. 12, n. 10, p. 2943-2949, oct. 2000.

64 CARRADO, K. A.; THIYAGARAJAN, P.; ELDER, D. L. Polyvinyl alcohol clay complexes formed by direct synthesis. **Clays and Clay Minerals,** v. 44, n. 4, p. 506-514, aug. 1996.

65 XU, J.; MENG, Y. Z.; LI, R. K. Y.; XU, Y.; RAJULU, A. V. Preparation and properties of poly(vinyl alcohol)-vermiculite nanocomposites. **Journal of Polymer Science Part B-Polymer Physics,** v. 41, n. 7, p. 749-755, apr. 2003.

66 FRANCIS, C. W. Adsorption of polyvinylpyrrolidone on reference clay minerals. **Soil Science,** v. 115, n. 1, p. 40-54, jan. 1973.

67 SEQUARIS, J. M.; HILD, A.; NARRES, H. D.; SCHWUGER, M. J. Polyvinylpyrrolidone adsorption on Na-Montmorillonite. Effect of the polymer interfacial conformation on the colloidal behavior and binding of chemicals. **Journal of Colloid and Interface Science,** v. 230, n. 1, p. 73-83, oct. 2000.

68 ATESOK, G.; SOMASUNDARAN, P.; MORGAN, L. J. Charge effects in the adsorption of polyacrylamides on sodium kaolinite and its flocculation. **Powder Technology,** v. 54, n. 2, p. 77-83, feb. 1988.

69 DENG, Y. J.; DIXON, J. B.; WHITE, G. N.; LOEPPERT, R. H.; JUO, A. S. R. Bonding between polyacrylamide and smectite. **Colloids and Surfaces a-Physicochemical and Engineering Aspects,** v. 281, n. 1-3, p. 82-91, june 2006.

70 ARANDA, P.; RUIZHITZKY, E. Poly(ethylene oxide)-silicate intercalation materials. **Chemistry of Materials,** v. 4, n. 6, p. 1395-1403, nov.-dec. 1992.

71 BOURGEAT-LAMI, E.; GUIMARAES, T. R.; PEREIRA, A. M. C.; ALVES, G. M.; MOREIRA, J. C.; PUTAUX, J.-L.; DOS SANTOS, A. M. High solids content, soap-free, film-forming latexes stabilized by Laponite clay platelets. **Macromolecular Rapid Communications,** v. 31, n. 21, p. 1874-1880, nov. 2010.

72 XU, X.; SMITH, A. E.; KIRKLAND, S. E.; MCCORMICK, C. L. Aqueous RAFT synthesis of pH-responsive triblock copolymer mPEO-PAPMA-PDPAEMA and formation of shell cross-linked micelles. **Macromolecules,** v. 41, n. 22, p. 8429-8435, 2008.

73 BOURSIER, T.; CHADUC, I.; RIEGER, J.; D'AGOSTO, F.; LANSALOT, M.; CHARLEUX, B. Controlled radical polymerization of styrene in miniemulsion mediated by PEO-based trithiocarbonate macromolecular RAFT agents. **Polymer Chemistry,** v. 2, n. 2, p. 355-362, feb. 2011.

74 BUETUEN, V.; ARMES, S. P.; BILLINGHAM, N. C. Selective quaternization of 2-(dimethylamino)ethyl methacrylate residues in tertiary amine methacrylate diblock copolymers. **Macromolecules,** v. 34, n. 5, p. 1148-1159, jan. 2001.

[75] ZHAO, W.; FONSNY, P.; FITZGERALD, P.; WARR, G. G.; PERRIER, S. Unexpected behavior of polydimethylsiloxane/poly(2-(dimethylamino)ethyl acrylate) (charged) amphiphilic block copolymers in aqueous solution. **Polymer Chemistry,** v. 4, n. 6, p. 2140-2150, feb. 2013.

[76] HASHIMOTO, N.; AOYAMA, T.; SHIOIRI, T. New methods and reagents in organic synthesis. 14. A simple efficient preparation of methyl esters with trimethylsilyldiazomethane ($TMSCHN_2$) and its application to gas chromatographic analysis of fatty acids. **Chemical & Pharmaceutical Bulletin,** v. 29, n. 5, p. 1475-1478, 1981.

[77] SAHNOUN, M.; CHARREYRE, M. T.; VERON, L.; DELAIR, T.; D'AGOSTO, F. Synthetic and characterization aspects of dimethylaminoethyl methacrylate reversible addition fragmentation chain transfer (RAFT) polymerization. **Journal of Polymer Science Part a-Polymer Chemistry,** v. 43, n. 16, p. 3551-3565, aug. 2005.

[78] LI, M.; LI, G. L.; ZHANG, Z.; LI, J.; NEOH, K.-G.; KANG, E.-T. Self-assembly of pH-responsive and fluorescent comb-like amphiphilic copolymers in aqueous media. **Polymer,** v. 51, n. 15, p. 3377–3386, july 2010.

[79] LIU, F.; URBAN, M. W. Dual temperature and pH responsiveness of poly(2-(n,n-dimethylamino)ethyl methacrylate-co-n-butyl acrylate) colloidal dispersions and their films. **Macromolecules,** v. 41, n. 17, p. 6531-6539, aug. 2008.

[80] MESPOUILLE, L.; DEGEE, P.; DUBOIS, P. Amphiphilic poly(n,n-dimethylamino-2-ethyl methacrylate)-g-poly(ε-caprolactone) graft copolymers: Synthesis and characterisation. **European Polymer Journal,** v. 41, n. 6, p. 1187–1195, june 2005.

[81] LANGMUIR, I. The adsorption of gases on plane surfaces of glass, mica and platinum. **Journal of the American Chemical Society,** v. 40, p. 1361-1403, jul.-dec. 1918.

[82] FREUNDLICH, H. Concerning adsorption in solutions. **Zeitschrift Fur Physikalische Chemie--Stochiometrie Und Verwandtschaftslehre,** v. 57, n. 4, p. 385-470, dec. 1906.

[83] HAGHSERESHT, F.; LU, G. Q. Adsorption characteristics of phenolic compounds onto coal-reject-derived adsorbents. **Energy & Fuels,** v. 12, n. 6, p. 1100-1107, nov.-dec. 1998.

[84] FOO, K. Y.; HAMEED, B. H. Insights into the modeling of adsorption isotherm systems. **Chemical Engineering Journal,** v. 156, n. 1, p. 2-10, jan. 2010.

[85] LIMOUSIN, G.; GAUDET, J. P.; CHARLET, L.; SZENKNECT, S.; BARTHES, V.; KRIMISSA, M. Sorption isotherms: A review on physical bases, modeling and measurement. **Applied Geochemistry,** v. 22, n. 2, p. 249-275, feb. 2007.

[86] ALLEN, S. J.; GAN, Q.; MATTHEWS, R.; JOHNSON, P. A. Comparison of optimised isotherm models for basic dye adsorption by kudzu. **Bioresource Technology,** v. 88, n. 2, p. 143-152, june 2003.

[87] SMITH, K. L.; WINSLOW, A. E.; PETERSEN, D. E. Association reactions for ... Poly(alkylene oxides) and polymeric poly(carboxylic acids). **Industrial and Engineering Chemistry,** v. 51, n. 11, p. 1361-1364, 1959.

[88] KABANOV, V. A.; PAPISOV, I. M. Formation of complexes between the complementary synthetic-polymers and oligomers in dilute-solutions. **Vysokomolekulyarnye Soedineniya Seriya A,** v. 21, n. 2, p. 243-281, 1979.

[89] NURKEEVA, Z. S.; MUN, G. A.; KHUTORYANSKIY, V. V.; BITEKENOVA, A. B.; DUBOLAZOV, A. V.; ESIRKEGENOVA, S. Z. Ph effects in the formation of interpolymer complexes between poly (n-vinylpyrrolidone) and poly(acrylic acid) in aqueous solutions. **European Physical Journal E,** v. 10, n. 1, p. 65-68, jan. 2003.

[90] KUNITSKAYA, L. R.; BERKOVA, S. A.; ZHELTONOZHSKAYA, T. B. Block-copolymers of polyacrylamide with poly(ethylene oxide) forming intramolecular polycomplexes. **Molecular Crystals and Liquid Crystals,** v. 497, p. 614-623, 2008.

[91] PERMYAKOVA, N. M.; ZHELTONOZHSKAYA, T. B.; OBOZNOVA, N. V. Double-hydrophilic block copolymers forming intramolecular polycomplexes. **Molecular Crystals and Liquid Crystals,** v. 497, p. 639-647, 2008.

[92] ZHUNUSPAYEV, D. E.; MUN, G. A.; HOLE, P.; KHUTORYANSKIY, V. V. Solvent effects on the formation of nanoparticles and multilayered coatings based on hydrogen-bonded interpolymer complexes of poly(acrylic acid) with homo- and copolymers of n-vinyl pyrrolidone. **Langmuir,** v. 24, n. 23, p. 13742-13747, dec. 2008.

[93] HEMKER, D. J.; FRANK, C. W. Dynamic light-scattering-studies of the fractal aggregation of poly(methacrylic acid) and poly(ethylene glycol). **Macromolecules,** v. 23, n. 20, p. 4404-4410, oct. 1990.

[94] KHUTORYANSKIY, V. V.; MUN, G. A.; NURKEEVA, Z. S.; DUBOLAZOV, A. V. Ph and salt effects on interpolymer complexation via hydrogen bonding in aqueous solutions. **Polymer International,** v. 53, n. 9, p. 1382-1387, sept. 2004.

[95] TRENS, P.; DENOYEL, R. Conformation of poly(ethylene glycol) polymers at the silica water interface - a microcalorimetric study. **Langmuir,** v. 9, n. 2, p. 519-522, feb. 1993.

[96] PAVLOVIC, M.; ADOK-SIPICZKI, M.; NARDIN, C.; PEARSON, S.; BOURGEAT-LAMI, E.; PREVOT, V.; SZILAGYI, I. Effect of macroRAFT copolymer adsorption on the colloidal stability of layered double hydroxide nanoparticles. **Langmuir,** v. 31, n. 46, p. 12609-12617, nov. 2015.

[97] GREGORY, J. Rates of flocculation of latex particles by cationic polymers. **Journal of Colloid and Interface Science,** v. 42, n. 2, p. 448-456, feb. 1973.

[98] SAKAI, K.; SMITH, E. G.; WEBBER, G. B.; SCHATZ, C.; WANLESS, E. J.; BUTUN, V.; ARMES, S. P.; BIGGS, S. Comparison of the adsorption of cationic diblock copolymer micelles from aqueous solution onto mica and silica. **Langmuir,** v. 22, n. 12, p. 5328-5333, june 2006.

[99] HOOGEVEEN, N. G.; STUART, M. A. C.; FLEER, G. J. Polyelectrolyte adsorption on oxides .1. Kinetics and adsorbed amounts. **Journal of Colloid and Interface Science,** v. 182, n. 1, p. 133-145, sept. 1996.

[100] WU, B.; LI, C.; YANG, H.; LIU, G.; ZHANG, G. Formation of polyelectrolyte multilayers by flexible and semiflexible chains. **Journal of Physical Chemistry B,** v. 116, n. 10, p. 3106-3114, mar. 2012.

[101] DAS, P.; ZHONG, W.; CLAVERIE, J. P. Copolymer nanosphere encapsulated CdS quantum dots prepared by RAFT copolymerization: Synthesis, characterization and mechanism of formation. **Colloid and Polymer Science,** v. 289, n. 14, p. 1519-1533, sept. 2011.

4 Synthesis of hybrid latexes

4.1 Introduction

Layered silicate polymer nanocomposites (LSPN) are an attractive alternative for diversifying the applications of conventional polymeric materials.[1-5] The presence of clay particles confers various advantages over the pure polymeric counterparts of these materials, including enhanced hardness, mechanical strength and scratch resistance, improved optical and thermal properties, reduced gas permeability, as well as the attribution of novel and specific properties, and significant reductions in weight and even in the cost of these materials. Numerous examples of LSPNs are already commercially available and, in recent years, increasing attention has been dedicated to soft film-forming LSPN latexes due to the outstanding properties that these materials can offer in diverse coating applications.[6-8]

The main focus in this chapter is to evaluate the effectiveness of macroRAFT-assisted encapsulating emulsion polymerization (REEP) strategy for the synthesis of anisotropic composite latex particles incorporating Laponite platelets using different RAFT copolymers. For this purpose, as described in Chapter 3, macroRAFT agents containing hydrophilic (ionisable and/or polar) and hydrophobic domains were, initially, designed and synthesized by solution polymerization. For the successful incorporation of anisotropic fillers into polymer matrixes, the adsorption of these molecules onto Laponite was then was performed in aqueous medium and studied, by adsorption isotherms. Finally, the emulsion polymerization of methyl methacrylate (MMA), or methyl acrylate (MA), and butyl acrylate (BA) was carried out in the presence of the CTA-modified clays to generate clay/polymer nanocomposite latex particles.

The REEP strategy adopted in this work has been previously used for the successful encapsulation of diverse particles, including hydrophobic organic (phthalocyanine blue pigment) and hydrophilic inorganic pigment particles (alumina and zirconia-coated titanium dioxide),[9] different metal, metal oxide and metal nitride spherical particles,[10] cadmium sulfide[11] and lead sulfide[12] quantum dots, cerium oxide,[13,14,15,16] carbon nanotubes,[17,18] Gibbsite,[19] Montmorillonite clay[20] and even graphene oxide.[21], as already presented in Chapter 2 (section 2.3.3.1.4) The major feature in the REEP technique that allows the encapsulation of inorganic particles is the use of RAFT copolymers, or oligomers, that can direct the growing of the polymer chains to the surface of the particles, restricting

(preferably) it to the inorganic substrate. Even though a similar result could be obtained by attaching a free radical initiator to the surface, in theory, the decomposition of one initiator in two radicals leaves, at least, one free radical in the aqueous phase, generating a significant amount of polymer chains that are not attached to the inorganic particles.[22] In addition, RAFT copolymers can act as stabilizers, discarding, in most cases, the need for additional surfactant.[23, 24]

When the REEP strategy is employed to high aspect ratio substrates, such as nanotubes or platelets, anisotropic latex particles can be produced if we consider that the final hybrid particles tend to assume the shape morphology of the substrate. However, the encapsulation of anisotropic nano-objects is not so trivial. The disk shape morphology, large aspect ratio and high surface energy of layered minerals difficult the encapsulation process and, while the encapsulation of spherical inorganic particles can be achieved by conventional emulsion or miniemulsion methods,[25-28] most attempts to encapsulate unmodified[29] and, in some cases, surface-modified[30, 31] clay platelets by emulsion polymerization result in the formation of the so-called armored structures. In fact, forming a polymer layer around the platelets implies in imposing a lower energy state to the particles and, to guarantee that the platelets are located and maintained, individually, inside each latex particle, several parameters, related especially to kinetic and/or thermodynamic control mechanisms, must be optimized. Being able to control the morphology of the hybrid particles and, therefore, having control over the orientation of the platelets in the final polymeric, is fundamental for the final coating properties of the material. For this reason, the individual encapsulation of platelets with a thin polymer layer, resulting in anisotropic flat composite latex particles that are more likely to induce anisotropy into the final film, is highly desirable since it potentially improves the properties of the composite material.

In this chapter, various parameters were explored in the RAFT-mediated emulsion polymerization in the presence of Laponite particles. The main parameter studied was the nature of the macroRAFT agent, and molecules with different compositions, hydrophilic-lipophilic balances and chain lengths were evaluated in the synthesis of the hybrid latexes. The structure of each molecule has already been described in details in previous chapters and will not be further discussed here. Some other important parameters that were studied in this work include the RAFT copolymer concentration, pH, type and concentration of initiator, monomer feed composition and temperature. The RAFT agent chosen was the 4-cyano-4-thiothiopropylsulfanyl pentanoic acid (CTPPA), a (thiocarbonyl)sulfanyil

derivative that carries a short hydrophobic alkyl chain end (thiopropyl) as Z group. CTPPA has been reported numerous times in the literature[13, 32-36] and, besides presenting a facile synthesis, it has proven to be a potential candidate to act as an efficient reversible addition-fragmentation chain transfer agent, presenting an adequate reactivity and conferring living characteristics on the polymerization of the monomers proposed in this work. Laponite platelets were chosen among the layered silicates since it is an ideal model substrate, presenting a high chemical purity, a uniform dispersity of the elementary platelets and the ability to produce clear dispersions. After the adsorption of the RAFT (co)polymers, they were chain extended to form a polymer shell around the Laponite platelets, by emulsion polymerization under semi-batch conditions and in the absence of surfactant, resulting in layered silicate polymer nanocomposite latex particles with diverse morphologies.

4.2 Bibliographic Review

4.2.1 Nanocomposites

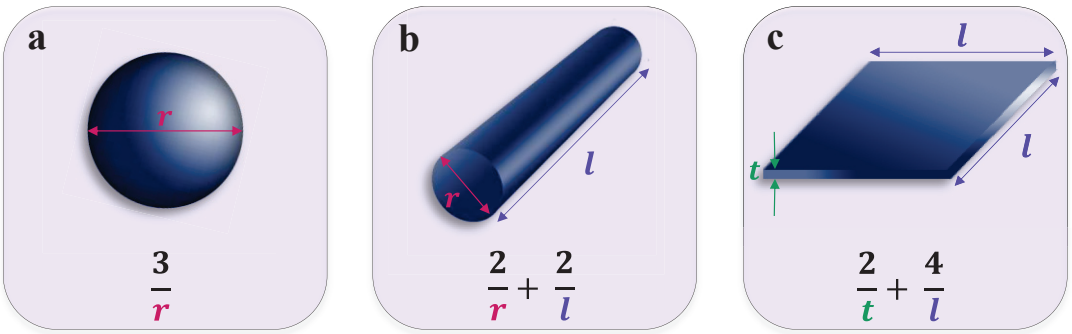
Nanocomposites are a class of composite materials composed of a matrix, or continuous phase, and dispersed fillers, or reinforcements, that possess at least one of the dimensions in the nanometric scale. The use of nano-sized fillers, instead of conventional micro and macro-sized particles, causes a considerable increase in the interfacial area and intensifies the physical interaction between the phases, resulting in significant improvements even at very low filler contents. Moreover, it is also possible to explore the addition of nanofillers with special properties to produce materials with specific and outstanding properties. Nanocomposites can be classified, in general, based on their structural component or based on the type of the matrix used (ceramic, metallic or polymeric). The focus in this thesis is restricted to polymer matrix nanocomposites; so the attention is dedicated exclusively to this type of materials.

Fillers have been added to polymer matrixes, historically, as cost effective materials, however, their role goes beyond being a mere inert additive. The creation of organic/inorganic nanocomposite materials has been as one of the most promising developments in the field of materials science.[37] By combining organic and inorganic components at the nanoscale, these materials take advantage of all the features that these components can offer, resulting in a unique composite material with improved properties. Each part has a specific purpose: polymeric matrixes attribute flexibility and processability

to the final material, while the incorporation of an inorganic component brings enhancements in rigidity and thermal stability, for instance. Nonetheless, the incorporation of nanometric particles in polymers does not, necessarily, cause improvements in the materials resistance. Excessively small particles are usually difficult to disperse and tend to agglomerate in the matrix. The lack of affinity between both phases is another factor responsible for particle agglomeration and, in most cases, the surface modification of the inorganic additives is necessary to facilitate the compatibility between organic and inorganic phases, increasing the dispersibility of the inorganic component and leading, therefore, to the production of composite materials with superior properties.

Based on the type of reinforcement used, it is possible to identify three categories of nanocomposites,[38] depending on the number of dimensions in the nanometric scale of the materials, as illustrated in Figure 4.1.

Figure 4.1 – Surface area/volume relations for different reinforcement geometries: (a) particulate materials (silica, metal, and other organic and inorganic particles); (b) fibrous materials (nanofibers and nanotubes) and (c) layered materials (graphite, layered silicate, and other layered minerals).



Source: adapted from ref. [38]

a) ***Nanoparticle-reinforced composites.*** These materials are reinforced with nano-sized particles that contain all three dimensions at the nanometer scale (isodimensional nanoparticles), such as silica,[39] metals[40-42] and other organic or inorganic spherical particles. Fillers are, in general, added to enhance the matrix elastic modulus and yield strength. But specifically for the case of nanoscale particulate additives, they can be associated additionally to improving the transmittance of visible light, when compared to additives with larger particle sizes.[43]

b) ***Nanofiber-reinforced composites.*** When two of the dimensions of the objects are in the nanometric scale, and the third one is not, causing the length of the particle to

be much greater than its cross-sectional dimensions, elongated structures are formed, such as nanotubes or nanofibers. Typical examples of particles that belong to this class of materials and are used in the synthesis of nanocomposites include cellulose fibers (whiskers)[44] and carbon nanotubes.[45]

c) ***Nanoplatelet-reinforced composites.*** In this type of nanocomposites, only one of the dimensions of the reinforcement is in the nanometer range. Two common examples that exist as layered materials in their bulk state are clays and graphite. Some of the advantages of nanoplatelet-reinforced polymer composites include improved stiffness, strength, toughness, thermal stability and gas-barrier properties, as well as reduced coefficient of thermal expansion.[46] The surface modification of particles is required, in most cases, to promote the compatibility between hydrophilic particles and the hydrophobic polymer phase, reducing, therefore, the agglomeration of the mineral in the polymer matrix.

4.2.1.1 Layered silicate polymer nanocomposites (LSPN)

Clays or layered silicates are natural or synthetic minerals that consist of very thin layers, usually hold together by the sharing of counter-ions. They have been the most widely investigated precursors for nanocomposites, probably due to their easy availability and largely studied intercalation chemistry.[4] However, it was only in 1993, after the Toyota group[47, 48] has reported the use of Mt platelets to reinforce Nylon-6, that LSPN and nanocomposites, in general, started to become an attractive field of research for both academia and industry.

For an efficient reinforcement behavior in nanocomposites, the layers must be well dispersed throughout the matrix phase and, in this aspect, different morphologies of clay/polymer nanocomposites are possible,[1, 4, 49] as illustrated in Figure 4.2. In the conventional miscible state, also known as phase separated state, silicate sheets are separated by a minimum interlayer space, since polymer chains do not intercalate between clay platelets (Figure 4.2b). The properties of the obtained material are similar to the ones of a micro-scale composite. The insertion of a single (or sometimes more) extended polymer chain into the gallery space between the adjacent layers causes the expansion of the spacing to form an intercalated structure (Figure 4.2b). In this type of structure, polymeric and inorganic layers are ordered in an alternate manner with a repeat distance between them. The third type of structure, the exfoliated or delaminated structures (Figure 4.2c), results in the

most significant enhances in mechanical, optical, electrical and thermal properties of the material and, for this reason, it is of particular interest. In this type of configuration, the complete and uniform separation of the layers leads to the individual dispersion of the platelets in the continuous polymer matrix, which maximizes clay-polymer interactions by making the surface of the platelets fully available for the polymer.

Figure 4.2 – Types of clay/polymer composites: (a) phase separated, (b) intercalated and (c) exfoliated.



Source: adapted from ref.[1]

Nonetheless, in a polymer matrix, small fillers with large internal surface (such as silicate layers) tend to agglomerate rather than to be homogeneously dispersed. In their pristine state, these materials are generally miscible with hydrophilic polymers and, to render them miscible with other polymers, clays are often submitted to a cation exchange process by the layer intercalation of an organic surfactant that increases the basal spacing and converts the material from hydrophilic to hydrophobic.

Several methods are available for the preparation of clay-based nanocomposites, the principal being: (i) melt intercalation; (ii) intercalation of polymers or prepolymers from solution; (iii) template synthesis (sol-gel technology) and (iv) *in situ* intercalative polymerization.[4] In the **melt intercalation** process, the layered silicate is mechanically blended with the polymer matrix at high temperature by conventional methods, such as extrusion or injection molding. If the filler is compatible with the matrix, either intercalated or exfoliated nanocomposites can be formed. However, if phases are incompatible, a poor distribution of the mineral in the polymer matrix is obtained. This technique is considered one of the most commercially attractive approaches for preparing clay/polymer nanocomposites due to its versatility and environmental benefits. In the second method, the **intercalation of polymer from solution**, also known as exfoliation-adsorption process,[1] a solvent (in which the polymer, or prepolymer in case of insoluble polymers, is soluble) is used to swell the layered silicate. Due to the weak forces that hold the layers together, layered

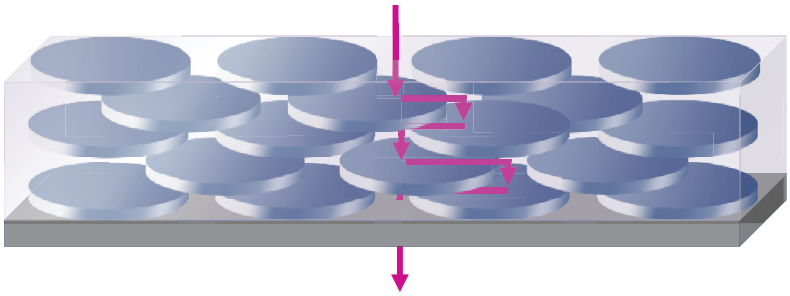
silicates can be easily dispersed in an adequate solvent, and polymer chains can be intercalated between the layers. After removal of the solvent, either by vaporization or precipitation, the nanocomposite is formed. Although this technique has been mostly reported for water-soluble polymers, the use of non-aqueous solutions is possible as well. Nanocomposites obtained through emulsion polymerization are also included in this technique. In the **template synthesis (sol-gel technology)** technique, the clay minerals are synthesized in the presence of an aqueous solution of the polymer matrix. This method is widely used for the synthesis of nanocomposites based on layered double hydroxides[50-52] however, some disadvantages of the technique must be considered for layered silicates. The high temperature required to synthesize most clay minerals may cause the decomposition of the polymer matrix. In addition, growing silicate particles tend to aggregate during the synthesis. The ***in situ*** **intercalative polymerization**, another commercially attractive technique to prepare LSPN, was the first method used to synthesize these materials. The initiator or catalyst is initially fixed through cationic exchange onto the platelets and the layered silicate is swollen by a monomer or a monomer solution. Then, by the migration of the monomers into the galleries of the clay, polymerization occurs between the intercalated sheets.

A variety of advantages makes layered silicate polymer nanocomposites competitive for different possible applications in industry, in sectors such as the automotive, construction, aerospace, food packaging, textile and others. Some of the aspects that make these materials more interesting and exciting than conventional composites is that they are lighter in weight and at lower filler contents, they exhibit significant enhancements not only in mechanical, barrier, flame-retardant and rheological properties, but also in crystallinity, biodegradation and thermal stability.[53, 54]

Additionally, clay/polymer nanocomposite films generally present an optical transparency similar to their polymer counterparts, which is not observed for conventional clay/polymer composites. This advantage, added to the gas barrier property, make LSPN well-acceptable materials in packaging industries, for applications as wrapping films and beverage containers. In fact, the ability of exfoliated fillers to form individual platelets in a polymer matrix result in considerable extension of shelf-life for different types of packaged food.[55] Impermeable platelet-shaped particles with sufficient aspect ratio, such as Mt and graphene, have the ability to change the diffusion path of small gas-penetrant molecules in polymer films, positively affecting the barrier properties of these materials. By producing a tortuous path for the species to travel through and extending, therefore, the diffusion pathway

of the permeating gas molecules, lamellar particles work as an aligned barrier structure for gases, as shown in Figure 4.3. To obtain LSPN with excellent permeability, the maximization of nanoplatelets aspect ratio and the effective dispersion of the fillers are of key importance. These factors contribute to a regular arrangement of the nanoplatelets within the polymer matrix, with the surface of the individual particles oriented in a perpendicular direction to the gas diffusion path.[56]

Figure 4.3 – Schematic representation of the "torturous diffusion path" in clay/polymer nanocomposites.



Source: adapted from ref.[2]

The alignment of high aspect ratio particles in polymer nanocomposites results in significant improvements in the mechanical properties (such as tension, compression, bending and fracture of the material) compared to virgin polymers, at very low filling levels (2-10 wt. %). The multi-layered silicate structure is also responsible for other interesting improvements in nanocomposites, including the increased thermal stability[53, 54] and ability to promote flame retardancy.[57-59] In these cases, the explanation to the improved properties can be found in the formation, under oxidative conditions, of a low permeability char, which behaves as a physical barrier for thermal insulation, separating the polymer from the superficial polymer zone that is under combustion.[58] The presence of organically modified layered silicates particles in nanocomposites may have, additionally, a considerable catalytic role in the biodegradation mechanism, leading to significant improvements in biodegradability of biodegradable polymers. These materials find several potential future applications as high-performance biodegradable materials.[3]

4.2.2 Colloidal nanocomposites

To overcome some of the issues observed in the synthesis of conventional composites (such as the melt processing irreproducibility, for instance), colloidal nanocomposites have

emerged as an alternative new category of nanocomposites.[60] In fact, waterborne processes can be considered versatile techniques for the production of nanocomposites, with numerous advantages that allow the design of highly ordered materials with tailored properties. Disposing of nanocomposite particles in the form of a colloidal dispersion in a continuous aqueous medium can confer very practical and interesting industrial applications to these materials. In the last decades, emulsion and miniemulsion polymerization processes have proven to be potential tools to produce polymer/inorganic particles and highly suitable to generate a wide variety of composite colloidal particles.[37] These materials are easily handled and can be further processed into films that, compared with their pure-polymer counterparts, possess improved mechanical, thermal, or barrier properties. Among some of the advantages of producing nanocomposites by emulsion polymerization, the use of water as dispersion medium can be cited as one of the most interesting ones, since it avoids the increase in viscosity, guarantees a good heat dissipation and allows adequate conditions for the exfoliation of the particles.[61]

To elaborate composite particles from inorganic colloids, such as metals, metal oxides, clays, among others, different strategies are available. In general, colloidal nanocomposites can be produced *ex situ,* from the preformed organic and inorganic colloids, or *in situ*, by the chemical reaction of the inorganic/organic precursors in the presence of the latex/mineral particles, or even by simultaneous reaction of organic and inorganic precursors.[62] Depending on the strategy used, the inorganic particles can be incorporated inside or at the surface of the latex particles. Indeed, the control of the morphology of the hybrid particles is a key factor to determine the properties of the final material. Various strategies are available for the incorporation of inorganic objects at the surface of the latex particles.[37, 60, 63] This process, known as "Pickering polymerization", represents a considerable simplification of the conventional emulsion polymerization process and it is, therefore, attracting increasing interest not only in the academic medium but also from industries. In some cases, nanocomposites can be successfully produced in the absence of surfactant.[64, 65] In these cases, however, the mechanism of particle nucleation involves mainly homogeneous nucleation and is less related to micellar nucleation, as in conventional emulsion polymerization. Final composite particles are composed of a polymeric core that is decorated with inorganic particles, forming an inorganic "protective armor". Nonetheless, the encapsulation of inorganic particles with a layer of binder polymer, creating polymer shells and inorganic cores, has shown to be of great interest in the last few years. The formation of core-shell particles by encapsulation techniques is an ultimate solution to avoid

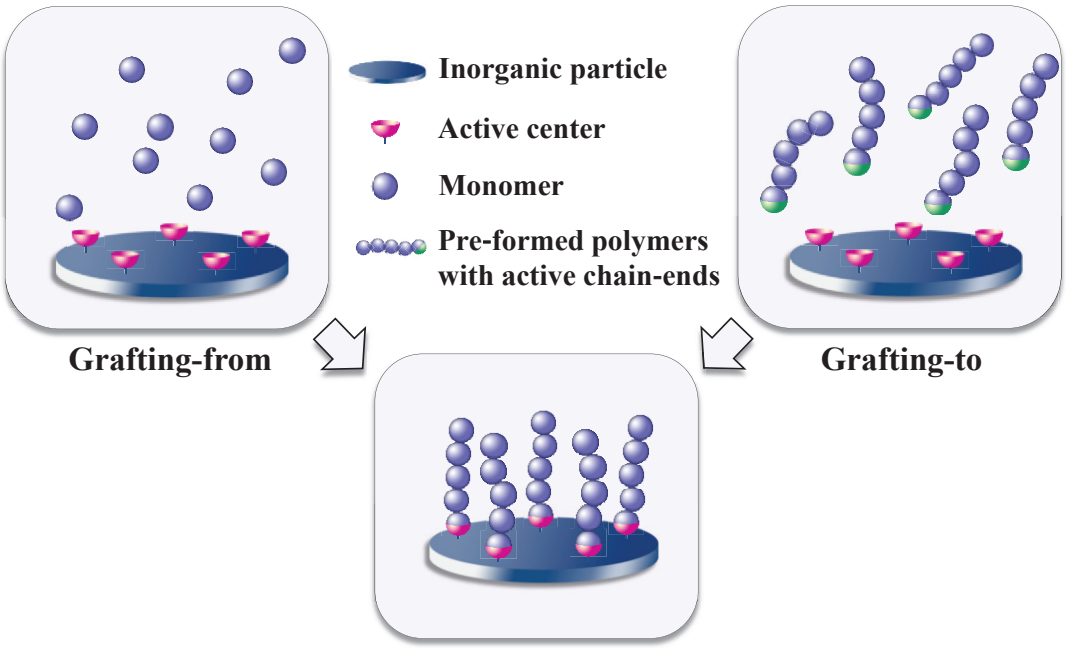
agglomeration of the inorganic objects and ensure that they remain separated during the film formation process. For this purpose, numerous works have reported the synthesis of hydrophobic organic/inorganic hybrid particles by the grafting-from, grafting-through, or grafting-to techniques in solution and aqueous-dispersed media, although only a limited number of contributions deal with aqueous dispersed systems.

4.2.2.1 Synthesis of colloidal nanocomposites

Different techniques can be used in the preparation of nanocomposite particles, either in solution or in aqueous dispersed media, including grafting-from, grafting-through, grafting-to, heterocoagulation, layer-by-layer deposition of functional polymers, self-assembly of block copolymers with inorganic particles, macroRAFT assisted polymer encapsulation of inorganic particles and so forth.

These techniques can be divided, mainly, into two classes, depending on the disposition of the polymer phase in the nanocomposite. In the first class, the polymer chains form a brush that is responsible for protecting the inorganic particles. In this aspect, the polymer brushes can be grown from the surface, in a process known as grafting-from, or attached to it, process known as grafting-to. Figure 4.4 illustrates the grafting-from and grafting-to approaches. The second strategy relies on the formation of a polymer shell around the inorganic particle. The difference, however, is that the polymer chains are not necessarily covalently bonded to the surface, and they are randomly distributed and not orderly arranged, as it is observed for polymer brushes. Among the techniques obtained through this approach, the layer-by-layer method, the block copolymers self-assembly in the presence of inorganic particles and the macroRAFT-assisted polymer-encapsulating emulsion polymerization (REEP) can be cited. While the first class of techniques involves essentially the modification of the inorganic particles, aiming to improve the compatibility between the inorganic filler and the polymer matrix, the second class of techniques produces particles that can not only be added to a polymer matrix but also be used directly to produce the final material. The focus of this section will be directed to the grafting-from, grafting-to, self-assembly of block copolymers with inorganic particles and the macroRAFT-assisted polymer-encapsulation of inorganic particles.

Figure 4.4 – Schematic representation of grafting-from and grafting-to techniques to graft polymer chains at the surface of inorganic particles.



Source: adapted from ref.[66-68]

The modification of inorganic particles by grafting polymer chains from its surface is an important technique for modifying the physical and chemical properties of the material, or even to introduce new functionalities to it. In the grafting-from strategy, the inorganic material is treated with organic molecules that carry both a functional group that can interact with the inorganic particle and a functional reactive group, such as an initiator, that participates in the polymerization. By the propagation of monomers from initiating species (reactive centers) fixed on the inorganic surface, the polymer is formed in a process also known as surface-initiated (SI) polymerization. In some cases, the functional reactive group can be the monomer. Controlled radical polymerization techniques can be successfully employed for the grafting-from method, leading to high efficiency and high grafting densities. Several examples can be found in the literature that illustrate the applications of ATRP, NMP and RAFT to grafting-from systems.[69-86] While ATRP and NMP grafting-from methods involve the grafting of an initiator to the surface, RAFT relies on the linking of the RAFT agent (either by the R or Z groups) to the inorganic particle.

A cationic RAFT agent was used by Chirowodza et al. to modify Laponite platelets and to control the surface initiated polymerization of styrene (sty).[87] The analysis of polymer chains by SEC indicated similar molar masses for the free and the bonded families of polymer chains, proving that even the grafted RAFT agents could successfully control the

polymerization. In fact, the characterization of grafted polymer chains requires the cleavage of the chains and their subsequent isolation. This process can be challenging, and, for this reason, the grafting-to technique is sometimes preferred. One of the advantages of employing the grafting-to over the grafting-from method is the possibility to characterize the polymers chains (in terms of molar mass and dispersity) prior to their attachment onto the surface.

The grafting-to technique consists in the covalent attachment of pre-formed polymers by their active chain-end with reactive centers present on the inorganic surface. For this purpose, polymer chains containing complementary functional groups that are able to react with the inorganic particle must be pre-synthesized. These reactive polymers are commonly prepared by reversible deactivation radical polymerization (RDRP) techniques, such as RAFT,[88, 89] ATRP[90, 91] and NMP,[90] nonetheless, polymers prepared by conventional methods, other than controlled/living radical polymerization techniques, can be effectively applied as well. The main drawback of the grafting-to method is the low grafting density, which is caused by the steric hindrance from the large previously attached polymers.

In this aspect, the covalent modification of inorganic surfaces by the grafting-from method can be generally associated to higher grafting densities on the surface of particles since monomers are less prone to suffer steric hindrance. Despite some of the drawbacks associated with the grafting-from approach (it is still a very complicated and time-consuming method, not suitable for large-scale production), it is considered the most effective method to produce highly dense polymer brushes on the surface of nanoparticles.

The use of block copolymers, instead of homopolymers, has become another fast-growing method for the production of nanocomposites. Different than a pair of linear homopolymers, in the melt state, block copolymers tend to segregate in a local scale, forming lamellar, cylindrical, cubic spherical or interconnected network morphologies, instead of phase separating. And these formed microdomain structures are particularly attractive for hosting nano-objects. In this aspect, two synthetic approaches allow the production of these block copolymers-based nanocomposites. In the first method, the particles are synthesized *in situ* and, in the second approach, the block copolymers, synthesized *ex situ*, self-assemble to generate the nanocomposites. There are several parameters that influence the self-assembly process of block copolymers in the production of nanocomposites, such as the polymer chain configuration, particle orientation, particle-particle and particle-polymer interactions, among others. An interesting review by Bockstaller et al. reports the self-

assembly of block copolymers in the presence of various inorganic particles and discusses how the inclusion of inorganic nano-objects with different particle morphologies influences the structure formation process in block copolymer-based nanocomposites.[92] Even though nanocomposites with well-defined morphologies that could find potential applications in diverse fields can be obtained by this method, in some cases long dialysis times are required and the process can be considered quite complicated.

The grafting-from, grafting-to, or self-assembly techniques often require the surface modification of preformed inorganic particles in organic solvents. The hybrid particles can be recovered after evaporation of the solvent and, for posterior applications, water-based systems might be needed. Volatile organic compounds have been progressively avoided in the last decades and coating formulators tend to migrate from solvent-borne processes to waterborne alternatives.[24] Emulsion polymerization, a widely used free radical polymerization process, can be considered one of the most interesting methods to synthesize colloidal nanocomposites. In many of the strategies reported, however, the use of surfactants is required to provide colloidal stability to the hybrid particles. It is known that these molecules migrate in materials, prejudicing the adhesive and mechanical properties of the films.[93] To overcome this issue, emulsion has been associated to the versatility of living polymerization techniques. Through the association of the polymerization-induced self-assembly (PISA) of amphiphilic block copolymers mechanism with inorganic particles, as presented in Chapter 2, RDRP-based methods have emerged as a promising alternative to obtain well-defined nanocomposites latex particles. By engineering/functionalizing the surface of the inorganic particle with adsorbed ATRP or NMP initiators or, even more commonly, with RAFT agents, these techniques allow an effective control over the particle composition and morphology and open doors to the production of well-defined materials that find a variety of new applications.

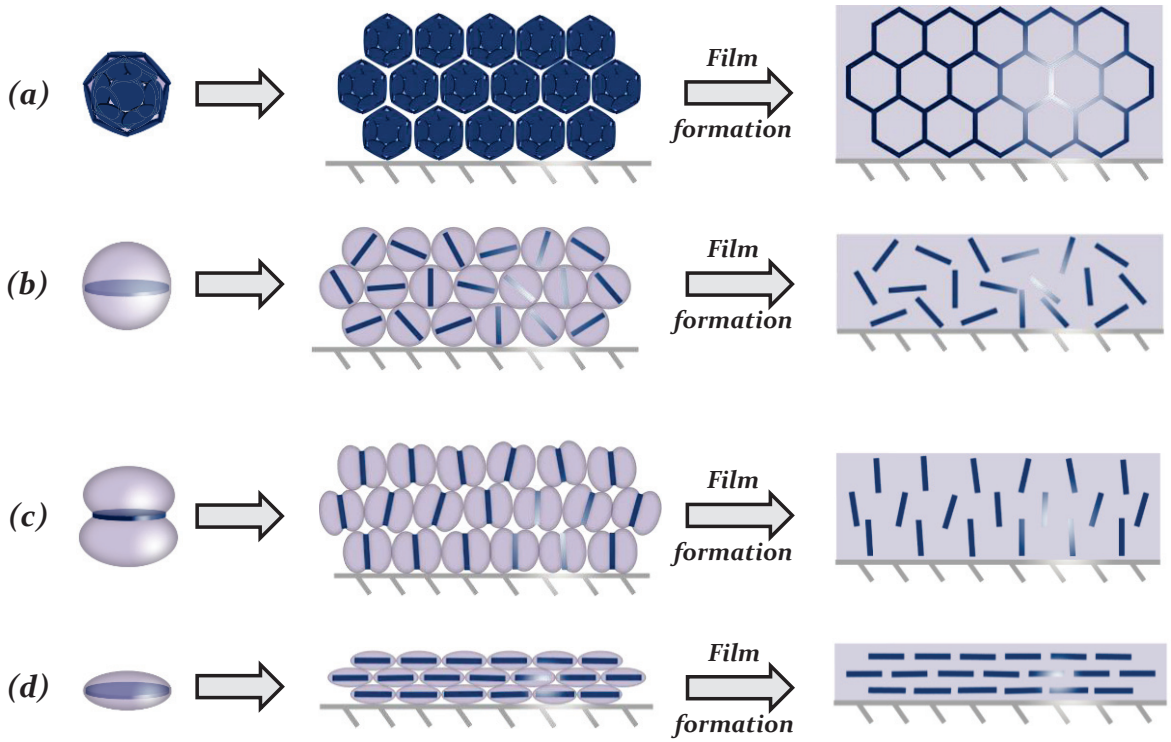
4.2.2.2 MacroRAFT-assisted encapsulating emulsion polymerization of layered particles

RAFT is shown to be an effective technique for the encapsulation of spherical and tubular inorganic nano-objects by emulsion polymerization, as described in details in section 2.3.3.1.4. of Chapter 2. The encapsulation of high aspect ratio inorganic particles (sheets or platelet-like particles, such as clays, for instance), however, is, according to van Herk et al.,[22] more challenging due to the high surface energy of these systems. Very hydrophilic particles

tend to minimize their contact with the hydrophobic polymeric phase by maintaining themselves in a state of minimal interfacial energy. The morphology obtained, in these cases, depends on the compatibility of the inorganic particle with the polymeric and aqueous phases.[20] Recently, hybrid latexes stabilized by clay platelets have been reported, in a process known as "Pickering polymerization".[29-31, 94, 95] In these processes, clay platelets are located on the surface of the latex particles, in contact with the aqueous phase, acting as a protective armor that stabilizes the system, forming the so-called armored particles. Multihollow Laponite-armored latexes particles were recently elaborated by macroRAFT-mediated emulsion polymerization in the presence of Laponite particles by Guimarães et al.[96] The anchoring of a PEG-based macroRAFT agent (2000 g mol^{-1}) on the surface of Laponite showed to be crucial for the controlled/living character of the polymerization, since it decreased the partitioning of the RAFT agent to the monomer droplets and avoided some inconvenient effects caused in the absence of clay, such as rate retardation, long induction period and poor colloidal stability.

The greatest advantage of the Pickering process is that the platelets are orderly distributed in the hybrid nanostructured film, forming a honeycomb-like structure that results in enhanced mechanical properties, as shown in Figure 4.5a. In fact, the orientation of the platelets in the hybrid film is a primordial factor for the properties of the material. The encapsulation of the platelets in a spherical morphology (Figure 4.5b) results in an aleatory (non-preferential) orientation of the platelets in the final film, which is not as effective for the enhancement of the coating properties as the nanostructuration of the platelets. For this purpose, the individual encapsulation of platelets in a way that preserves the anisotropic character of the platelets, to produce, preferably, plate-like flat composite latex particles (Figure 4.5d) is the most advantageous approach. In the process of film formation, flat particles tend to be organized in a nanostructured manner, inducing anisotropy and, potentially, improving the barrier properties and the scratch resistance of the final nanocomposite films.

Figure 4.5 – Schematic representation of the expected orientation of clay platelets in the final film using latexes with different particle morphologies: (a) armored particles; (b) spherical particles; (c) dumbbell particles and (d) flat particles.



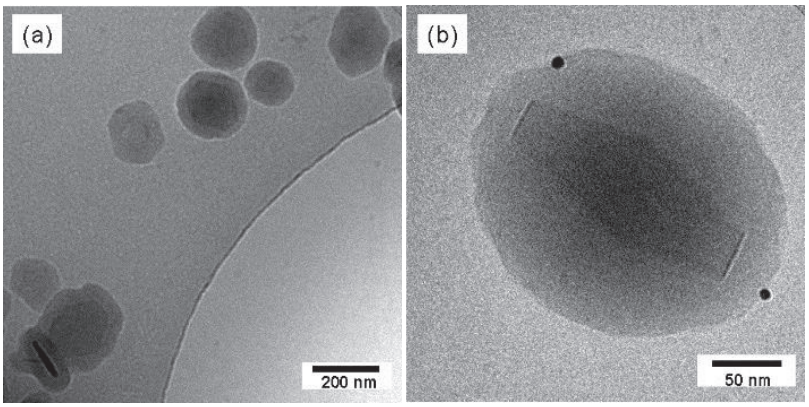
Source: adapted from ref.[19]

Samakande et al.[97, 98] used miniemulsion polymerization to encapsulate Montmorillonite particles. The copolymerizarion of styrene and BA was mediated by trithiocarbonate and dithiobenzoate RAFT agents that, containing a quaternary ammonium group, were anchored by their leaving group (R) to the clay surface through cation exchange. The CTA-modified clays were successfully dispersed in the monomer phase and, by increasing the hydrophobicity of the clay sheets, allowed the controlled synthesis of clay/polymer nanocomposites. The morphology of the final particles, however, could not be firmly assessed by TEM and platelets could only be visualized within ultramicrotomed cross sections, by embedding the dried latex in an epoxy resin, and most of the clay platelets presented an intercalated morphology. A similar strategy was used by Chakrabarty et al. to synthesize fluorinated copolymers by RAFT miniemulsion polymerization using Laponite nanoparticles.[99] To enhance the compatibility between the fluorinated copolymers and the clay, the authors used a cationic RAFT agent that, by inducing sufficient hydrophobicity to Laponite platelets, it guaranteed that the platelets remained at oil−water interface rather than in aqueous phase, allowing, therefore, the platelets to act as stabilizers in the formation of armored particles. One could expect, however, that clay platelets would get encapsulated by

this strategy but, as fluorinated polymers are more hydrophobic than the surface-functionalized clays, the platelets tend to stay in the oil-water interface, as a matter of interfacial energy. In addition, in opposition to the work of Samakande et al.[97, 98], the platelets were initially dispersed in the water phase. The presence of the cationic RAFT agent showed to affect the Pickering miniemulsion polymerization and polymers with controlled molar masses and narrow dispersities were obtained. However, among the disadvantages of the miniemulsion process, one can cite the fact that the individual encapsulation of the platelets is almost impossible. In addition, the hydrophobic modification of the clay particles is necessary in most cases to predisperse the platelets in the monomer phase and, last but not least, the industrial implementation of miniemulsion polymerization is still not considered advantageous.

The first successful encapsulation of anisotropic particles by RAFT emulsion polymerization was reported in 2009 by Ali and coworkers,[19] as shown in Figure 4.6. They used amphipathic trithiocarbonate RAFT agents to encapsulate cationic synthetically produced Gibbsite platelets with a P(MMA-*co*-BA) layer, under starve-feed conditions. By manipulating the composition of these random RAFT copolymers with different combinations of acrylic acid and butyl acrylate, the authors promoted the stabilization of the core-shell particles, prevented the self-assembly of these molecules in the aqueous phase (limiting the formation of pure polymeric particles) and promoted the chain extension from the inorganic surface, directing polymer growth to the clay platelets.

Figure 4.6 – Encapsulated Gibbsite platelets obtained by using RAFT copolymers (a) BA_5-*co*-AA_{10} and (b) BA_5-*co*-AA_5 with a feed composition ratio of MMA:BA=10:1.



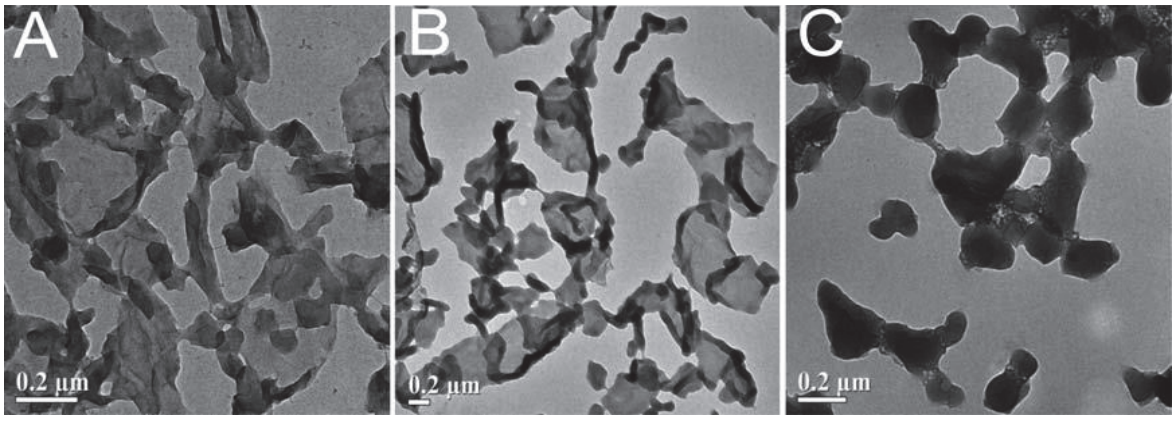
Source: Copied with permission from ref. [19]

In a more recent work, Mballa Mballa et al.[20, 100] proposed a method for the encapsulation of negatively charged Montmorillonite clay by copolymerization of MMA

with BA (with a molar ratio 10 : 1) using cationic dimethylaminoethyl acrylate (DMAEA)-based RAFT copolymers. In the approach proposed by the authors, the macroRAFT agent in aqueous solution was able to efficiently adsorb on the clay by electrostatic interaction and, by acting as a stabilizer, encapsulate the inorganic particles, resulting in flat nanocomposite particles with a "cornflake" morphology.

Graphene oxide (GO) sheets were successfully encapsulated by RAFT-mediated emulsion polymerization.[21] Considering that GO is often considered as an inorganic compound, it is worth mentioning this effort since it can offer interesting insights towards the better understanding of the encapsulation of high aspect ratio materials. The authors used an anionic macroRAFT agent composed of random units of sodium styrene sulfonate, acrylic acid, and butyl acrylate, with a low molar mass, to encapsulate GO particles with MMA and BA under starve-feed conditions. The strategy used in this work was similar to the methodology used to encapsulate inorganic particles through the REEP process, however, the GO surface was pretreated with poly(allylamine hydrochloride) (PAH) to alter the surface charge of GO and enhance the adsorption, by electrostatic interaction, of the anionic copolymer onto the GO sheets. Encapsulated particles with a uniform polymer layer were obtained. By varying the amount of PAH, partial polymer coatings of the GO could be achieved and by changing the amount of monomer fed into the system, the thickness of the polymer layer could be easily tailored, as shown in Figure 4.7.

Figure 4.7 – GO particles coated with P(MMA-co-BA) using 15 mg of PAH, 100 mg of macro-RAFT copolymer, 10 mg of GO, and (A) 186 mg, (B) 465 mg, and (C) 930 mg of a 10/1 w/w mixture of MMA and BA.



Source: copied with permission from ref.[21]

In general, some common aspects among the works involving the REEP strategy can be cited as important prerequisites for the successful encapsulation of inorganic particles.

Even though these prerequisites are not universally required to ensure effective encapsulation, they seem to positively affect the process:

- The existence of a **strong interaction** between the RAFT (co)polymers and the inorganic particles. When this condition is satisfied, polymerization is encouraged to be located at the inorganic surface (or even restricted to this interface);
- The incorporation of **hydrophobic units** (i.e. BA) to the RAFT chains. The presence of hydrophobic domains increases the affinity between the hydrophobic monomers and the inorganic particles, directing the polymerization locus to the inorganic surface and avoiding secondary nucleation. The number of hydrophobic units, however, must be envisaged for an adequate hydrophilic/hydrophobic balance. Too hydrophilic copolymers tend to remain in the water phase, leading to secondary nucleation, while too hydrophobic copolymers can aggregate into micelle-like formations, leading to secondary nucleation as well;
- The **random distribution** of the hydrophilic and hydrophobic units along the RAFT copolymer chain. This condition avoids the self-assembly of the molecules into micelles, reducing the formation of pure polymeric particles via micellar nucleation;
- An **adequate molar mass** for the macroRAFT agent. Short polymers, or even oligomers, are generally preferred over long chains since these molecules allow a higher number of RAFT functional units per particle. In addition, long chains are more likely to collapse, due to their lower solubility in water, resulting in secondary nucleation. Nonetheless, a minimal chain length in necessary to provide sufficient colloidal stability of the encapsulated particles;
- A **slight excess of macroRAFT agent**. It seems that a minimal amount of macroRAFT agent must be free in the aqueous phase to adsorb on the hybrid particles during the encapsulation process, in order to maintain the colloidal stability of the growing polymeric layer. For this reason, the total concentration of macroRAFT agent must be superior to the concentration necessary to cover the inorganic surface (to guarantee that an excess will exist in solution) without, however, being excessive enough to encourage the formation of pure polymeric particles;
- An **adequate pH**. The pH is another key parameter for the successful encapsulation since it alters the ionization state of ionic RAFT (co)polymers and defines the surface and/or edge charges of numerous inorganic particles, thus affecting the adsorption process;

- A suitable selection of the **monomer composition** of the hydrophobic shell. Highly hydrophobic polymeric shells cause a high interfacial tension, driving the inorganic particles to the polymer/water interface. In addition, the glass transition temperature (T_g) of the shell, when below the polymerization temperature, facilitates the migration of the particle to the water interface, affecting the final morphology of the particles.[13,19]
- The use of **starve-feed process**. Even though it is not proven to be an indispensable factor, the use of starve-feed conditions[20,19,21,9,101,17,102,13,14,15, 16] is generally preferred over the batch process[10,11] since it prevents the partitioning of the RAFT chains between the monomer droplets and aqueous phase. In addition, the accumulation of monomer in droplets, avoided under the starve-feed conditions, decreases the T_g of the polymeric shell due to the plasticizer effect of the accumulated monomer, and leads to a phase separation process that can cause the formation of an uneven polymer coating.
- The **living character** of the RAFT molecules. So far, there has not been any clear evidence of a direct relationship between the controlled character of polymerization (controlled molar mass and low dispersity) and the success of encapsulation. In some cases, uncontrolled or poorly controlled polymerizations led to the formation of encapsulated particles,[16,10,12,18] revealing the secondary character of this parameter. However, the ability that dormant RAFT molecules have to be reactivated and suffer chain extension is crucial for the encapsulation process. The key role of the RAFT agent is, therefore, related mainly to the living character, rather than to the controlled aspect, of the process.

To conclude, the REEP strategy represents an efficient and universal technique for the encapsulation of a variety of inorganic particles, with different surface chemistries, particle morphologies and aspect ratios. With an adequate selection of macroRAFT agents and reaction conditions, any filler can be potentially encapsulated. Even though the number of studies involving the encapsulation of inorganic objects via RAFT polymerization in aqueous dispersed media is increasing in the last few years, a few works report the encapsulation of anisotropic particles and, more specifically, of Laponite clay. Both works that have been reported, so far, using Laponite as fillers with cationic[99] and nonionic[96] macroRAFT agents via miniemulsion and emulsion polymerization, respectively, resulted in Laponite-decorated armored particles. In addition, most works that describe successful encapsulation strategies do not progress towards film-forming studies and, for this reason, the real potential of the method to produce nanostructured films, where platelets are aligned in the polymer matrix, has not been well explored yet.

4.3 Experimental Section

4.3.1 Materials

MacroRAFT agents were synthesized and purified as described previously in Chapter 3. Laponite RD particles used in this work were supplied by BYK Additives Ltd (former Rockwood Additives Ltd). The initiators: 4,4′-azobis(cyanovaleric acid) (ACPA, ≥98%, Sigma-Aldrich), azobis(2-methylpropionamide) dihydrochloride (AIBA, 98%, Acros Organics) and 2,2'-azobis[2-(2-imidazolin-2-yl)propane]dihydrochloride (ADIBA, 99%, Wako) were used without further purification. Tetrahydrofuran (THF, Sigma-Aldrich), sodium hydroxide (NaOH 1N, standard, Acros Organics), hydrochloric acid (HCl 1N, standard, Acros Organics), sodium pyrophosphate tetrabasic ($Na_4P_2O_7$, 98%, Synth), and THF (HPLC, stabilized/BHT, Sigma-Aldrich) were all used as received. The monomers: methyl methacrylate (MMA, 99%, Sigma-Aldrich), *n*-butyl acrylate (BA, 99%, Sigma-Aldrich) and methyl acrylate (MA, 99%, stabilized, Acros Organics) were used without further purification.

4.3.2 Methods

Hybrid polymer/Laponite latexes were synthesized in the presence of various macroRAFT agents using a semi-continuous process. In a typical run, 0.1250 g of Laponite and, in some cases, 0.0125 g of peptizing agent: sodium pyrophosphate tetrabasic ($Na_4P_2O_7$), were added into a flask containing 10 mL of water. The dispersion was left under vigorous stirring for 30 minutes while, in parallel, the required amount of macroRAFT agent (2.2 mM unless stated otherwise) was added into a flask and 10 mL of water were used to dissolve the polymer. In some cases, droplets of HCl or NaOH solution were added for pH adjustments. The Laponite dispersion was added into the flask containing the macroRAFT solution and, if necessary, a second pH adjustment was made at this point. The Laponite/macroRAFT suspension was left stirring for 60 minutes and transferred to a 50 mL three-neck round-bottom flask, where 0.1 g of the monomer mixture (typically MMA/BA 80/20 wt/wt) and the initiator solution were added. The initiator solution was previously prepared by adding the required amount of initiator (typically 3 times less than the molar concentration of macroRAFT) to the necessary amount of water to complete a total volume

of 22.6 mL. The water-soluble azo initiator, ACPA, was used for the polymerizations mediated by AA or PEGA-based macroRAFTs, and a small amount of NaOH solution was added to dissolve this initiator in water. AIBA or ADIBA initiators, which are cationic, were used for polymerizations mediated by DMAEMA-based macroRAFTs. The system was adapted to a reflux condenser, a stirring plate and purged with nitrogen for 30 minutes. The monomer mixture was purged in a separate flask. To start polymerization, the system was heated to 80 ºC and 2.4 mL of the monomer mixture were fed at a rate of 0.6 mL h^{-1} during 4 hours. The polymerization was left for 1 to 3 additional hours after the end of the monomer addition and samples were taken every hour for kinetics study. A typical recipe and conditions used in the synthesis are shown in Table 4.1.

Table 4.1 – Typical recipe and conditions used in the synthesis of hybrid latexes by RAFT-mediated emulsion polymerization in the presence of various macroRAFT agents.

[Laponite] (g L^{-1})	5
[macroRAFT]/[Initiator]	3
Monomer initial shot (mL)	0.1
Monomer added (mL)	2.4
Monomer addition rate (mL h^{-1})	0.6
Monomer mixture (%wt MMA:BA)	80:20
Total volume (mL)	25
Temperature (°C)	80

Source: elaborated by the author.

4.3.3 Characterizations

Monomer conversion was determined by gravimetric analysis and calculation was made considering a semi-continuous process, taking into account that, at a given time, different amounts of monomer were being taken and added into the reactor. For size exclusion chromatography (SEC) analysis, polymer was separated from the clay and extracted from the dried hybrid latex by stirring with THF for 24 hours, followed by centrifugation at 60000 rpm[96] (using a Sorvall™ MTX 150 Micro-Ultracentrifuge, from Thermo Scientific). The supernatant was used for determination of M_n and $Đ$ by SEC in THF, according to the methodology described in Section 3.3.1.3. The hydrodynamic average particle diameter ($Z_{av.}$) and the dispersity of the samples (Poly value) were determined by Dynamic Light Scattering (DLS) in a NanoZetasizer Malvern instrument, as described in section 3.4.1.3 of Chapter 3. Even though this technique is recommended for spherical

particles, it can be considered as an indicative for the non-spherical particles obtained in this work. Particles morphology was determined by cryogenic transmission electron microscopy (cryo-TEM) using a Philips CM120 transmission electron microscope from the Centre Technologique des Microstructures (CTμ), platform of the Université Claude Bernard Lyon 1, in Villeurbanne, France. A drop of the dilute suspension was deposited on a holey carbon-coated copper grid and, before introduction in the microscope, the excess of liquid was removed from the grid with filter paper. The grid was then immersed into a liquid ethane bath cooled with liquid nitrogen and positioned on the cryo-transfer holder, which kept the sample at –180 °C and guaranteed a low-temperature transfer to the microscope. Images of the frozen hydrated latex specimens were acquired at an accelerating voltage of 120 kV.

For the observation of the Laponite polymer nanocomposites microstructure in a larger scale, samples were sectioned and observed using a dual column Focused Ion Beam (FIB)–Scanning Electron Microscope (SEM) ZEISS NVision40, with a Ga^{2+} ion beam accelerated at 30 kV. Analyses were carried out by Dr. Florent Dalmas, Dr. Laurent Chazeau and Baptiste Gary from MATEIS laboratory (INSA of Lyon). To guarantee the observation of the materials with minimum charging effects, high resolution and a good contrast between the phases, a bulk nanocomposite trapezoid, previously metalized with gold, was, first, milled at high current beam (4 nA), in order to guarantee an imaging of the shorter face by the electron beam up to at least a 15 μm depth. A final polishing of the observed surface was, then, carried out with a fine current beam (80 pA). The SEM images of the polished surface were recorded under low voltage conditions (2 kV) using an in-lens secondary electron (SE) detector.

The thermo-mechanical response of the material was evaluated through dynamic mechanical analysis (DMA). The measurements, realized by Dr. Florent Dalmas, Dr. Laurent Chazeau and Baptiste Gary from MATEIS laboratory, were performed in a homemade apparatus (MATEIS, INSA of Lyon) in torsion mode at a fixed frequency of 1 Hz from and from 150 K to 400 K with a heating rate of 1 K min^{-1}. All samples were dried before analysis and their dimensions were about 10 mm long, 3 mm wide and 0.6 mm thick. The variation of the storage (G') and the loss (G'') moduli of the complex shear modulus (G^*) with temperature was measured and the mechanical main relaxation temperature was defined as the temperature at the maximum of loss modulus (G'').

4.4 Results and discussion

Initially, the influence of the macroRAFT agent nature on particles morphology and latex stability was evaluated during the synthesis of polymer/Laponite nanocomposite latexes. Twelve different macroRAFT structures were evaluated and the results are described below, organized according to these structures. Polymerizations were carried out following the typical recipe shown in Table 4.1, but some parameters were varied for specific macroRAFTs, in order to obtain a better study and understanding of the process, and will be specified in the corresponding items.

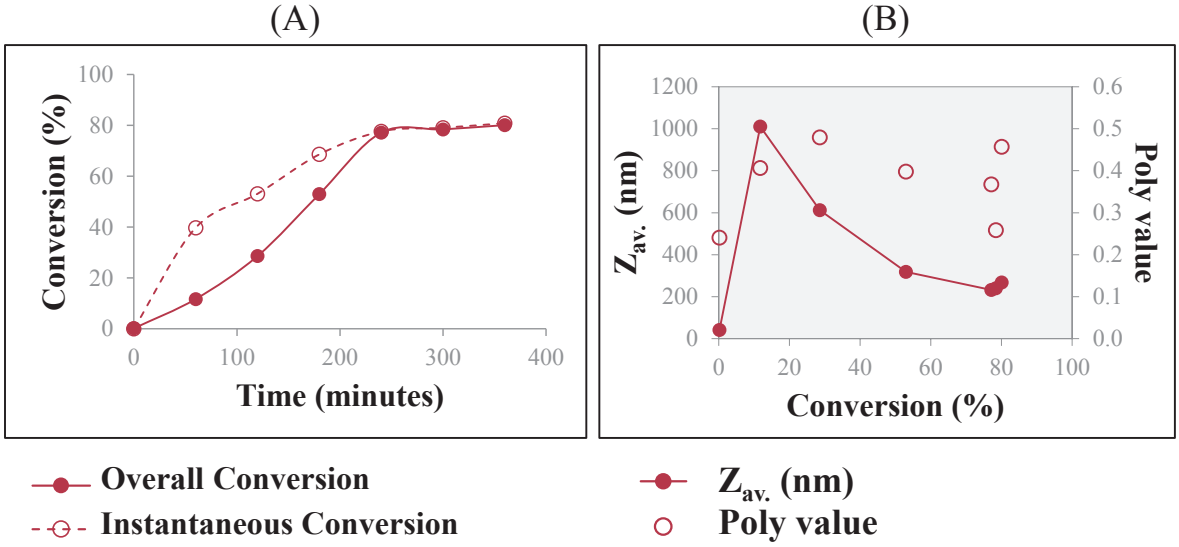
4.4.1 Synthesis of hybrid latexes in the presence of PEG_{45}-CTPPA

The macroRAFT composed of a nonionic polar linear block containing 45 units of PEG was used to mediate the semi-continuous emulsion copolymerization of MMA with BA in the presence of Laponite platelets modified with peptizing agent: sodium pyrophosphate tetrabasic. The adsorption study revealed a high affinity of the macroRAFT for Laponite. So, before polymerization, a significant part of the CTA was immobilized on the surface of the platelets. Figure 4.8A shows overall and instantaneous conversions versus time curves obtained for the polymerization. A conversion of 75% was obtained after 6 hours of reaction, confirming the ability of the macroRAFT/Laponite "complex" to nucleate particles. Samples were also analyzed in terms of particle size. The evolution of particles sizes and poly value with conversion, measured by DLS, is shown in Figure 4.8. The addition of PEG-CTPPA into the Laponite dispersion did not result initially in a significant change in particle size but, during polymerization, particle sizes increased in the first hour of reaction, from 42 nm to 1011 nm, and decreased again to 267 nm during the final 5 hours.

The emulsion polymerization of styrene mediated by PEG-based macroRAFT agents under batch conditions, in the absence of inorganic objects, has been described in the literature and low polymerization rates with long induction periods were reported.[103] In fact, similar PEG-based RAFT polymers seem to be incapable of efficiently stabilizing the latex particles, due to their partition between the aqueous and the monomer phases.[105] This partition phenomenon retards the growth of the polymer chains and prejudices the nucleation process, leading, therefore, to the formation of particles with poor colloidal stability. The mechanism that leads to the formation of the particles in the hybrid polymer Laponite systems may be more complex, however, and it has not been completely elucidated yet. A

similar system has already been reported by our group before for the polymerization of styrene in a batch process, in the presence of Laponite platelets [96] and, by partitioning between the water phase and the Laponite surface, the PEG chains lead to the formation of, respectively, molecules that chain extend and self-assemble in water and PEG/Laponite complexes, that may or not chain extend. Both paths may result in the aggregation of growing particles (either from the macroRAFT/clay complex and the self-assembled block copolymers), which are stabilized by clay platelets and adsorbed PEG segments. However, in the case of the batch emulsion polymerization of styrene, clay platelets tend also to adsorb on monomer droplets, decreasing the amount of clay available for stabilization of the aqueous phase nucleated latex particles. As these particles grow, they need more platelets for stabilization, situation that is achieved at high conversions, upon the release of clay platelets from the consumption of monomer droplets. At this point, which is after 30% conversion, the system regains stability and the formed aggregates disappeared, resulting in a drop of the particle size. At the end of polymerization, clay-armored composite latex particles are obtained.

Figure 4.8 – Evolutions of: (A) overall monomer conversion (full line) and instantaneous conversion (dashed line) with time and (B) evolution of the average hydrodynamic diameters and poly value with conversion during the synthesis of P(MMA-*co*-BA)/Laponite nanocomposite latex by RAFT-mediated emulsion polymerization using PEG_{45}-CTPPA macroRAFT agent at pH = 10.



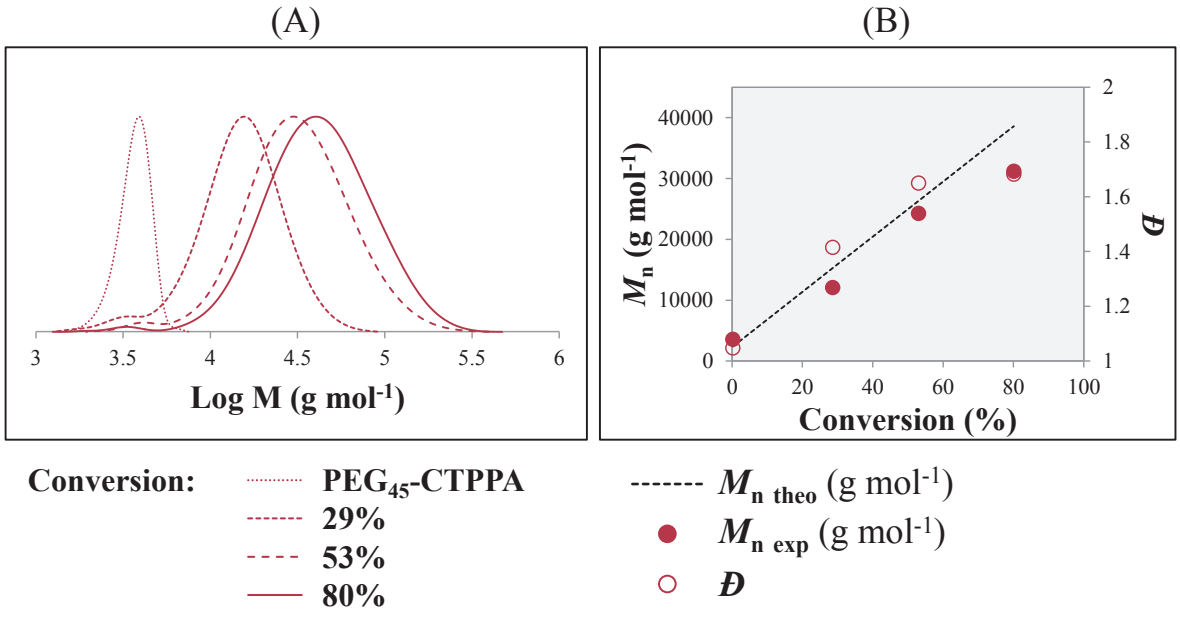
Source: elaborated by the author.

Different conditions, however, were used in this work and the adoption of starve-feed conditions was expected to guarantee the absence of monomer droplets in the system.

Nevertheless, in the case, part of the monomer apparently got accumulated anyway, as seen in the conversion versus time curves of Figure 4.8, since, due to the high solubility of MMA and its oligomers in water, the amphiphilic objects may have been generated later the case of the MMA/BA mixture than in the case of styrene. Therefore, a similar mechanism that leads to the temporary aggregation phenomenon could be equally applied here.

The controlled character of the growing amphiphilic polymer chains was investigated by the determination of their molar mass and dispersity by SEC in THF, after the removal of Laponite.[96] The chromatograms are shown in Figure 4.9A, while the evolution of molar mass and dispersity with conversion is shown in Figure 4.9B. It is possible to observe that monomodal curves were obtained, with a satisfactory shift of the chromatograms, indicating an almost complete consumption of the starting PEG-CTPPA macroRAFT agent. A small shoulder can be observed in the region of low molar mass due to PEG-CTPPA molecules that did not chain extend. Even though all experimental M_n data points fall close to the theoretical line and increase linearly with conversion, which would indicate consistency with RAFT-controlled systems, the high dispersity ($Đ$ = 1.68) is in agreement with the partitioning of PEG-CTPPA molecules, as the presence of residual PEG-CTPPA suggest that only a fraction of the macroRAFT agents was involved in chain extension process.

Figure 4.9 – Evolutions of: (A) the size exclusion chromatograms with monomer conversion (SEC THF, PS calibration), and (B) the number-average molar masses (M_n) and dispersities (Đ) with monomer conversion during the synthesis of P(MMA-*co*-BA)/Laponite nanocomposite latex by RAFT-mediated emulsion polymerization using PEG_{45}-CPP macroRAFT agent at pH = 10. The straight lines in the M_n versus conversion plots correspond to the theoretical values.



Source: elaborated by the author.

Final latex was colloidally stable, however sedimentation could be observed after some months.

4.4.2 Synthesis of hybrid latexes in the presence of PAA_{40}-CTPPA

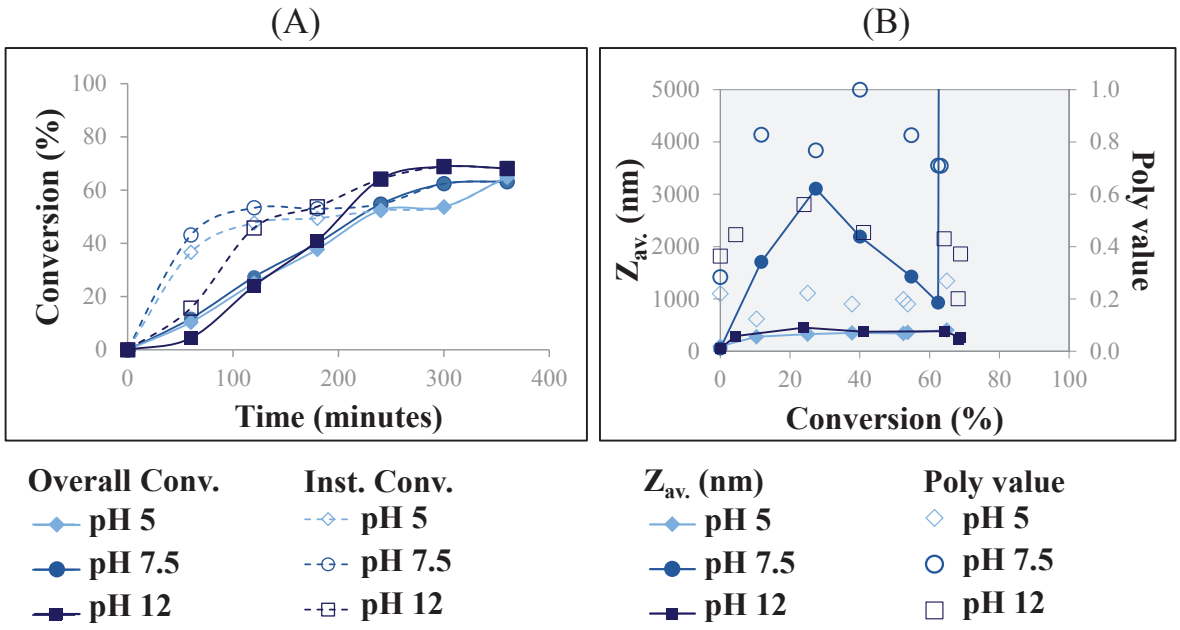
The macroRAFT agent containing 40 units of acrylic acid was used as mediator in the synthesis of polymer/Laponite nanocomposite latexes. This homopolymer is purely hydrophilic, so it is not expected to form micelles, and is pH dependent, presenting an anionic character under alkaline conditions. For this reason, three different pH values were tested: an acidic (pH = 5.0), a neutral (pH = 7.5) and an alkaline (pH = 12) value. Considering that the pK_a of poly(acrylic acid) is ~4.5,[104] it is expected that, in all the conditions studied, the macroRAFT is deprotonated and, consequently, negatively charged. However, the amount of charged acid units in the structure depends on the pH, so at a pH high enough, such as 12, it is expected that all acid units are deprotonated.

Final latexes had poor colloidal stability for all the pH values tested, which was indicated by the sedimentation of particles during polymerization (even though this is not evidenced by the data shown in Figure 4.10B for polymerizations at pH 5 and 12). Overall and instantaneous conversions versus time curves are shown in Figure 4.10A. Results were slightly better under alkaline conditions (pH 12), for which an overall conversion of 70% was achieved after 6 hours of reaction, against 63% obtained at pH 7.5. However, as shown in Figure 4.10B, the presence of large aggregated particles during polymerization could be observed in all cases, and might have prejudiced the withdrawn of samples, giving unreal values of conversion.

It is expected that, in the emulsion polymerization mediated by hydrophilic macroRAFT agents, nucleation starts in the aqueous phase according to the polymerization-induced self-assembly (PISA) mechanism, resulting in amphiphilic block copolymers that self-assemble and produce self-stabilized latexes particles, in the presence or not of clay. When clay platelets are present, a part of the macroRAFT agent is adsorbed on their surface and consequently the polymerization locus is moved to the inorganic surface. In this scenario, hybrid particles would be efficiently nucleated and stabilized by the Laponite/macroRAFT complex. However, the presence of PAA-CTPPA seems to affect this kinetics of particle formation, as the formation of aggregates is observed since the early stages of polymerization. This situation was also observed during the synthesis of hybrid

particles mediated by PEG-CTPPA, but the main difference in this case was that the aggregation was a temporary phenomenon that could be reverted upon the release of clay platelets and macroRAFT molecules by the monomer droplets (as they were being consumed). In addition, the analysis of PAA-CTPPA's adsorption isotherm, carried out at pH 7.5 and shown in Chapter 3 (Figure 3.22), indicates that a weak interaction is promoted between the macroRAFT and the clay surface and, therefore, most of the macroRAFT is in the aqueous phase. This observation excludes the hypothesis of macroRAFT partitioning between the water phase and the clay surface, eliminating the existence of macroRAFT/Laponite complexes. In the presence of Laponite platelets, it is possible that either the repulsion between oppositely charged chains and clay surface prevented PAA from adsorbing on the edges or the positive charge density on the edges were not enough for an effective interaction with AA units. Therefore, it is likely that the mechanisms of particle formation and, as a consequence, the stability problem, could be related to the secondary nucleation of particles and to the events taking place in water.

Figure 4.10 – Effect of pH on the evolutions of: (A) overall monomer conversion (full line) and instantaneous conversion (dashed line) with time and (B) the average hydrodynamic diameters and poly value with conversion during the synthesis of P(MMA-*co*-BA)/Laponite nanocomposite latexes by RAFT-mediated emulsion polymerization using PAA_{40}-CTPPA macroRAFT agent. .

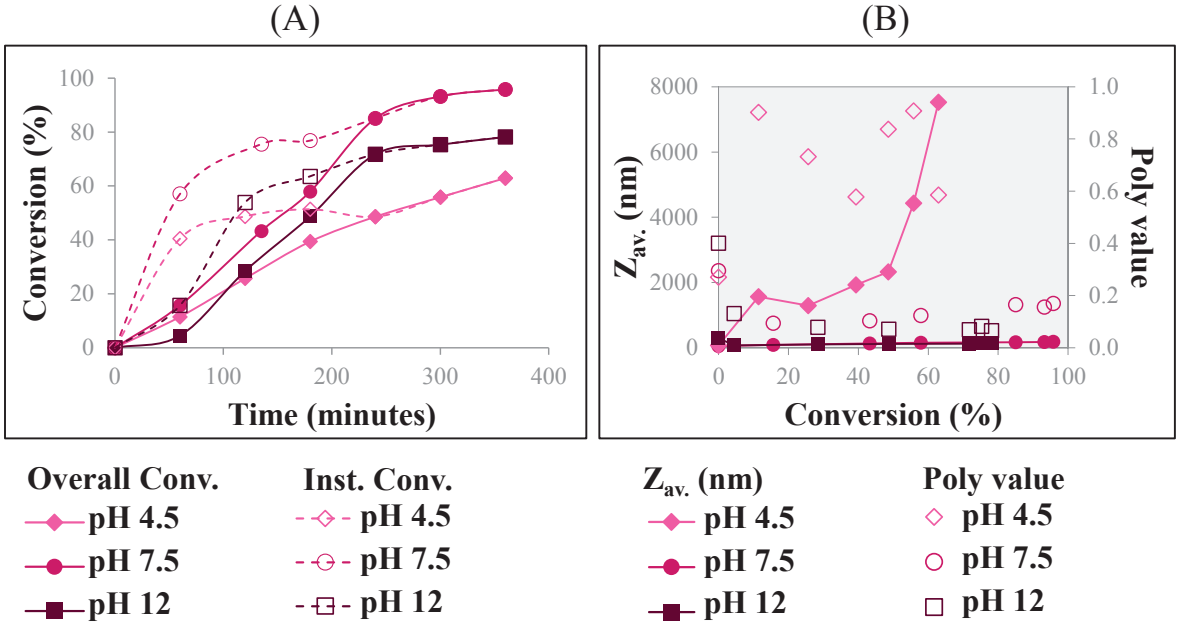


Source: elaborated by the author.

4.4.3 Synthesis of hybrid latexes in the presence of PEG_{45}-*b*-PAA_{42}-CTPPA

In the sequence, hybrid latexes were synthesized in the presence of a double-hydrophilic macroRAFT agent that combines the PEG and PAA blocks. With this association, it was expected that the macroRAFT agent would be able to adsorb on the surface of Laponite and, possibly, on the edges as well due to the presence of the PAA block (although the adsorption isotherm of PAA shown in Chapter 3 suggests that this adsorption might not occur, PEG chains could help increasing the adsorption of the AA block on the edges of the platelets due to screening of the clay surface charge). The block copolymer PEG_{45}-*b*-PAA_{42}-CTPPA was evaluated in the synthesis of hybrid latexes for 3 different pHs. Latexes obtained at low pH (4.5) presented no colloidal stability, but when a higher pH value was used (pH = 7.5 and 12.0), final latexes were stable with higher monomer conversions, as shown in Figure 4.11A. Regarding particle size, at low pH, the instability of the system led to a polydisperse latex, with the formation of particles larger than 7500 nm.

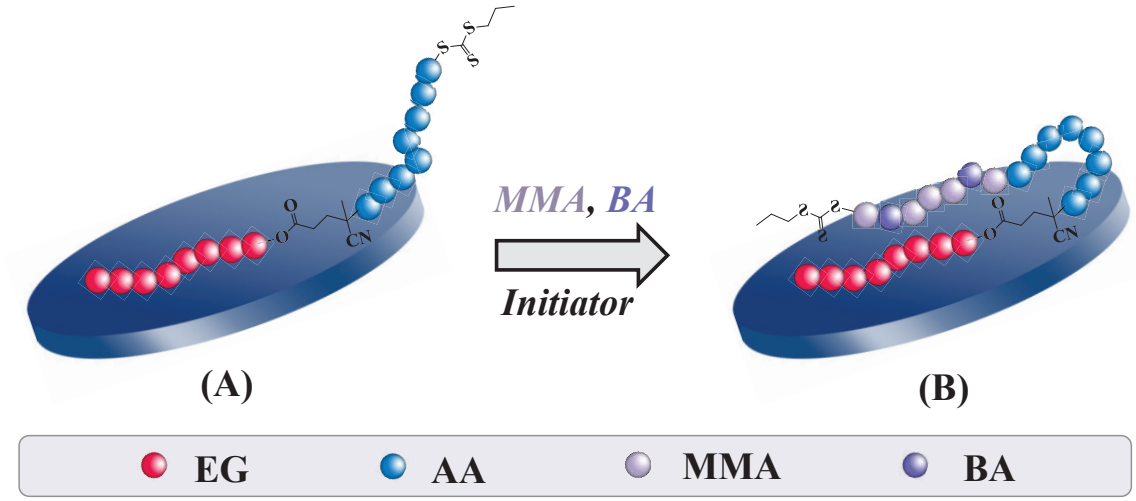
Figure 4.11 – Effect of pH on the evolutions of: (A) overall monomer conversion (full line) and instantaneous conversion (dashed line) with time, and (B) evolution of the average hydrodynamic diameters and poly value with conversion during the synthesis of P(MMA-*co*-BA)/Laponite nanocomposite latexes by RAFT-mediated emulsion polymerization using PEG_{45}-*b*-PAA_{42}-CTPPA macroRAFT agent.



Source: elaborated by the author.

At low pH ranges, hydrogen bonds can be formed between the ether units of PEG and the carboxyl groups of PAA, resulting in water-insoluble intramolecular complexes, if the composition of the complexes is stoichiometric. In our case, the pHs tested were probably above the critical pH of complexation, since stable macroRAFT/Laponite suspensions were obtained in all cases. This was not the case, however, for the latex particles, as they were unstable at pH = 4.5. If there were an excess of either EO or AA units, it could be expected that the macroRAFT agent could stabilize the hybrid particles. However, with part of the units adsorbed on the platelets (as shown in the adsorption isotherm of Chapter 3) and part possibly forming intramolecular hydrogen bonds, this molecule's capacity to stabilize the nanocomposite latex particles was prejudiced. At higher pH, some of the carboxylic groups were dissociated and did not participate in hydrogen bonding with PEO, so both segments could be free to stabilize the hybrid particles and to interact with the clay surface. One great feature of this block copolymer is that the interaction of the ethylene glycol groups with the Laponite surface promotes the approaching of the highly hydrophilic AA segment to the inorganic particle. So, while some carboxylic groups are free in the aqueous phase, surrounding the platelets, the PEG block interact with Laponite, generating a double effect of stabilization (electrosteric). However, this copolymer has a disadvantage (besides favoring the formation of the intramolecular complexes): the configuration of the molecule forces the growing hydrophobic block to be located outside the particle, leaving the hydrophilic AA segment buried inside the polymer shell or configured as a loop (both situations may not be enough for stabilization purposes), according to the schematic representation shown in Figure 4.12.

Figure 4.12 – Schematic representation of (A) Laponite platelets with adsorbed macroRAFT agent PEG_{45}-*b*-PAA_{42}-CTPPA and (B) during the synthesis of P(MMA-*co*-BA)/Laponite nanocomposite latexes by RAFT-mediated emulsion polymerization using PEG_{45}-*b*-PAA_{42}-CTPPA macroRAFT agent.



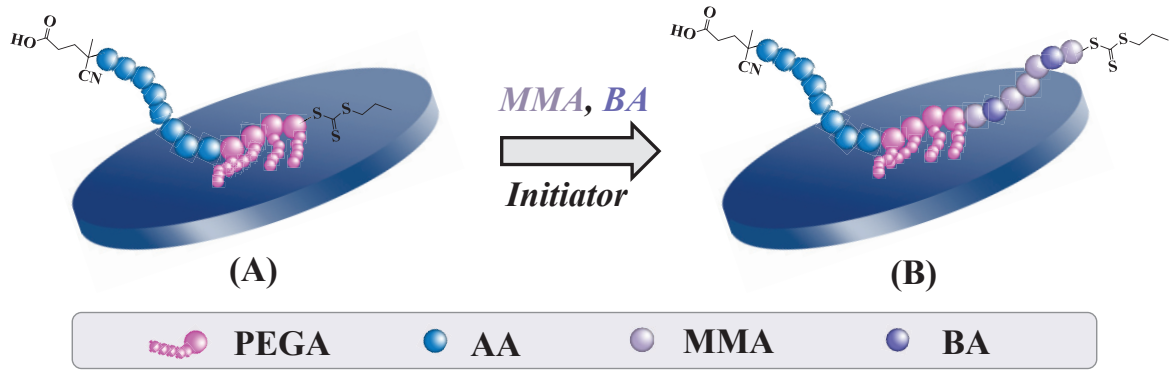
Source: elaborated by the author.

To avoid both drawbacks, a simple change in the configuration the molecule was made with the next macroRAFT agent, P(AA_{40}-*b*-$PEGA_4$)-CTPPA, as described in the following section.

4.4.4 Synthesis of hybrid latexes in the presence of P(AA_{40}-*b*-$PEGA_4$)-CTPPA

The macroRAFT P(AA_{40}-*b*-$PEGA_4$)-CTPPA was designed considering the two main drawbacks observed in the structure of PEG_{45}-*b*-PAA_{42}-CTPPA. First, the linear PEG block was replaced by a PEGA block, with pending ethylene glycol units, in order to avoid the hydrogen bonding between the ether units of PEG and the carboxyl groups of PAA (or at least reduce the formation of such bonds, as it is known that they will not be totally avoided).[105] The second factor considered was the position of this PEGA block in the structure, closer to the C=S reactive double bond of the macroRAFT agent's Z group. This configuration guarantees that the hydrophobic poly(MMA-*co*-BA) block grows closer to the PEGA units and leaves the AA segment free in the other extremity of the molecule, in a tail configuration, to be more effective as stabilizing block, as shown in Figure 4.13.

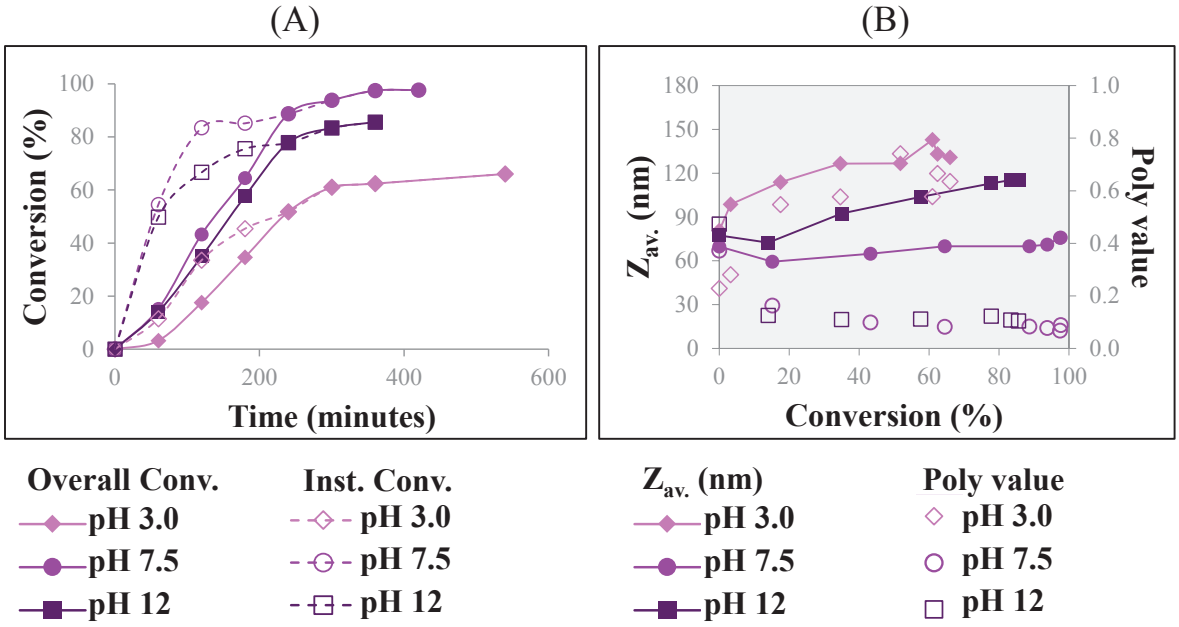
Figure 4.13 – Schematic representation of (A) Laponite platelets with adsorbed macroRAFT agent P(AA_{40}-*b*-$PEGA_4$)-CTPPA and (B) during the synthesis of P(MMA-*co*-BA)/Laponite nanocomposite latexes by RAFT-mediated emulsion polymerization using P(AA_{40}-*b*-$PEGA_4$)-CTPPA macroRAFT agent.



Source: elaborated by the author.

The synthesis of hybrid latexes in the presence of the macroRAFT agent P(AA_{40}-*b*-$PEGA_4$)-CTPPA were carried out in three different pH values (3.0, 7.5 and 12) and stable latexes were obtained in all experiments, even under acidic condition, suggesting that the pending configuration of ethylene glycol units is, in fact, more effective in avoiding the formation of hydrogen bonds than the linear configuration (while the linear block contains 45 units of ethylene glycol, in a proportion close to stoichiometry to the number of AA units, the PEGA-based macroRAFT contains 36 units, which should leave more free AA units as well). However, the pH seemed to have effects on particle size and particle size distribution. While one population of small particles of 76 nm was obtained when polymerization was carried out at pH 7.5, the presence of two populations of particles at pH 3.0 resulted in high poly values. This result might indicate that, in an acidic medium, larger aggregates were produced due to the formation of some hydrogen bonds and/or to the neutralization of PAA side chains. The kinetic behavior of the synthesis also seemed to be affected by the pH, as shown in Figure 4.14. The lowest conversion (66%) was obtained at low pH (3.0), while a conversion of 98% was obtained at pH 7.5. This low conversion obtained could be explained, in part, by insolubility of ACPA at pH 3, since this initiator is only soluble in alkaline water ($pK_a \sim 3.85$).

Figure 4.14 – (A) Evolution of overall monomer conversion (full line) and instantaneous conversion (dashed line) with time and (B) evolution of the average hydrodynamic diameters and poly value with conversionduring the synthesis of P(MMA-*co*-BA)/Laponite nanocomposite latex by RAFT-mediated emulsion polymerization using P(AA_{40}-*b*-$PEGA_4$)-CTPPA macroRAFT agent.

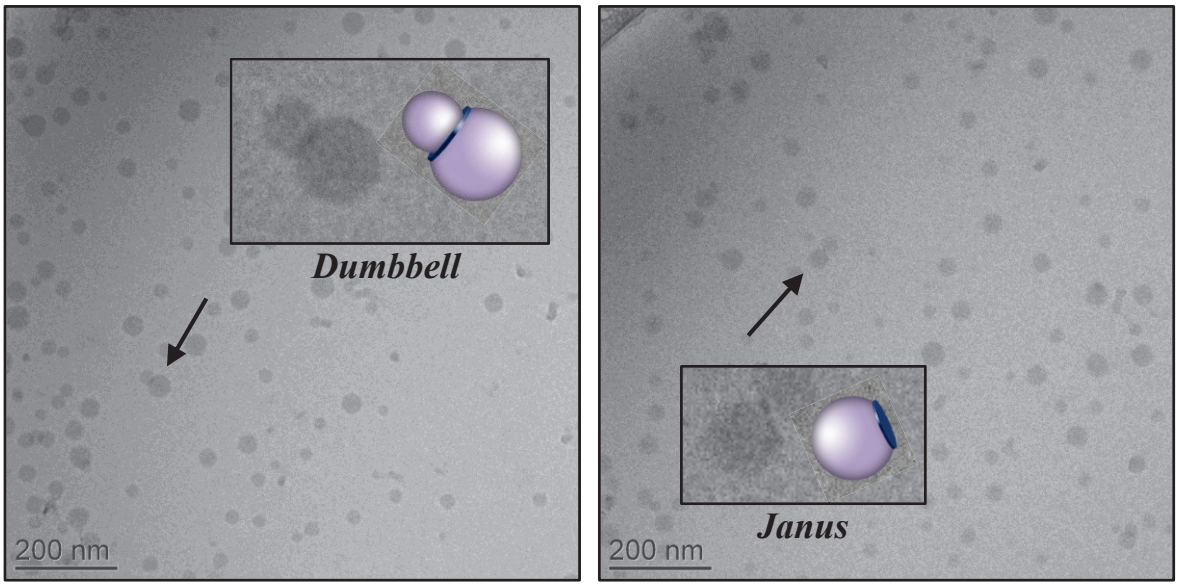


Source: elaborated by the author.

The hybrid latex synthesized at pH 7.5 was characterized by cryo-TEM and images are shown in Figure 4.14B. Even though micrographs are not very clear, they indicate that the Laponite platelets were not truly encapsulated by the polymer shell but, instead, some polymeric nodules can be seen surrounding the inorganic particles. Some dumbbell, or peanut-shaped, and janus particles can be seen as well. It is clear, though, that there is a large number of free polymeric particles in the water phase. These results can be explained by the large amount of free macroRAFT agent that was in the water phase at the beginning of polymerization, since these highly hydrophilic molecules, composed of two hydrophilic blocks, tend to stay in the water phase. According to the adsorption isotherms shown in Chapter 3, about 85% of the macroRAFT agent is free in the aqueous phase, while only 15% is adsorbed onto Laponite surface. The block copolymers that were not adsorbed on the surface of the platelets can be responsible for the formation of pure polymeric secondary particles, according to the PISA mechanism of nucleation. Therefore, the amphiphilic block copolymers formed *in situ* by the addition of the hydrophobic monomer units that were soluble in the water phase (until the point in which the critical chain length was achieved) suffered self-assembly and generated self-stabilized objects. It is expected that, under ideal conditions, the macroRAFT-modified clays behave as the main polymerization locus and,

together with the use of a semi-batch process, inhibit homogeneous nucleation. For this reason, to decrease the hydrophilicity and avoid the tendency of the macroRAFT agents to stay in the aqueous phase, a more hydrophobic block copolymer, PAA_{40}-*b*-P($PEGA_6$-*co*-BA_4)-CTPPA was evaluated, as shown in the following section.

Figure 4.15 – Cryo-TEM images of hybrid particles obtained by the copolymerization of MMA:BA 80:20, at 80 ºC, in the presence of 2.2 mM of macroRAFT agent P(AA_{40}-*b*-$PEGA_4$)-CTPPA and 5 g L^{-1} of Laponite at pH 7.5.

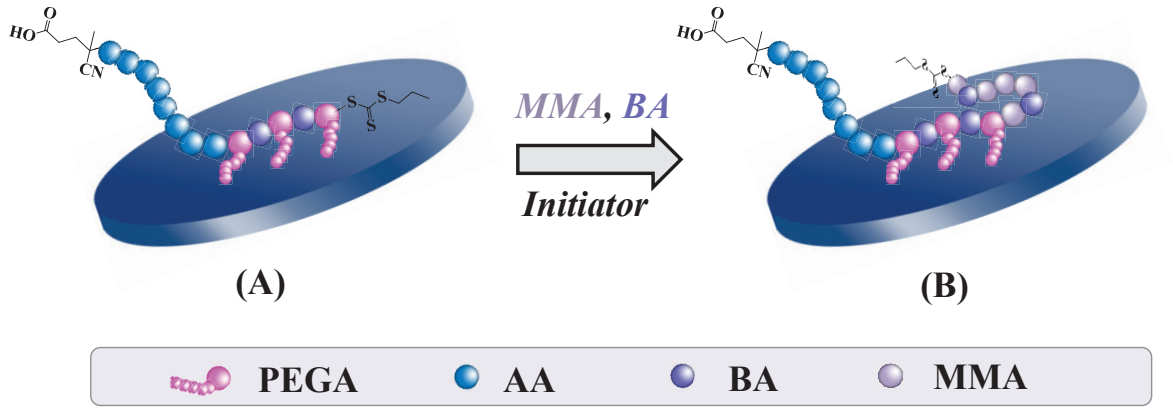


Source: elaborated by the author.

4.4.5 Synthesis of hybrid latexes in the presence of PAA_{40}-*b*-($PEGA_6$-*co*-BA_4)-CTPPA

Considering the high hydrophilicity of P(AA_{40}-*b*-$PEGA_4$)-CTPPA, the macroRAFT PAA_{40}-*b*-P($PEGA_6$-*co*-BA_4)-CTPPA was designed containing hydrophobic units of BA along the PEGA block. Besides contributing to increase the tendency of the hydrophobic poly(MMA-*co*-BA) block to grow closer to the surface of Laponite, as illustrated in Figure 4.16, the BA units also contribute to decrease the hydrophilicity of the molecule, decreasing thus the predisposition that highly hydrophilic macroRAFT agents have to stay preferentially in the aqueous phase.

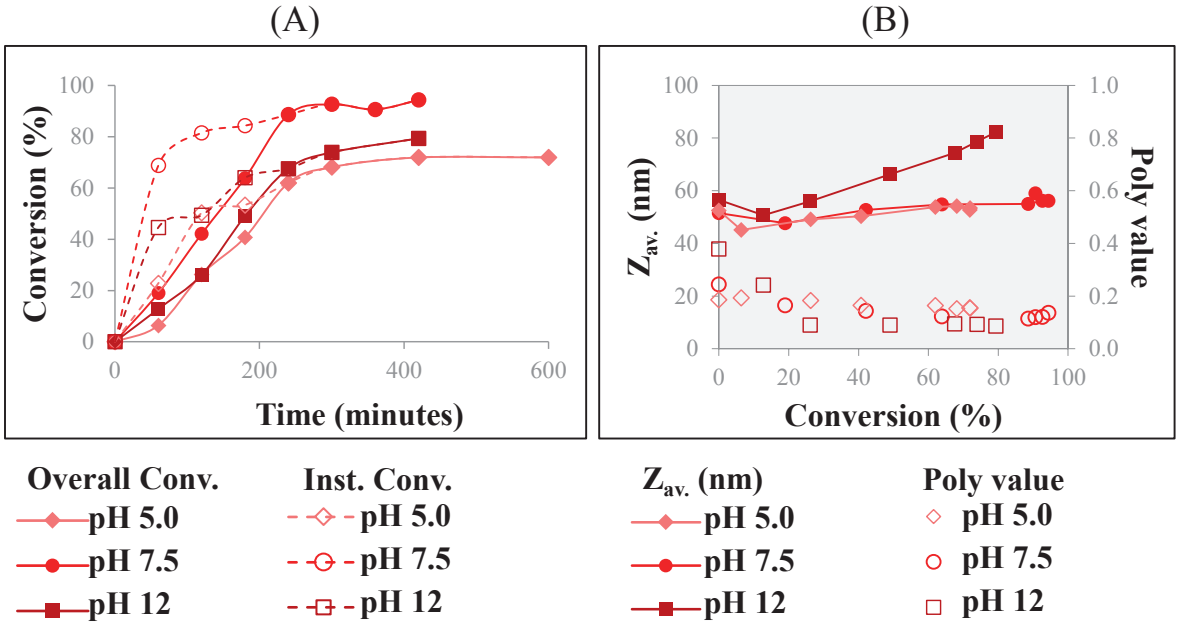
Figure 4.16 – Schematic representation of (a) Laponite platelets with adsorbed macroRAFT agent PAA_{40}-*b*-P($PEGA_6$-*co*-BA_4)-CTPPA and (b) during the synthesis of Poly(MMA-*co*-BA)/Laponite nanocomposite latex by RAFT-mediated emulsion polymerization using PAA_{40}-*b*-P($PEGA_6$-*co*-BA_4)-CTPPA macroRAFT agent (MR6).



Source: elaborated by the author.

Stable latexes were obtained for all three different pH values tested (5.0, 7.5 and 12) and, again, the pH seemed to affect conversion, since the highest instantaneous and overall conversions were obtained at neutral pH. The effect of pH on particle size and particle size distribution, on the other hand, was slight.

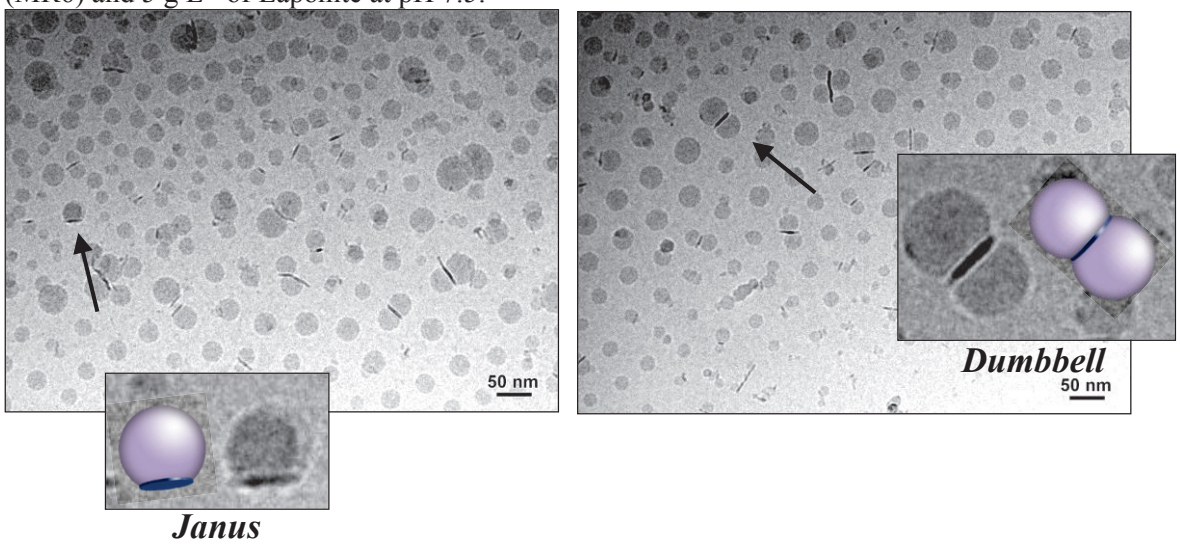
Figure 4.17 – (A) Evolution of overall monomer conversion (full line) and instantaneous conversion (dashed line) with time and (B) evolution of the average hydrodynamic diameters and poly value with conversion during the synthesis of P(MMA-*co*-BA)/Laponite nanocomposite latex by RAFT-mediated emulsion polymerization using PAA_{40}-*b*-P($PEGA_6$-*co*-BA_4)-CTPPA macroRAFT agent (MR6).



Source: elaborated by the author.

The hybrid latex synthesized at pH 7.5 was characterized by cryo-TEM and images are shown in Figure 4.18. It is possible to identify dumbbell and janus particles with more defined morphologies, in comparison to the latex synthesized with highly hydrophilic macroRAFT agents. Although it also seems that there are less free polymeric particles in the water phase, no conclusion can be drawn regarding the effective number of particles that do not contain Laponite platelets. To be identified on the images, platelets must have their basal planes oriented in parallel to the electron beam, since this disposition forces the electrons to pass through the entire length of the platelet. Transmission of electrons is, therefore, minimal and platelets can be seen as dark lines. If platelets, on the other hand, are perpendicularly orientated to the beam, electrons penetrate through the thickness of the clay sheets, which is negligible, and suffer an undetectable absorption, resulting in no change in brightness. In this situation, even hybrid particles that contain clay platelets can be erroneously detected as pure polymer particles, if these particles are positioned in a way that the basal plane of the platelets is in perpendicular to the electron beam. Even though, in theory, some idea could be traced by plotting the evolution of the particle number with conversion (if there were in fact secondary nucleation, it should increase with conversion) the complex particle morphology (dumbbell and janus), the shape anisotropy and the high size distribution might make quantitative estimations quite complicated in this case. Considering the constant particle size in Figure 4.17B, it is very likely that there is secondary nucleation for polymerizations carried out at pH = 5 and 7.5.

Figure 4.18 – Cryo-TEM images of hybrid particles obtained by the copolymerization of MMA:BA 80:20, at 80ºC, in the presence of 2.2 mM of macroRAFT agent PAA_{40}-*b*-P($PEGA_6$-*co*-BA_4)-CTPPA (MR6) and 5 g L^{-1} of Laponite at pH 7.5.



Source: elaborated by the author.

Recent studies have demonstrated that the individual encapsulation of clay platelets is driven by kinetic and thermodynamic factors.[20, 22, 100] From the kinetical point of view, the use of RDRP techniques is expected to ensure a slow and controlled growth of polymer chains on the surface of each nanofiller, thanks to the kinetic features of the RDRP mechanisms. While polymer chains would grow in a fast manner by conventional free radical polymerization, leading to the formation of long hydrophobic chains on the surface of the particles, which favor aggregation, by RDRP mechanisms, initiation and propagation of chains require significantly larger periods of time to occur. For this reason, in the case of RAFT mechanism, the time necessary to activate the chain transfer agent, known as induction period, and the slow growth of polymer chains are expected to difficult the aggregation of platelets and allow the individual encapsulation of nanofillers.

Therefore, the formation of dumbbell and janus particles instead of the true encapsulation can be a result of thermodynamic factors. Clays, for being very hydrophilic, tend to minimize the contact with the polymeric phase (hydrophobic) by maintaining themselves in a state of minimal interfacial energy. Depending on the mobility that the inorganic phase has in the polymer matrix, the inorganic nanoparticle can migrate from inside the hydrophobic inner part of the growing latex particles to the polymer/water interface, or simply exclude itself (phase separate) from the growing polymer nodule, generating particles with janus morphology. In this aspect, the selection of an adequate ratio between the comonomers MMA and BA must take into account the glass transition temperature (T_g) of the final copolymer. To avoid the mobility of the filler inside the latex particles towards the polymer/water interface, resulting in a thermodynamically favored morphology, the T_g of the copolymer should be superior to the temperature used during the synthesis of the nanocomposite latex particles by emulsion polymerization.

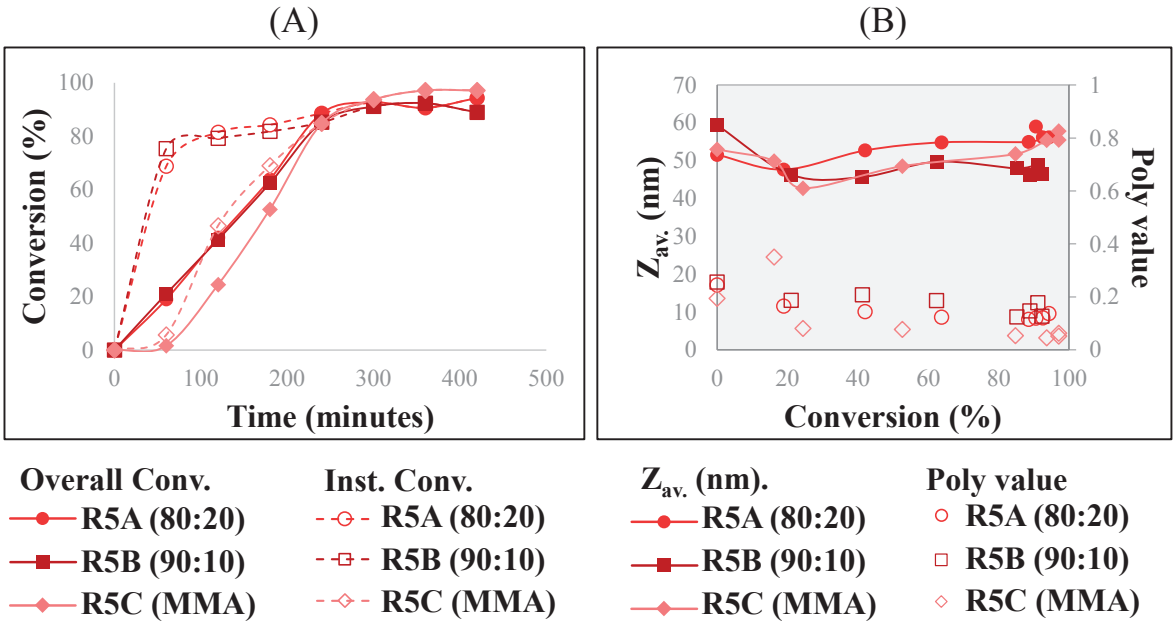
In our case, the use of a MMA-rich feeding might be necessary to guarantee the formation of core-shell hybrid latex particles, since it favors the formation of kinetically trapped morphologies. Hence, two additional experiments (under the same conditions of the experiment carried out at pH 7.5, which was denominated R5A) were carried out to evaluate the effect of different MMA:BA mixtures by increasing the MMA molar ratio from 80% to 90% (R5B, MMA:BA 90:10) and to 100% (R5C).

Evolution of overall and instantaneous conversion with time, as well as the evolution of particle size and poly value with conversion, are shown in Figure 4.19 A and B, respectively. The comparison between the curves indicates that similar profiles were

obtained for all monomer compositions chosen. It can be observed, however, that polymerization of pure MMA (R5B) presented an induction period. Generally related to the nucleation mechanism, induction periods may correspond to the first chain transfer reactions necessary for the copolymer to self-assemble in water (right after the hydrophobic block has reached a sufficient length).[96] Therefore, the main factor that may have led to this phenomenon during polymerization with MMA is the high hydrophilicity of the monomer, which increases the critical length of the hydrophobic block necessary for the self-assembly process, retarding the nucleation of particles. In this scenario, it is possible that, after the self-assembly of amphiphilic block copolymers, the generated particles adsorb onto the macroRAFT/clay complex, forming the janus or dumbbell structures. It should also be considered, though, that the self-assembly process can also involve block copolymers grown from the clay surface with block copolymers formed in water.

From Figure 4.19B, it is possible to see, as well, that the synthesis of hybrid latexes with pure MMA presented lower instantaneous conversions. It is known that, besides forming droplets (which compete for macroRAFT stabilizers and Laponite platelets), accumulated monomer might act as plasticizer and decrease the T_g of the polymer shell.

Figure 4.19 – (A) Evolution of overall monomer conversion (full line) and instantaneous conversion (dashed line) with time and (B) evolution of the average hydrodynamic diameters and poly value with conversion during the synthesis of polymer/Laponite nanocomposite latex by RAFT-mediated emulsion polymerization using PAA_{40}-*b*-P($PEGA_6$-*co*-BA_4)-CTPPA macroRAFT agent (MR6) with different molar ratios of monomers MMA and BA: MMA:BA 80:20 (R5A); MMA:BA 90:10 (R5B) and pure MMA (R5C).



Source: elaborated by the author.

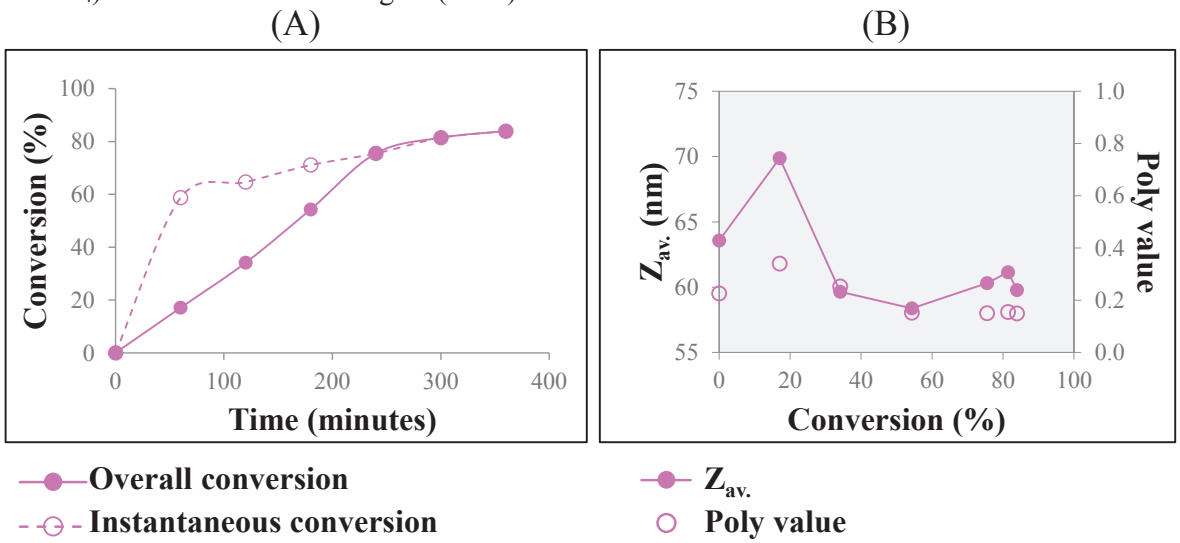
For the aforementioned reasons, the following experiments were carried out with the monomer mixture MMA:BA 90:10, as this mixture guarantees that the copolymer shell has a T_g higher than the reactional temperature, favoring the formation of kinetically controlled (or trapped) morphologies (core-shell) instead of thermodynamically stable morphologies (e.g. janus), and ensures satisfactory instantaneous conversion.

In addition, for the following experiments with the other AA-containing macroRAFT agents, the only pH tested was 7.5. It was considered that, as a general rule, lower values of pH result in lower conversions due to the solubility issues that the initiator (ACPA) presents under such conditions and high pHs are not good for the RAFT functionality, in general, regardless of the structure of the macroRAFT agent.

4.4.6 Synthesis of hybrid latexes in the presence of P(AA_{16}-*co*-BA_{16})-*b*-(P(EGA_6-*co*-BA_4)-CTPPA

An even more hydrophobic macroRAFT agent containing random BA units distributed along the PAA block was tested, the P(AA_{16}-*co*-BA_{16})-*b*-P($PEGA_6$-*co*-BA_4)-CTPPA. The pH of the macroRAFT/Laponite dispersion, as mentioned above, was adjusted to 7.5 and the monomer mixture used was MMA:BA 90:10 (mol%). A stable hybrid latex was obtained after 360 minutes of polymerization, with a final overall conversion of 84%, as shown in Figure 4.20A.

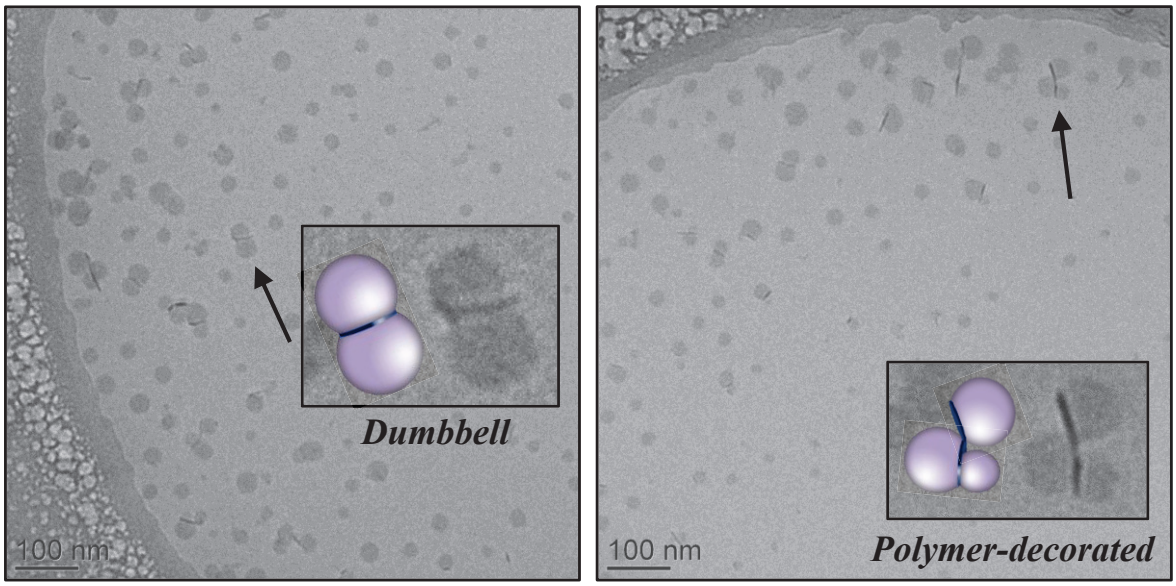
Figure 4.20 – (A) Evolution of overall monomer conversion (full line) and instantaneous conversion (dashed line) with time and (B) evolution of the average hydrodynamic diameters and poly value with conversion during the synthesis of P(MMA-*co*-BA)/Laponite nanocomposite latex (MMA:BA = 90:10 mol%) by RAFT-mediated emulsion polymerization using P(AA_{16}-*co*-BA_{16})-*b*-P($PEGA_6$-*co*-BA_4)-CTPPA macroRAFT agent (MR7).



Source: elaborated by the author.

Cryo-TEM images of the final latex are shown in Figure 4.21. As compared to PAA_{40}-*b*-P($PEGA_6$-*co*-BA_4)-CTPPA, a very similar result in terms of particle morphology was obtained, with the formation of polymer-decorated clay particles. In such morphologies, polymer nodules surround Laponite platelets, generating decorated platelets with one (janus), two (dumbbell) or more polymeric nodules. This result indicates that, in this case, the modification of the hydrophobic/hydrophilic balance of the stabilizing block did not result in a notable effect on the morphology of the particles. It was expected that this modification on the macroRAFT structure could result in the coating of the rims of the platelet with polymer, since the adsorbed PAA block containing hydrophobic units could attract the growing polymer layer close to the edges of Laponite, however this did not occur. Moreover, no conclusive information can be extracted from the images concerning the effect of increasing the hydrophobicity of the RAFT copolymer on the formation of pure polymer (secondary) particles. However, the analysis of the evolution of particle size and poly value with conversion, shown in Figure 4.21, suggest that secondary nucleation happened, in fact, as a decrease in particle size is observed after polymerization reached 20% conversion.

Figure 4.21 – Cryo-TEM images of hybrid particles obtained by the copolymerization of MMA:BA 90:10, at 80ºC, in the presence of 2.2 mM of macroRAFT agent P(AA_{16}-*co*-BA_{16})-*b*-P($PEGA_6$-*co*-BA_4)-CTPPA (MR7) and 5 g L^{-1} of Laponite at pH 7.5.

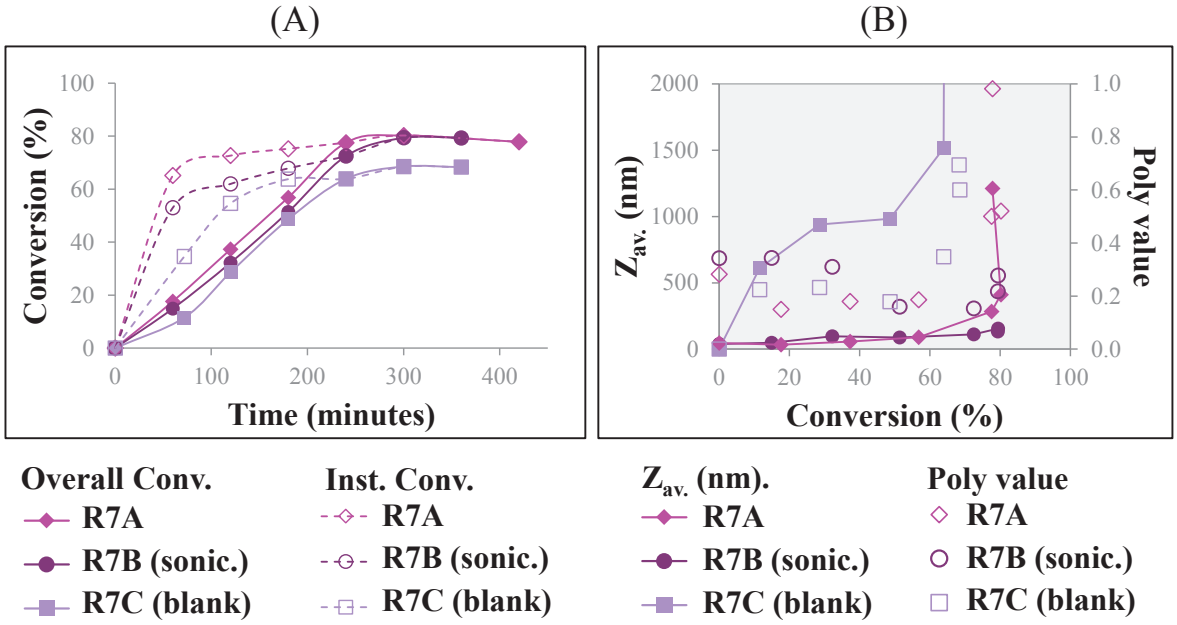


Source: elaborated by the author.

4.4.7 Synthesis of hybrid latexes in the presence of P($PEGA_5$-*co*-BA_3)-CTPPA

A nonionic macroRAFT agent, the P($PEGA_5$-*co*-BA_3)-CTPPA, was evaluated as mediator in the synthesis of the nanocomposite particles by emulsion polymerization. Since this macroRAFT does not contain AA units along its structure, the pH of the macroRAFT/Laponite suspension was not adjusted prior to the emulsion polymerization and peptizer was added to neutralize the rim charges of Laponite. However, the first experiment (R7A) resulted in unstable final latexes because the absence of a PAA block reduced the macroRAFT's capacity to provide stability to the hybrid latex particles. To increase the colloidal stability of the hybrid particles, the experiment was repeated by submitting the colloidal suspension of this macroRAFT agent and Laponite to 5 minutes of sonication at 30% amplitude before polymerization (R7B). To verify the stability of the particles in the absence of Laponite platelets, a blank experiment was carried out (R7C) without Laponite. The evolution of overall and instantaneous conversions with time obtained for all experiments are shown in Figure 4.22A, and evolution of particle size and poly value are in Figure 4.22B.

Figure 4.22 – (A) Evolution of overall monomer conversion (full line) and instantaneous conversion (dashed line) with time and (B) evolution of the average hydrodynamic diameters and poly value with conversion during the synthesis of P(MMA-*co*-BA)/Laponite nanocomposite latex (MMA:BA = 90:10 mol%) by RAFT-mediated emulsion polymerization using P($PEGA_5$-*co*-BA_3)-CTPPA macroRAFT agent (MR8) for experiments R7A, R7B (with five-minute sonication process, at 30% amplitude) and R7C (blank, without Laponite).



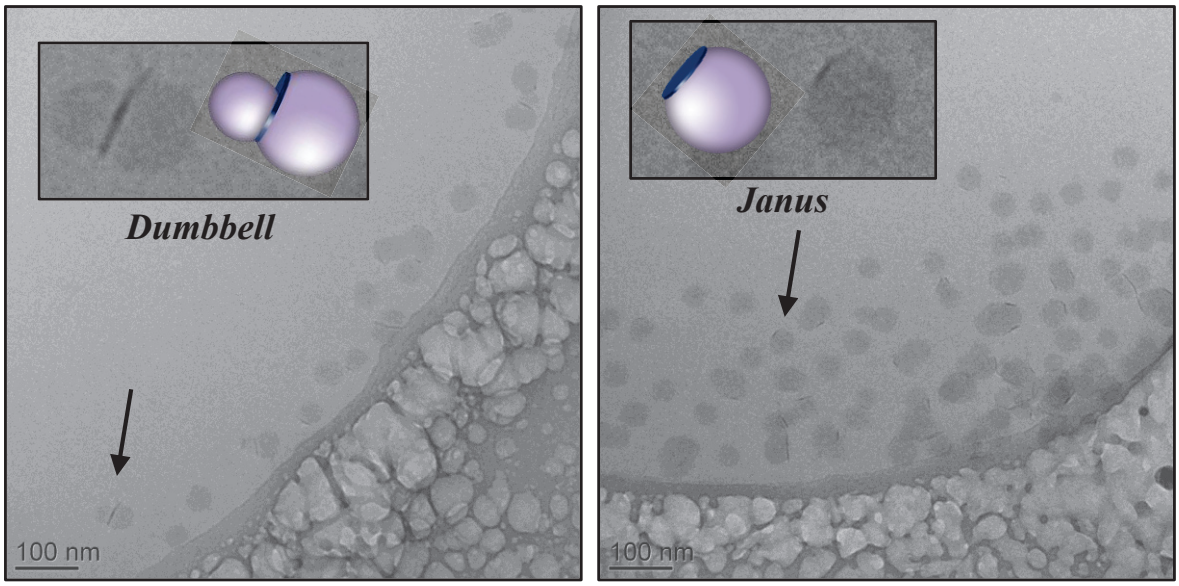
Source: elaborated by the author.

From the evolution of particle size and poly value (Figure 4.22B), it is possible to presume that, although this nonionic macroRAFT agent adsorbs efficiently onto Laponite, this copolymer does not behave as an efficient stabilizer for the pure latex particles. This may be related to the fact that this macroRAFT agent can dissolve in the monomer phase and, therefore, due to its partitioning between the monomer phase and the clay platelets, a lower than the expected amount of macroRAFT is available to stabilize the forming particles. The hybrid particles are more stable, although the destabilization of the final particles can be observed at the end of polymerization.

The cryo-TEM images of the R7B nanocomposite particles, shown in Figure 4.23, reveal a tendency of the platelets to be located at the edges of the polymeric particles, forming janus structures, or sandwiched between two polymer particles, forming dumbbell structures. In this configuration, the platelets may play an important role in stabilizing the hybrid particles. In a recent work developed by our group (Bourgeat-Lami et al., soon submitted for publication), spherical silica particles were successfully encapsulated by this same approach used with P($PEGA_5$-*co*-BA_3)-CTPPA (adapting the conditions of experiment R7B to colloidal silica), resulting in mono and multiencapsulated silica particles, depending

on the size of the silica spheres. Many questions still remain unanswered though, concerning specially the location of the macroRAFT agent chains on the encapsulated particles so they can efficiently adsorb on the silica nanospheres and stabilize the nanocomposite latex particles. Therefore, many aspects still need to be elucidated to fully understand all the elements involved in the encapsulation of inorganic substrates using this nonionic RAFT copolymer. This macroRAFT agent is, without a doubt, a promising system for the encapsulation of inorganic particles, yet it could be considered very sensitive to the morphology and/or surface chemistry of the inorganic particle and susceptible to colloidal stability issues.

Figure 4.23 – Cryo-TEM images of hybrid particles obtained by the copolymerization of MMA:BA 90:10, at 80ºC, in the presence of 2.2 mM of macroRAFT agent P($PEGA_5$-*co*-BA_3)-CTPPA (MR8) and 5 g L^{-1} of Laponite (R7B).

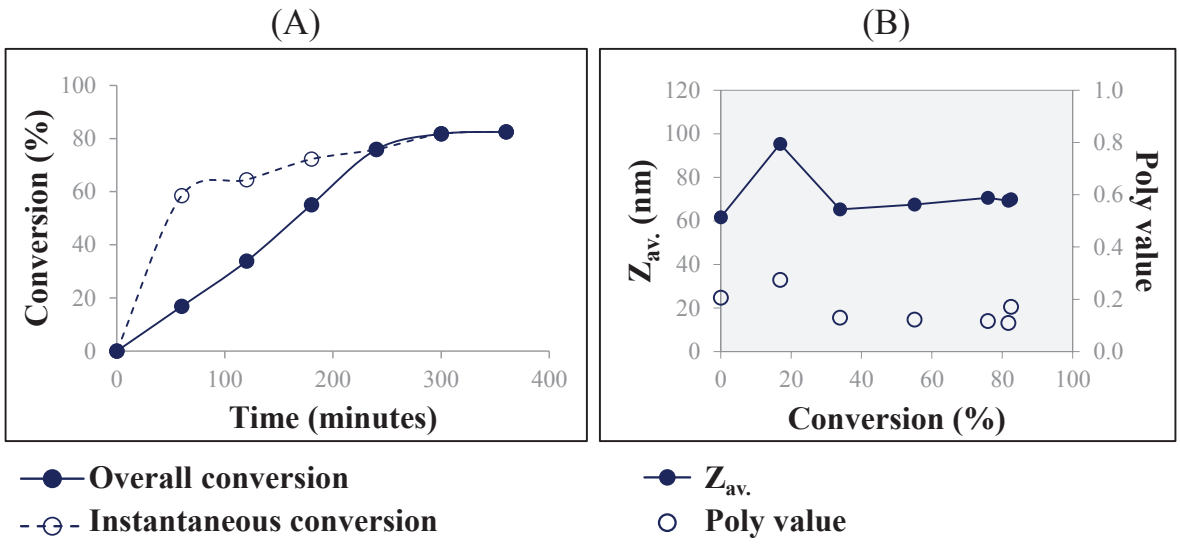


Source: elaborated by the author.

4.4.8 Synthesis of hybrid latexes in the presence of P(AA_{16}-*co*-BA_{16})-CTPPA

Emulsion polymerization mediated by P(AA_{16}-*co*-BA_{16})-CTPPA macroRAFT agent was carried out at pH 7.5, using MMA:BA 90:10 (mol%) as monomer mixture. A stable latex was obtained with a final conversion of 82%, as shown in Figure 4.24A. A discrete increase in particle size was observed during the first hour of polymerization but particle size was maintained constant during the rest of the process and poly value was kept below 0.17 (Figure 4.24B).

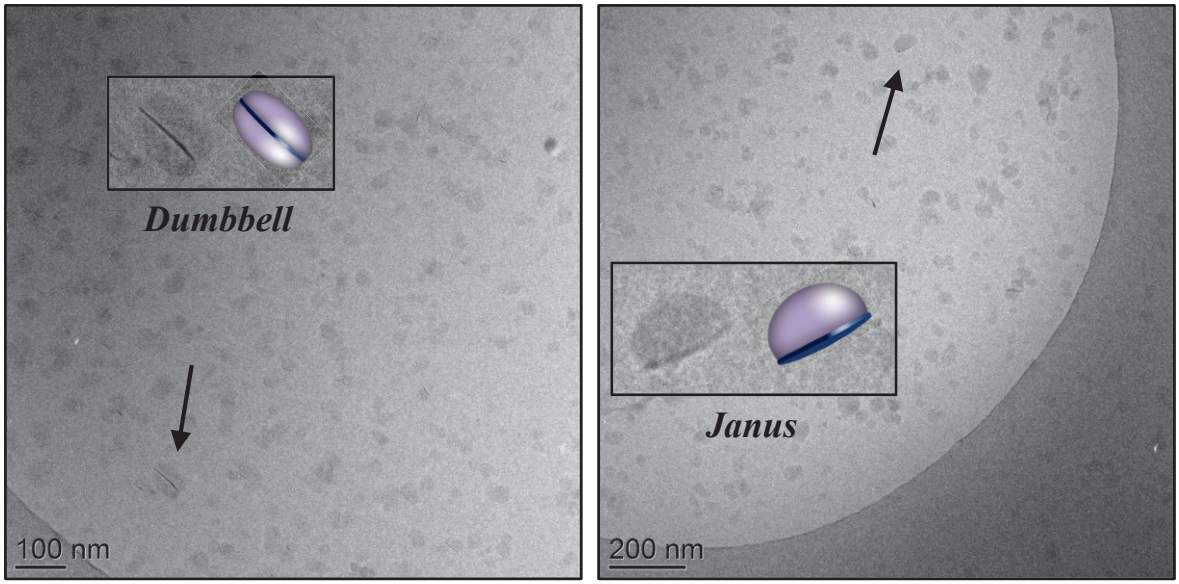
Figure 4.24 – (A) Evolution of overall monomer conversion (full line) and instantaneous conversion (dashed line) with time and (B) evolution of the average hydrodynamic diameters and poly value with conversion during the synthesis of P(MMA-*co*-BA)/Laponite nanocomposite latex (MMA:BA = 90:10 mol%) by RAFT-mediated emulsion polymerization using 2.2 mM of P(AA_{16}-*co*-BA_{16})-CTPPA macroRAFT agent (MR2) at pH 7.5.



Source: elaborated by the author.

Flat dumbbell and flat janus particles were obtained, as indicated in the cryo-TEM images of Figure 4.25. Several works have reported the successful encapsulation of various inorganic particles using P(AA-*co*-BA) RAFT copolymers or oligomers, with different compositions and chain lengths.[9, 12, 13, 19] In fact, in all those cases, RAFT copolymers present a high affinity with the oppositely charged inorganic surface and were, therefore, capable of adsorbing onto the particles via strong electrostatic interaction. In the case of Laponite, on the other hand, the different charges presented by the surface and the rims of the particles add more complexity to the process, and it is very likely that the negatively charged copolymers suffer a strong influence of the repulsive negative charges of the surface of the clay, rather than being attracted by the positive edges. However, from the micrographs it is possible to infer that this macroRAFT agent seems to be more susceptible to follow the shape anisotropy of the particle, producing non-spherical flat morphologies, than the PEG-based molecules.

Figure 4.25 – Cryo-TEM images of hybrid particles obtained by the copolymerization of MMA:BA 90:10, at 80ºC, in the presence of 2.2 mM of macroRAFT agent P(AA_{16}-*co*-BA_{16})-CTPPA (MR2) and 5 g L^{-1} of Laponite at pH 7.5.



Source: elaborated by the author.

4.4.9 Synthesis of hybrid latexes in the presence of P(AA-*co*-PEGA-*co*-BA)-CTPPA

Two random copolymers composed of AA, PEGA and BA with different chain lengths, P(AA_4-*co*-$PEGA_4$-*co*-BA_4)-CTPPA and P(AA_9-*co*-$PEGA_9$-*co*-BA_9)-CTPPA, were evaluated on the synthesis of P(MMA-*co*-BA)/Laponite nanocomposite latex particles. The monomer ratio used was MMA:BA 90:10 (mol%) and polymerizations were carried out at pH 7.5 with two different concentrations of macroRAFT agents. Results are listed in Table 4.2:

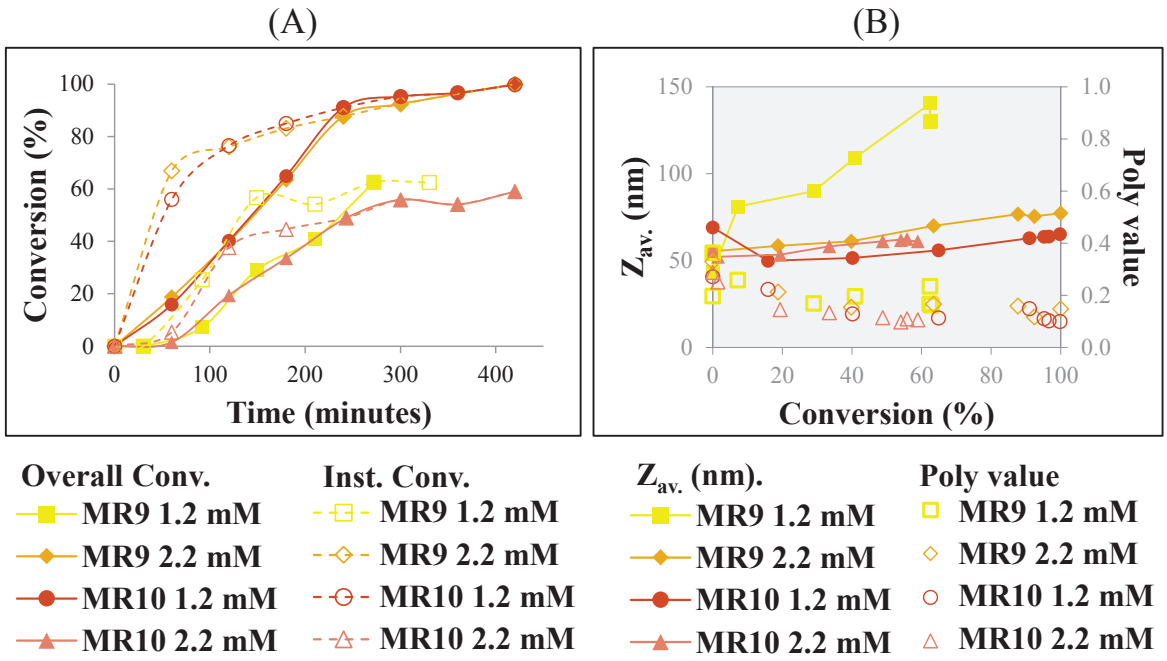
Table 4.2 – Results obtained in the synthesis of hybrid latexes mediated by P(AA-*co*-PEGA-*co*-BA)-CTPPA macroRAFT agents using a monomer composition of MMA:BA 90:10 (mol%), 5 g L^{-1} of Laponite and at pH 7.5.

RAFT agent	[RAFT] (mM)	Conversion (%)	$Z_{av.}$ (nm)	Poly
P(AA_4-*co*-$PEGA_4$-*co*-BA_4)-CTPPA	1.2	62	130	0.16
	2.2	100	77	0.15
P(AA_9-*co*-$PEGA_9$-*co*-BA_9)-CTPPA	1.2	99.8	65	0.10
	2.2	59	61	0.11

Source: elaborated by the author.

The evolution of overall and instantaneous conversions with time, shown in Figure 4.26A, reveal that higher conversions were obtained for the systems mediated by P(AA_4-*co*-$PEGA_4$-*co*-BA_4)-CTPPA at a concentration of 2.2 mM and by P(AA_9-*co*-$PEGA_9$-*co*-BA_9)-CTPPA at a concentration of 1.2 mM, which, interestingly, represent the same mass concentration of copolymer. Oppositely, systems mediated by 1.2 mM of P(AA_4-*co*-$PEGA_4$-*co*-BA_4)-CTPPA and by 2.2 mM of P(AA_9-*co*-$PEGA_9$-*co*-BA_9)-CTPPA presented a low polymerization rate with an induction period. As mentioned before, induction periods can be generally associated to the nucleation mechanism and correlated to the process of chain extension of copolymers that leads to the self-assembly of the molecules in water, once the hydrophobic block critical length is surpassed. In this aspect, it is understandable that a longer hydrophilic copolymer requires that the hydrophobic block reaches a higher critical length to suffer the self-assembly, while the high concentration of this copolymer consumes more monomer units (which are being fed into the reactor), consequently retarding the nucleation of particles. For this reason, an excess of P(AA_9-*co*-$PEGA_9$-*co*-BA_9)-CTPPA can be prejudicial for the polymerization kinetics. In a similar manner, the low concentration of the short copolymer presented a final conversion leveling off at around 60% with an induction period. Indeed, short RAFT copolymers are more susceptible to migrate to the aqueous phase during the encapsulation process, suffering partition between the monomer droplets and the aqueous phase and impeding, therefore, the fast growth of the hydrophobic block. In addition, it is known that, during the encapsulation process, a certain excess of macroRAFT agent must exist in the aqueous phase (free macroRAFT, i.e. non-adsorbed on Laponite) to be able to adsorb on the growing hybrid objects, in order to maintain their colloidal stability. Indeed, 1.2 mM of P(AA_4-*co*-$PEGA_4$-*co*-BA_4)-CTPPA macroRAFT resulted in larger particle sizes ($Z_{av.}$ = 130 nm).

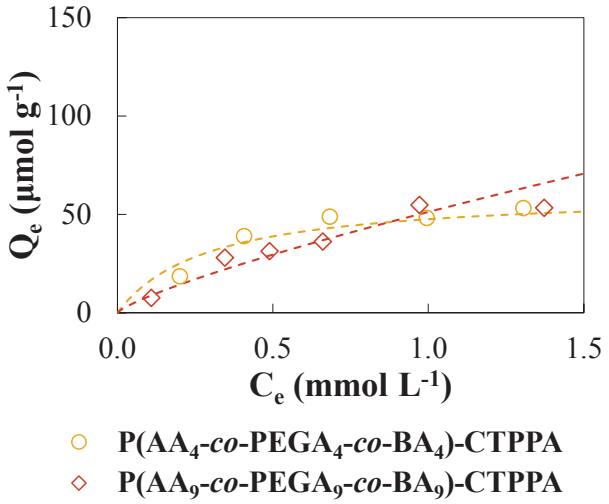
Figure 4.26 – (A) Evolution of overall monomer conversion (full line) and instantaneous conversion (dashed line) with time and (B) evolution of the average hydrodynamic diameters and poly value with conversion during the synthesis of P(MMA-*co*-BA)/Laponite nanocomposite latex (MMA:BA = 90:10 mol%) by RAFT-mediated emulsion polymerization using P(AA_4-*co*-$PEGA_4$-*co*-BA_4)-CTPPA (MR9) and P(AA_9-*co*-$PEGA_9$-*co*-BA_9)-CTPPA (MR10) macroRAFT agents at the concentrations of 1.2 and 2.2 mM, and at pH 7.5.



Source: elaborated by the author.

For the successful encapsulation of inorganic particles, it is highly desirable that the RAFT copolymer chains should be as short as possible to provide the largest number of RAFT end groups per particle while maintaining the colloidal stability of the hybrid particles. In this aspect, the selection of P(AA_4-*co*-$PEGA_4$-*co*-BA_4)-CTPPA copolymer could be preferred over P(AA_9-*co*-$PEGA_9$-*co*-BA_9)-CTPPA. However, the adsorption isotherms of these macroRAFT agents, recalled in Figure 4.27, suggest that both molecules present very similar adsorption profiles, in terms of molar concentration, onto Laponite surface. This means that, for the same amount of RAFT chain ends adsorbed on Laponite, larger adsorption in terms of mass of copolymer is found for P(AA_9-*co*-$PEGA_9$-*co*-BA_9)-CTPPA. Thus, allowing more acrylic acid units to stabilize the hybrid particles with similar RAFT functional end groups to control polymerization, P(AA_9-*co*-$PEGA_9$-*co*-BA_9)-CTPPA might be a more interesting choice.

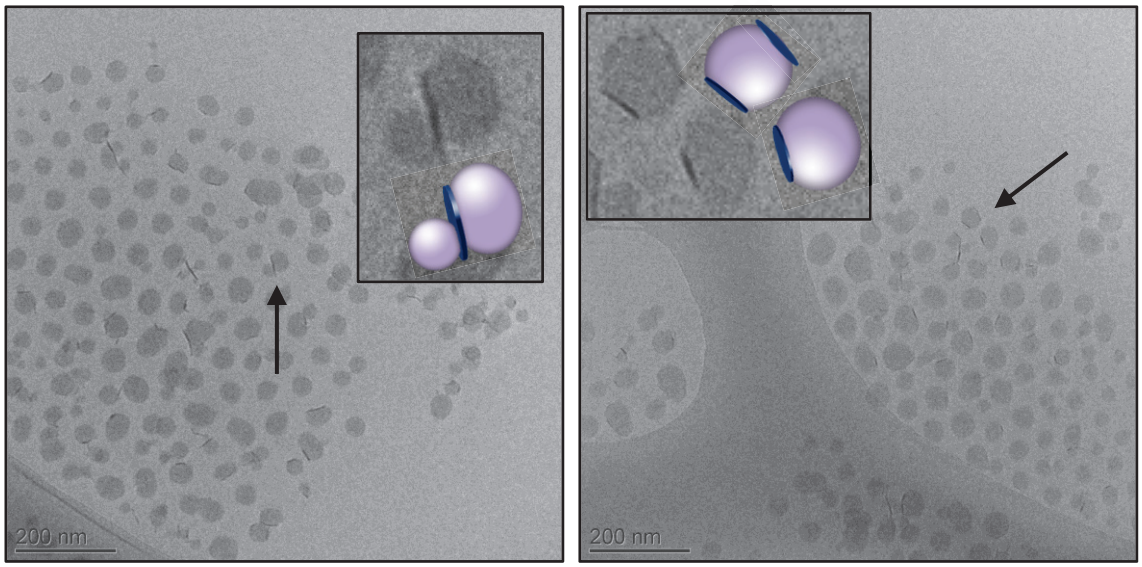
Figure 4.27 – Isotherm for macroRAFT P(AA$_4$-*co*-PEGA$_4$-*co*-BA$_4$)-CTPPA (MR9) and = P(AA$_9$-*co*-PEGA$_9$-*co*-BA$_9$)-CTPPA (MR10) adsorption onto Laponite surface at pH 7.5 in terms of molar concentration. Laponite = 5.0 g L^{-1}. Dashed lines are the fitting to the Langmuir (MR9) and Freundlich (MR10) equations.



Source: elaborated by the author.

Figure 4.28 shows the cryo-TEM images of latex particles obtained in the polymerization mediated by 1.2 mM of P(AA$_9$-*co*-PEGA$_9$-*co*-BA$_9$)-CTPPA. Micrographs reveal that Laponite platelets are located predominantly in the edge of the polymer particles, generating janus structures, or trapped between two polymer particles, generating dumbbell particles.

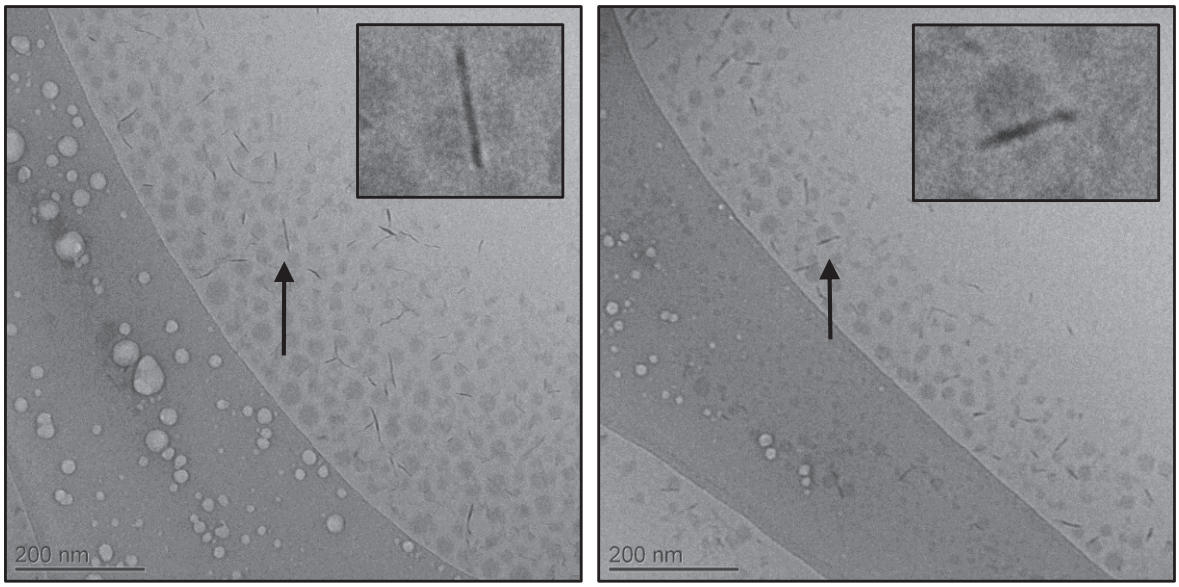
Figure 4.28 – Cryo-TEM images of hybrid particles obtained by the copolymerization of MMA:BA 90:10, at 80ºC, in the presence of 1.2 mM of macroRAFT agent P(AA$_9$-*co*-PEGA$_9$-*co*-BA$_9$)-CTPPA (MR10) and 5 g L^{-1} of Laponite at pH 7.5.



Source: elaborated by the author.

In order to verify the effect of monomer addition rate, polymerization in the presence of 1.2 mM of P(AA_9-*co*-$PEGA_9$-*co*-BA_9)-CTPPA was repeated with a different monomer addition rate profile, as an attempt to guarantee complete monomer starvation. For this purpose, the feeding time was kept in 4 hours and the flow rate was decreased from 0.6 to 0.135 mL h^{-1}, which resulted in a latex with final solids content of 2%. In this case, the monomer-starved condition was expected to avoid the formation of monomer droplets, which could cause macroRAFT partitioning by competing with Laponite. Cryo-TEM images of the final product of this polymerization (Figure 4.29) show that, even at a very low monomer addition rate, the same type of morphology is obtained.

Figure 4.29 – Cryo-TEM images of hybrid particles obtained by the copolymerization of MMA:BA 90:10, at 80ºC, in the presence of 1.2 mM of macroRAFT agent P(AA_9-*co*-$PEGA_9$-*co*-BA_9)-CTPPA (MR10) and 5 g L^{-1} of Laponite at pH 7.5 with a monomer feed of 0.135 mL h^{-1}.



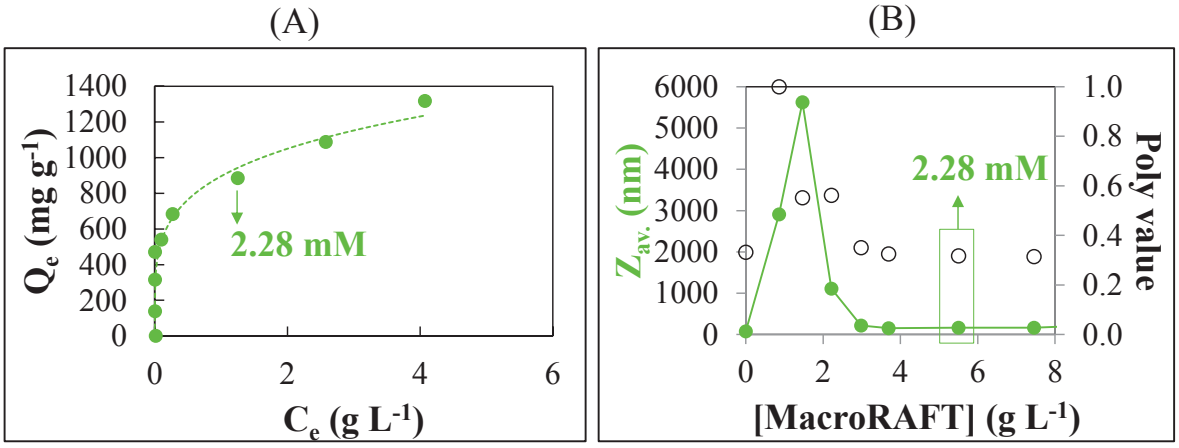
Source: elaborated by the author.

4.4.10 Synthesis of hybrid latexes in the presence of P(DMAEMA$_{10}$-*co*-BA$_4$)-CTPPA

Polymerizations mediated by DMAEMA-based macroRAFT agents were carried out in the presence of a cationic initiator: AIBA instead of ACPA, since ACPA may interact with the charged amine groups of DMAEMA by electrostatic interactions, and affect the stabilization of the hybrid particles. For the synthesis of nanocomposite latexes by emulsion polymerization, the quaternized P(qDMAEMA$_{10}$-*co*-BA_4)-CTPPA was preferred over the non-quaternized molecule due to the permanent charge that this copolymer possesses regardless of the pH of the medium (while the unmodified macroRAFT agent requires a low

pH for the ionization of the DMAMEA moieties, working at high pH values could be more interesting due to the neutralization of the positive charges from the edges of Laponite) The concentration of macroRAFT agent was selected based on the adsorption isotherm of this copolymer, as already shown in Chapter 3 and recalled, in Figure 4.30. A concentration of 5.6 g L^{-1} (or 2.28 mM, based on the theoretical molar mass of this quaternized copolymer, 2460 g mol^{-1}) was used since, at this concentration, the Laponite surface is saturated with the copolymer and there are some free chains in the aqueous phase to stabilize the nanocomposite latex particles.

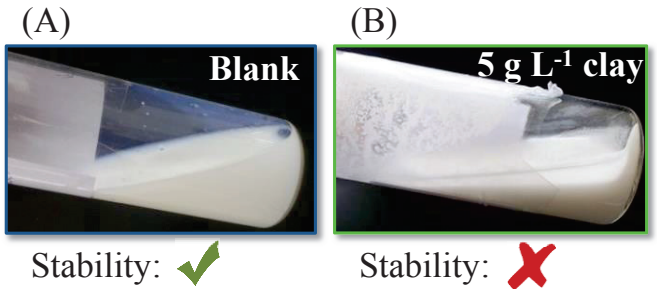
Figure 4.30 – (A) Adsorption isotherm of P(qDMAEMA$_{10}$-*co*-BA$_4$)-CTPPA (MR11q) onto Laponite 5 g L^{-1} and (B) evolution of the average hydrodynamic diameters and poly value of macroRAFT-modified Laponite platelets with macroRAFT concentration.



Source: elaborated by the author.

For this experiment (R10A), a final conversion of 75% was achieved after 6 hours of polymerization, however, the latex presented poor colloidal stability since the very early stages of polymerization. This polymerization was repeated under the same conditions but in the absence of Laponite (blank experiment, R10B) and 76% conversion was achieved, with good colloidal stability ($Z_{av.}$ = 144 nm and poly value = 0.01), as shown in Figure 4.31.

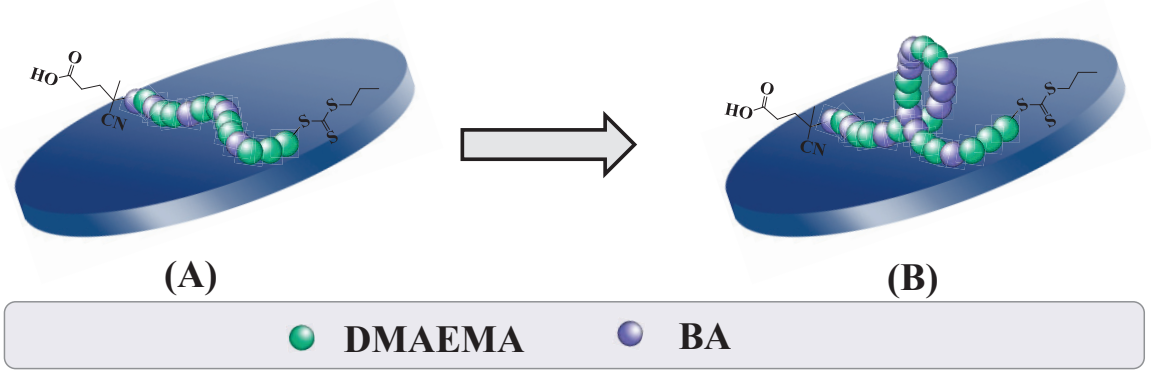
Figure 4.31 – Final latexes obtained via copolymerization of MMA with BA (90:10 mol%) using P(qDMAEMA$_{10}$-*co*-BA$_4$)-CTPPA macroRAFT agent (MR11q) (A) in the absence of clay (blank) and (B) in the presence of 5 g L^{-1} of Laponite (or 5 wt%, based on total mass of monomer).



Source: elaborated by the author.

It has been discussed in Chapter 3 that short cationic polymer chains are more prone to adsorb onto Laponite in a flat extended configuration. In this situation, it is very likely that the adsorbate will not be able to stabilize the nanocomposite latex particles and, if the concentration of macroRAFT agents in the aqueous phase is insufficient to provide additional stability to these particles, aggregation may occur. In this aspect, the use of longer, less charged (highly charged molecules tend to be disposed in an extended configuration due to intramolecular repulsive interactions) and more flexible (softer) copolymer chains can be more interesting since they allow the formation of loops and tails along the chain, as illustrated in Figure 4.32, which are essential for stabilizing the particles. For this reason, the macroRAFT agent P(qDMAEMA$_{19}$-*co*-BA$_{14}$)-CTPPA was designed as an alternative to overcome the stability issues caused by the use of P(qDMAEMA$_{10}$-*co*-BA$_4$)-CTPPA.

Figure 4.32 – Schematic representation of Laponite platelets with adsorbed macroRAFT agents (A) P(qDMAEMA$_{10}$-*co*-BA$_4$)-CTPPA (MR11) in an extended configuration and (B) P(qDMAEMA$_{19}$-*co*-BA$_{14}$)-CTPPA (MR12) in a non-extended configuration containing loops and tails.

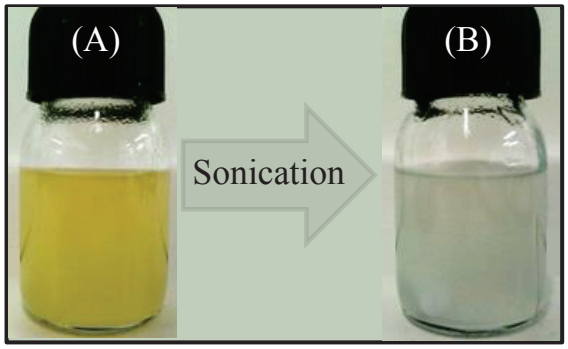


Source: elaborated by the author.

4.4.11 Synthesis of hybrid latexes in the presence of P(qDMAEMA$_{19}$-*co*-BA$_{14}$)-CTPPA

For the P(DMAEMA$_{19}$-*co*-BA$_{14}$)-CTPPA-mediated synthesis of polymer/Laponite hybrid latexes, the quaternized copolymer was initially preferred over the non-modified molecule, for the same reason elucidated in the previous item. However, all attempts to use the quaternized molecule resulted in a significant loss of the dispersion color, as shown in Figure 4.33, either during the five-minute sonication pre-polymerization process, performed at 30% amplitude, or as soon as the dispersion was submitted to the heating process, at 80 ºC, to start polymerization. The yellowish tone is very typical of CTPPA RAFT agent and, it could be presumable that the quaternization process with methyl iodide might have affected the double bond of this macroRAFT agent, since higher amount of methyl iodide was necessary for this copolymer, specifically. As the copolymer was not purified after quaternization, the possible double bond degradation could have been caused by residual methyl iodide under strong experimental conditions (sonication and heating).

Figure 4.33 – Colloidal suspension of P(qDMAEMA$_{19}$-*co*-BA$_{14}$)-CTPPA (MR12q) with Laponite 5 g L^{-1} (A) before and (B) after a five-minute sonication process, at 30% amplitude.



Source: elaborated by the author.

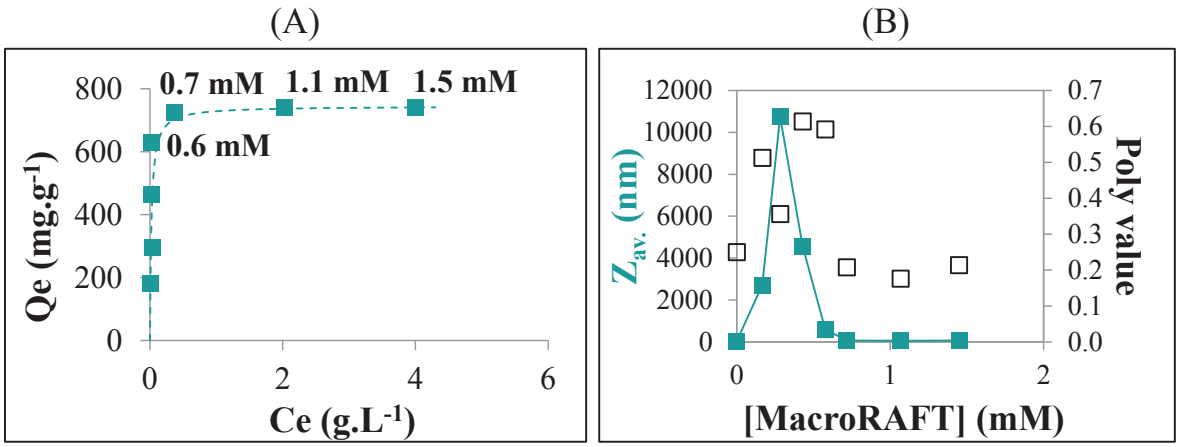
The next experiments were therefore, carried out with unquaternized P(DMAEMA$_{19}$-*co*-BA$_{14}$)-CTPPA. It is known that, especially at high pH values, primary amidine groups may suffer hydrolysis during the homolysis of AIBA. For this reason, the pH of the media was carefully selected and adjusted since the hydrolysis process can be minimized if this key parameter is maintained below 7.[106] Thus, polymerizations that had AIBA as initiator were carried out at pH 6. In fact, at this pH value DMAEMA-based CTA is protonated and, in addition, as seen by the pH scan carried out for the adsorption study, shown in Chapter 3, this pH value is ideal for DMAEMA-containing systems.

The following parameters were studied: macroRAFT concentration, monomer composition (in order to obtain film-forming latexes), initiator, clay content and temperature.

4.4.11.1 Effect of macroRAFT concentration

The macroRAFT agent concentration was selected based on the adsorption isotherm of this copolymer onto Laponite, shown in Figure 4.34 (and already shown in Chapter 3). It can be seen in the adsorption isotherm that at a concentration of 0.7 mM of macroRAFT, the surface of Laponite is saturated and maximum adsorption has been reached. However, at this concentration, the amount of macroRAFT that is free in the aqueous phase is likely to be insufficient to provide stability to the system, so four concentrations of P(DMAEMA$_{19}$-*co*-BA$_{14}$)-CTPPA were studied in the synthesis of hybrid latexes. Experiments were carried out in the presence of: 1.1 mM of macroRAFT; 1.5 mM, which is the concentration that corresponds to the last point of the isotherm; 2.2 mM, which is an extrapolation of the isotherm and is the typical concentration that has been used in this work for the other macroRAFT agents; and finally, in the absence of macroRAFT agent.

Figure 4.34 – (A) Adsorption isotherm of P(DMAEMA$_{19}$-*co*-BA$_{14}$)-CTPPA onto Laponite (5 g L^{-1}) at pH 6 and (B) evolution of the average hydrodynamic diameters (full symbols) and poly value (open symbols) with macroRAFT concentration.



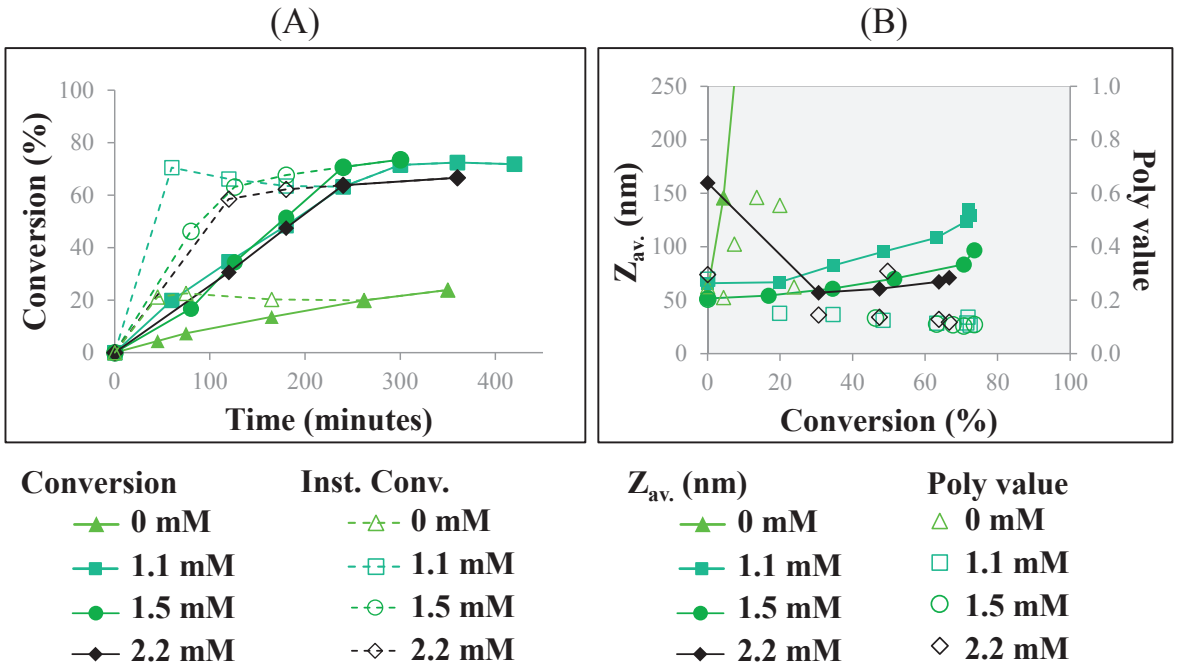
Source: elaborated by the author.

The use of P(DMAEMA$_{19}$-*co*-BA$_{14}$)-CTPPA macroRAFT agent at pH 6 led to the production of stable nanocomposite latexes. The evolution of overall and instantaneous conversions versus time is shown in Figure 4.35A. It is possible to observe that there is no significant difference in the conversion profile of the curves for all macroRAFT

concentrations, except for the experiment carried out in the absence of macroRAFT. However, the low conversions obtained for this experiment cannot be considered as a reliable result, as the high instability of the system, and the formation of aggregates, prejudiced the samples withdrawn.

Despite the good stability provided by different concentrations of cationic macroRAFT agent, it can be observed that limiting values of conversion (between 67 and 74%) were obtained. Even though the polymerization system (reactor and reflux condenser) was carefully checked for possible monomer loss during the reactions, the emulsion polymerizations mediated by most of the macroRAFT agents used in this work seem to always reach a limiting conversion of ~70%, which is usually not considered as a high value of conversion. We will come back to this point later in the discussion.

Figure 4.35 – (A) Overall monomer conversion (straight line) and instantaneous conversion (hashed line) versus time and (B) evolution of the average hydrodynamic diameters and poly value versus conversion for the polymerization of MMA:BA 90:10 in the presence of 0 mM, 1.1 mM, 1.5 mM and 2.2 mM of P(DMAEMA$_{19}$-*co*-BA$_{14}$)-CTPPA macroRAFT agent and 5 g L^{-1} of Laponite at 80°C and pH 6.



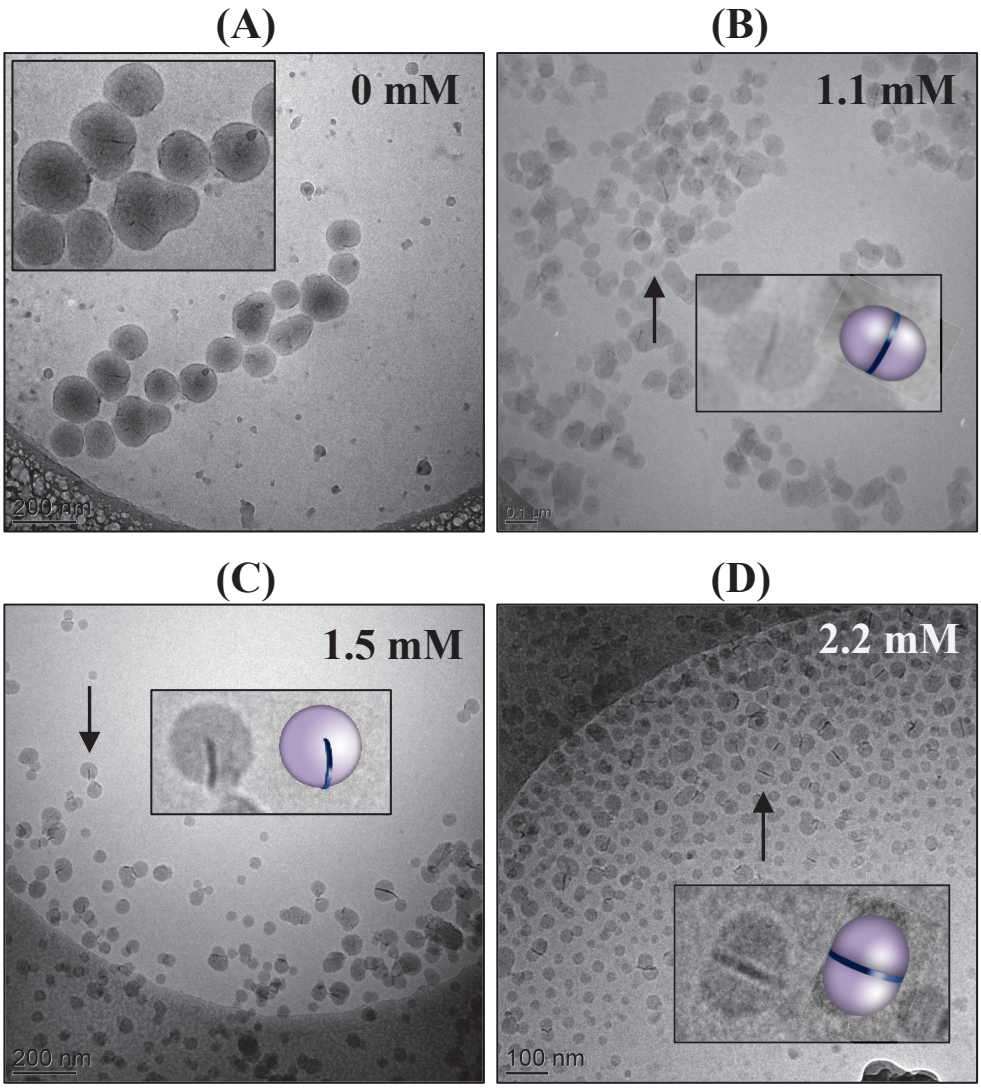
Source: elaborated by the author.

Concerning the evolution of particle sizes, it is possible to see a significant difference between the experiments carried out with 1.1 and 2.2mM of macroRAFT. The higher macroRAFT concentration led to lower particle size values. However, if we take a look at the initial values of $Z_{av.}$ for all CTA concentrations, we can observe the formation of

aggregates ($Z_{av.}$ ~150 nm) when macroRAFT/Laponite dispersions are produced using higher CTA concentration. Despite the strong interaction between clay and CTA, it is presumable that disaggregation occurs, since a significant decrease on particle size and poly value is observed during polymerization.

Cryo-TEM images of these latexes are shown in Figure 4.36 and, even though the latex synthesized in the absence of macroRAFT was unstable (R11.1A), indicating the formation of big aggregated particles, only non-spherical clay-containing latex particles of around 200 nm in diameter can be seen on the image of Figure 4.36A. The destabilization of the system could be explained by an initial destabilization of clay platelets upon addition of the initiator (AIBA) which can adsorb on the clay surface through cation exchange and neutralize the surface charges of Laponite. In addition, it is possible that the positively charged oligomers grown from or adsorbing on the clay surface during polymerization convert the clay from hydrophilic to hydrophobic and, as there is no surfactant in the system, at some point the formed particles should get destabilized. Laponite platelets can be seen either buried inside these aggregated particles or located outside, at the particles surface. In the presence of 1.1 mM of macroRAFT agent (Figure 4.36B, R11.1B), stable dumbbell-like particles (135 nm) were obtained. Similar morphology was obtained with 1.5 mM of macroRAFT (R11.1C), however, particles seemed (from the cryo-TEM images) to be less vulnerable to agglomeration in this case and several Laponite platelets can be seen almost fully covered with polymer, with only one of the extremities uncovered. When macroRAFT concentration was increased to 2.2 mM (R11.1D), the major part of the particles presented a dumbbell-like morphology, but it seems that at a higher macroRAFT concentration, more free latex particles (smaller than the hybrid ones) were obtained.

Figure 4.36 – Cryo-TEM images of hybrid particles obtained by the copolymerization of MMA:BA 90:10 in the presence of (A) 0 mM, (B) 1.1 mM, (C) 1.5 mM and (D) 2.2 mM of P(DMAEMA$_{19}$-*co*-BA$_{14}$)-CTPPA macroRAFT agent and 5 g L^{-1} of Laponite at 80°C and pH 6.



Source: elaborated by the author.

4.4.11.2 Effect of monomer composition

To evaluate the effect of the monomer mixture composition, the macroRAFT concentration was fixed at 1.5 mM. The purpose of this study was to migrate from a non-film-forming monomer composition to an adequate film-forming mixture, so different monomer compositions were tested. In addition to the non-film-forming mixture MMA:BA 90:10, two mixtures richer in BA and that are capable of forming film at room temperature were evaluated, MMA:BA 50:50 and Sty:BA 50:50. A more hydrophilic film-forming monomer mixture was tested as well, the MA:BA 80:20, as listed in Table 4.3.

Table 4.3 – Glass transition temperature (T_g) and solubility in water of the monomers and monomer mixtures used in the synthesis of hybrid latexes by RAFT mediated emulsion polymerization in the presence of P(DMAEMA$_{19}$-*co*-BA$_{14}$)-CTPPA macroRAFT agent.

Monomer mixture m_1/m_2	$T_{g,1}/T_{g,2}$ (K) [a]	Solubility in water (wt%) [b]	Mixture (mol%)	Tg (°C) [c]	Entry#
MMA / BA	368 / 208	1.59 / 0.14	90 / 10	72	R11.1C
			50 / 50	-7	R11.2A
Sty / BA	368 / 208	0.02 / 0.14	50 / 50	-7	R11.2B
MA / BA	281 / 208	6.0 / 0.14	80 / 20	-7	R11.2C

Fox equation

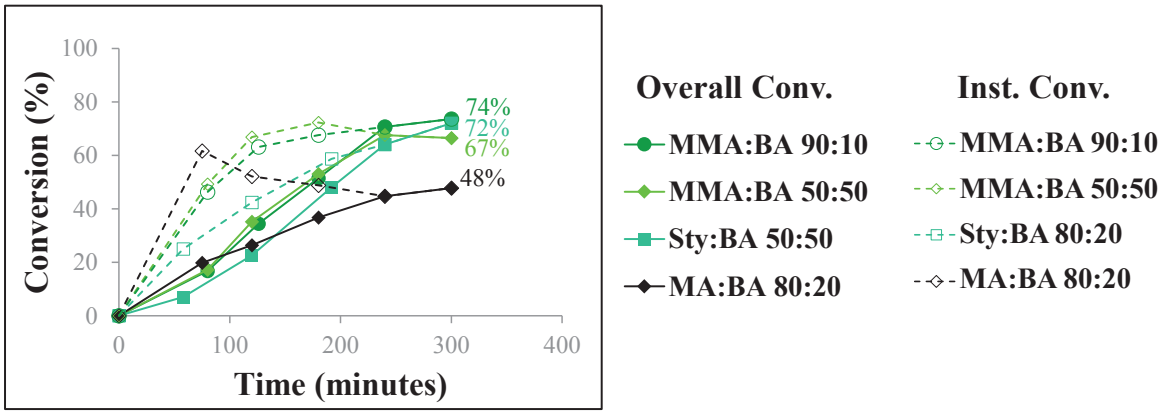
$$\frac{1}{T_g} = \frac{w_{m1}}{T_{g,m1}} + \frac{w_{m2}}{T_{g,m2}}$$

w_{m1} and w_{m2} = weight fraction of monomers m1 and m2
$T_{g,m1}$ and $T_{g,m2}$ = Tg of homopolymers composed of monomers m1 and m2 (K)

[a] Tg of the resulting homopolymers formed by the repeating units m1 and m2.[107]
[b] Solubility (wt%) of monomers m1 and m2 in water at 25 ºC.[108, 109]
[c] Tg of the copolymers calculated according to the Fox equation.
Source: elaborated by the author.

Kinetic results are shown in Figure 4.37. It can be seen that a low conversion was obtained for the film-forming acrylate-based monomer mixture of R11.2C (MA:BA 80:20; X = 48%). For the MMA:BA and Sty:BA film-forming mixtures, conversions were, respectively 67 and 72%, while 74% conversion was achieved for the MMA:BA 90:10 mixture (R11.1C).

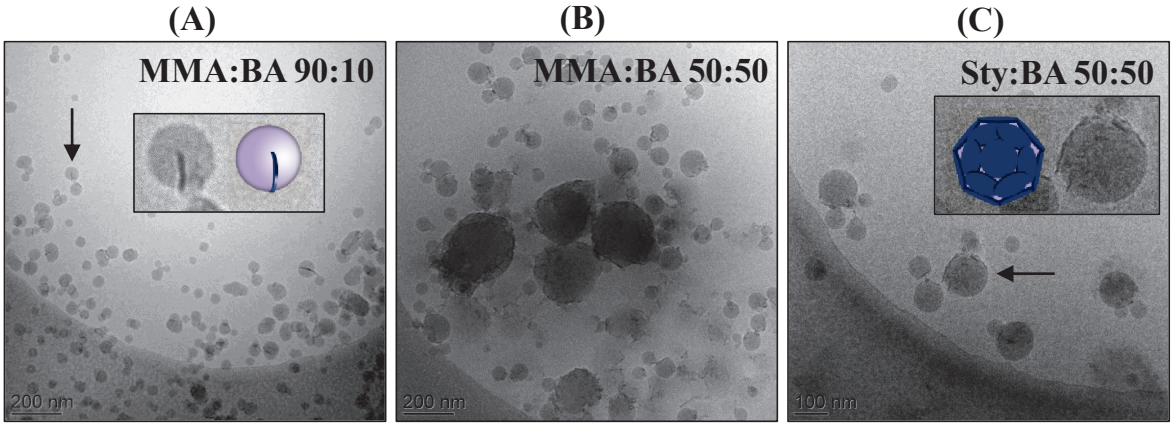
Figure 4.37 – Overall monomer conversion (straight line) and instantaneous conversion (hashed line) versus time for the polymerization of MMA:BA 90:10 (R11.1C), MMA:BA 50:50 (R11.2A), Sty:BA 50:50 (R11.2B) and MA:BA 80:20 (R11.2C) in the presence of 1.5 mM of macroRAFT agent and 5 g L^{-1} of Laponite at 80°C and pH 6.



Source: elaborated by the author.

Due to the conversion obtained in the experiment with MA:BA 80:20 (lower than 50%), some experiments were carried out as an attempt to increase the conversion with this monomer mixture (as shown in the following sections) before the imaging of the sample by cryo-TEM. Figure 4.38 shows, therefore, the cryo-TEM images of the latexes R11.1C, R12.1A and R12.1B. The images indicate that, for the film-forming mixtures MMA:BA 50:50 (R11.2A) and Sty:BA 50:50 (R11.2B), similar results were obtained in terms of particle morphology, with the formation of large armored particles. The effect of monomer composition seems to be in agreement with what has been reported in the literature. When the T_g of the polymeric shell is low, inorganics tend to migrate to the polymer/water interface during polymerization, searching a thermodynamically-favored morphology.

Figure 4.38 – Cryo-TEM images of hybrid particles obtained by the copolymerization of (A) MMA:BA 90:10 (R11.1C), (B) MMA:BA 50:50 (R11.2A) and (C) Sty:BA 50:50 (R11.2B) in the presence of 1.5 mM of P(DMAEMA19-co-BA14)-CTPPA macroRAFT agent and 5 g L-1 of Laponite at 80°C and pH 6.

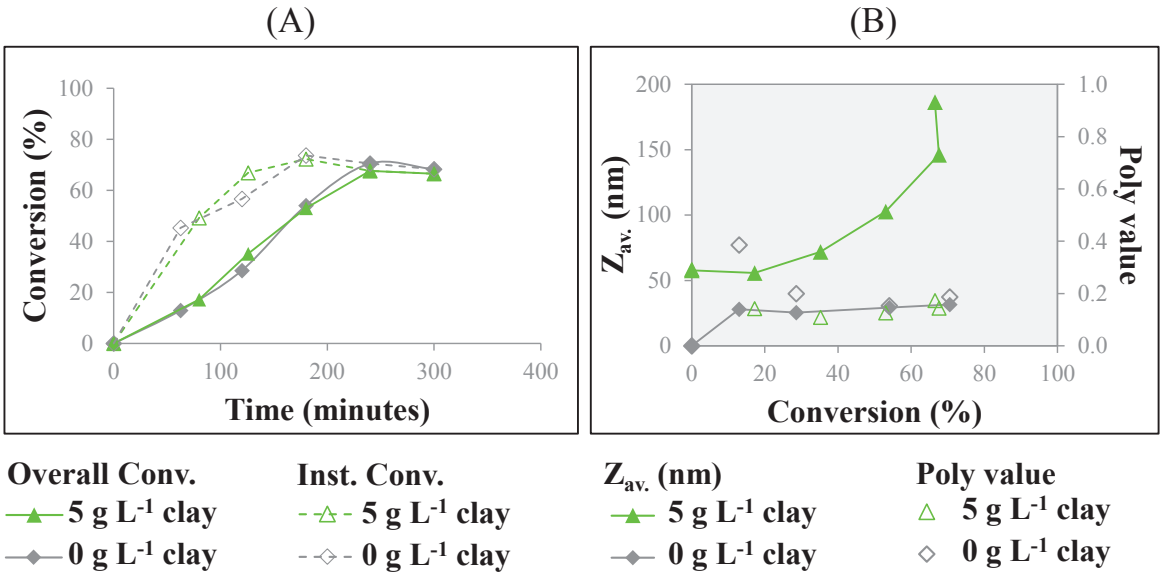


Source: elaborated by the author.

The increase in particle size, observed for the film-forming monomer mixtures R11.2A and R11.2B, could be explained by the effect of the T_g of the copolymers, as well. As clays migrate to the polymer/water interface, the macroRAFT agents become, possibly, no longer exposed to the aqueous phase and, at some point, the particles lose colloidal stability, generating large armored particles. The loss of colloidal stability could happen either during the nucleation stage, which can be similar for the film-forming monomer mixtures and for the copolymers with high T_g (resulting in dumbbell-shaped particles), or after nucleation, if we consider that the morphology of the nucleated particles is affected by the T_g of the copolymer.

It is also possible that the particles formed initially with the film-forming mixtures are less stable (compared to the high T_g formulation) simply because they are soft particles. So, a blank experiment was carried out to verify the particle size evolution in the film-forming formulation MMA:BA 50:50 in the absence of clay (R11.2D) Results are shown in Figure 4.39.

Figure 4.39 – (A) Evolution of overall monomer conversion (full line) and instantaneous conversion (dashed line) with time and (B) evolution of the average hydrodynamic diameters and poly value with conversion during the synthesis of P(MMA-*co*-BA) by RAFT-mediated emulsion polymerization using P(DMAEMA$_{19}$-*co*-BA$_{14}$)-CTPPA with a 50:50 molar composition of MMA:BA monomers in the presence of 5 g L^{-1} of Laponite (R11.2A) and in the absence of the clay (R11.2D).



Source: elaborated by the author.

A comparison between both experiments indicate similar results in terms of overall and instantaneous conversions, however, the polymerization carried out in the absence of clay presented a different profile of particle size evolution. These results suggest a different nucleation mechanism between the experiments with film-forming and non-film-forming monomer mixtures and contradict the hypothesis that the lack of stability of the initial hybrid particles is caused by the soft character of the copolymers. The formation of larger particles for experiments carried out with the film-forming monomer composition in the presence of clay platelets could be a consequence, therefore, of the more hydrophobic nature of this composition and of the reduced availability that the macroRAFT copolymers present in nanocomposite particles, since part of the copolymer chains is adsorbed on the inorganic surface and fewer molecules are free to stabilize the growing hydrophobic particles (which

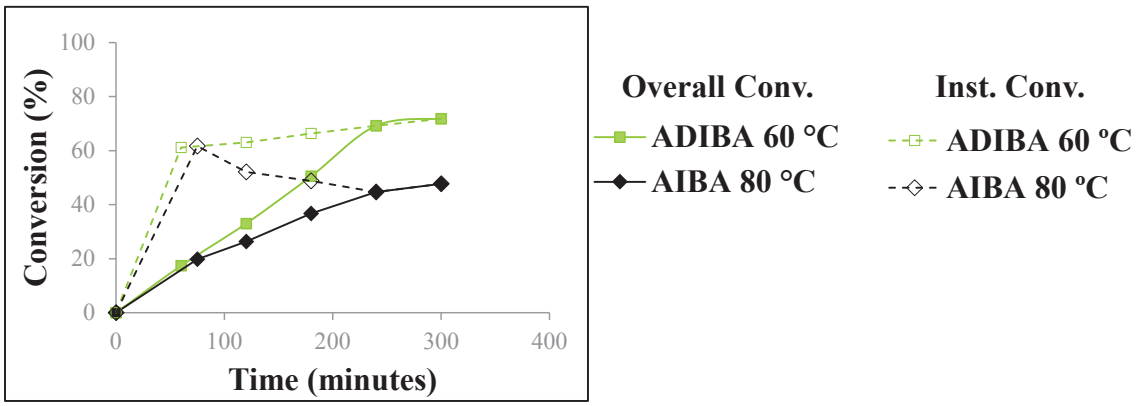
is not the case in the absence of clay). A comparison with the MA:BA 80:20 monomer mixture support this hypothesis, since stable nanocomposite latex particles were obtained with this more hydrophilic monomer mixture.

Nonetheless, to confirm this hypothesis, it can be fundamental to evaluate the copolymerization of the more hydrophilic film-forming mixture with MA and BA. Since a low conversion was obtained for this experiment (R11.2C, MA:BA 80:20, X = 48%), the effect of the initiator was studied as an attempt to improve conversion for this polymerization in particular.

4.4.11.3 Effect of the nature of the initiator

The low conversion obtained in the copolymerization of the more hydrophilic film-forming mixture with MA and BA can be attributed to monomer evaporation, which may happen through the condenser and is more critical in the film-forming monomer mixture composed of MA, since this monomer has a lower boiling point (80 °C) than MMA (101 °C). As the initiator ADIBA has a half-life decomposition time in water, at 80°C, nearly 3 times lower than AIBA,[106] it was used to replace AIBA in the emulsion polymerizations, giving the possibility to reduce the reaction temperature. Besides, ADIBA is more pH tolerant than AIBA, as it does not suffer hydrolysis even at high pH values (even though the pH of the reaction medium was adjusted at the beginning of polymerization to avoid hydrolysis of the amidine groups from the initiator, this precaution was not enough to maintain the pH sufficiently low during the rest of the polymerization in order to avoid these undesired reactions, and a slight pH increase was observed after polymerizations started). So, the emulsion polymerization carried out with the MA:BA film-forming monomer mixture, which presented an unsatisfactory conversion, was repeated with ADIBA replacing AIBA, at 60 ºC (R11.3A). Results obtained for this experiment, shown in Figure 4.40, indicate that, while a final conversion of 48% was achieved for the polymerization initiated by AIBA (R11.2C), a final conversion of 72% was obtained when ADIBA was used as initiator (R11.3A), which supports the above-mentioned assumptions.

Figure 4.40 – Overall monomer conversion (straight line) and instantaneous conversion (hashed line) versus time for the polymerization of MA:BA 80:20 in the presence of 1.5 mM of P(DMAEMA$_{19}$-*co*-BA$_{14}$)-CTPPA macroRAFT agent, 5 g L^{-1} of Laponite and different initiators: AIBA at 80°C (R11.2C) and ADIBA at 60°C (R11.3A).

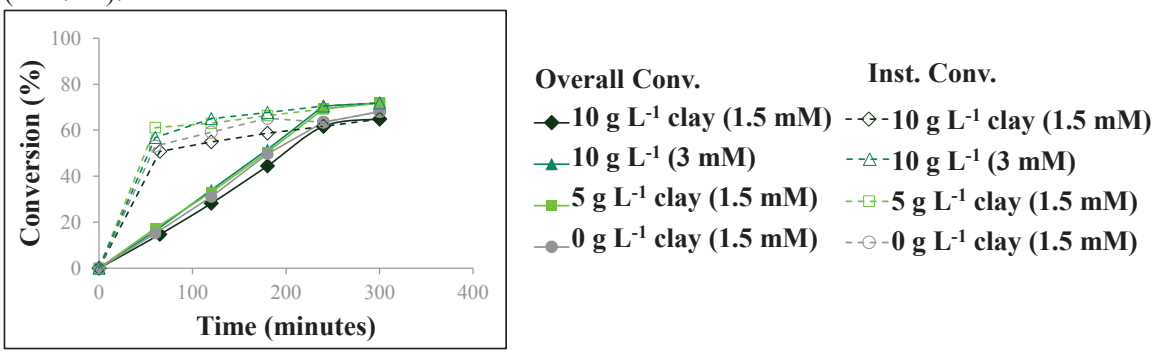


Source: elaborated by the author.

4.4.11.4 Effect of clay content

To study the effect of the clay content in the polymerization and in the formation of the hybrid particles, three different systems were compared to the basic formulation containing 5 g L^{-1} of Laponite (which also represents 5% weight of clay, based on the monomer mass), 1.5 mM of macroRAFT agent and using the film-forming formulation with MA and BA (R11.3A). A blank experiment was carried out in the absence of clay (R11.4A) and two experiments were carried out increasing the Laponite content to 10 g L^{-1}, with two different macroRAFT concentrations: 1.5 (R11.4B) and 3 mM (R11.4C). All polymerizations were initiated by ADIBA. Results, shown in Figure 4.41 indicate that very similar conversion profiles were obtained for all experiments.

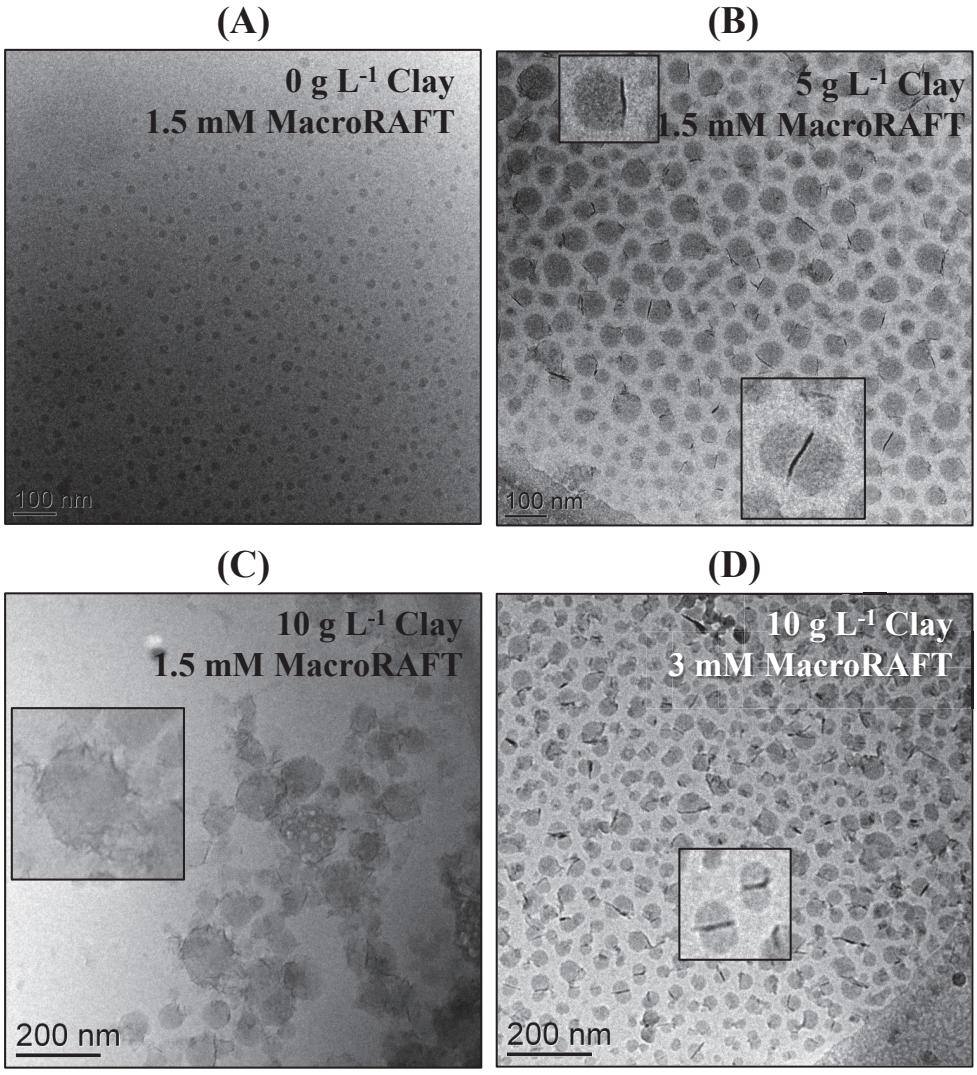
Figure 4.41 – Overall monomer conversion (straight line) and instantaneous conversion (hashed line) versus time for the copolymerization of MA:BA 80:20 using ADIBA as initiator at 60°C in the presence of 1.5 mM of P(DMAEMA$_{19}$-*co*-BA$_{14}$)-CTPPA macroRAFT agent and 10 g L^{-1} of Laponite (R11.4B); 3 mM of macroRAFT agent and 10 g L^{-1} of Laponite (R11.4C); 1.5 mM of macroRAFT agent and 5 g L^{-1} of Laponite (R11.3C) and 1.5 mM of macroRAFT agent and 0 g L^{-1} of Laponite (R11.4A).



Source: elaborated by the author.

Cryo-TEM images of the latexes are shown in Figure 4.42. A comparison between images (A), (B) and (C), which correspond respectively to 0, 5 and 10 g L^{-1} of Laponite, and with a fixed macroRAFT concentration of 1.5 mM, reveals that the variation in the clay content results in a clear change in the particles size. While very small particles (~20nm) were obtained in the absence of clay, hybrid particles with dumbbell morphology of around 110 nm were formed in the presence of 5 g L^{-1} of Laponite, which might indicate that the platelets play a crucial role in the mechanism of particle formation. However, if the clay content is increased to 10 g L^{-1}, 1.5 mM of macroRAFT is no longer enough to provide stability to the growing particles and they aggregate forming armored structures. If we consider a competition between the CTA and the clay in the stabilization of the system, these results are interesting and corroborate our first results for armored latexes. An equivalent amount of macroRAFT (3mM) was used to guarantee the stabilization of particles in the presence of 10 g L^{-1} of Laponite, as shown in Figure 4.42D. In this case, the higher amount of macroRAFT adsorbed on the platelets, with Laponite platelets working as an efficient polymerization locus and, therefore, reducing the proportional amount of monomer available to form the polymeric shell around each macroRAFT/Laponite particle, led to the formation of smaller dumbbell particles (~75nm).

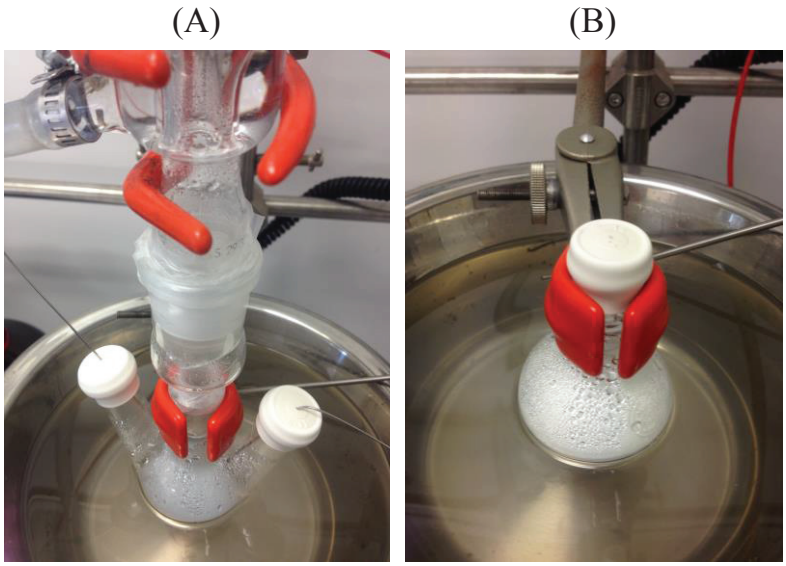
Figure 4.42 – Cryo-TEM images of hybrid particles obtained by the copolymerization of MA:BA 80:20 using ADIBA as initiator at 60°C in the presence and of (A) 1.5 mM of P(DMAEMA$_{19}$-*co*-BA$_{14}$)-CTPPA macroRAFT agent and 0% Laponite (B) 1.5 mM of macroRAFT agent and 5 g L^{-1} of Laponite; (C) 1.5 mM of macroRAFT agent and 10 g L^{-1} of Laponite and (d) 3 mM of macroRAFT agent and 10 g L^{-1} of Laponite.



Source: elaborated by the author.

But again, experiments were still trapped in ~70% limiting conversions. These low conversions could be attributed to the use of a deficient reaction system (reactor + condenser) that might facilitate monomer evaporation and, as already mentioned before, this evaporation is more critical in the film-forming monomer mixture composed of MA. It can be seen in Figure 4.43A that drops of water and, possibly, MA are condensed in the connection adapter and in the lower part of the reflux condenser. So, to prove this hypothesis, the polymerization was repeated using a one-neck flask, without the reflux condenser (R11.4D), as shown in Figure 4.43B.

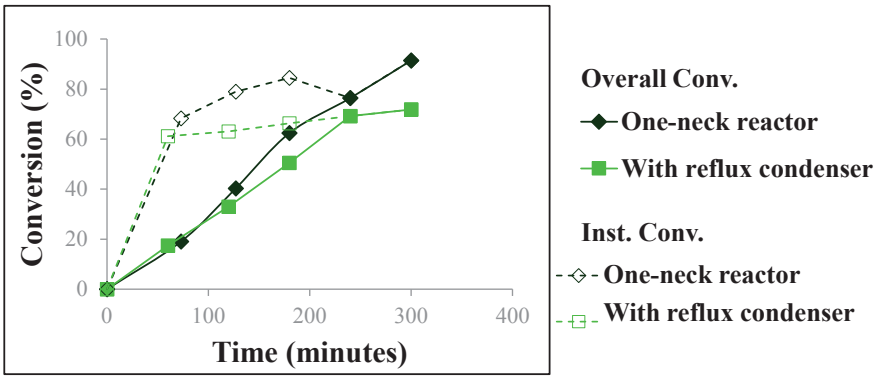
Figure 4.43 – Reactors used in the emulsion polymerization of MA:BA 80:20 in the presence of 1.5 mM of P(DMAEMA$_{19}$-*co*-BA$_{14}$)-CTPPA macroRAFT agent, 5 g L^{-1} of Laponite and ADIBA at 60°C.



Source: elaborated by the author.

The results, shown in Figure 4.44, indicate that higher overall and instantaneous conversions were, in fact, obtained when the reflux condenser was not used. The use of a simpler system (Figure 4.43B) resulted in an overall conversion of 91%, while only 72% was achieved with the reflux condenser (R11.2C). This result proves that a significant part of the monomer mixture is lost by evaporation or is condensed along the condenser walls.

Figure 4.44 – Overall monomer conversion (straight line) and instantaneous conversion (hashed line) versus time for the copolymerization of MA:BA 80:20 using ADIBA as initiator at 60°C and in the presence of 1.5 mM of P(DMAEMA$_{19}$-*co*-BA$_{14}$)-CTPPA macroRAFT agent and 5 g L^{-1} of Laponite using three-neck reactor with reflux condenser (R11.2C) and one-neck reactor (R11.4D).



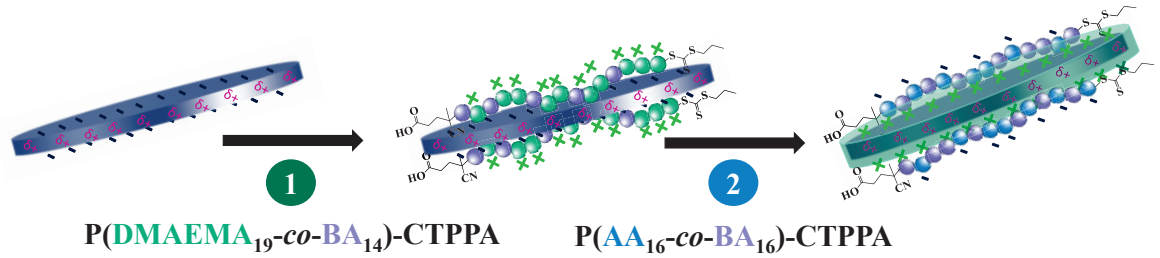
Source: elaborated by the author.

4.4.12 Layer-by-layer technique

As the previous conditions used to synthesize polymer/Laponite nanocomposite latex particles did not result in the fully encapsulation of the platelets, and led, instead, mainly to janus and dumbbell-shaped particles, the layer-by-layer technique was evaluated as an attempt to achieve true and uniform encapsulation of Laponite with a film-forming formulation. This approach involved the use of two macroRAFT agents. Initially, Laponite was coated with 0.6 mM of P(DMAEMA$_{19}$-*co*-BA$_{14}$)-CTPPA (MR12) and the pH of the suspension was adjusted to 6 by the addition of HCl. The amount of cationic macroRAFT was selected based on the adsorption isotherm of Figure 4.34. It was considered that, at the selected concentration, the amount of macroRAFT should be enough to change the surface charge of Laponite with minimal formation of aggregates, but it is crucial to guarantee, as well, that this amount is not too large to allow the presence of free molecules in water. A five-minute sonication process (30% amplitude) was necessary to increase the stability of the dispersion due to the low macroRAFT concentration used. A second layer of P(AA$_{16}$-*co*-BA$_{16}$)-CTPPA (MR2, 1.6 mM, also adjusted to the pH of 6 by the addition of NaOH 1N) was, then, added to this suspension and it was, again, sonicated for five minutes.

P(DMAEMA$_{19}$-*co*-BA$_{14}$)-CTPPA was initially used to cause the charge inversion of the surface of the Laponite and facilitate, therefore, the subsequent adsorption of negatively charged P(AA$_{16}$-*co*-BA$_{16}$)-CTPAA onto their surface via electrostatic interactions, as schematically represented in Figure 4.45. The layer-by-layer technique is expected to be less affected by the different rim and surface charges of Laponite, and it also allows the use of the negatively charged macroRAFT copolymer as dispersant, which can potentially adsorb onto the entire platelet.

Figure 4.45 – Schematic representation of the sequential adsorption of macroRAFT copolymers P(DMAEMA$_{19}$-*co*-BA$_{14}$)-CTPPA (layer 1) and P(AA$_{16}$-*co*-BA$_{16}$)-CTPPA (layer 2) at pH 6 onto Laponite platelets to generate a uniformly charged particle.



Source: elaborated by the author.

Three emulsion polymerizations were carried out in the presence of these Laponite platelets modified by the layer-by-layer technique, as listed in Table 4.4. As the general formulation used in experiment R12A, with a monomer addition time of 4 hours, presented stability problems, it was, initially, repeated under the same conditions but the reaction was stopped after 2 hours of polymerization, before the loss of stability, which led to lower solids content (R12B). In a second attempt, R12A was repeated increasing the concentration of P(AA_{16}-*co*-BA_{16})-CTPPA macroRAFT agent from 1.6 to 2.2 mM (R12C).

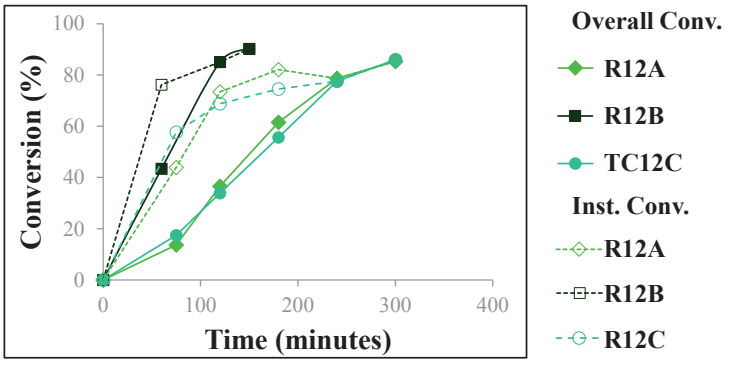
Table 4.4– Type of macroRAFT agent used and monomer addition time (at 0.6 mL/h) during experiments R12A, R12B and R12C.

Entry#	Monomer addition time (h)	[P(AA_{16}-*co*-BA_{16})-CTPPA] (mM)
R12A	4	1.6
R12B	2	1.6
R12C	4	2.2

Source: elaborated by the author.

Results, shown in Figure 4.46, indicate that different conversion profiles were obtained with higher overall and instantaneous conversions for experiment R12B. However, these curves cannot be considered as a reliable result due to the poor stability of the medium that might have led to a heterogeneous and, therefore, not representative, sample withdrawn.

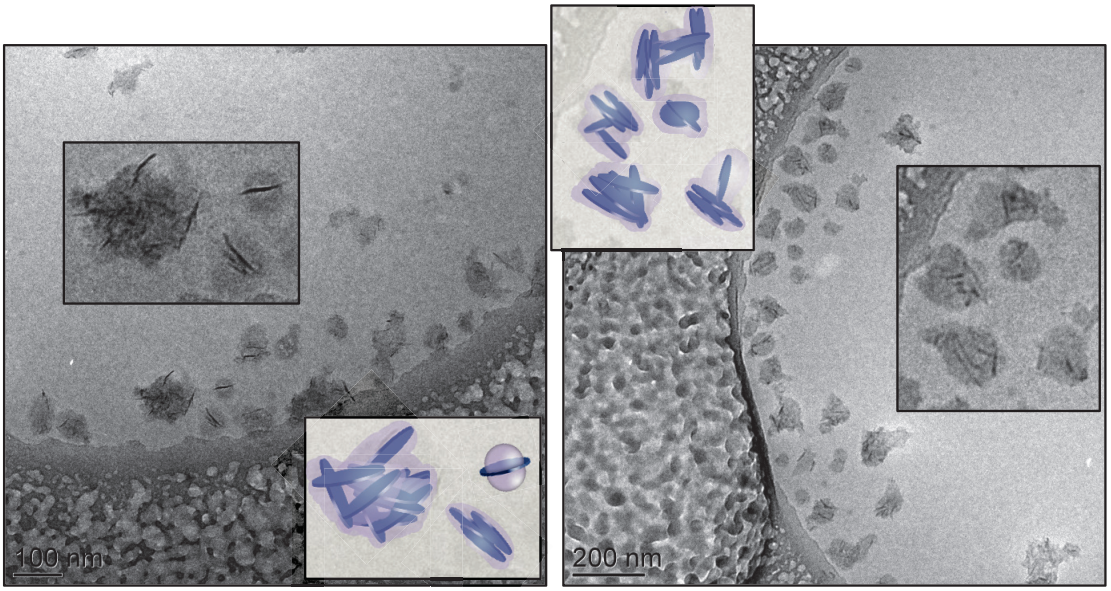
Figure 4.46 – Overall monomer conversion (straight line) and instantaneous conversion (hashed line) versus time for the polymerization of MA:BA 80:20 in the presence of 0.6 mM of P($DMAEMA_{19}$-*co*-BA_{14})-CTPPA and 1.6 mM of P(AA_{16}-*co*-BA_{16})-CTPPA, 5 g L^{-1} of Laponite and initiator ACPA at 80°C.



Source: elaborated by the author.

Experiment R12B (with lower polymer content) was characterized by cryo-TEM and the images are shown in Figure 4.47. It can be seen that the hybrid particles contain multiple platelets inside. When the layer-by-layer technique is compared to the other techniques used in this work, it can be seen that the hybrid particles are less spherical and platelets have a higher tendency to stay inside the polymeric shell. Besides, it seems that the formation of the shell is restricted to the inorganic surface since almost no free polymeric particles are observed, indicating that secondary nucleation was minimal.

Figure 4.47 – Cryo-TEM images of hybrid particles obtained by the copolymerization of MA:BA 80:20 in the presence of ACPA at 60°C and 5 g L^{-1} of Laponite coated with 0.6 mM of P(DMAEMA$_{19}$-*co*-BA$_{14}$)-CTPPA and 1.6 mM of macroRAFT agent P(AA$_{16}$-*co*-BA$_{16}$)-CTPPA, via the layer-by-layer technique (R12B).



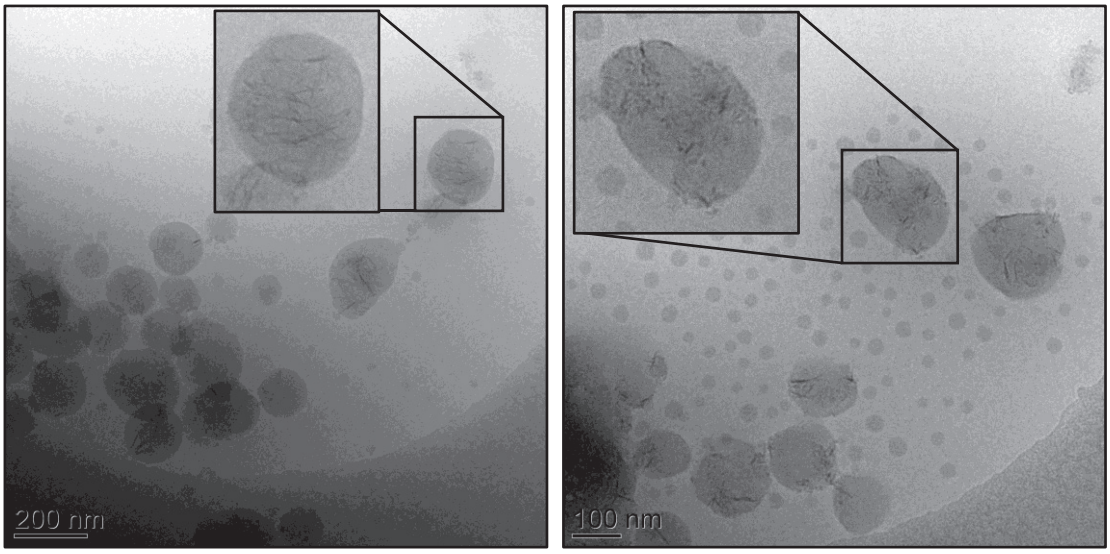
Source: elaborated by the author.

Considering that the multiple encapsulation could be attributed to a possible poor colloidal stability of the clay platelets initial dispersion (that, being unstable, tend to form aggregates), an attempt to improve the dispersion of the macroRAFT/Laponite particles via the layer-by-layer approach was carried out using a higher concentration of P(AA$_{16}$-*co*-BA$_{16}$)-CTPPA. For this experiment (R12C), the conditions were similar to polymerization R12A, but the concentration of the negatively charged macroRAFT agent P(AA$_{16}$-*co*-BA$_{16}$)-CTPPA was increased from 1.6 mM to 2.2 mM.

Micrographs of Figure 4.48 show that, similarly to R12B, Laponite was successfully encapsulated in the polymer particles. However, similarly to sample R12B, each particle contained several platelets. Final latex was, in fact, more stable with 2.2 mM of P(AA$_{16}$-*co*-

BA_{16})-CTPPA than with 1.6 mM of this macroRAFT agent, nonetheless, free polymeric particles can be seen, which indicates that the excess of macroRAFT led to secondary nucleation.

Figure 4.48 – Cryo-TEM images of hybrid particles obtained by the copolymerization of MA:BA 80:20 in the presence of ACPA at 60°C and 5 g L^{-1} of Laponite coated with 0.6 mM of P($DMAEMA_{19}$-*co*-BA_{14})-CTPPA and 2.2 mM of macroRAFT agent P(AA_{16}-*co*-BA_{16})-CTPPA, via the layer-by-layer technique (R12C).



Source: elaborated by the author.

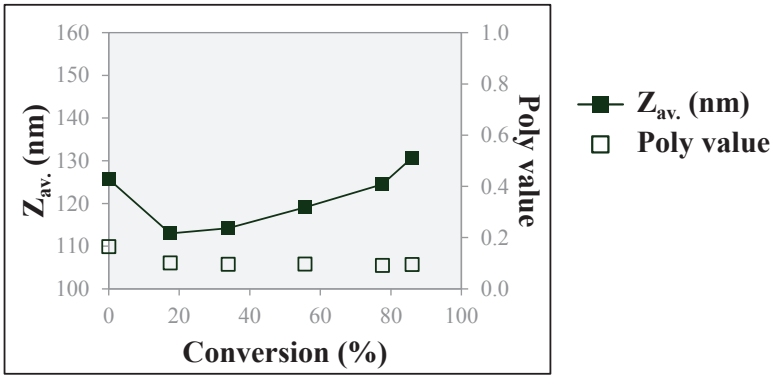
A comparison between the particle sizes of the initial macroRAFT/Laponite dispersion, obtained after the adsorption of the first layer of P($DMAEMA_{19}$-*co*-BA_{14})-CTPPA (93 nm) and of the second dispersion, obtained after the adsorption of the second layer of P(AA_{16}-*co*-BA_{16})-CTPPA (125 nm), indicates that the adsorption of the second layer of P(AA_{16}-*co*-BA_{16})-CTPPA caused a modest increase in particle size. However, the formation of these particles with various encapsulated platelets, instead of individual encapsulation, could be attributed to a possible negative effect that the cationic macroRAFT agent had on the dispersion of the platelets, or it could have been caused by the adsorption of the anionic macroRAFT layer (which could have decreased the stability of the clays before polymerization). Some of the clay platelets modified with different concentrations of P($DMAEMA_{19}$-*co*-BA_{14})-CTPPA at pH 6 were characterized by X-ray diffraction to verify how the presence of the cationic macroRAFT affected the basal spacing of Laponite. In fact, results (Annex 3) indicate that the presence of 0.6 mM of macroRAFT agent caused an increase in the basal spacing of Laponite that suggests that molecules were intercalated. A

similar increase in the basal spacing of Laponite, however, was obtained by higher amounts (1.5 mM) of macroRAFT agent.

The size of the clay clusters (aggregates) of nanocomposite latex R12B is of the same order of magnitude of the diameter determined before polymerization (around 100 nm), which suggests that clay aggregates were already formed before the start of the feeding of the monomer mixture and that polymerization was carried out within these clusters (aggregates), possibly generating sandwiched structures or even tactoids. It is, nevertheless, possible as well that aggregation occurs during polymerization (as the clay is getting buried inside the particles, the stability can be lost).

The evolution of particle size and poly value with conversion (Figure 4.49) show that, as soon as polymerization starts, there is a decrease in particle size, probably due to the formation of small secondary particles. During polymerization, however, particles increase until a final average hydrodynamic diameter of 130 nm.

Figure 4.49 – Evolution of the average hydrodynamic diameters and poly value with conversion for the polymerization of MA:BA 80:20 in the presence of 0.6 mM of P(DMAEMA$_{19}$-*co*-BA$_{14}$)-CTPPA and 2.2 mM of P(AA$_{16}$-*co*-BA$_{16}$)-CTPPA, 5 g L^{-1} of Laponite and initiator ACPA at 80°C.



Source: elaborated by the author.

4.4.13 Mechanical behavior and microstructural characterization of Laponite polymer nanocomposite films

Two nanocomposite latexes synthesized in the presence of P(DMAEMA$_{19}$-*co*-BA$_{14}$)-CTPPA and with different Laponite contents (R11.3A and R11.3C), as well as the corresponding pure polymer counterparts (denominated matrix), were selected for the production of films (by the casting method), for the determination of the thermo-mechanical behavior of the films (by dynamic-mechanical analysis, DMA), and for the investigation of

the microstructure of a 2D cross-section of the material (by FIB-SEM). Some of the characteristics of these latexes are reviewed in Table 4.5.

Table 4.5 – Latex samples selected to be analyzed by DMA.

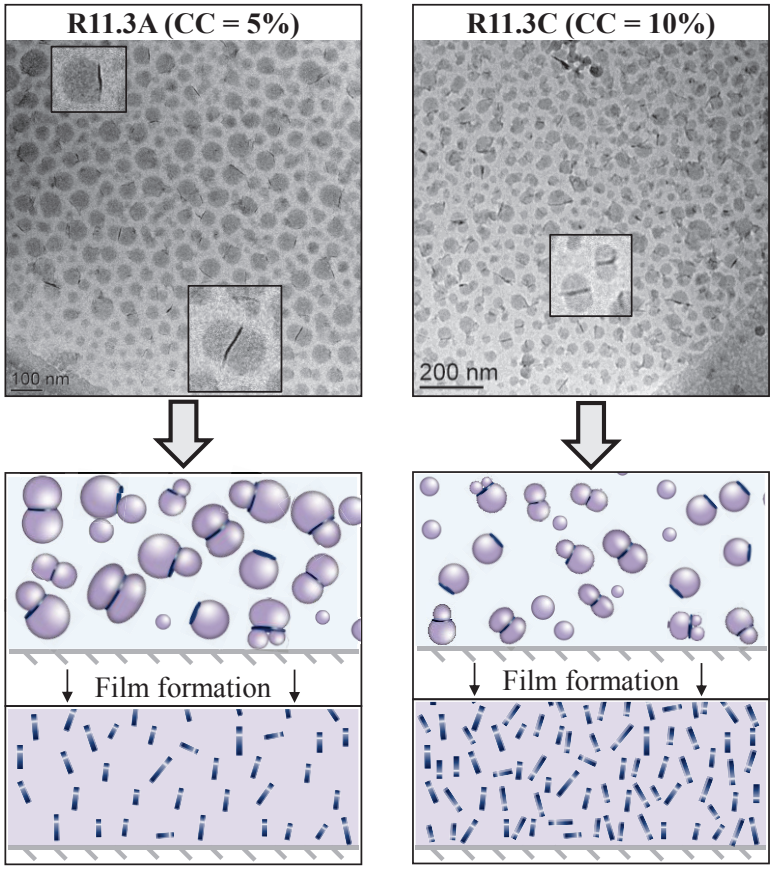
Entry#	CC (wt%)[a]	[MR] (mM)[b]	Monomer mixture (mol:mol)	SC (%)[c]	$Z_{av.}$ (nm)[d]
R11.3A	5	1.5	MA:BA 80:20	8.6	110
R11.3C	10	3.0	MA:BA 80:20	9.4	76

[a] CC = clay content. Weight percentage based on the total mass of polymer.
[b] MR = P(DMAEMA$_{19}$-*co*-BA$_{14}$)-CTPPA
[c] Solids content, measured by gravimetric analysis.
[d] Measured by DLS.
Source: elaborated by the author.

Besides the different clay contents, these latex samples also differ in the macroRAFT concentration. They were selected, mainly, due to the predominating dumbbell morphology of the hybrid particles. In order to give better insights regarding the orientation of the platelets in the nanocomposite film, it could be interesting to obtain quantitative information about the morphologies produced. However, as it can be quite complicated to image Laponite-containing latex particles properly, it can be risky to rely on the determination of the percentages of each morphology by cryo-TEM images and, for this reason, the counting of the particles was not carried out.

As schematically represented in Figure 4.50, such morphologies are expected to, after film forming, give origin to nanocomposite films with a homogeneous distribution (and even a certain organization) of the platelets in the polymer matrix that are likely to present interesting mechanical behaviors.

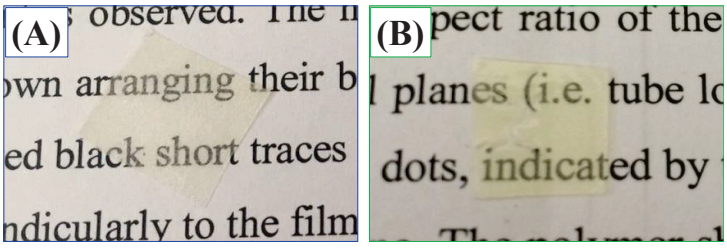
Figure 4.50 – Schematic representation of the expected homogeneous and structured organization of the composite particles obtained after the film-formation process of latexes with different clay contents: R11.3A and R11.3C.



Source: elaborated by the author.

The visual aspect of the final nanocomposite films R11.3A and R11.3C is shown in Figure 4.51. The high transparency of the films can lead to the assumption of a positive uniform distribution of the Laponite platelets within the polymer matrix. It is clear that the film presented a stronger yellowish color at a higher macroRAFT concentration (Figure 4.51B) than at a lower concentration of the RAFT copolymer (Figure 4.51A).

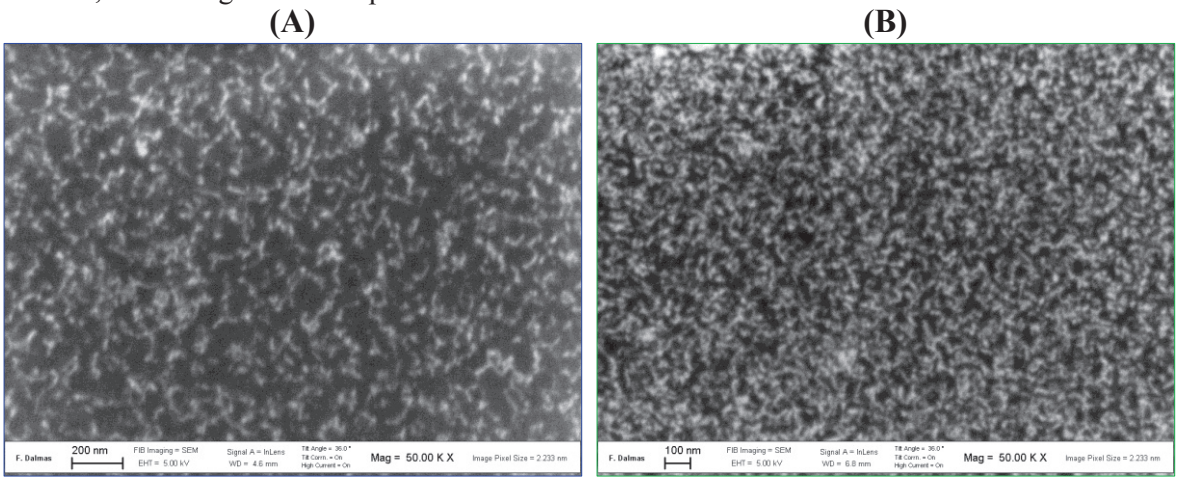
Figure 4.51 – Photographic images illustrating the visual aspect of the films (A) R11.3A and (B) R11.3C.



Source: elaborated by the author.

In order to better understand the effect exerted by Laponite on the final mechanical properties of the films, nanocomposite films had their microstructure investigated by imaging a 2D cross-section of the material via FIB–SEM. Images are shown in Figure 4.52. The different contrasts in the images indicate the presence of Laponite platelets (which are the bright phase) and the polymer matrix (which is the dark background). However, the reduced size of Laponite particles does not allow an individual observation of the platelets. It is possible to see, nonetheless, that there is a homogeneous distribution of the platelets in the polymer matrix, generating, at large scale, a network structure. These connected and homogeneous structures are even more pronounced for the higher clay content (Figure 4.52B).

Figure 4.52 – FIB–SEM observation of samples (A) R11.3A, containing 5 wt% of Laponite and (B) R11.3C, containing 10 wt% Laponite.

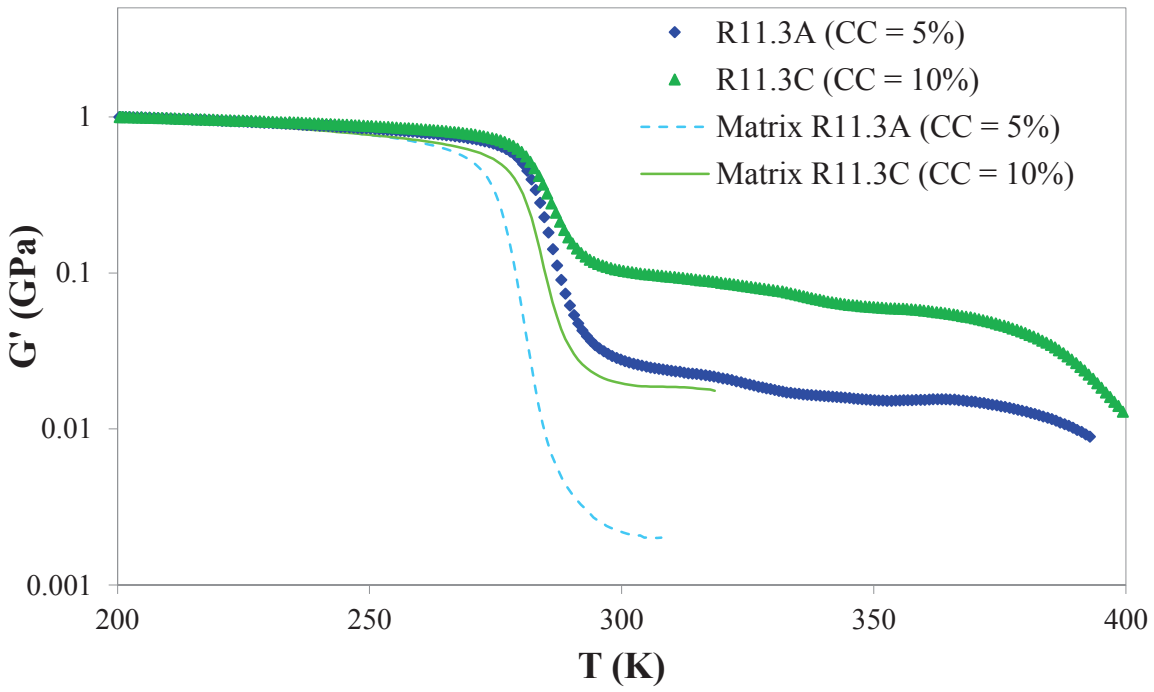


Source: elaborated by the author.

The mechanical behavior of the Laponite-reinforced films, as well as the corresponding pure polymer matrixes, was investigated by DMA and the plotting of the shear storage modulus G′ versus the temperature is shown in Figure 4.53. Due to the large uncertainty on the thickness of such thin film samples (which leads to a three times higher uncertainty on the modulus value), the modulus curves of all samples have been normalized at 1 GPa at 200 K. The expected modulus for the unfilled matrix should, in fact, be around this value, but the filled samples would be expected to have a modulus between 2 and 3 times higher. This error, however, has no consequences on the following discussion, which is based on the modulus value at temperature above that of the main relaxation, as the mechanical contrast between the inorganic particles and the matrix is expected to be of the order of a decade or more.[110] A comparison of the shear storage modulus, G′, between the

matrix and the corresponding nanocomposite in the rubbery plateau shows that there is a stiffening effect due to the presence of the platelets. A long plateau followed by a drop of the modulus at high temperatures, and an increase in modulus of around 10 times the one of the matrix is observed with the addition of 5 wt% of Laponite. Although less abrupt, a similar enhancing effect is observed in the mechanical properties of the material when the nanocomposite is reinforced with 10 wt% of Laponite, as well. This behavior could be attributed to the formation of a stiff layer network in the film, as already reported recently for graphene[111] and layered double hydroxide[110] nanocomposites. The formation of such networks in nanocomposites can be described by the mechanical percolation model,[112, 113] which considers that, in these materials, there is a parallel mechanical coupling of the rigid phase (the platelets) in the soft phase (the polymer matrix).

Figure 4.53 – Storage shear modulus, G′, as a function of temperature for the Laponite nanocomposite films and for the correspondent unfilled matrix.



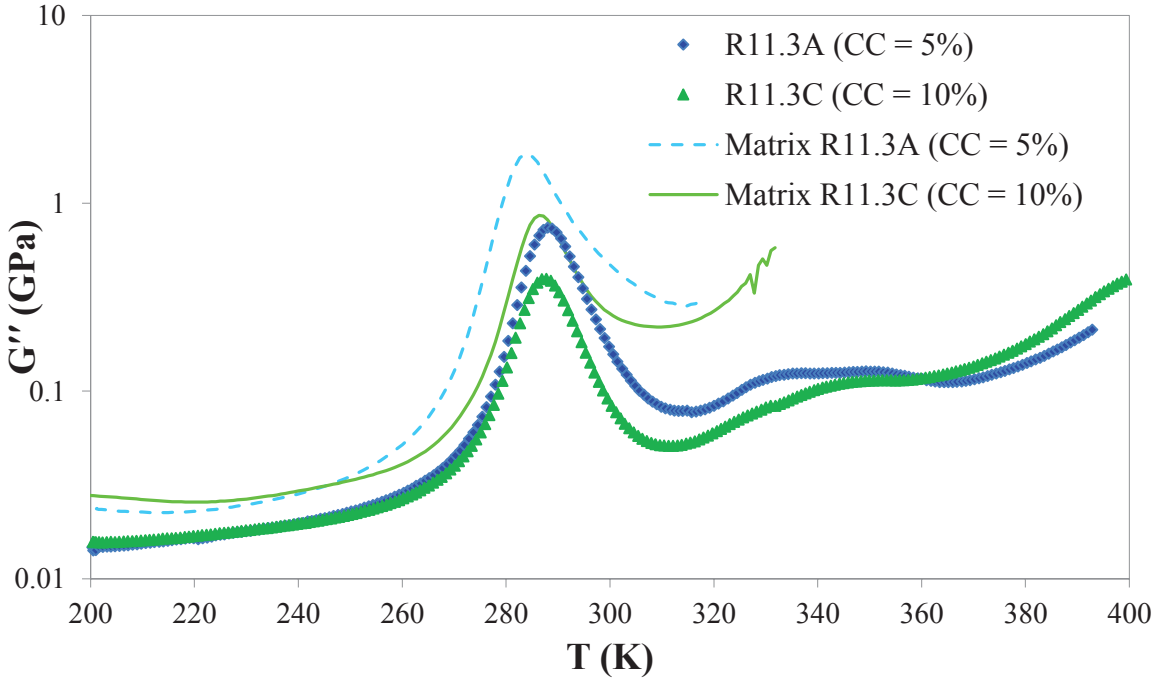
Source: elaborated by the author.

Regarding the behavior of the matrix, it is interesting to observe, that an increase in the macroRAFT concentration led to an increase in the modulus in the rubbery state. It has been shown by Chenal et al.[114] that, in core-shell-based films formed by macroRAFT block copolymers (in which the core is composed of a soft polymer and the shell is composed of PAA), the PAA shell behaves as the hard phase, forming a thin honeycomb percolating

network. A similar behavior could be expected for the DMAEMA-based macroRAFT agents, the macroRAFT phase causing an increase in the stiffening of the matrix.

In fact, in such nanocomposite systems, it is expected, therefore, to exist two percolating networks; one formed by Laponite platelets and a second one formed by the macroRAFT chains. Figure 4.54 shows the loss modulus, G″, as a function of temperature. By the analysis of the nanocomposite curves, it is possible to observe one main relaxation temperature (Tα) that can be attributed to the polymer phase and a second relaxation peak that might be the response of the macroRAFT phase. Finally at high enough temperatures, the polymer begins to flow as evidenced by a decrease in modulus. The clay networks formed in these samples are therefore less rigid than it would be expected if there were direct contact between the platelets. As already mentioned before, the DMAEMA-based macroRAFT agent adsorbs on the clay platelets by ionic bonds. It is possible that with temperature, there is an increase in the mobility of the ionic links that connect macroRAFT chains and clay platelets in the formation of such networks, giving rise to a decrease in modulus.

Figure 4.54 – Loss modulus, G″, as a function of temperature for the Laponite nanocomposite films and for the correspondent unfilled matrix.



Source: elaborated by the author.

Since matrixes are equally composed of polymer and macroRAFT agent, one could expect a similar behavior of these materials, with two relaxation temperatures and a similar

increase in the mobility of the macroRAFT or macroRAFT/clay networks at high temperature (flowing).

Due to experimental issues, however, the analysis of the matrixes could not continue throughout the whole temperature range, until higher values of temperature, and only one main relaxation temperature could be observed, which did not allowed us to confirm our hypothesis. Therefore, as a future perspective, it could be interesting to try to reproduce these experiments with the matrixes until higher temperature values to evidence the second relaxation peak, allowing a better understanding of the behavior of this macroRAFT phase with temperature.

4.5 Conclusions

In this chapter, the preparation of polymer/Laponite nanocomposite latexes by RAFT-mediated emulsion polymerization, via the REEP strategy, is described. The synthetic strategy proposed led to the formation of nanocomposite particles with a variety of different morphologies. In fact, the individual encapsulation of the Laponite platelets with a thin polymer layer, in order to maintain the shape anisotropy of the particles, which was the main objective of this work, has shown to be an extremely challenging and complicated task. The lamellar shape of the platelets, their high aspect ratio and surface energy and opposite charges on the surface and on the edges of the platelets may have made their effective encapsulation difficult to be achieved.

A careful selection of the experimental conditions was, for this purpose, necessary. Different parameters were explored in the RAFT emulsion polymerization in the presence of Laponite platelets. The main parameter studied was the nature of the macroRAFT agent, including its hydrophobic-hydrophilic balance and its molar mass. AA, PEG and DMAEMA-based macroRAFT agents were tested as mediators and cryo-TEM analysis revealed the formation of nanocomposite particles with different morphologies, including armored, janus, dumbbell, or multi-encapsulated particles (several platelets encapsulated inside each latex particle).

The incorporation of such units (AA, PEGA, BA and DMAEMA) in the macroRAFT agents had specific purposes. PEG (linear or pendent chains) was incorporated to adsorb on the basal faces of Laponite. The linear PEG-CTPPA macroRAFT agent suffered partitioning (part of the macroRAFT, therefore, was not available to stabilize the forming particles) and

presented a possible "hydrophobicity" (as this macroRAFT can partition between hydrophilic and hydrophobic phases, it should be more "hydrophobic" than the others) led to a poor stabilizing capacity of the macroRAFT agent and to the formation of armored particles. However, in general, the use of macroRAFT agents with incorporated pending PEG chains worked well and led to the formation of, predominately, polymeric nodules on the surface of Laponite, resulting in polymer-decorated particles (such as the dumbbell and janus morphologies), as could be expected (if we consider the edges to be highly hydrophilic and not covered by macroRAFT).

AA, on the other hand, was expected to interact with the edges of the clay, which are positively charged. However, this approach seemed to be, in fact, not so efficient, according to the adsorption isotherm and to the poor improvement in the morphology of the particles. The charge repulsion provided by the clay surface might have prevented PAA from adsorbing on the edges. Moreover, it is possible that the positive charge density on the edges was not high enough for adsorption of the AA units. In addition, the high hydrophilicity of the AA-based mediator led to secondary nucleation due to the presence of a high amount of macroRAFT in water, which resulted in stability issues. It is clear, therefore, that macroRAFT agents cannot be too hydrophilic, to avoid that the nucleation process starts in the aqueous phase, according to the polymerization-induced self-assembly (PISA) mechanism.

The incorporation of an AA block into a linear PEG macroRAFT was also evaluated, as well as the incorporation of pending PEGA chains into a PAA macroRAFT. It was expected that, by associating PAA and PEG blocks, macroRAFT agents could adsorb on both the surface and the edges of the platelets. In addition, the adsorption of PEG chains could, perhaps, help increasing the adsorption of the AA block on the edges of the platelets (due to screening of the clay surface charge). However, special attention should be paid in this case to the formation, at low pH, of hydrogen bonds between the ether units of PEG and the carboxyl groups of PAA, resulting in water-insoluble intramolecular complexes, especially for the macroRAFT agent with the linear configuration. Another factor that makes the copolymer with the PEG pending blocks more advantageous than the one with the linear block is the position of the PEG chains in this structure (closer to the C=S reactive double bond of the macroRAFT agent's Z group), which guarantees that the hydrophobic polymer grows closer to the PEGA units and leaves the AA segment free in the other extremity of the molecule, in a tail configuration, to either adsorb on the edges of the clay, or to stabilize in a more effective manner the nanocomposite latex particle. However, this macroRAFT agent

was not able to generate truly encapsulated particles and, instead, polymeric nodules were formed around the platelets, generating structures with dumbbell and janus morphologies. The large amount of free macroRAFT agent in the aqueous phase at the beginning of polymerization (~85%) resulted in a large number of free polymeric particles, formed according to the PISA nucleation mechanism.

Therefore, the incorporation of BA units into the macroRAFT agents aimed to increase the hydrophobicity of these molecules and, therefore, decrease the tendency that such hydrophilic block copolymers have to stay in the aqueous phase, inhibiting homogeneous nucleation and directing the growth of the polymer shell to the macroRAFT-modified clays. More hydrophobic block copolymer containing random BA units along the PEGA and AA blocks were evaluated and cryo-TEM images indicate that platelets were still not fully encapsulated, being partially covered or decorated by the polymeric particles.

An interesting result was obtained with P(AA-*co*-BA) macroRAFT, which also resulted in dumbbell or janus structures. However, apparently, a better wetting of the clay surface was obtained by this copolymer than by any other macroRAFT compositions. This experiment, which can be seen as a control experiment, validate our hypothesis that PAA does not cover Laponite edges as efficiently as expected. The surface energy of the edge can be considered still higher than the surface energy of the basal faces (that could be considered "hydrophobic") and, therefore, the polymer chains still phase separate from the edges. A better wetting of the basal faces, however, is obtained by the adsorption of P(AA-*co*-BA) than by the adsorption of PEG chains, which means that the PEG would render the faces less hydrophobic.

It is known that there is an important relationship between the nature (monomer composition) of the macroRAFT agents and the kinetic control of the nanocomposite particles morphology. In this regard, the initial colloidal suspension formed by the adsorption of macroRAFT onto Laponite platelets is a decisive point in determining the final morphology of the particles. Some aspects, such as the adsorbed amount of macroRAFT, the concentration of macroRAFT agent free in the aqueous phase (non-adsorbed), the dispersibility of the platelets, and even the configuration that the macroRAFT chains adopt on the adsorbate are of key importance on the mechanisms that lead to the encapsulation of the particles.

The incorporation of DMAEMA units into the macroRAFT agents was expected to allow a strong interaction between the macroRAFT and the oppositely charged surface of

the clays by electrostatic attraction. In addition, some BA units were included, generating P(DMAEMA-co-BA) copolymers, considering the importance of the incorporation of hydrophobic units, as it has been shown in the previous results. The chain length of these copolymers seemed to be a crucial factor for the stability of the nanocomposite latex particles. Short copolymers were unable to stabilize with efficiency the particles and, in this aspect, the longer chain was a more efficient mediator. The strong adsorption of the DMAEMA-based copolymer led to a better wettability of the inorganic surface and to the formation of partially encapsulated particles, with clay platelets sandwiched between two polymer particles or, in some cases, with the edges and the basal surfaces covered with polymer.

Indeed, the existence of a strong interaction between the macroRAFT agent and the surface of the clay seems to be a crucial factor for defining the clay environment as the polymerization locus and, therefore, for a successful encapsulation process. In the case of the DMAEMA-based macroRAFT agent, even though it presented a strong adsorption onto Laponite, the different charges of the edges and the surface of the platelets may have led to the production of mostly bare-edged particles, such as the dumbbell morphology.

The DMAEMA-based formulation was, then, adapted to film-forming monomer mixtures. The more hydrophobic mixtures (MMA:BA and Sty:BA 50:50) led to the formation of armored particles. The use of a more hydrophilic mixture (MA:BA 80:20) resulted in small dumbbell particles. The clay content was also studied and, even though conversion profile was not affected by this factor, different particle morphologies were obtained. Small spherical particles of 20 nm were obtained in the absence of clay and dumbbell or janus morphologies of ~100 nm were formed in the presence of 5 g L^{-1} of clay. However, when the content was increased to 10 g L^{-1}, armored structures were formed, indicating that it is crucial to increase the macroRAFT concentration as well, to guarantee the stability of the janus and dumbbell particles.

Finally, the layer-by-layer approach was investigated as an attempt to achieve true and uniform encapsulation of Laponite, by the initial surface charge inversion of Laponite platelets through the adsorption of a small quantity of P($DMAEMA_{19}$-*co*-BA_{14})-CTPPA, followed by the adsorption of P(AA_{16}-*co*-BA_{16})-CTPPA. In this case, it is likely that the AA-based macroRAFT can efficiently cover the edges of the clay, as it can adsorb on the entire particle surface (which has been rendered positive by the adsorption of the DMAEMA-based copolymer) and images show that by this approach it is possible to obtain multiple encapsulated hybrid particles.

Two formulations of DMAEMA-based latexes that led to dumbbell particles with different clay contents were selected for a further investigation of the thermo-mechanical behavior of the films, by DMA, as well as of their microstructure, by FIB-SEM. A homogeneous distribution of the platelets within the polymer matrix was observed by FIB-SEM and, in comparison to the pure polymer matrix, the presence of the clay platelets, as well as the macroRAFT agents, has increased the stiffness of the material. Such enhancement could be attributed to the formation of a connected network of platelets in the matrix, as well as a percolating network formed by the DMAEMA-based macroRAFT chains. In this aspect, the dumbbell morphology of the particles might have been crucial for the arrangement of the platelets in this mechanical percolation structure since, by having uncoated edges, the dumbbell particles allowed platelet–platelet interactions within the polymer matrix.

References

1 ALEXANDRE, M.; DUBOIS, P. Polymer-layered silicate nanocomposites: Preparation, properties and uses of a new class of materials. **Materials Science & Engineering R-Reports,** v. 28, n. 1-2, p. 1-63, jun. 2000.

2 RAY, S. S.; OKAMOTO, M. Polymer/layered silicate nanocomposites: A review from preparation to processing. **Progress in Polymer Science,** v. 28, n. 11, p. 1539-1641, nov. 2003.

3 OKAMOTO, M. Recent advances in polymer/layered silicate nanocomposites: An overview from science to technology. **Materials Science and Technology,** v. 22, n. 7, p. 756-779, july 2006.

4 PAVLIDOU, S.; PAPASPYRIDES, C. D. A review on polymer-layered silicate nanocomposites. **Progress in Polymer Science,** v. 33, n. 12, p. 1119-1198, dec. 2008.

5 RAY, S. S. Recent trends and future outlooks in the field of clay-containing polymer nanocomposites. **Macromolecular Chemistry and Physics,** v. 215, n. 12, p. 1162-1179, june 2014.

6 SUGAMA, T. Polyphenylenesulfied/montomorillonite clay nanocomposite coatings: Their efficacy in protecting steel against corrosion. **Materials Letters,** v. 60, n. 21-22, p. 2700-2706, sept. 2006.

7 MAJUMDAR, D.; BLANTON, T. N.; SCHWARK, D. W. Clay-polymer nanocomposite coatings for imaging application. **Applied Clay Science,** v. 23, n. 5-6, p. 265-273, oct. 2003.

[8] YEH, J. M.; HUANG, H. Y.; CHEN, C. L.; SU, W. F.; YU, Y. H. Siloxane-modified epoxy resin-clay nanocomposite coatings with advanced anticorrosive properties prepared by a solution dispersion approach. **Surface & Coatings Technology,** v. 200, n. 8, p. 2753-2763, jan. 2006.

[9] NGUYEN, D.; ZONDANOS, H. S.; FARRUGIA, J. M.; SERELIS, A. K.; SUCH, C. H.; HAWKETT, B. S. Pigment encapsulation by emulsion polymerization using macro-RAFT copolymers. **Langmuir,** v. 24, n. 5, p. 2140-2150, 2008.

[10] DAIGLE, J.-C.; CLAVERIE, J. P. A simple method for forming hybrid core-shell nanoparticles suspended in water. **Journal of Nanomaterials,** v. 2008, p. 1-8, 2008.

[11] DAS, P.; ZHONG, W.; CLAVERIE, J. P. Copolymer nanosphere encapsulated CdS quantum dots prepared by RAFT copolymerization: Synthesis, characterization and mechanism of formation. **Colloid and Polymer Science,** v. 289, n. 14, p. 1519-1533, sept. 2011.

[12] DAS, P.; CLAVERIE, J. P. Synthesis of single-core and multiple-core core-shell nanoparticles by RAFT emulsion polymerization: Lead sulfide-copolymer nanocomposites. **Journal of Polymer Science Part A: Polymer Chemistry,** v. 50, n. 14, p. 2802-2808, jul. 2012.

[13] ZGHEIB, N.; PUTAUX, J.-L.; THILL, A.; BOURGEAT-LAMI, E.; D'AGOSTO, F.; LANSALOT, M. Cerium oxide encapsulation by emulsion polymerization using hydrophilic macroRAFT agents. **Polymer Chemistry,** v. 4, n. 3, p. 607-614, 2013.

[14] GARNIER, J.; WARNANT, J.; LACROIX-DESMAZES, P.; DUFILS, P. E.; VINAS, J.; VANDERVEKEN, Y.; VAN HERK, A. M. An emulsifier-free RAFT-mediated process for the efficient synthesis of cerium oxide/polymer hybrid latexes. **Macromolecular Rapid Communications,** v. 33, n. 16, p. 1388-1392, aug. 2012.

[15] GARNIER, J.; WARNANT, J.; LACROIX-DESMAZES, P.; DUFILS, P.-E.; VINAS, J.; VAN HERK, A. Sulfonated macro-RAFT agents for the surfactant-free synthesis of cerium oxide-based hybrid latexes. **Journal of Colloid and Interface Science,** v. 407, p. 273-281, oct. 2013.

[16] WARNANT, J.; GARNIER, J.; VAN HERK, A.; DUFILS, P.-E.; VINAS, J.; LACROIX-DESMAZES, P. A CeO_2/PVDC hybrid latex mediated by a phosphonated macro-RAFT agent. **Polymer Chemistry,** v. 4, n. 23, p. 5656-5663, dec. 2013.

[17] NGUYEN, D.; SUCH, C. H.; HAWKETT, B. S. Polymer coating of carboxylic acid functionalized multiwalled carbon nanotubes via reversible addition-fragmentation chain transfer mediated emulsion polymerization. **Journal of Polymer Science Part A: Polymer Chemistry,** v. 51, n. 2, p. 250-257, jan. 2013.

[18] ZHONG, W.; ZEUNA, J. N.; CLAVERIE, J. P. A versatile encapsulation method of noncovalently modified carbon nanotubes by RAFT polymerization. **Journal of Polymer Science Part A: Polymer Chemistry,** v. 50, n. 21, p. 4403-4407, 2012.

19 ALI, S. I.; HEUTS, J. P. A.; HAWKETT, B. S.; VAN HERK, A. M. Polymer encapsulated gibbsite nanoparticles: Efficient preparation of anisotropic composite latex particles by RAFT-based starved feed emulsion polymerization. **Langmuir,** v. 25, n. 18, p. 10523-10533, sept. 2009.

20 MBALLA MBALLA, M. A.; ALI, S. I.; HEUTS, J. P. A.; VAN HERK, A. M. Control of the anisotropic morphology of latex nanocomposites containing single montmorillonite clay particles prepared by conventional and reversible addition-fragmentation chain transfer based emulsion polymerization. **Polymer International,** v. 61, n. 6, p. 861-865, 2012.

21 HUYNH, V. T.; NGUYEN, D.; SUCH, C. H.; HAWKETT, B. S. Polymer coating of graphene oxide via reversible addition-fragmentation chain transfer mediated emulsion polymerization. **Journal of Polymer Science Part A: Polymer Chemistry,** v. 53, n. 12, p. 1413-1421, june 2015.

22 VAN HERK, A. M. Polymer encapsulation of single clay platelets by emulsion polymerization approaches, thermodynamic, and kinetic factors. **Macromolecular Reaction Engineering**, p. n/a-n/a, 2015.

23 ZETTERLUND, P. B.; THICKETT, S. C.; PERRIER, S.; BOURGEAT-LAMI, E.; LANSALOT, M. Controlled/living radical polymerization in dispersed systems: An update. **Chemical Reviews,** v. 115, p. 9745−9800, 2015.

24 BOURGEAT-LAMI, E.; D'AGOSTO, F.; LANSALOT, M. Synthesis of nanocapsules and polymer/inorganic nanoparticles through controlled radical polymerization at and near interfaces in heterogeneous media. In: VANA, P. (Ed.). **Controlled radical polymerization at and from solid surfaces**. Heidelberg: Springer International Publishing, 2016. v.270, p.123-161. (Advances in polymer science).

25 ERDEM, B.; SUDOL, E. D.; DIMONIE, V. L.; EL-AASSER, M. S. Encapsulation of inorganic particles via miniemulsion polymerization. I. Dispersion of titanium dioxide particles in organic media using OLOA 370 as stabilizer. **Journal of Polymer Science Part a-Polymer Chemistry,** v. 38, n. 24, p. 4419-4430, dec. 2000.

26 YANG, Y.; KONG, X. Z.; KAN, C. Y.; SUN, C. G. Encapsulation of calcium carbonate by styrene polymerization. **Polymers for Advanced Technologies,** v. 10, n. 1-2, p. 54-59, jan.-feb. 1999.

27 TIARKS, F.; LANDFESTER, K.; ANTONIETTI, M. Encapsulation of carbon black by miniemulsion polymerization. **Macromolecular Chemistry and Physics,** v. 202, n. 1, p. 51-60, jan. 2001.

28 VIALA, P.; BOURGEAT-LAMI, E.; GUYOT, A.; LEGRAND, P.; LEFEBVRE, D. Pigment encapsulation by emulsion polymerisation, redespersible in water. **Macromolecular Symposia,** v. 187, p. 651-661, sept. 2002.

[29] CAUVIN, S.; COLVER, P. J.; BON, S. A. F. Pickering stabilized miniemulsion polymerization: Preparation of clay armored latexes. **Macromolecules,** v. 38, n. 19, p. 7887-7889, sept. 2005.

[30] NEGRETE-HERRERA, N.; PUTAUX, J.-L.; DAVID, L.; DE HAAS, F.; BOURGEAT-LAMI, E. Polymer/Laponite composite latexes: Particle morphology, film microstructure, and properties. **Macromolecular Rapid Communications,** v. 28, n. 15, p. 1567-1573, aug. 2007.

[31] PUTLITZ, B. Z.; LANDFESTER, K.; FISCHER, H.; ANTONIETTI, M. The generation of "armored latexes" and hollow inorganic shells made of clay sheets by templating cationic miniemulsions and latexes. **Advanced Materials,** v. 13, n. 7, p. 500-503, apr. 2001.

[32] XU, X.; SMITH, A. E.; KIRKLAND, S. E.; MCCORMICK, C. L. Aqueous RAFT synthesis of ph-responsive triblock copolymer mPEO-PAPMA-PDPAEMA and formation of shell cross-linked micelles. **Macromolecules,** v. 41, n. 22, p. 8429-8435, 2008.

[33] BOURSIER, T.; CHADUC, I.; RIEGER, J.; D'AGOSTO, F.; LANSALOT, M.; CHARLEUX, B. Controlled radical polymerization of styrene in miniemulsion mediated by PEO-based trithiocarbonate macromolecular RAFT agents. **Polymer Chemistry,** v. 2, n. 2, p. 355-362, feb. 2011.

[34] CHADUC, I.; ZHANG, W.; LANSALOT, M.; D'AGOSTO, F.; CHARLEUX, B. Amphiphilic block copolymers from a direct and one-pot RAFT synthesis in water. **Macromolecular Rapid Communications,** v. 32, n. 16, p. 1270-1276, aug. 2011.

[35] CHADUC, I.; CREPET, A.; BOYRON, O.; CHARLEUX, B.; D'AGOSTO, F.; LANSALOT, M. Effect of the pH on the RAFT polymerization of acrylic acid in water. Application to the synthesis of poly(acrylic acid)-stabilized polystyrene particles by RAFT emulsion polymerization. **Macromolecules,** v. 46, n. 15, p. 6013-6023, aug. 2013.

[36] CHADUC, I.; GIROD, M.; ANTOINE, R.; CHARLEUX, B.; D'AGOSTO, F.; LANSALOT, M. Batch emulsion polymerization mediated by poly(methacrylic acid) macroRAFT agents: One-pot synthesis of self-stabilized particles. **Macromolecules,** v. 45, n. 15, p. 5881-5893, july 2012.

[37] BOURGEAT-LAMI, E.; LANSALOT, M. Organic/inorganic composite latexes: The marriage of emulsion polymerization and inorganic chemistry. **Advances in Polymer Science,** v. 233, p. 53-123, may 2010.

[38] THOSTENSON, E. T.; LI, C. Y.; CHOU, T. W. Nanocomposites in context. **Composites Science and Technology,** v. 65, n. 3-4, p. 491-516, mar. 2005.

[39] ZOU, H.; WU, S.; SHEN, J. Polymer/silica nanocomposites: Preparation, characterization, properties, and applications. **Chemical Reviews,** v. 108, n. 9, p. 3893-3957, sept. 2008.

40 SIH, B. C.; WOLF, M. O. Metal nanoparticle - conjugated polymer nanocomposites. **Chemical Communications**, n. 27, p. 3375-3384, 2005.

41 FAUPEL, F.; ZAPOROJTCHENKO, V.; STRUNSKUS, T.; ELBAHRI, M. Metal-polymer nanocomposites for functional applications. **Advanced Engineering Materials,** v. 12, n. 12, p. 1177-1190, dec. 2010.

42 CASERI, W. Nanocomposites of polymers and metals or semiconductors: Historical background and optical properties. **Macromolecular Rapid Communications,** v. 21, n. 11, p. 705-722, july 2000.

43 NAGANUMA, T.; KAGAWA, Y. Effect of particle size on the optically transparent nano meter-order glass particle-dispersed epoxy matrix composites. **Composites Science and Technology,** v. 62, n. 9, p. 1187-1189, 2002.

44 MIAO, C.; HAMAD, W. Y. Cellulose reinforced polymer composites and nanocomposites: A critical review. **Cellulose,** v. 20, n. 5, p. 2221-2262, oct. 2013.

45 PANDEY, G.; THOSTENSON, E. T. Carbon nanotube-based multifunctional polymer nanocomposites. **Polymer Reviews,** v. 52, n. 3-4, p. 355-416, 2012.

46 YANG, Y.; ZHU, Z. K.; YIN, J.; WANG, X. Y.; QI, Z. E. Preparation and properties of hybrids of organo-soluble polyimide and montmorillonite with various chemical surface modification methods. **Polymer,** v. 40, n. 15, p. 4407-4414, july 1999.

47 USUKI, A.; KAWASUMI, M.; KOJIMA, Y.; OKADA, A.; KURAUCHI, T.; KAMIGAITO, O. Swelling behavior of montmorillonite cation exchanged for omega-amino acids by epsilon-caprolactam. **Journal of Materials Research,** v. 8, n. 5, p. 1174-1178, may 1993.

48 KOJIMA, Y.; USUKI, A.; KAWASUMI, M.; OKADA, A.; FUKUSHIMA, Y.; KURAUCHI, T.; KAMIGAITO, O. Mechanical-properties of nylon 6-clay hybrid. **Journal of Materials Research,** v. 8, n. 5, p. 1185-1189, may 1993.

49 LUO, J. J.; DANIEL, I. M. Characterization and modeling of mechanical behavior of polymer/clay nanocomposites. **Composites Science and Technology,** v. 63, n. 11, p. 1607-1616, aug. 2003.

50 ORIAKHI, C. O.; FARR, I. V.; LERNER, M. M. Incorporation of poly(acrylic acid), poly(vinylsulfonate) and poly(styrenesulfonate) within layered double hydroxides. **Journal of Materials Chemistry,** v. 6, n. 1, p. 103-107, jan. 1996.

51 _____. Thermal characterization of poly(styrene sulfonate) layered double hydroxide nanocomposites. **Clays and Clay Minerals,** v. 45, n. 2, p. 194-202, apr. 1997.

52 WILSON, O. C.; OLORUNYOLEMI, T.; JAWORSKI, A.; BORUM, L.; YOUNG, D.; SIRIWAT, A.; DICKENS, E.; ORIAKHI, C.; LERNER, M. Surface and interfacial properties of polymer-intercalated layered double hydroxide nanocomposites. **Applied Clay Science,** v. 15, n. 1-2, p. 265-279, sept. 1999.

[53] ZANETTI, M.; BRACCO, P.; COSTA, L. Thermal degradation behaviour of PE/clay nanocomposites. **Polymer Degradation and Stability,** v. 85, n. 1, p. 657-665, july 2004.

[54] VYAZOVKIN, S.; DRANCA, I.; FAN, X. W.; ADVINCULA, R. Kinetics of the thermal and thermo-oxidative degradation of a polystyrene-clay nanocomposite. **Macromolecular Rapid Communications,** v. 25, n. 3, p. 498-503, feb. 2004.

[55] DUNCAN, T. V. Applications of nanotechnology in food packaging and food safety: Barrier materials, antimicrobials and sensors. **Journal of Colloid and Interface Science,** v. 363, n. 1, p. 1-24, nov. 2011.

[56] CUI, Y.; KUMAR, S.; KONA, B. R.; VAN HOUCKE, D. Gas barrier properties of polymer/clay nanocomposites. **Rsc Advances,** v. 5, n. 78, p. 63669-63690, 2015.

[57] BLUMSTEIN, A. Polymerization of adsorbed monolayers. Ii. Thermal degradation of the inserted polymer. **Journal of Polymer Science Part A: General Papers,** v. 3, n. 7, p. 2665-2672, july 1965.

[58] BEYER, G. Nanocomposites: A new class of flame retardants for polymers. **Plastics, Additives and Compounding,** v. 4, n. 10, p. 22-28, oct. 2002.

[59] PORTER, D.; METCALFE, E.; THOMAS, M. J. K. Nanocomposite fire retardants - a review. **Fire and Materials,** v. 24, n. 1, p. 45-52, jan.-feb. 2000.

[60] BALMER, J. A.; SCHMID, A.; ARMES, S. P. Colloidal nanocomposite particles: Quo vadis? **Journal of Materials Chemistry,** v. 18, n. 47, p. 5722-5730, dec. 2008.

[61] MITTAL, V. Chapter 1 polymer nanocomposites in emulsion and suspension: An overview. In: (Ed.). **Polymer nanocomposites by emulsion and suspension polymerization**: The Royal Society of Chemistry, 2011. p.1-31.

[62] ZGHEIB, N. **Elaboration de particules de latex composites a base d'oxyde de cerium par polymerisation radicalaire en milieu aqueux disperse**. 2011. 268 (NNT : 2011LYO10218).

[63] BOURGEAT-LAMI, E.; SHEIBAT-OTHMAN, N.; DOS SANTOS, A. M. Chapter 13 polymer-clay nanocomposite particles and soap-free latexes stabilized by clay platelets: State of the art and recent advances. In: MITTAL, V. (Ed.). **Polymer nanocomposites by emulsion and suspension polymerization**: The Royal Society of Chemistry, 2011. p.269-311.

[64] BARTHET, C.; HICKEY, A. J.; CAIRNS, D. B.; ARMES, S. P. Synthesis of novel polymer-silica colloidal nanocomposites via free-radical polymerization of vinyl monomers. **Advanced Materials,** v. 11, n. 5, p. 408-410, mar. 1999.

[65] PERCY, M. J.; BARTHET, C.; LOBB, J. C.; KHAN, M. A.; LASCELLES, S. F.; VAMVAKAKI, M.; ARMES, S. P. Synthesis and characterization of vinyl polymer-silica colloidal nanocomposites. **Langmuir,** v. 16, n. 17, p. 6913-6920, aug. 2000.

66 CARLSSON, L.; FALL, A.; CHADUC, I.; WAGBERG, L.; CHARLEUX, B.; MALMSTRORN, E.; D'AGOSTO, F.; LANSALOT, M.; CARLMARK, A. Modification of cellulose model surfaces by cationic polymer latexes prepared by RAFT-mediated surfactant-free emulsion polymerization. **Polymer Chemistry,** v. 5, n. 20, p. 6076-6086, oct. 2014.

67 QIAO, X. **Synthesis of silica-polymer hybrid particles via controlled radical polymerization in aqueous dispersed media** 2013. (Ph.D.). Universite Claude Bernard Lyon I

68 LEE, H.-I.; PIETRASIK, J.; SHEIKO, S. S.; MATYJASZEWSKI, K. Stimuli-responsive molecular brushes. **Progress in Polymer Science,** v. 35, n. 1-2, p. 24-44, jan.-feb. 2010.

69 CHARLEUX, B.; D'AGOSTO, F.; DELAITTRE, G. Preparation of hybrid latex particles and core-shell particles through the use of controlled radical polymerization techniques in aqueous media. In: VAN HERK, A. M.;LANDFESTER, K. (Ed.). **Hybrid latex particles: Preparation with (mini) emulsion polymerization**. Berlin Heidelberg: Springer, 2010. p.125-183. (Advances in polymer science).

70 BARBEY, R.; LAVANANT, L.; PARIPOVIC, D.; SCHUEWER, N.; SUGNAUX, C.; TUGULU, S.; KLOK, H.-A. Polymer brushes via surface-initiated controlled radical polymerization: Synthesis, characterization, properties, and applications. **Chemical Reviews,** v. 109, n. 11, p. 5437-5527, nov. 2009.

71 BRINKS, M. K.; STUDER, A. Polymer brushes by nitroxide-mediated polymerization. **Macromolecular Rapid Communications,** v. 30, n. 13, p. 1043-1057, jul 2009.

72 PAN, G.; MA, Y.; ZHANG, Y.; GUO, X.; LI, C.; ZHANG, H. Controlled synthesis of water-compatible molecularly imprinted polymer microspheres with ultrathin hydrophilic polymer shells via surface-initiated reversible addition-fragmentation chain transfer polymerization. **Soft Matter,** v. 7, n. 18, p. 8428-8439, 2011.

73 QU, Z.; HU, F.; CHEN, K.; DUAN, Z.; GU, H.; XU, H. A facile route to the synthesis of spherical poly(acrylic acid) brushes via RAFT polymerization for high-capacity protein immobilization. **Journal of Colloid and Interface Science,** v. 398, p. 82-87, may 2013.

74 LI, C.; HAN, J.; RYU, C. Y.; BENICEWICZ, B. C. A versatile method to prepare RAFT agent anchored substrates and the preparation of PMMA grafted nanoparticles. **Macromolecules,** v. 39, n. 9, p. 3175-3183, may 2006.

75 LI, C. Z.; BENICEWICZ, B. C. Synthesis of well-defined polymer brushes grafted onto silica nanoparticles via surface reversible addition-fragmentation chain transfer polymerization. **Macromolecules,** v. 38, n. 14, p. 5929-5936, july 2005.

76 ROTZOLL, R.; VANA, P. Synthesis of poly(methyl acrylate) loops grafted onto silica nanoparticles via reversible addition-fragmentation chain transfer

polymerization. **Journal of Polymer Science Part a-Polymer Chemistry,** v. 46, n. 23, p. 7656-7666, dec. 2008.

77 YANG, Y.; YANG, Z.; ZHAO, Q.; CHENG, X.; TJONG, S. C.; LI, R. K. Y.; WAN, X.; XIE, X. Immobilization of RAFT agents on silica nanoparticles utilizing an alternative functional group and subsequent surface-initiated RAFT polymerization. **Journal of Polymer Science Part a-Polymer Chemistry,** v. 47, n. 2, p. 467-484, jan. 2009.

78 OHNO, K.; MA, Y.; HUANG, Y.; MORI, C.; YAHATA, Y.; TSUJII, Y.; MASCHMEYER, T.; MORAES, J.; PERRIER, S. Surface-initiated reversible addition-fragmentation chain transfer (RAFT) polymerization from fine particles functionalized with trithiocarbonates. **Macromolecules,** v. 44, n. 22, p. 8944-8953, nov. 2011.

79 HOJJATI, B.; SUI, R.; CHARPENTIER, P. A. Synthesis of TiO_2/PAA nanocomposite by RAFT polymerization. **Polymer,** v. 48, n. 20, p. 5850-5858, sept. 2007.

80 HOJJATI, B.; CHARPENTIER, P. A. Synthesis and kinetics of graft polymerization of methy methacrylate from the RAFT coordinated surface of nano-TiO_2. **Journal of Polymer Science Part a-Polymer Chemistry,** v. 46, n. 12, p. 3926-3937, june 2008.

81 YE, Y.-S.; SHEN, W.-C.; TSENG, C.-Y.; RICK, J.; HUANG, Y.-J.; CHANG, F.-C.; HWANG, B.-J. Versatile grafting approaches to star-shaped poss-containing hybrid polymers using RAFT polymerization and click chemistry. **Chemical Communications,** v. 47, n. 38, p. 10656-10658, 2011.

82 SKAFF, H.; EMRICK, T. Reversible addition fragmentation chain transfer (RAFT) polymerization from unprotected cadmium selenide nanoparticles. **Angewandte Chemie-International Edition,** v. 43, n. 40, p. 5383-5386, 2004.

83 LI, Q.; ZHANG, L.; BAI, L.; ZHANG, Z.; ZHU, J.; ZHOU, N.; CHENG, Z.; ZHU, X. Multistimuli-responsive hybrid nanoparticles with magnetic core and thermoresponsive fluorescence-labeled shell via surface-initiated RAFT polymerization. **Soft Matter,** v. 7, n. 15, p. 6958-6966, 2011.

84 BECKERT, F.; FRIEDRICH, C.; THOMANN, R.; MUELHAUPT, R. Sulfur-functionalized graphenes as macro-chain-transfer and RAFT agents for producing graphene polymer brushes and polystyrene nanocomposites. **Macromolecules,** v. 45, n. 17, p. 7083-7090, sept. 2012.

85 CUI, L.; LIU, J.; WANG, R.; LIU, Z.; YANG, W. A facile "graft from" method to prepare molecular-level dispersed graphene-polymer composites. **Journal of Polymer Science Part a-Polymer Chemistry,** v. 50, n. 21, p. 4423-4432, nov. 2012.

86 KONN, C.; MOREL, F.; BEYOU, E.; CHAUMONT, P.; BOURGEAT-LAMI, E. Nitroxide-mediated polymerization of styrene initiated from the surface of Laponite clay platelets. **Macromolecules,** v. 40, n. 21, p. 7464-7472, oct. 2007.

87 CHIROWODZA, H.; WEBER, W.; HARTMANN, P.; PASCH, H. Surface-initiated reversible addition fragmentation chain transfer (RAFT) polymerization of styrene from Laponite clay surfaces. **Macromolecular Symposia,** v. 313-314, n. 1, p. 135-145, mar. 2012.

88 CHENG, J.; HE, J.; LI, C.; YANG, Y. Facile approach to functionalize nanodiamond particles with v-shaped polymer brushes. **Chemistry of Materials,** v. 20, n. 13, p. 4224-4230, july 2008.

89 LIU, J.; YANG, W.; TAO, L.; LI, D.; BOYER, C.; DAVIS, T. P. Thermosensitive graphene nanocomposites formed using pyrene-terminal polymers made by RAFT polymerization. **Journal of Polymer Science Part a-Polymer Chemistry,** v. 48, n. 2, p. 425-433, jan. 2010.

90 HOMENICK, C. M.; LAWSON, G.; ADRONOV, A. Polymer grafting of carbon nanotubes using living free-radical polymerization. **Polymer Reviews,** v. 47, n. 2, p. 265-290, 2007.

91 BADRI, A.; WHITTAKER, M. R.; ZETTERLUND, P. B. Modification of graphene/graphene oxide with polymer brushes using controlled/living radical polymerization. **Journal of Polymer Science Part A: Polymer Chemistry,** v. 50, n. 15, p. 2981-2992, aug. 2012.

92 BOCKSTALLER, M. R.; MICKIEWICZ, R. A.; THOMAS, E. L. Block copolymer nanocomposites: Perspectives for tailored functional materials. **Advanced Materials,** v. 17, n. 11, p. 1331-1349, june 2005.

93 MCKENNA, T. F. L.; CHARLEUX, B.; BOURGEAT-LAMI, E.; D'AGOSTO, F.; LANSALOT, M. Novel technologies and chemistries for waterborne coatings. **Journal of Coatings Technology and Research,** v. 11, n. 2, p. 131-141, mar. 2014.

94 BOURGEAT-LAMI, E. Organic-inorganic nanostructured colloids. **Journal of Nanoscience and Nanotechnology,** v. 2, n. 1, p. 1-24, feb. 2002.

95 BOURGEAT-LAMI, E.; GUIMARAES, T. R.; PEREIRA, A. M. C.; ALVES, G. M.; MOREIRA, J. C.; PUTAUX, J.-L.; DOS SANTOS, A. M. High solids content, soap-free, film-forming latexes stabilized by Laponite clay platelets. **Macromolecular Rapid Communications,** v. 31, n. 21, p. 1874-1880, nov. 2010.

96 GUIMARAES, T. R.; CHAPARRO, T. D. C.; D'AGOSTO, F.; LANSALOT, M.; DOS SANTOS, A. M.; BOURGEAT-LAMI, E. Synthesis of multi-hollow clay-armored latexes by surfactant-free emulsion polymerization of styrene mediated by poly(ethylene oxide)-based macroRAFT/Laponite complexes. **Polymer Chemistry,** v. 5, n. 22, p. 6611-6622, nov. 2014.

97 SAMAKANDE, A.; SANDERSON, R. D.; HARTMANN, P. C. Encapsulated clay particles in polystyrene by RAFT mediated miniemulsion polymerization. **Journal of Polymer Science Part a-Polymer Chemistry,** v. 46, n. 21, p. 7114-7126, nov. 2008.

98 _____. Rheological properties of RAFT-mediated poly(styrene-co-butyl acrylate)-clay nanocomposites p(S-co-BA)-PCNS : Emphasis on the effect of structural parameters on thermo-mechanical and melt flow behaviors. **Polymer,** v. 50, n. 1, p. 42-49, jan. 2009.

99 CHAKRABARTY, A.; ZHANG, L.; CAVICCH, K. A.; WEISS, R. A.; SINGHA, N. K. Tailor-made fluorinated copolymer/clay nanocomposite by cationic RAFT assisted pickering miniemulsion polymerization. **Langmuir,** v. 31, n. 45, p. 12472-12480, nov. 2015.

100 MBALLA, M. A. M.; HEUTS, J. P. A.; VAN HERK, A. M. Encapsulation of non-chemically modified montmorillonite clay platelets via emulsion polymerization. **Colloid and Polymer Science,** v. 291, n. 3, p. 501-513, mar. 2013.

101 NGUYEN, D.; SUCH, C.; HAWKETT, B. Polymer-TiO_2 composite nanorattles via RAFT-mediated emulsion polymerization. **Journal of Polymer Science Part a-Polymer Chemistry,** v. 50, n. 2, p. 346-352, jan. 2012.

102 ALI, S. I.; HEUTS, J. P. A.; VAN HERK, A. M. Controlled synthesis of polymeric nanocapsules by RAFT-based vesicle templating. **Langmuir,** v. 26, n. 11, p. 7848-7858, june 2010.

103 DOS SANTOS, A. M.; POHN, J.; LANSALOT, M.; D'AGOSTO, F. Combining steric and electrostatic stabilization using hydrophilic macroRAFT agents in an ab initio emulsion polymerization of styrene. **Macromolecular Rapid Communications,** v. 28, n. 12, p. 1325-1332, june 2007.

104 GEBHARDT, J. E.; FUERSTENAU, D. W. Adsorption of polyacrylic acid at oxide/water interfaces. **Colloids and Surfaces,** v. 7, n. 3, p. 221-231, aug. 1983.

105 ZHANG, W.; D'AGOSTO, F.; BOYRON, O.; RIEGER, J.; CHARLEUX, B. Toward a better understanding of the parameters that lead to the formation of nonspherical polystyrene particles via RAFT-mediated one-pot aqueous emulsion polymerization. **Macromolecules,** v. 45, n. 10, p. 4075-4084, may 2012.

106 RAMOS, J.; FORCADA, J. Which are the mechanisms governing in cationic emulsion polymerization? **European Polymer Journal,** v. 43, n. 11, p. 4647–4661, nov. 2007.

107 BRANDRUP, J.; IMMERGUT, E. H.; A, G. E. **Polymer handbook**. 4th. New York: J. Wiley & Sons., Inc., 1999. 2336.

108 SHAW, D. G.; MACZYNSKI, A.; GORAL, M.; WISNIEWSKA-GOCLOWSKA, B.; SKRZECZ, A.; OWCZAREK, I.; BLAZEJ, K.; HAULAIT-PIRSON, M. C.; HEFTER, G. T.; MACZYNSKA, Z.; SZAFRANSKI, A. IUPAC-nist solubility data series. 81. Hydrocarbons with water and seawater-revised and updated. Part 6. C_8H_8-C_8H_{10} hydrocarbons with water. **Journal of Physical and Chemical Reference Data,** v. 34, n. 3, p. 1489-1553, sept. 2005.

[109] GREEN, D. P. R. **Perry's chemical engineers' handbook**. 8th. New York, Chicago, San Francisco, Lisbon, London, Madrid, Mexico City, Milan, New Delhi, San Juan, Seoul, Singapore, Sydney, Toronto: McGraw-Hill, 2008. 2400.

[110] VESCHAMBRES, C.; HALMA, M.; BOURGEAT-LAMI, E.; CHAZEAU, L.; DALMAS, F.; PREVOT, V. Layered double hydroxides: Efficient fillers for waterborne nanocomposite films. **Applied Clay Science**, 2016. In press.

[111] NOËL, A.; FAUCHEU, J.; CHENAL, J.-M.; VIRICELLE, J.-P.; BOURGEAT-LAMI, E. Electrical and mechanical percolation in graphene-latex nanocomposites. **Polymer,** v. 55, n. 20, p. 5140-5145, sept. 2014.

[112] OUALI, N.; CAVAILLE, J. Y.; PEREZ, J. Elastic, viscoelastic and plastic behavior of multiphase polymer blends. **Plastics, Rubber and Composites Processing Applications**, p. 55-60, 1991.

[113] KOLAŘK, J. Simultaneous prediction of the modulus, tensile strength and gas permeability of binary polymer blends. **European Polymer Journal,** v. 34, n. 5–6, p. 585-590, may 1998.

[114] CHENAL, M.; RIEGER, J.; VÉCHAMBRE, C.; CHENAL, J.-M.; CHAZEAU, L.; CRETON, C.; BOUTEILLER, L. Soft nanostructured films with an ultra-low volume fraction of percolating hard phase. **Macromolecular Rapid Communications,** v. 34, n. 19, p. 1524-1529, oct. 2013.

5 Conclusions and perspectives

In this thesis, the macroRAFT-assisted encapsulating emulsion polymerization (REEP) technique was used to synthesize polymer-Laponite nanocomposite latexes capable of forming nanocomposite films that present a controlled microstructure and a homogeneous nanoparticle distribution in the matrix. The REEP technique is a versatile and efficient method for the encapsulation of a large variety of inorganic (or even organic, in some cases) particles that associates all the advantages of emulsion polymerization and RDRP techniques. One of the key features of the method is the use of amphipathic RAFT agents that work as coupling agents between the platelets and the polymer phase and stabilizers of the hybrid particles. One of the advantages of this technique is that, since no sophisticated chemical treatment of the inorganic surface is required, nanocomposite latex particles can be synthesized by one simple step of emulsion polymerization through the PISA mechanism. Moreover, it eliminates the need for conventional surfactants to stabilize the final latex particles, which is desirable for environmental and for quality-related reasons, since the presence of free surfactant in the latex may have a negative effect on the properties of the film.

The successful encapsulation of inorganic particles by the REEP strategy strongly depends on the use of carefully selected amphipathic macroRAFT agents that, by carrying suitable anchor groups, can adsorb on the inorganic particles and control the polymerization of the polymeric shell from the inorganic surface. In this aspect, the existence of some hydrophobic monomer units is crucial to increase the affinity between the macroRAFT/inorganic particles and the hydrophobic monomer and decrease the hydrophilicity of the macroRAFT agents (which forces molecules to stay, mainly, in the water phase, leading to secondary nucleation of particles). This characteristic can be responsible to direct, therefore, the growing of the polymer chains to the inorganic surface. Nevertheless, some molecules must be free in the aqueous phase to adsorb on the growing hybrid particles and stabilize the new objects that are being formed. In addition, the hydrophilic and hydrophobic units must be, preferably, randomly distributed in the copolymers to avoid their self-assembly into micelles and, consequently, the formation of new particles by micellar nucleation. To avoid the presence of monomer droplets in the water phase, which could lead to the partitioning of macroRAFT (or even the inorganic particles) between the macroRAFT/inorganic particle complexes, the water phase and the monomer

droplets, the system (as some works indicate) should be under monomer starve-feed conditions.

So, to guarantee that the macroRAFT agent has an adequate hydrophilic/hydrophobic balance, a careful selection of its structure must be performed. In addition, to guarantee an adequate adsorption of the macroRAFT agent onto the inorganic surface, the chemical nature of the inorganic particle must be taken into account. Indeed, the adsorption is a crucial factor for the success of the REEP strategy.

For this purpose, during the initial step of this work towards the production of polymer/Laponite nanocomposite latexes by RAFT-mediated emulsion polymerization, 12 different macroRAFT agents were carefully designed and synthesized by solution polymerization. In chapter 3 it is shown that polymerizations were successfully carried out and the synthesis of most macroRAFT agents followed a controlled behavior, according to the RAFT mechanism. The low molar masses of the homo and copolymers at low conversions, however, as well as the use of PEGA macromonomer and the methylation agent for SEC analysis, prejudiced the characterization of some of the products, giving unrealistic values of M_n and $Đ$. However, as obtaining controlled and uniform (in terms of dispersity) copolymers is not of fundamental importance for the synthesis of the nanocomposite particles by the REEP strategy, the homo and copolymers obtained were adequate for the intention proposed in this work.[1].

The second step towards the production of polymer/Laponite nanocomposite latexes by RAFT-mediated emulsion polymerization, also shown in Chapter 3, was the formation of the polymer/Laponite colloidal suspensions. A study of the equilibrium adsorption of PAA, PEGA and DMAEMA-based macroRAFT agents by graphically plotting the solid phase concentration of these molecules (adsorbed chains) against their liquid phase concentration (free chains), in adsorption isotherms, was carried out. However, the conformation of the polymeric chain can have a strong influence on the adsorption process and the interpretation of these isotherms can be, sometimes, arduous. Moreover, a considerable number of factors can interfere in this conformation, including the pH of the medium, the flexibility of the molecules, their cationicity, molar mass, concentration, and so forth. The isotherms obtained in this work were either of the L-type or the high-affinity type of curves, and results were fitted to the Langmuir and Freundlich models.

In this stage, the nature of the macroRAFT agent, including its composition, hydrophobic-hydrophilic balance and molar mass, is crucial for the adsorption process and,

therefore, has a direct impact, later, on the mechanisms that govern the synthesis of nanocomposite latex particles and on their final morphology. Therefore, the structures of the macroRAFT agents were designed considering, above all, their interactions with Laponite. While linear or pendent chains of PEG were chosen due to their capacity to adsorb on the basal faces of Laponite, AA, on the other hand, was expected to interact with the positively charged edges of the clay. BA units were incorporated into some macroRAFT agents in order to increase the hydrophobicity of the molecule (increasing, therefore, the hydrophobicity of the macroRAFT/Laponite particles to consequently enhance the affinity of the polymer shell for the platelets). DMAEMA was selected, as well, due to its capacity to adsorb on Laponite basal faces via strong electrostatic interaction.

The adsorption isotherms of anionic PAA_{40}-CTPPA macroRAFT agent, carried out at pH 7.5, indicated that a possible charge repulsion between the clay surface and the macroRAFT might have prevented PAA from adsorbing on the edges, since very low adsorption was observed in this case. It should also be considered that the positive charge density on the edges might not have been high enough for adsorption of the AA units. A comparison with the adsorption isotherm of P(AA_{16}-*co*-BA_{16})-CTPPA, carried out at pH 7.5 as well, revealed that, the presence of hydrophobic domains was essential for the adsorption process. While the adsorption of PAA_{40}-CTPPA was almost nonexistent at neutral pH, the adsorption of the BA-containing copolymer, P(AA_{16}-*co*-BA_{16})-CTPPA, fitted to the Freundlich model, presenting a high adsorption capacity.

The favorable effect of BA units on adsorption was also revealed by the isotherms of PEGA-based macroRAFT agents. The association of AA and PEG blocks in some macroRAFT structures was performed aiming to promote macroRAFT adsorption on both the surface and the edges of the platelets. However, this adsorption seemed to be dependent on the linear or pending configuration of the PEG chains, since, intermolecular complexes can be formed between AA and PEG segments, interfering in adsorption of the macroRAFT agent PEG_{45}-$_b$-PAA_{42}-CTPPA. This effect, nonetheless, was reduced when ethylene glycol units were disposed as pending segments, as in P(AA_{40}-*b*-$PEGA_4$)-CTPPA, for which a higher adsorption plateau was obtained. The isotherms of random copolymers composed of AA, BA and PEGA indicated that the random distribution of these monomers in the structure of the macroRAFT agent is less favorable for adsorption than their segmental distribution in blocks. The only two totally uncharged macroRAFT agents, PEG_{45}-CTPPA and P($PEGA_5$-*co*-BA_3)-CTPPA, presented a high affinity for Laponite and, fitting well to the Langmuir model, as expected from the L-type shape of curves, they presented high adsorbed amounts

of macroRAFT agents at saturation (Q_{max}), in agreement with what has been reported in the literature for the adsorption of a similar molecule (PEG-CTPPA) onto Laponite.[2]

High-affinity-type curves were also obtained for the adsorption of cationic macroRAFT agents onto Laponite, and all data fitted well to the Langmuir adsorption model. The adsorption of quaternized molecules (at pH 10) was compared to the adsorption of unmodified molecules (adjusted to pH 6) and the quaternization of the macroRAFT agents seemed to have an effect on adsorption. When compared to the untreated copolymer, a different profile, with higher adsorption plateau, was obtained for the quaternized molecule. A considerably higher affinity of the positively charged molecules for Laponite surface can be observed when comparing the adsorption isotherms of cationic, nonionic and anionic macroRAFT agents. Even though cationic systems can be more challenging in terms of colloidal stability, due to the greater ability of polycations to cause coagulation and bridging effects, which affects their effectiveness as stabilizers, the strong adsorption of these molecules onto clay minerals make them promising coupling agents for the synthesis of nanocomposites. However, uncharged macroRAFT agents PEG_{45}-CTPPA and P($PEGA_5$-*co*-BA_3)-CTPPA can be quite efficient for this purpose as well, considering that a relatively strong adsorption was observed for these molecules. Furthermore, they do not cause the charge inversion of the clay platelets and, consequently, are not associated with the stability issues caused by this phenomenon.

The synthesis of nanocomposites, which was the third step of the synthetic strategy proposed in this work, (described in Chapter 4), strongly relied on the colloidal suspension formed initially by the macroRAFT-modified Laponite platelets (and, therefore, on the adsorption of these molecules onto Laponite). In this aspect, a high amount of macroRAFT agent must be, preferably, adsorbed on the platelets with minimal free macroRAFT agent in the aqueous phase, to avoid that the nucleation process starts in the aqueous phase and follows the polymerization-induced self-assembly (PISA) mechanism to generate pure polymer particles.

During the synthesis of nanocomposites mediated by the linear PEG-CTPPA, macroRAFT chains suffered partitioning between the hydrophilic and hydrophobic phases and part of the macroRAFT, therefore, was not available to stabilize the forming particles. In addition, as this macroRAFT can partition, it should be more “hydrophobic” than the others, which led to a poor stabilizing capacity of the macroRAFT agent and to the formation of armored particles.

The use of macroRAFT agents with incorporated pending PEG chains, in general, led to the formation of polymeric nodules on the surface of Laponite, resulting in polymer-decorated particles (such as the dumbbell and janus morphologies). Indeed, considering that the edges of the platelets are highly hydrophilic, it could be expected that they might not get covered by PEG-based macroRAFT agents, since polymer chains could be forced to phase-separate from the edges. However, the association of AA moieties into PEG-based macroRAFT agents was expected to overcome such limitation, since these molecules could potentially adsorb on both the surface and the edges of the platelets. However, these macroRAFT agents were not able to generate truly encapsulated particles and, instead, polymeric nodules were formed around the platelets, generating structures with dumbbell and janus morphologies. The large amount of free macroRAFT agent (~85%) in the aqueous phase at the beginning of polymerization mediated by P(AA_{40}-*b*-$PEGA_4$)-CTPPA resulted in a large number of free polymeric particles, formed according to the PISA nucleation mechanism.

In this regard, the incorporation of BA units into the macroRAFT structure is a crucial strategy to increase the hydrophobicity of these molecules and to inhibit homogeneous nucleation during emulsion polymerization. In a similar manner to the PEG-based systems, the presence of a considerable amount of PAA-CTPPA macroRAFT in water (due to the high hydrophilicity of this molecule and to its low adsorption onto Laponite) led to secondary nucleation when this polymer was used as mediator in the synthesis of nanocomposites. The use of PAA-based macroRAFT agent resulted in stability issues. This was not the case for the P(AA-*co*-BA) copolymer, which on top of that gave surprising results in terms of morphology. The formation of dumbbell and janus structures seems to suggest that this copolymer can cause a better wetting of the clay surface than any other macroRAFT compositions used. This result corroborated the hypothesis that PAA is incapable of efficiently covering Laponite edges and suggested that PEG chains might render the faces of the clay less hydrophobic.

The use of DMAEMA-based copolymers containing random units of BA as mediators led to an even better wettability of the inorganic surface and to the formation of partially encapsulated particles, with clay platelets sandwiched between two polymer particles or, in some cases, with the edges and the basal surfaces covered with polymer. The strong adsorption of DMAEMA-based copolymers is among the main reasons for these results, since it helped to define the clay environment as the polymerization locus. However, a short chain length seemed to affect the stability of the nanocomposite latex particles and,

in this aspect, the longer chain was more efficient as stabilizer and, therefore, as mediator of the polymerization.

As an attempt to reach film-forming nanocomposite latexes, The DMAEMA-based formulation was adapted for different monomer mixtures. While the more hydrophobic mixtures (MMA:BA and Sty:BA 50:50) led to the formation of armored particles, the use of a more hydrophilic mixture (MA:BA 80:20) resulted in small dumbbell particles. Another parameter studied was the clay content and different particle morphologies were obtained. Small spherical particles of 20 nm were obtained in the absence of the clay and dumbbell or janus morphologies of ~100 nm were formed in the presence of 5 wt% of clay (based on the monomer mass). However, when the content was increased to 10 %, armored structures were formed, indicating that it is crucial to increase the macroRAFT concentration as well, to guarantee the stability of the janus and dumbbell particles formed. As a general rule, the DMAEMA-based copolymer offered a good coverage of the basal planes of Laponite with polymer. Nonetheless, this still did not happen for the edges of the platelets, and mostly uncovered-edges morphologies, such as dumbbell and janus, were obtained with this copolymer.

The different charges of the edges and the surface of the platelets may have led to the production of such morphologies and, for this purpose, the layer-by-layer approach was investigated as an attempt to achieve true and uniform encapsulation of Laponite. Relying on the initial surface charge inversion of Laponite platelets by the adsorption of P(DMAEMA$_{19}$-*co*-BA$_{14}$)-CTPPA macroRAFT agent, the layer-by-layer approach was expected to guarantee a full coverage of the platelets by the adsorption a second layer of oppositely charged P(AA$_{16}$-*co*-BA$_{16}$)-CTPPA macroRAFT agents to efficiently cover the modified surfaces as well as the positive edges of the clay. Indeed, images show that by this approach it was possible to obtain multiple encapsulated hybrid particles.

Two hybrid latexes synthesized in the presence of DMAEMA-based macroRAFT agent with different clay contents were selected for a further investigation of the thermo-mechanical behavior of the films (by DMA) as well as of their microstructure (by FIB-SEM). The dumbbell morphology of the particles obtained in both cases led to a homogeneous distribution of the platelets within the polymer matrix, as observed by FIB-SEM. The dumbbell morphology may have been crucial for the formation of a connected network of platelets in the matrix, which resulted in a significant increase in the stiffness of the material, in comparison to the pure polymer matrix. By having uncoated edges, such dumbbell

particles allowed platelet–platelet interactions within the polymer matrix and allowed the arrangement of the platelets in a mechanical percolation structure.

In summary, the synthetic strategy proposed led to the formation of nanocomposite particles with a variety of different morphologies. In fact, the individual encapsulation of the Laponite platelets with a thin polymer layer, in order to maintain the shape anisotropy of the particles, which was the main objective of this work, has shown to be an extremely challenging and complicated task. The lamellar shape of the platelets, their high aspect ratio, high surface energy and opposite charges on the surface and on the edges may have made the effective encapsulation of the particles difficult to be achieved. Some other aspects can be considered fundamental for the formation of the particles obtained in this work, such as the low compatibility of the edges of the clay with the coupling agent and, therefore, with the polymer phase. In this aspect, even though the layer-by-layer approach can be quite complicated in terms of colloidal stability, it can represent an interesting and promising strategy for encapsulation. In fact, the emulsion polymerizations mediated by each macroRAFT agent in the presence of Laponite platelets represent, individually, a rich and complex system that offers numerous possibilities for encapsulation. Even though, unfortunately, the depth study of each one of them was not the main objective of this thesis and, for this reason, this work was not explored further into this direction, it represents a potential approach for future attempts to encapsulate Laponite.

Another possible interesting approach would be to try to extend the use of the REEP technique to other RDRP techniques, such as NMP. This field has not been well explored yet. There are mechanism differences between these techniques that could be interesting for encapsulation purposes. While NMP and ATRP operate via a reversible termination reaction, RAFT operates via reversible transfer reactions In RAFT emulsion polymerization, a water-soluble initiator is used and initiation takes place in the water phase. In the case of NMP and ATRP, this process would suffer a major change, since the designed macroinitiators would be attached to the inorganic surface. This study could give interesting insight regarding the events involved in the REEP process as well.

Despite requiring a careful planning of best conditions and selection of components, the REEP of inorganic particles is a versatile process that can be easily implemented. Final materials obtained by this method could find applications in diverse fields, such as paints, coatings, adhesives or in the biomedical field.

References

1 DAS, P.; ZHONG, W.; CLAVERIE, J. P. Copolymer nanosphere encapsulated CdS quantum dots prepared by RAFT copolymerization: Synthesis, characterization and mechanism of formation. **Colloid and Polymer Science,** v. 289, n. 14, p. 1519-1533, sept. 2011.

2 GUIMARAES, T. R.; CHAPARRO, T. D. C.; D'AGOSTO, F.; LANSALOT, M.; DOS SANTOS, A. M.; BOURGEAT-LAMI, E. Synthesis of multi-hollow clay-armored latexes by surfactant-free emulsion polymerization of styrene mediated by poly(ethylene oxide)-based macroRAFT/Laponite complexes. **Polymer Chemistry,** v. 5, n. 22, p. 6611-6622, nov. 2014.

Annexes

Nº d'ordre Année 2016

THÈSE

Présentée devant

L'UNIVERSITÉ DE SÃO PAULO – L'ÉCOLE D'INGÉNIERIE DE LORENA

et

L'UNIVERSITÉ CLAUDE BERNARD – LYON 1

ECOLE DOCTORALE DE CHIMIE (ED206)

Spécialité : Chimie

DIPLOME DE DOCTORAT

(arrêté du 7 août 2006)

SYNTHESIS OF NANOCOMPOSITES WITH ANISOTROPIC PROPERTIES BY CONTROLLED RADICAL EMULSION POLYMERIZATION

Soutenue publiquement le 29 Mars 2016

par Thaíssa DE CAMARGO CHAPARRO

Directrice de thèse : Elodie BOURGEAT-LAMI

Co-directeur de thèse : Amilton Martins dos SANTOS

Soutenue devant le jury composé de :

M. Philippe CASSAGNAU	Professeur, Université Lyon 1	Examinateur
M. Johan P. A. HEUTS	Professeur, Eindhoven University of Technology	Rapporteur
M^{me} Vanessa PRÉVOT	Chargée de recherche, CNRS	Rapporteur
M. Reinaldo GIUDICI	Professeur, University of São Paulo	Examinateur
M^{me} Elodie BOURGEAT-LAMI	Directeur de recherche, CNRS	Directrice
M. Amilton Martins dos SANTOS	Professeur, University of São Paulo	Co-directeur

UNIVERSITE CLAUDE BERNARD - LYON 1

Président de l'Université	**M. François-Noël GILLY**
Vice-président du Conseil d'Administration	M. le Professeur Hamda BEN HADID
Vice-président du Conseil des Etudes et de la Vie Universitaire	M. le Professeur Philippe LALLE
Vice-président du Conseil Scientifique	M. le Professeur Germain GILLET
Directeur Général des Services	M. Alain HELLEU

COMPOSANTES SANTE

Faculté de Médecine Lyon Est – Claude Bernard	Directeur : M. le Professeur J. ETIENNE
Faculté de Médecine et de Maïeutique Lyon Sud – Charles Mérieux	Directeur: Mme la Professeure C. BURILLON
Faculté d'Odontologie	Directeur : M. le Professeur D. BOURGEOIS
Institut des Sciences Pharmaceutiques et Biologiques	Directeur : Mme la Professeure C. VINCIGUERRA
Institut des Sciences et Techniques de la Réadaptation	Directeur : M. le Professeur Y. MATILLON
Département de formation et Centre de Recherche en Biologie Humaine	Directeur : Mme. la Professeure A-M. SCHOTT

COMPOSANTES ET DEPARTEMENTS DE SCIENCES ET TECHNOLOGIE

Faculté des Sciences et Technologies	Directeur : M. F. DE MARCHI
Département Biologie	Directeur : M. le Professeur F. FLEURY
Département Chimie Biochimie	Directeur : Mme Caroline FELIX
Département GEP	Directeur : M. Hassan HAMMOURI
Département Informatique	Directeur : M. le Professeur S. AKKOUCHE
Département Mathématiques	Directeur : M. le Professeur Georges TOMANOV
Département Mécanique	Directeur : M. le Professeur H. BEN HADID
Département Physique	Directeur : M. Jean-Claude PLENET
UFR Sciences et Techniques des Activités Physiques et Sportives	Directeur : M. Y.VANPOULLE
Observatoire des Sciences de l'Univers de Lyon	Directeur : M. B. GUIDERDONI
Polytech Lyon	Directeur : M. P. FOURNIER
Ecole Supérieure de Chimie Physique Electronique	Directeur : M. G. PIGNAULT
Institut Universitaire de Technologie de Lyon 1	Directeur : M. le Professeur C. VITON
Ecole Supérieure du Professorat et de l'Education	Directeur : M. le Professeur A. MOUGNIOTTE
Institut de Science Financière et d'Assurances	Directeur : M. N. LEBOISNE

Annex 1 Extended abstracts

Résumé

Les nanocomposites ont suscité un intérêt croissant au cours de ces dernières années en raison des nombreux avantages qu'ils offrent par rapport aux composites traditionnels. Parmi eux, les nanocomposites à charges lamellaires sont particulièrement intéressants, car ils combinent les meilleurs attributs des silicates lamellaires avec la facilité de transformation et de manipulation des polymères organiques.[1-6] Comme l'efficacité de renforcement des charges minérales est fortement liée à leur facteur de forme, des particules anisotropes, comme des plaquettes d'argile, ont un attrait tout particulier. En plus de permettre d'améliorer les propriétés mécaniques du matériaux, notamment sa dureté et sa résistance aux rayures, les plaquettes d'argile peuvent aussi contribuer à améliorer d'autres propriétés, telles que des propriétés optiques et de barrière aux gaz, tout en réduisant de manière significative le poids et donc le coût des matériaux résultants.

Cependant, parvenir à disperser uniformément des nano-objets anisotropes à l'échelle nanométrique afin de maintenir leur intégrité tout en préservant leurs propriétés physiques uniques, est particulièrement difficile. Des nombreux travaux ont porté sur le contrôle de l'arrangement de telles nanoparticules et sur leur distribution au sein de matrices polymères. En outre, leur alignement permettrait d'influencer considérablement les propriétés mécaniques, électriques ou optiques, ainsi que les performances macroscopiques des matériaux résultants. Un moyen efficace pour réaliser une bonne dispersion d'objets anisotropes avec une distribution contrôlée des nanoparticules est de les encapsuler par une couche de polymère. Parmi les méthodes de synthèse décrites dans la littérature, les techniques de polymérisation radicalaire par désactivation réversible (PRDR) présentent l'avantage de permettre un contrôle précis de la composition, de l'épaisseur et de la fonctionnalité de la couche de polymère.

Bien qu'il existe beaucoup de stratégies de synthèse en milieu solvant utilisant la PRDR afin de revêtir la surface de particules inorganiques par des polymères, les procédés en milieux aqueux dispersés tels que la polymérisation en émulsion, en suspension, en dispersion ou en miniémulsion ont été encore peu explorés jusqu'ici. La polymérisation en emulsion, un procédé de polymérisation radicalaire utilisé industriellement pour fabriquer des adhésifs, des peintures ainsi que divers autres produits, est particulièrement intéressante.

Les stratégies actuellement disponibles pour produire des particules inorganiques encapsulées par polymérisation en émulsion, présentent cependant encore des limitations qui les empêchent d'être des techniques universelles. En effet, l'utilisation de la polymérisation en émulsion classique (non contrôlée) pour encapsuler des particules inorganiques de façon individuelle conduit rarement à la morphologie coeur-écorce désirée et des objets de morphologie plus complexe tels que des particules « bonhommes de neige », « marguerites », des particules « framboises » ou encore des particules « Janus » sont généralement obtenus.

Récemment, un nouveau procédé de synthèse de nanocomposites organique / inorganique par polymérisation en émulsion via l'utilisation de la technique de transfert de chaîne réversible par addition-fragmentation (RAFT),[7] a été reporté par Hawkett et al.[8] pour encapsuler des pigments organiques (bleu de phtalocyanine) et des particules inorganiques hydrophiles (dioxyde de titane), et par la suite étendu par Daigle et Claverie[9] à l'encapsulation de différents types de particules inorganiques telles que des métaux ou des oxydes métalliques. Cette stratégie d'encapsulation par polymérisation en émulsion assistée par des macro-agents RAFT,[10, 11] repose sur l'utilisation de macro-agents de contrôle (appelés macro-agents RAFT ou macroRAFTs) hydrophiles comme agents de couplage et comme précurseurs de stabilisants.

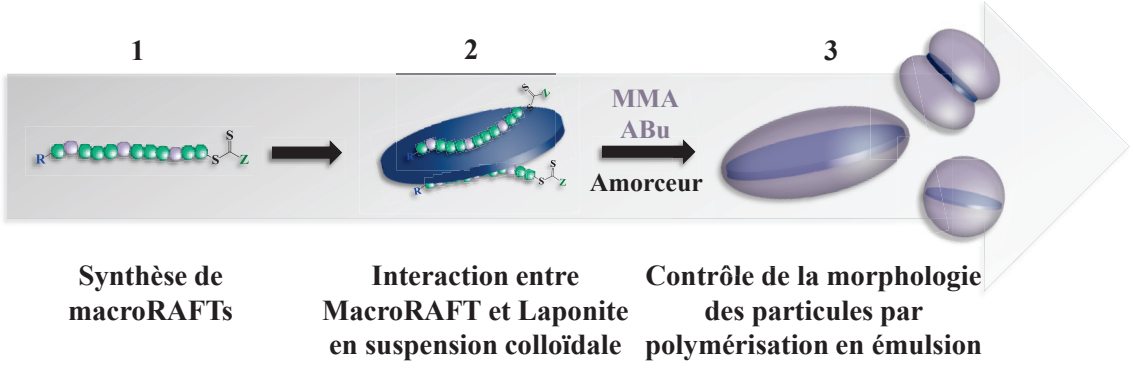
Diverses autres particules ont été encapsulées avec succès par ce procédé, y compris des nanoparticules de sulfure de cadmium[12] et de sulfure de plomb,[13] de l'oxyde de cérium,[14-17] des nanotubes de carbone,[18, 19] des plaquettes d'argile (Gibbsite,[20] Montmorillonite[21]) ou encore des feuillets d'oxyde de graphite.[22] L'encapsulation de nano-objets anisotropes tels que des argiles par ce procédé, n'est cependant pas trivial. La forme plaquettaire des particules, leur facteur de forme élevé et leur forte énergie de surface entravent le processus d'encapsulation et la plupart des tentatives pour encapsuler des plaquettes d'argile non chimiquement modifiées[23] ou modifiées en surface[24-26] par polymérisation en émulsion conduisent à la formation de particules de morphologie « carapace » (particules de latex décorées en surface par les plaquettes d'argile). Plusieurs paramètres liés notamment à des mécanismes de contrôle cinétique et/ou thermodynamique, doivent être optimisés pour le succès de l'encapsulation. Outre l'encapsulation, un autre objectif est de former une couche mince de polymère à la surface des particules de telle sorte que l'anisotropie de forme des particules soit conservée. La production de telles particules de latex anisotropes de morphologie cœur-écorce suscite un intérêt croissant car ces particules sont susceptibles

d'induire une anisotropie dans le film final, ce qui est particulièrement intéressant afin de former des matériaux ayant des propriétés potentiellement améliorées qui peuvent trouver des applications dans les domaines des revêtements ou des adhésifs,[27] par exemple. Pour cette raison, contrôler l'orientation des plaquettes d'argile dans le film polymère, est essentiel en vue d'obtenir les propriétés désirées pour le revêtement final.

L'objectif de ce travail de thèse était de préparer des latex nanocomposites à base d'argile, la Laponite RD, en émulsion aqueuse, à l'aide de la polymérisation radicalaire contrôlée par transfert de chaîne réversible par addition-fragmentation (RAFT) en utilisant la stratégie d'encapsulation par polymérisation en émulsion assistée par des macro-agents RAFT. Les plaquettes de Laponite ont été choisies comme charge inorganique surtout pour leur anisotropie de forme, ce qui pourrait permettre l'elaboration de films nanostructurés, mais aussi pour leurs propriétés thermiques et mécaniques, leur pureté chimique élevée et la distribution uniforme en taille des plaquettes. Le principal défi est de maintenir les particules d'argile à l'intérieur des particules de latex, de façon individuelle tout en préservant leur anisotropie de forme et la stabilité colloïdale du milieu.

La stratégie de synthèse proposée dans ce travail pour encapsuler les particules de Laponite, permet potentiellement l'élaboration d'une grande variété de morphologies de particules pouvant conduire à des films composites de nanostructures contrôlées. Elle est composée de trois étapes principales, comme représenté schématiquement sur la Figure A1.1.

Figure A1.1 – Schéma illustrant les différentes étapes de synthèse de la stratégie adoptée.



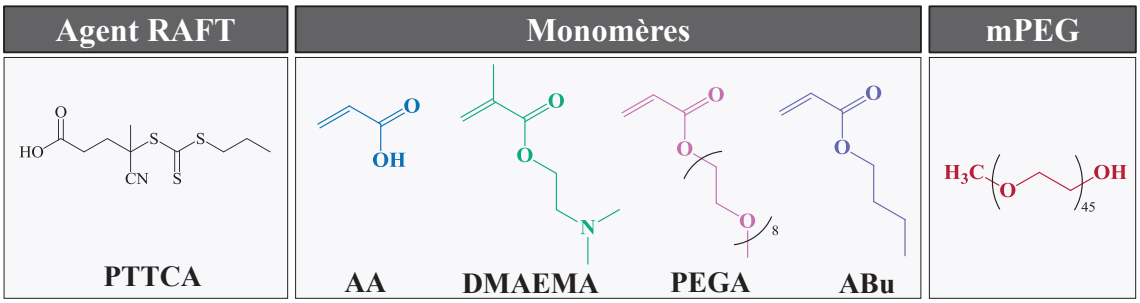
Source : Élaboré par l'auteur.

Dans une première partie, la **synthèse des macro-agents RAFT** a été réalisée. Des polymères hydrophiles (macroRAFTs) à base de polyéthylène glycol (PEG), d'acide acrylique (AA) ou de méthacrylate de N,N- diméthylaminoéthyle (DMAEMA) et

comportant des unités hydrophobes d'acrylate de *n*-butyle (ABu) (dans certains cas) et un groupe trithiocarbonate terminal ont été tout d'abord synthétisés par polymérisation en solution en utilisant l'acide 4-cyano-4-(propylsulfanylthiocarbonyl) sulfanyl pentanoïque, comme agent de transfert.

Douze macro-agents RAFT de structures différentes ont été conçus en tenant compte de leur capacité à interagir avec les particules inorganiques (via des groupes d'ancrage appropriés) et à contrôler la polymérisation du méthacrylate de méthyle (MMA), ou de l'acrylate de méthyle (MA) avec l'ABu à partir de la surface des particules inorganiques. L'agent RAFT, les monomères et le poly(éthylène glycol) éther de méthyle (mPEG) utilisés pour la synthèse des macro-agents RAFT sont représentés sur la Figure A1.2.

Figure A1.2 – Agent RAFT, monomères et mPEG utilisés pour la synthèse des macro-agents RAFT.



Source : Élaboré par l'auteur.

Ensuite, **l'interaction entre les macroRAFTs et l'argile en suspension colloïdale** a été étudiée à travers le tracé des isothermes d'adsorption. Les données ont été modélisés en appliquant les modèles d'adsorption de Langmuir et Freundlich. Alors que les macro-agents RAFT à base de DMAEMA présentent une forte interaction avec la surface de l'argile par échange cationique (courbes de type H), le PEGA et, en particulier les macroRAFTs à base d'AA ont montré des adsorptions plus faibles.

Dans une troisième partie, le **contrôle de la morphologie des particules hybrides par polymérisation en émulsion** sans tensioactif a été evalué. En agissant comme des agents de couplage et des stabilisants, les macroRAFTs ont eté utilisés dans la copolymérisation en émulsion du mélange MMA/ABu 90/10 en mode semi-continu en presence d'argile. Une sélection minutieuse des conditions expérimentales a été nécessaire. Différents paramètres ont été explorés dans la polymérisation RAFT en émulsion en présence des particules de Laponite. Les principaux paramètres étudiés sont la nature du macro-agent RAFT, sa balance hydrophobe-hydrophile et sa masse molaire.

Des particules de différentes morphologies ont été obtenues et les morphologies ont été reliées à la nature et à la concentration de l'agent macroRAFT, à la température de transition vitreuse du copolymère final (fonction de la composition du mélange de monomères hydrophobes) et aux conditions de polymérisation. Les analyses par cryo-microscopie électronique en transmission (cryo-MET) ont mis en évidence la formation de particules de latex en surface des plaquettes d'argile, des particules de morphologie « haltère », « Janus », « carapace » ou encore des particules multi-encapsulées (plusieurs plaquettes encapsulées dans chaque particule de latex).

L'utilisation des macro-agents RAFT à base de PEG a conduit surtout à la formation de nodules de polymère sur la surface de la Laponite, donnant lieu à des particules de polymère décorées (tels que des morphologies « haltères » et « Janus ») ou à des particules « carapace ». Le macro-agent RAFT à base d'AA a conduit à des particules « haltères » et « Janus », tandis que la forte adsorption des copolymères à base de DMAEMA a conduit à une meilleure mouillabilité de la surface inorganique et à la formation de particules encapsulées, avec des plaquettes d'argile prises en sandwich entre deux particules de polymère, et dans certains cas, avec les bords et les faces des plaquettes recouvertes de polymère. Une approche « *couche par couche* » a été également évaluée, en adsorbant successivement des copolymères à base d'AA et des copolymères à base de DMAEMA. Cette approche a conduit à la formation de particules multi-encapsulées.

Les latex composites les plus prometteurs ont été adaptés à des formulations conduisant à des latex filmifiables possédant par conséquent des températures de transition vitreuse plus faibles. Les films de polymère/Laponite ont été préparés par séchage et les propriétés mécaniques des films ont été étudiées par spectrométrie mécanique dynamique pour comprendre la relation entre les paramètres de synthèse (et donc la morphologie des particules), la microstructure 3D des films obtenus et leur renforcement.

Resumo

Nanocompósitos têm atraído crescente atenção nos últimos anos devido aos inúmeros benefícios que eles podem oferecer em relação aos compósitos tradicionais. Entre estes materiais, os nanocompósitos de cargas lamelares são particularmente interessantes por combinarem os melhores atributos dos filossilicatos com a facilidade de processamento e manuseio dos polímeros orgânicos.[1-6] Uma vez que a eficiência de reforço das cargas minerais está fortemente relacionada com o seu fator de forma, partículas anisotrópicas, como as lamelas de argila, são particularmente interessantes. Além de atribuir melhores propriedades mecânicas aos materiais, em particular com relação à dureza e à resistência ao risco, a presença de lamelas de argila também pode contribuir para melhorar outras propriedades, tais como as propriedades óticas e de barreira a gases, enquanto reduzem significativamente o peso e, portanto, o custo dos materiais resultantes.

No entanto, dispersar nano-objetos anisotrópicos de maneira uniforme e em escala nanométrica a fim de manter sua integridade, preservando suas propriedades físicas únicas, é um desafio particularmente difícil. Inúmeros estudos têm sido dedicados ao controle do arranjo dessas nanopartículas e de sua distribuição nas matrizes poliméricas. Além disso, o alinhamento das partículas pode influenciar significativamente as propriedades mecânicas, eléctricas ou óticas, assim como o desempenho macroscópico dos materiais resultantes. Uma forma eficaz de conseguir uma boa dispersão dos objetos anisotrópicos, com uma distribuição controlada das nanopartículas, é encapsulá-los com uma camada de polímero. Entre os métodos de síntese descritos na literatura, técnicas de polimerização radicalar por desativação reversível (RDRP) tem a vantagem de permitir um controle preciso da composição, espessura e funcionalidade da camada de polímero

Embora existam muitas estratégias de síntese utilizando RDRP em solvente para revestir a superfície de partículas inorgânicas com polímero, os métodos em meio aquoso, tais como polimerização em emulsão, suspensão, dispersão ou miniemulsão ainda têm sido pouco explorados. A polimerização em emulsão, um processo de polimerização radicalar amplamente utilizado na indústria para a produção de adesivos, tintas e outros produtos, é particularmente interessante. As estratégias disponíveis atualmente para a encapsulação de partículas inorgânicas via polimerização em emulsão, no entanto, ainda têm limitações que as impedem de ser técnicas universais. De fato, a utilização da polimerização em emulsão convencional (não controlada) para a encapsulação de partículas inorgânicas de forma

individual raramente conduz à morfologia do tipo núcleo-casca desejada e morfologias mais complexas, tais como partículas do tipo *snowman*, *daisy*, *raspberry* ou partículas *janus,* são geralmente obtidas.

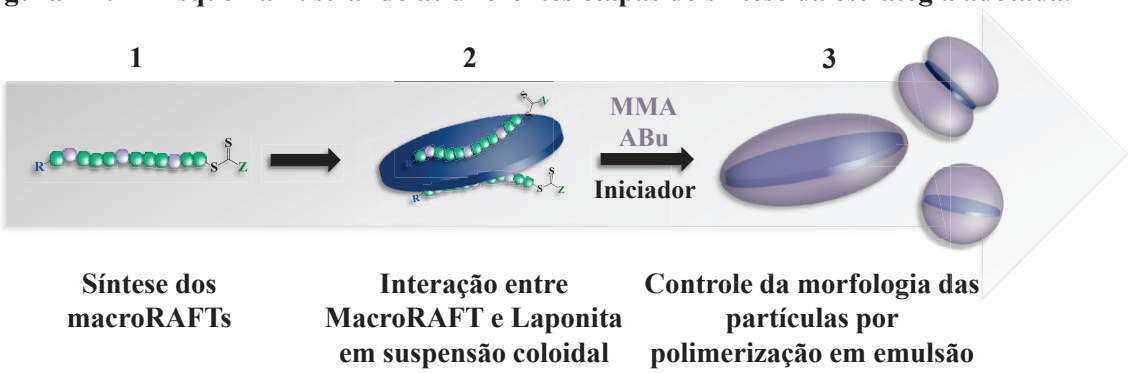
Recentemente, um novo método de síntese de nanocompósitos orgânicos/inorgânicos via polimerização em emulsão, utilizando a técnica de polimerização radicalar controlada por transferência de cadeia via adição-fragmentação reversível (RAFT),[7] foi reportada por Hawkett et al.[8] para encapsular pigmentos orgânicos (azul de ftalocianina) e partículas inorgânicas hidrofílicas (dióxido de titânio), e subsequentemente utilizado por Daigle e Claverie[9] para a encapsulação de diferentes tipos de partículas inorgânicas, tais como metais e óxidos metálicos. Esta estratégia de encapsulação via polimerização em emulsão assistida por macroagentes RAFT[10, 11] baseia-se na utilização de macroagentes de controle (chamados de macroagentes RAFT ou macroRAFTs) hidrofílicos como agentes de acoplamento e precursores de estabilizantes.

Diversas outras partículas foram encapsuladas com sucesso por este método, incluindo nanopartículas de sulfeto de cádmio[12] e de chumbo,[13] óxido de cério,[14-17] nanotubos de carbono,[18, 19] lamelas de argila (gibsita[20] e Montmorilonita[21]) ou óxido de grafite.[22] A encapsulação de nanopartículas anisotrópicas, tais como as argilas, por este método, no entanto, não é trivial. A forma lamelar das partículas, a sua alta razão de aspecto e a elevada energia superficial dificultam o processo de encapsulação e a maioria das tentativas de encapsular partículas de argila não modificadas quimicamente[23] ou modificadas em sua superfície[24-26] via polimerização em emulsão resultou na formação de partículas armadas ou blindadas (partículas de látex decoradas na superfície com as lamelas de argila). Diversos parâmetros, relacionados principalmente aos mecanismos de controle cinético e/ou termodinâmico, devem ser otimizados para uma encapsulação bem-sucedida. O objetivo, além de encapsular as partículas inorgânicas, é formar uma fina camada de polímero sobre a superfície das partículas de modo que a sua anisotropia de forma seja mantida. A produção de tais partículas anisotrópicas de látex com morfologia núcleo-casca têm atraído crescente atenção nos últimos anos, visto que estas partículas podem induzir anisotropia ao filme final, o que é desejável para a obtenção de materiais com propriedades melhoradas que podem, potencialmente, encontrar aplicações nos campos de revestimentos ou adesivos,[27] por exemplo. Por esta razão, controlar a orientação das lamelas de argila no filme polimérico é essencial para a obtenção de materiais de revestimento que apresentem as propriedades desejadas.

O objetivo deste trabalho de tese foi a preparação de látices nanocompósitos à base da argila Laponita RD em emulsão aquosa, via polimerização radicalar controlada por transferência de cadeia via adição-fragmentação reversível (RAFT), usando a estratégia de encapsulação via polimerização em emulsão assistida por macroagentes RAFT. A Laponita foi escolhida como carga inorgânica devido principalmente à forma anisotrópica de suas lamelas, o que permite a elaboração de filmes nanoestruturados, mas também por suas propriedades térmicas e mecânicas, por sua alta pureza química e pela distribuição uniforme, em termos de tamanho, de suas partículas. O principal desafio é manter as partículas de argila dentro das partículas de látex, individualmente, mantendo a sua anisotropia de forma e a estabilidade coloidal do meio.

A estratégia de síntese proposta neste trabalho para encapsular as partículas de Laponita permite o desenvolvimento de uma ampla variedade de morfologias de partícula, podendo levar à formação de filmes nanocompósitos com estrutura controlada. Ela é composta de três etapas principais, como mostrado esquematicamente na Figura A1.1.

Figura A1.1 – Esquema ilustrando as diferentes etapas de síntese da estratégia adotada.



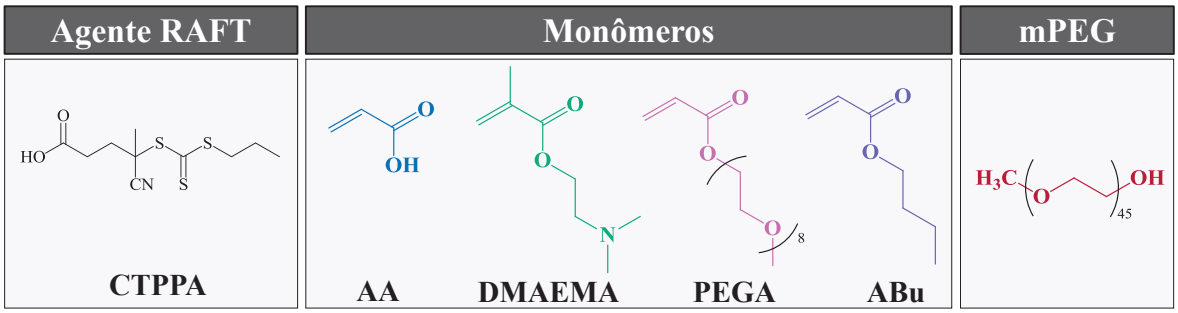
Fonte: elaborado pela autora.

Na primeira etapa, foi realizada a **síntese dos macroagentes RAFT**. Polímeros hidrofílicos (macroRAFTs) à base de poli(etileno glicol) (PEG), de ácido acrílico (AA) ou de metacrilato de N,N-dimetilaminoetila (DMAEMA) que contêm unidades hidrofóbicas de acrilato de *n*-butila (ABu) (em alguns casos) e um grupo tritiocarbonílico terminal foram inicialmente sintetizados por polimerização em solução utilizando o ácido 4-ciano-4-(propilsulfaniltiocarbonil) sulfanil pentanóico como um agente de transferência de cadeia.

Doze macroagentes RAFT de diferentes estruturas foram sintetizados levando em conta a sua capacidade de interagir com as partículas inorgânicas (pela presença de grupos âncoras adequados) e de controlar a polimerização do metacrilato de metila (MMA), ou do

acrilato de metila (MA), com o ABu à partir da superfície das partículas inorgânicas. O agente RAFT, os monômeros e o poli(etileno glicol) metil éter (mPEG), utilizados na síntese dos macroagentes RAFT estão representados na Figura A1.2.

Figura A1.2 – Agente RAFT, monômeros e mPEG utilizados para a síntese dos macroagentes RAFT.



Fonte: elaborado pela autora.

Em seguida, a **interação entre os macroRAFTs e a argila em suspensão coloidal** foi estudada por isotermas de adsorção. Os resultados foram ajustados aos modelos de adsorção de Langmuir e Freundlich. Enquanto os macroagentes RAFT à base de DMAEMA apresentam uma forte interação com a superfície da argila por troca catiônica (curvas do tipo H), os macroagentes RAFT à base de PEGA e, em especial, de AA apresentaram uma adsorção mais fraca.

Em uma terceira etapa, o **controle da morfologia das partículas híbridas por polimerização em emulsão** sem surfatante foi avaliado. Atuando como agentes de acoplamento e estabilizantes, esses macroRAFTs foram então utilizados na copolimerização em emulsão da mistura MMA/ABu 90/10, em processo semicontínuo, na presença da argila Laponita. Para tanto, uma seleção minuciosa das condições experimentais foi necessária. Diferentes parâmetros foram explorados na polimerização RAFT em emulsão na presença das partículas de Laponita. Os principais parâmetros estudados foram a natureza do macroagente RAFT, o balanço hidrofóbico-hidrofílico da molécula e sua massa molar.

Partículas de látex híbrido de diferentes morfologias foram obtidas e os resultados foram correlacionados à natureza e à concentração dos macroRAFTs, à temperatura de transição vítrea do copolímero final (função da composição da mistura de monômeros) e às condições de polimerização. As análises de microscopia eletrônica de transmissão à temperatura criogênica (Cryo-TEM) evidenciaram a formação de lamelas de Laponita decoradas com partículas de polímero (várias partículas de látex localizadas na superfície das lamelas), de partículas do tipo *dumbbell*, *janus*, blindadas (partículas de látex decoradas

com lamelas de argila em sua superfície) ou ainda de partículas multiencapsuladas (diversas lamelas encapsuladas dentro de uma única partícula de látex).

A utilização de macroagentes RAFT à base de PEG resultou, principalmente, na formação de nódulos poliméricos na superfície da Laponita, levando à formação de partículas de polímero decoradas (tais como as morfologias *dumbbell* e *janus*) ou partículas blindadas. O macroagente RAFT à base de AA levou à obtenção de partículas *dumbbell* e *janus*, enquanto a forte adsorção dos copolímeros à base de DMAEMA resultou em uma melhor molhabilidade da superfície inorgânica e na formação de partículas encapsuladas, com as lamelas de argila dispostas em forma de sanduíche entre duas partículas de polímero e, em alguns casos, com as bordas e as faces das lamelas cobertas de polímero. Uma abordagem "camada por camada" também foi adotada pela adsorção sucessiva de copolímeros à base de AA e copolímeros à base de DMAEMA na superfície da argila. Esta abordagem levou à formação de partículas multiencapsuladas.

Os látices compósitos mais promissores foram adaptados a formulações que conduzem à látices capazes de formar filme e que possuem, consequentemente, temperatura de transição vítrea mais baixa. Os filmes nanocompósitos foram preparados e suas propriedades mecânicas foram estudadas por análise dinâmico-mecânica para compreensão da relação entre os parâmetros de síntese (e, portanto, a morfologia das partículas), a microestrutura 3D dos filmes e seu reforço.

References

1 ALEXANDRE, M.; DUBOIS, P. Polymer-layered silicate nanocomposites: Preparation, properties and uses of a new class of materials. **Materials Science & Engineering R-Reports,** v. 28, n. 1-2, p. 1-63, jun. 2000.

2 RAY, S. S.; OKAMOTO, M. Polymer/layered silicate nanocomposites: A review from preparation to processing. **Progress in Polymer Science,** v. 28, n. 11, p. 1539-1641, nov. 2003.

3 OKAMOTO, M. Recent advances in polymer/layered silicate nanocomposites: An overview from science to technology. **Materials Science and Technology,** v. 22, n. 7, p. 756-779, july 2006.

4 PAVLIDOU, S.; PAPASPYRIDES, C. D. A review on polymer-layered silicate nanocomposites. **Progress in Polymer Science,** v. 33, n. 12, p. 1119-1198, dec. 2008.

[5] RAY, S. S. Recent trends and future outlooks in the field of clay-containing polymer nanocomposites. **Macromolecular Chemistry and Physics,** v. 215, n. 12, p. 1162-1179, june 2014.

[6] MITTAL, V. Polymer layered silicate nanocomposites: A review. **Materials,** v. 2, n. 3, p. 992-1057, sept. 2009.

[7] BARNER-KOWOLLIK, C. Introduction. In: _____ (Ed.). **Handbook of RAFT polymerization**: Wiley-VCH Verlag GmbH & Co. KGaA, 2008. p.1-4.

[8] NGUYEN, D.; ZONDANOS, H. S.; FARRUGIA, J. M.; SERELIS, A. K.; SUCH, C. H.; HAWKETT, B. S. Pigment encapsulation by emulsion polymerization using macro-RAFT copolymers. **Langmuir,** v. 24, n. 5, p. 2140-2150, 2008.

[9] DAIGLE, J.-C.; CLAVERIE, J. P. A simple method for forming hybrid core-shell nanoparticles suspended in water. **Journal of Nanomaterials,** v. 2008, p. 1-8, 2008.

[10] PAVLOVIC, M.; ADOK-SIPICZKI, M.; NARDIN, C.; PEARSON, S.; BOURGEAT-LAMI, E.; PREVOT, V.; SZILAGYI, I. Effect of macroRAFT copolymer adsorption on the colloidal stability of layered double hydroxide nanoparticles. **Langmuir,** v. 31, n. 46, p. 12609-12617, nov. 2015.

[11] CENACCHI-PEREIRA, A. M. **Synthesis of anisotropic polymer/inorganic composite particles via RAFT-mediated emulsion polymerization**. 2014. 286 (Ph.D.). École doctorale de chimie, University of Lyon, Lyon.

[12] DAS, P.; ZHONG, W.; CLAVERIE, J. P. Copolymer nanosphere encapsulated CdS quantum dots prepared by RAFT copolymerization: Synthesis, characterization and mechanism of formation. **Colloid and Polymer Science,** v. 289, n. 14, p. 1519-1533, sept. 2011.

[13] DAS, P.; CLAVERIE, J. P. Synthesis of single-core and multiple-core core-shell nanoparticles by RAFT emulsion polymerization: Lead sulfide-copolymer nanocomposites. **Journal of Polymer Science Part A: Polymer Chemistry,** v. 50, n. 14, p. 2802-2808, jul. 2012.

[14] ZGHEIB, N.; PUTAUX, J.-L.; THILL, A.; BOURGEAT-LAMI, E.; D'AGOSTO, F.; LANSALOT, M. Cerium oxide encapsulation by emulsion polymerization using hydrophilic macroRAFT agents. **Polymer Chemistry,** v. 4, n. 3, p. 607-614, 2013.

[15] GARNIER, J.; WARNANT, J.; LACROIX-DESMAZES, P.; DUFILS, P. E.; VINAS, J.; VANDERVEKEN, Y.; VAN HERK, A. M. An emulsifier-free RAFT-mediated process for the efficient synthesis of cerium oxide/polymer hybrid latexes. **Macromolecular Rapid Communications,** v. 33, n. 16, p. 1388-1392, aug. 2012.

[16] GARNIER, J.; WARNANT, J.; LACROIX-DESMAZES, P.; DUFILS, P.-E.; VINAS, J.; VAN HERK, A. Sulfonated macro-RAFT agents for the surfactant-free synthesis of cerium oxide-based hybrid latexes. **Journal of Colloid and Interface Science,** v. 407, p. 273-281, oct. 2013.

17 WARNANT, J.; GARNIER, J.; VAN HERK, A.; DUFILS, P.-E.; VINAS, J.; LACROIX-DESMAZES, P. A CeO_2/PVDC hybrid latex mediated by a phosphonated macro-RAFT agent. **Polymer Chemistry,** v. 4, n. 23, p. 5656-5663, dec. 2013.

18 NGUYEN, D.; SUCH, C. H.; HAWKETT, B. S. Polymer coating of carboxylic acid functionalized multiwalled carbon nanotubes via reversible addition-fragmentation chain transfer mediated emulsion polymerization. **Journal of Polymer Science Part A: Polymer Chemistry,** v. 51, n. 2, p. 250-257, jan. 2013.

19 ZHONG, W.; ZEUNA, J. N.; CLAVERIE, J. P. A versatile encapsulation method of noncovalently modified carbon nanotubes by RAFT polymerization. **Journal of Polymer Science Part A: Polymer Chemistry,** v. 50, n. 21, p. 4403-4407, 2012.

20 ALI, S. I.; HEUTS, J. P. A.; HAWKETT, B. S.; VAN HERK, A. M. Polymer encapsulated gibbsite nanoparticles: Efficient preparation of anisotropic composite latex particles by RAFT-based starved feed emulsion polymerization. **Langmuir,** v. 25, n. 18, p. 10523-10533, sept. 2009.

21 MBALLA MBALLA, M. A.; ALI, S. I.; HEUTS, J. P. A.; VAN HERK, A. M. Control of the anisotropic morphology of latex nanocomposites containing single montmorillonite clay particles prepared by conventional and reversible addition-fragmentation chain transfer based emulsion polymerization. **Polymer International,** v. 61, n. 6, p. 861-865, 2012.

22 HUYNH, V. T.; NGUYEN, D.; SUCH, C. H.; HAWKETT, B. S. Polymer coating of graphene oxide via reversible addition-fragmentation chain transfer mediated emulsion polymerization. **Journal of Polymer Science Part A: Polymer Chemistry,** v. 53, n. 12, p. 1413-1421, june 2015.

23 CAUVIN, S.; COLVER, P. J.; BON, S. A. F. Pickering stabilized miniemulsion polymerization: Preparation of clay armored latexes. **Macromolecules,** v. 38, n. 19, p. 7887-7889, sept. 2005.

24 NEGRETE-HERRERA, N.; PUTAUX, J.-L.; DAVID, L.; DE HAAS, F.; BOURGEAT-LAMI, E. Polymer/Laponite composite latexes: Particle morphology, film microstructure, and properties. **Macromolecular Rapid Communications,** v. 28, n. 15, p. 1567-1573, aug. 2007.

25 PUTLITZ, B. Z.; LANDFESTER, K.; FISCHER, H.; ANTONIETTI, M. The generation of "armored latexes" and hollow inorganic shells made of clay sheets by templating cationic miniemulsions and latexes. **Advanced Materials,** v. 13, n. 7, p. 500-503, apr. 2001.

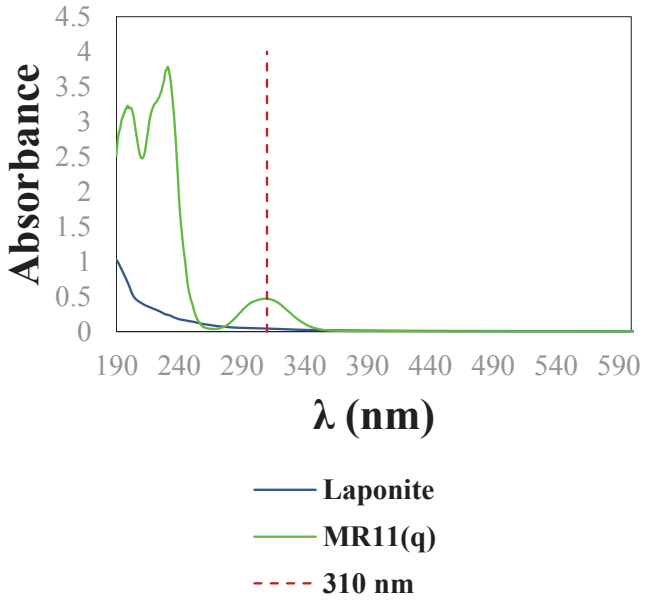
26 BOURGEAT-LAMI, E. Organic-inorganic nanostructured colloids. **Journal of Nanoscience and Nanotechnology,** v. 2, n. 1, p. 1-24, feb. 2002.

27 WANG, T.; COLVER, P. J.; BON, S. A. F.; KEDDIE, J. L. Soft polymer and nano-clay supracolloidal particles in adhesives: Synergistic effects on mechanical properties. **Soft Matter,** v. 5, n. 20, p. 3842-3849, 2009.

Annex 2 Calibration curves for the adsorption isotherms

For the determination of the equilibrium concentration of macroRAFT agent in the supernatant, C_e (g L^{-1}) and, consequently, the adsorbed amount of macroRAFT agent, Q_e (mg g^{-1}), as shown in Chapter 3, ultraviolet-visible (UV-vis) spectroscopy was used. For this purpose, the wavelength was, initially, determined by a comparison between the spectrum of a P(qDMAEMA$_{10}$-*co*-BA$_4$)-CTPPA (MR11q) macroRAFT agent solution in water and the spectrum of the supernatant of a 5 g L^{-1} dispersion of Laponite (the dispersion was submitted to a 1-hour centrifugation process at 60000 rpm, in a procedure similar to the one adopted for the isotherms). Both samples were submitted to a scan in the spectral region between 190 and 600 nm. Results, shown in Figure A2.1, indicate that at 310 nm, the trithiocarbonate chain end of the macroRAFT agent presents an intense peak of absorbance with minimal interference of Laponite.[1] A similar result was obtained for the other macroRAFT agents and, for this reason, this wavelength was selected to carry out the measurements for the calibration curves, as well as for the adsorption study.

Figure A2.1 – UV-vis spectra of Laponite (blue line) and P(qDMAEMA$_{10}$-co-BA$_4$)-CTPPA (MR12q, green line) in water.



Source: elaborated by the author.

For the adsorption study, a calibration curve was previously prepared for each macroRAFT agent by UV-vis spectroscopy at 310 nm. By the linearization of the data and

comparison of the results with the Beer-Lambert law, the molar absorptivity (ε) and correlation coefficient were determined, as listed in Table A2.1.

Table A2.1 – Beer-Lambert law and the molar absorptivity (ε) and correlation coefficient obtained, by UV visible spectroscopy, for the calibration curves of the macroRAFT agents.

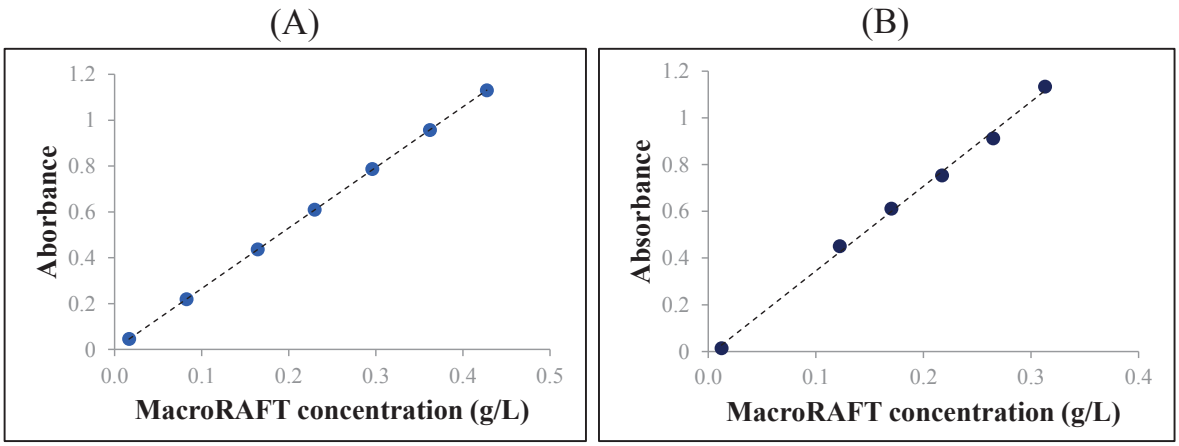
MacroRAFT	ε	**Corr. coef.**
MR1	2.641	0.99998
MR2	6.318	0.99690
MR3	4.259	0.99989
MR4	2.130	0.97629
MR5	2.211	0.99990
MR6	1.233	0.99970
MR7	1.344	0.99948
MR8	2.926	0.99995
MR9	3.335	0.99976
MR10	1.448	0.99988
MR11(q)	2.457	0.99965
MR12	1.344	0.99869
MR12(q)	2.844	0.99369

Beer-Lambert law: $A = \varepsilon\, c\, l$	A = Absorbance of the sample ε = molar absorptivity (L mol^{-1} cm^{-1}) c = concentration of the sample (mol L^{-1}) l = length of the light path through the sample (cm)

Source: this work.

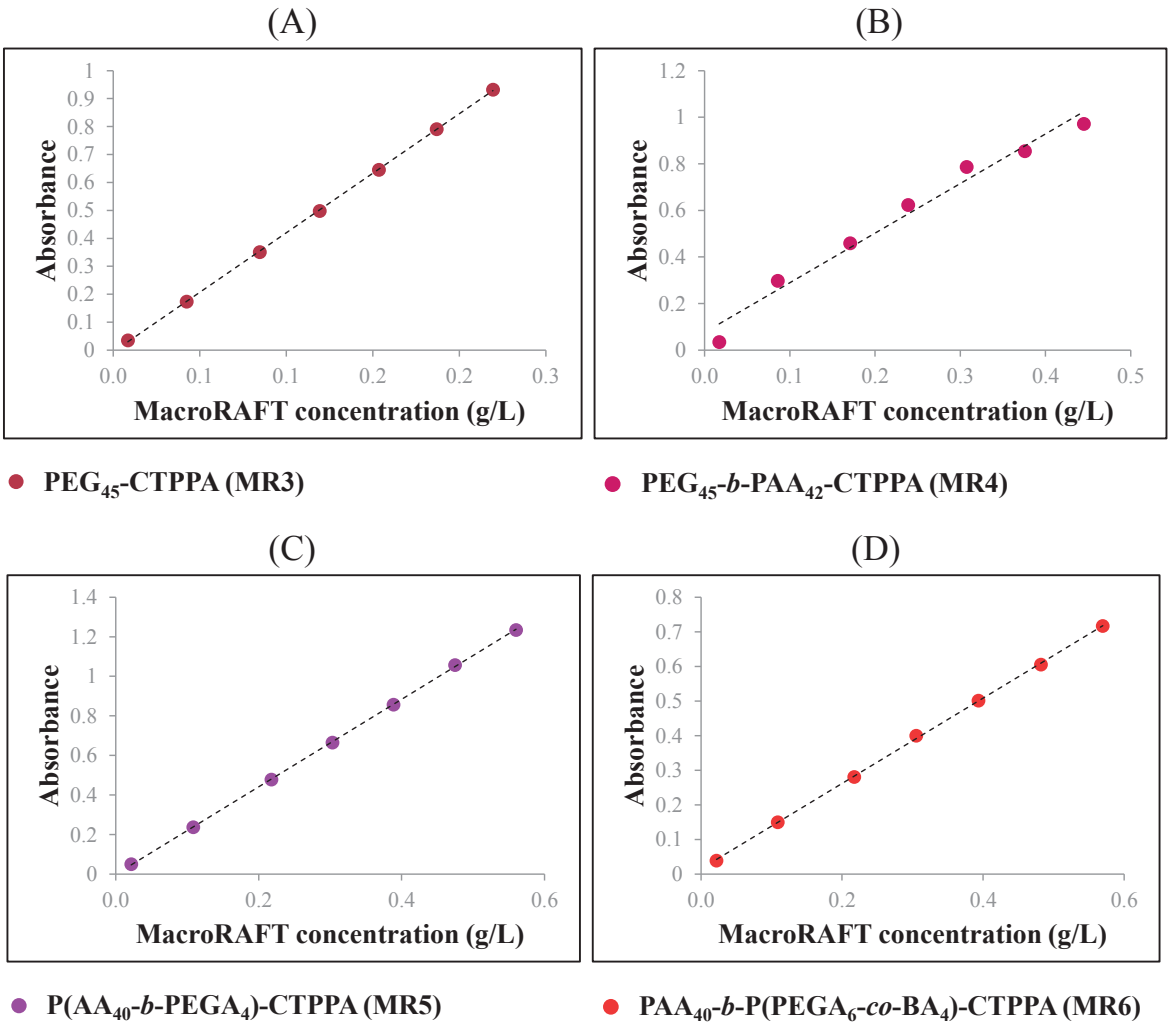
The calibration curves (shown in Figure A2.2, for the AA-based, PEGA-based and DMAEMA-based macroRAFT agents, respectively), as well as the correlation coefficients of Table A2.1, indicate that, for the concentration range observed, the relationship between the concentration of macroRAFT and the absorbance is linear according to the Beer-Lambert law. Therefore, the calibration curves obtained in this study can be used for the determination of the free macroRAFT concentration in the aqueous phase.

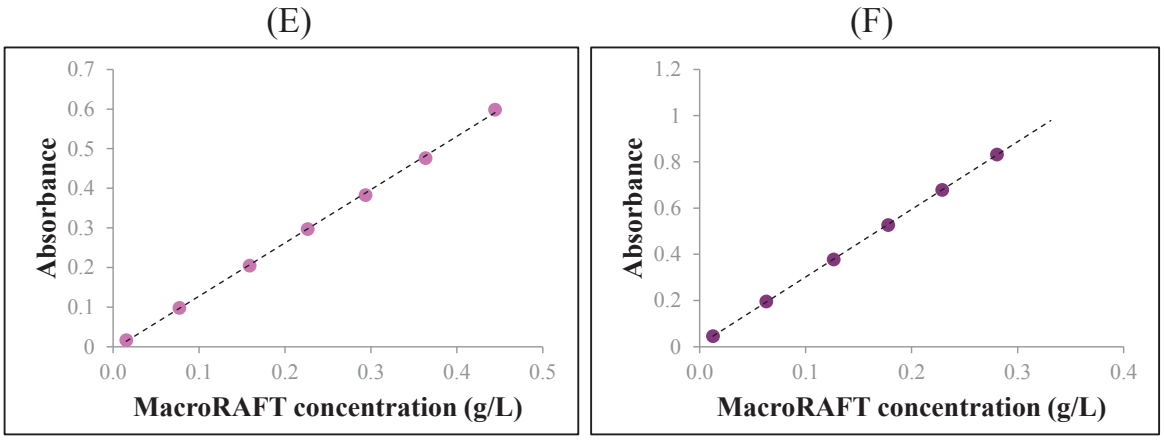
Figure A2.2 – Calibration curves for AA-based macroRAFT agents: (A) PAA_{40}-CTPPA at pH 7.5 and (B) P(AA_{16}-co-BA_{16})-CTPPA at pH 7.5 (λ = 310 nm).



Source: this work.

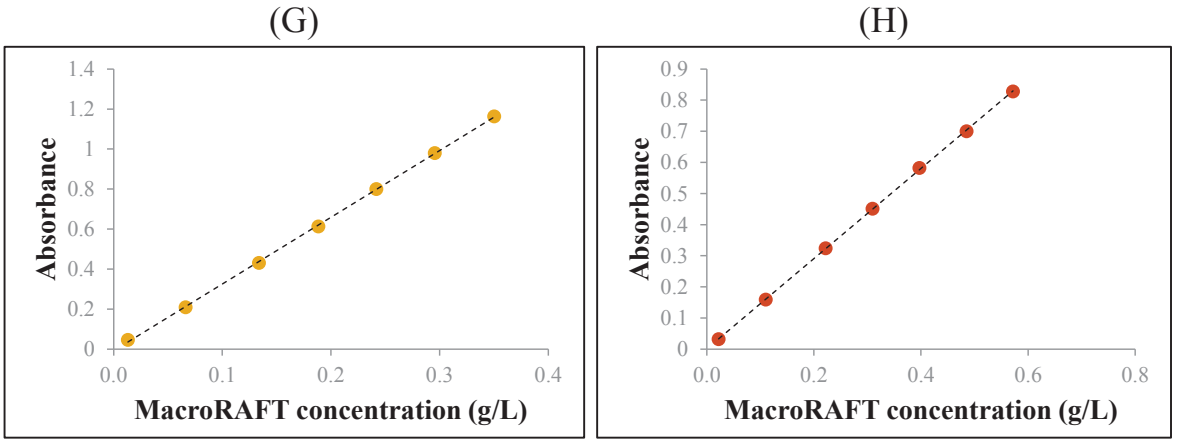
Figure A2.3 – Calibration curves for PEGA-based macroRAFT agents: (A) PEG_{45}-CTPPA at pH 10, (B) PEG_{45}-*b*-PAA_{42}) at pH 7.5 (λ = 310 nm), (C) P(AA_{40}-*b*-$PEGA_4$) at pH 7.5, (D) PAA_{40}-*b*-($PEGA_6$-*co*-BA_4) at pH 7.5, (E) P(AA_{16}-*co*-BA_{16})-*b*-($PEGA_6$-*co*-BA_4) at pH 7.5, (F) P($PEGA_5$-*co*-BA_3) at pH 10, (G) P(AA_4-*co*-$PEGA_4$-*co*-BA_4) at pH 7.5 and (H) P(AA_9-*co*-$PEGA_9$-*co*-BA_9) at pH 7.5.





● **P(AA$_{16}$-*co*-BA$_{16}$)-*b*- P(PEGA$_6$-*co*-BA$_4$)-CTPPA (MR7)**

● **P(PEGA$_5$-*co*-BA$_3$)-CTPPA (MR8)**

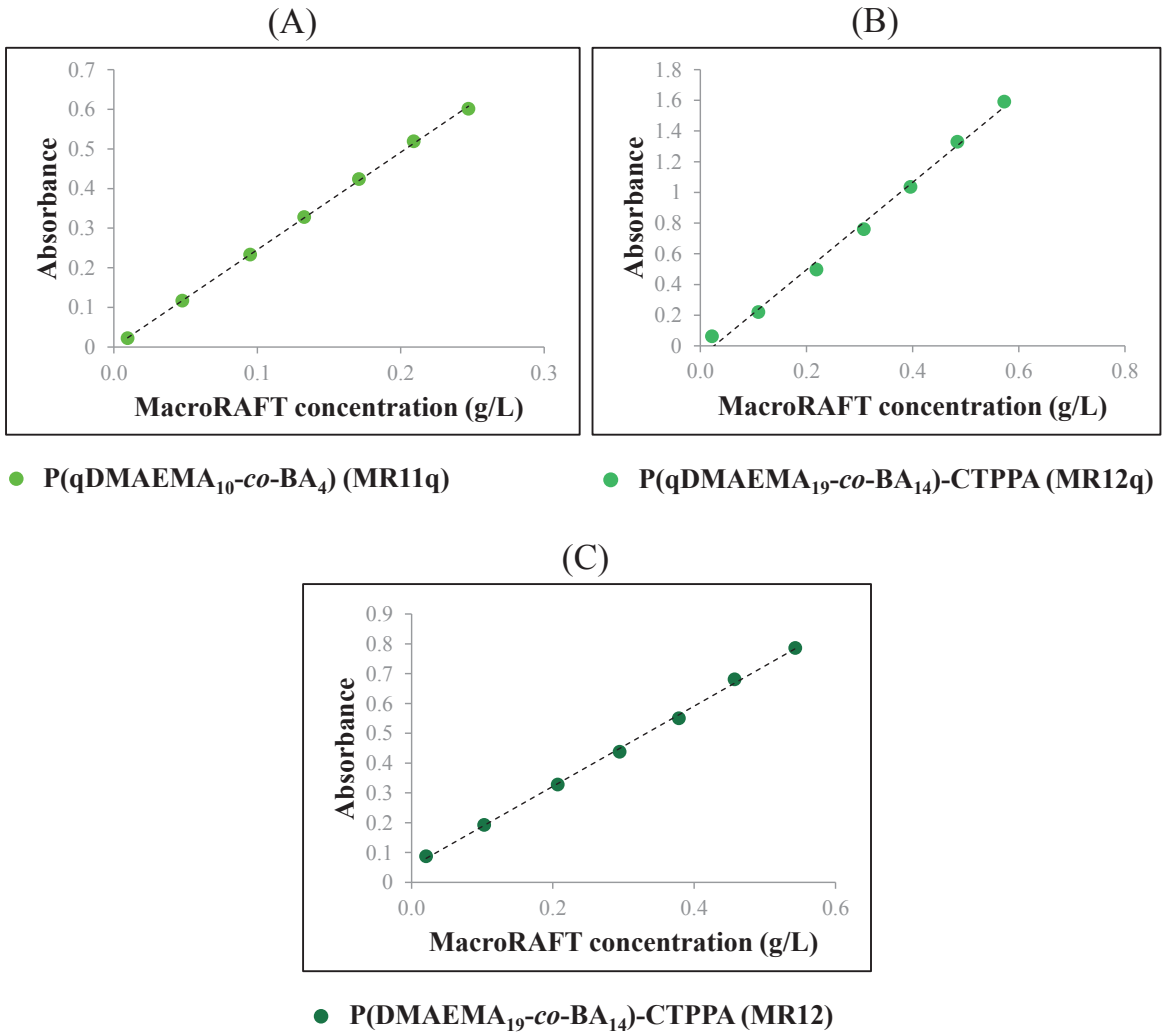


● **P(AA$_4$-*co*-PEGA$_4$-*co*-BA$_4$) (MR9)**

● **P(AA$_9$-*co*-PEGA$_9$-*co*-BA$_9$)-CTPPA (MR10)**

Source: elaborated by the author.

Figure A2.4 – Calibration curves for DMAEMA-based macroRAFT agents: (A) P(qDMAEMA$_{10}$-*co*-BA$_4$) at pH 10, (B) P(qDMAEMA$_{19}$-*co*-BA$_{14}$) at pH 10 (λ = 310 nm) and (C) P(DMAEMA$_{19}$-*co*-BA$_{14}$) at pH 6.



Source: elaborated by the author.

References

1 GUIMARAES, T. R.; CHAPARRO, T. D. C.; D'AGOSTO, F.; LANSALOT, M.; DOS SANTOS, A. M.; BOURGEAT-LAMI, E. Synthesis of multi-hollow clay-armored latexes by surfactant-free emulsion polymerization of styrene mediated by poly(ethylene oxide)-based macroRAFT/Laponite complexes. **Polymer Chemistry,** v. 5, n. 22, p. 6611-6622, nov. 2014.

Annex 3 X-ray diffraction analysis

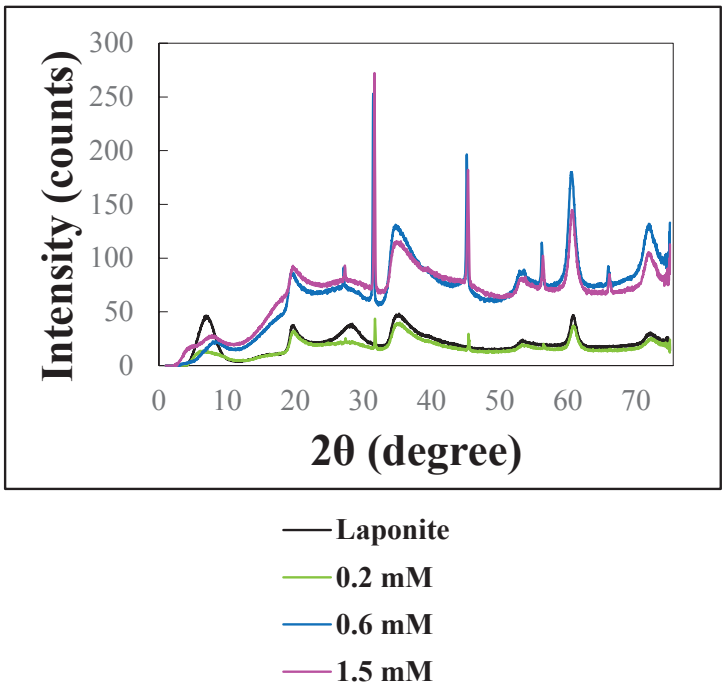
X-Ray diffraction (XRD) analysis were carried out in the *Laboratório de Caracterização Tecnológica* (*Depto. de Engenharia de Minas e de Petróleo*) from *Escola Politécnica da USP*, São Paulo, Brazil. Powder X-ray diffraction data were collected on a Bruker D8 Endeavor diffractometer operating at 40 kV and 40 mA for Cu Kα (λ = 1.54056 Å), with a scan speed of 0.5s per step and a step size of 0.02 ° in 2 θ.The angular domain analyzed was comprised between 1.5 and 75 °.

Four samples were prepared by, initially dispersing 0.9 g of Laponite into 45 mL of water. The dispersion was left under vigorous stirring while a solution of macroRAFT agent was prepared in parallel by adding 0.51 g of macroRAFT agent P(DMAEMA$_{19}$-*co*-BA$_{14}$)-CTPPA and 17g of water into a 30 mL flask. The solution was left stirring and had its pH adjusted to 6 by the addition of HCl. Samples were prepared by adding 10 mL of the Laponite dispersion into an adequate volume of the macroRAFT and completed with water until a total volume of 40 mL (in order to obtain a 5 g L^{-1} dispersion of Laponite containing different concentrations of macroRAFT agent). The concentration of macroRAFT agent in the final dispersion was selected based on the adsorption isotherm of this macroRAFT agent and the evolution of Zeta Potential (Figure 3.26 and Figure **3.25**, respectively). Therefore, four concentrations were analysed, as listed below:

- Pure **Laponite** RD (after being submitted to the dispersion procedure);
- Dispersion of Laponite (5 g L^{-1}) and **0.2 mM** of P(DMAEMA$_{19}$-*co*-BA$_{14}$)-CTPPA (this point is below the point of charge inversion of macroRAFT-modified Laponite platelets);
- Dispersion of Laponite (5 g L^{-1}) and **0.6 mM** P(DMAEMA$_{19}$-*co*-BA$_{14}$)-CTPPA (this point is above the point of charge inversion of macroRAFT-modified Laponite platelets and there is no free macroRAFT agent in the aqueous phase);
- Dispersion of Laponite (5 g L^{-1}) and **1.5 mM** of P(DMAEMA$_{19}$-*co*-BA$_{14}$)-CTPPA (this point is above the point of charge inversion of macroRAFT-modified Laponite platelets and there is an excess of macroRAFT agent that is free in the aqueous phase).

XRD results are shown in Figure A3.1.

Figure A3.1 – XRD analysis of Laponite (5 g L^{-1}) modified with different concentrations of P(DMAEMA$_{19}$-*co*-BA$_{14}$)-CTPPA macroRAFT agent at pH 6.



Source: elaborated by the author.

XRD pattern of Laponite in the sodium cation form presents a broad peak at about 6.9º (2θ) associated to a (001) basal spacing of ~ 0.79 nm. At low macroRAFT concentration (0.2 mM), a peak of lower intensity is observed at 6.4º (2θ), which can be associated to a basal spacing of ~ 0.77 nm. This means that, at low concentration of macroRAFT, the basal spacing of the mineral does not suffer a significant change. Confirming the close interaction between the clay platelets and P(DMAEMA$_{19}$-*co*-BA$_{14}$)-CTPPA chains at a concentration of 0.6 mM of macroRAFT, a small peak can be noticed around 7.9º (2θ) associated to a Laponite basal spacing of 0.88 nm. This expansion in the basal spacing after contact with 0.6 mM of DMAEMA-based copolymer suggests the intercalation of the polymer chains. Increasing the concentration of macroRAFT to 1.5 mM does not affect the basal spacing of Laponite, as very similar results were obtained at this concentration (2θ = 7.8 º with a basal spacing of 0.87 nm), indicating that the excess of macroRAFT does not intercalate but stays free in the aqueous phase.